

Road Erosion, Sediment Delivery, and Consequence in the Simonette Watershed West-Central Alberta

by

Kenneth Jared Fath

A thesis submitted in partial fulfillment of the requirements for the degree of

Doctor of Philosophy

in

Water and Land Resources

Department of Renewable Resources
University of Alberta

© Kenneth Jared Fath, 2022

Abstract

Gravel and dirt resource roads in the Alberta foothills are critical economic infrastructure, used to explore for, manage, and extract natural resources from this region. Resource roads are also known to add sediment to nearby streams and rivers, causing habitat stress for fish. Understanding road erosion and sediment delivery processes, and how road sediment moves through the stream network is therefore crucial to reducing habitat damage from these roads. The environment of west-central Alberta contains several features which make it susceptible to road erosion and sediment delivery problems: abundant glacial silt and clay deposits, seasonal freeze and thaw cycles, heavy industrial traffic, and a precipitation regime dominated by summer storms. This thesis examines factors and processes controlling road erosion and sediment delivery processes in the Simonette watershed, a 5400 km² watershed that spans the foothills and boreal plains regions in west-central Alberta. An understanding of these processes was used to develop and evaluate road impact indicators and test them against physical measures of stream condition. This research thus provides baseline data on road erosion, sediment delivery, stream condition, and appropriate indicators of impact that may be used by future watershed assessors in prioritizing and remediating areas of problematic sediment contribution in west-central Alberta foothills watersheds. It was initially hypothesized that sedimentation, and infiltration rates would be strongly determined by mapped surficial geology on site, with significant differences between fine-textured (glaciolacustrine), sandy (glaciofluvial, aeolian), and mixed (morainal) sites. Higher-traffic roads were also expected to generate higher amounts of sediment than lower-traffic roads. The main hypothesis regarding sediment deposition was that the size and extent of road sediment discharge plumes was controlled by the ability of the ground to absorb the discharge generated in the road area. The relationship between contributing area of sediment plumes, and runout area would be related to different infiltration rates in the road and plume area, and precipitation intensity. Road sediment delivery

impacts in streams were expected in stream features that promoted settlement of finer sediment, such as pools and areas of flow into the streambed.

The strongest driver of erosion in the Simonette watershed was how efficient road segments were at producing runoff from rain events. There was some evidence that surficial geology and traffic influenced sedimentation rate: the highest producing site was a high-traffic road in silty morainal deposits, and the lowest-producing site was a well-drained, sandy, low-traffic road. Both sites were also on end members of a continuum of hydrological responses for the studied road segments: sites with better-drained soils produced less sediment than sites with poorly-drained soils. Overall, sedimentation rates from these Alberta study roads were moderate to high compared to studies of other dirt roads in North America. Potential connectivity of road segments was also driven by hydrology: strong geometric relationships existed between flow-generating areas in the road network, and flow-absorbing areas downslope of road drain points. The area of road sediment plumes was strongly correlated with the product of road-related contributing area and slope, and the length of road plumes was correlated with road-related contributing area. Road erosion and consequence models calibrated to the findings of the erosion and deposition studies in the Simonette watershed were tested for their effectiveness in predicting instream sedimentation pressure. Proportion of clay and silt in streambed gravel matrix was positively related to the number or density of upstream road crossings and with estimated sedimentation pressure from a hydrologically-based road model. Overall, road hydrology was found to be the single best predictor of sedimentation rate and delivery potential to streams. Stream impacts in the region were not well-correlated with the commonly-used metric of road density, but instead with road crossings. This study supports a growing body of literature that suggests that the use of basic hydrological models is effective in predicting and assessing road sedimentation risk.

Preface

This is a paper-based thesis comprising three original research papers and front and back matter which help to introduce and contextualize the topic. The thesis includes material that I previously released in unpublished reports to the Forest Resources Improvement Association of Alberta (FRIAA).

The first report is:

Kenneth Jared Fath, 2018. “Combining field and LiDAR modelling tools to move beyond indicator-based approaches to surface erosion: Simonette as a test area for the Foothills natural region.” FRIAA Progress Report, dated January 22, 2018.

This report details preliminary and provisional results of the erosion study from 2016 to 2017.

The second report is:

Kenneth Jared Fath, 2019. “Combining field and LiDAR modeling tools to move beyond indicator-based approaches for surface erosion: Simonette as a test area for the Foothills natural region.” FRIAA Progress Report, dated June 11, 2019

This report describes the final dataset as of Summer 2019.

Portions of the thesis have also been presented at conferences:

CWRA Alberta Branch Conference, Red Deer, Alberta, April 14-16, 2019

American Geosciences Union Fall Meeting 2019, San Francisco, California, December 9-13, 2019

Brief summaries of findings from the thesis are provided in a series of quick notes from fRI Research:

“Erosion, Sediment Delivery, and Consequence from Roads in Foothills Watersheds in West-Central Alberta: A Case-Study in the Simonette”

-- Part 1: Road Surfaces

-- Part 2: Gully Erosion

-- Part 3: Diverting Sediment from Streams

-- Part 4: Instream Consequences and Road Crossings

Dedication

To all those who set out to measure the Earth (and usually fail):

Where were you when I laid the foundation of the Earth?

Tell me, if you possess understanding!

Who set its measurements – if you know –

Or who stretched a plumb line across it?

On what were its bases set,

Or Who laid its cornerstone –

When the morning stars all sang in a chorus

And the sons of God shouted for joy?

Job 38:4-7 (ESV)

Acknowledgements

This thesis would not be where it is without a great deal of grace, provision, and assistance. I am thankful to Axel Anderson for giving me the chance to examine, define, and delineate a challenging topic in contemporary hydrology. I came into this wanting to know “where the dirt goes” when people start disturbing watersheds and ended up coming away with more questions than answers. This is probably a good outcome for a thesis. Axel also pointed me towards a generous Mitacs grant which supported me in my first three years of the program. I am thankful for those at Mitacs, my first cohort of reviewers who had to wade through my radical (and over-ambitious) proposal, and also to Canfor, who generously provided funds and in-kind resources for the completion of the project. They also connected me with a campsite at the Timber Pro logging camp where I spent two rather enjoyable summers in 2017 and 2018.

During my first summer I had the fortune of staying in a rustic log cabin owned by Arvid Thiessen. Arvid also provided a very helpful hand when we bogged down our Toyota Tacoma in a muddy section of forest road in Spring Creek. He provided great service for an unbeatable price. Besides from that I and my field assistants were able to feast ourselves quite happily on his wife’s donuts at the Crooked Creek Convenience store (which are in my opinion the best I have eaten). I am also incredibly thankful for the times spent arguing politics and history, drinking tea, and playing Cribbage with Shane Lafleur, our Timber Pro camp security staff. He made the experience memorable, and at times hilarious, with his extremely detailed and precise camp reports (which included weather observations), and his helpful suggestions derived from a lifetime of leading young men in the Canadian Military.

I was helped immensely by my field assistants: The first was Haitao Li, a senior PhD student who helped me get my own PhD off to a good start. Our first two weeks out in the Simonette were filled with remarkable discoveries and missteps. I was glad for his help and his company. He remains a friend. Matthew Rayner showed up mid-season and helped me build the foundation of my project. He helped me do my first surveys and install my first silt fences without complaining. I enjoyed our conversations and his late night AM talk radio. Kyle Stratechuk was very talented and organized and undertook the gruelling and punishing job of installing all of our monitoring stations. He was with me in the worst mudholes, and he pulled our truck out of some slippery situations not once, but twice: without him I would have incurred loss. Jon Yasinski came along in the third season, and his patience, humour, wit, and incredible physical strength got us through the hard work of

maintaining our fussy sediment tanks and carrying out stream surveys while carrying around 70 pounds of equipment. Axel also assisted in our winter takedowns, and I was constantly impressed at his speed, strength, and efficiency. He is a formidable force. My dad, Benno, also helped me out with my first formal plume survey in Fall 2016, and instead of ordering me around he took my orders. His humility, grace, and patience are amazing.

My committee members have provided invaluable help in steering this project forward, improving the writing style, and most importantly, in helping me to see its ultimate significance and utility. I would not have had the confidence to finish this without them.

My parents provided constant support. My mother found me a “job” when I was in Vancouver Island debating my future career options, a job which turned out to be a PhD project. I hope that I have given her reason to be proud. My dad has always been a good and solid sounding board for life advice, and I needed a lot of that during this degree. My brother Dylan and his wife Breanna gave me a second home, friendship, and inspiration when I needed them most, and his two (now three) kids have provided me boundless joy as an uncle.

Much thanks also go to my wife Mavis (Suhua). She was willing to move from the warm, rainy, West Coast to the cold and tempestuous Prairies – an incredible sacrifice. She helped support me in the final two years of thesis writing. Many thanks to my daughter Noa (Nuoen) who will forever bear the burden of a strange name, and of being born in a strange time. She provided the final little push I needed to finish this long project. May she live under better times than the ones she was born in, and may I do my part in making those times, and a better future for all, possible.

God, who above all things, through the many valleys and mountains, and through the streams, forests, and foothills, carried me, deserves the last and best credit. My final prayer and hope is that this and all the future works of my hands may be used to produce the better world he is endlessly building out of all our flawed works.

Table of Contents

Abstract.....	ii
Preface	iv
Dedication	v
Acknowledgements.....	vi
Table of Contents	viii
List of Tables.....	xii
List of Figures	xiii
1. Introduction.....	1
1.1 Impact of road fines on fish and fish habitat	1
1.2 Controls on sediment production and delivery in the road environment	2
1.2.1 Road geometry, construction, and materials	2
1.2.2 Effects of traffic and maintenance	4
1.2.3 Fate of road sediment.....	4
1.3 Assessing and verifying road sedimentation pressure in watersheds.....	5
1.4 Fate of sediment in streams.....	7
1.5 Road impacts in Alberta watersheds.....	7
1.6 Unsealed resource roads in the Simonette watershed	8
1.7 Research contribution and study area	9
1.8 References	12
1.9 Tables	19
1.10 Figures	20
2 Hydrological Controls and Thresholds for Road Erosion in a Foothills Watershed, West-Central Alberta	26
2.1 Introduction	26
2.2 Methods and materials	28

2.2.1	Study site	28
2.2.2	Road surface sedimentation and data collection	29
2.2.2.1	Settling tank plots	30
2.2.2.2	Silt fences	32
2.2.2.3	Sedimentation plume survey data	33
2.3	Results	34
2.3.1	Settling tank sedimentation plots	34
2.3.2	Silt fences	35
2.3.3	Gullies and sediment plumes	36
2.4	Discussion	36
2.4.1	Hydrological behaviour and erosion risk	36
2.4.2	Effects of traffic and geology	37
2.4.3	Effect of road and ditch maintenance	38
2.4.4	Erosion rates in the Simonette compared to other studies	39
2.4.5	Management and modelling implications	40
2.5	Conclusion	41
2.6	References	42
2.7	Tables	48
2.8	Figures	54
3	Road-Related Contributing Area as a Driver of Sediment Plume Size for Unsealed Roads In West-Central Alberta, Canada	60
3.1	Introduction	60
3.1.1	Factors influencing road sediment connectivity	60
3.1.2	Conceptual model of plume formation	61
3.1.3	Research objectives	63
3.2	Study area and methods	63
3.2.1	Study area	63

3.2.2	Field data collection	65
3.2.2.1	Site selection.....	65
3.2.2.2	Sediment plume data collection	65
3.2.2.3	Sediment plume area calculations.....	66
3.2.3	Statistical methods.....	66
3.2.4	Steady-state plume hydrological model calibration	67
3.3	Results	67
3.3.1	Empirical relationships	67
3.3.1.1	Data summary and primary correlations	67
3.3.1.2	Plume length and area relationships, and outlier analysis.....	68
3.3.1.3	Sediment plume empirical model selection.....	69
3.3.2	Road infiltration modelling	69
3.4	Discussion	71
3.5	Conclusion.....	72
3.6	References	74
3.7	Tables	78
3.8	Figures.....	81
4	Sediment Contributions from Road-Stream Crossings Cause Downstream Gravel Matrix-Fining in a Foothills Watershed in Alberta, Canada.....	86
4.1	Introduction.....	86
4.1.1	Selection of appropriate indicators	87
4.1.2	Erosion and sedimentation modelling and indicators	88
4.1.3	Objective.....	88
4.2	Study site	89
4.2.1	Sample design: sub-watershed selection.....	90
4.2.2	Erosion simulations.....	91
4.2.2.1	GRAIP_Lite simulation.....	91
4.2.2.2	READI simulations	92

4.2.3	Stream physical attribute study.....	93
4.2.4	Lab analysis of freeze core samples	94
4.2.5	Statistical analysis of stream physical parameters and road pressure variables.....	94
4.3	Results	94
4.4	Discussion	95
4.5	Conclusion.....	98
4.6	References	100
4.7	Tables	105
4.8	Figures	110
5	Lessons learned: How studies in the Simonette watershed inform resource management....	116
5.1	Introduction.....	116
5.2	Research and infrastructure challenges in Alberta foothills watersheds	116
5.3	Road segment hydrology	117
5.4	Contributing area thresholds in the road prism.....	118
5.5	Road crossings as impact sites.....	119
5.6	Stream dynamics predict the location of impact.....	119
5.7	Road crossing inventories and watershed monitoring.....	120
5.8	General recommendations for resource road management	121
5.9	Road infrastructure management options to improve watershed health	122
5.10	References	123
5.11	Tables	127
5.12	Figures	128
	References.....	132
	Appendices	145

List of Tables

Table 1-1. Estimates of road-based sedimentation compared to other sources of sediment in forested watersheds (from Elliot, 2013).....	19
Table 1-2. Relative magnitude of road erosion in selected studies	19
Table 2-1. Climate variability in and near the Simonette watershed (Canadian Climate Normals 1981-2010).....	48
Table 2-2. Location and description of settling tank and silt fence sites	49
Table 2-3. Precipitation, rain energy, water yield, settling tank masses, and fines estimates: settling tank plots, 2017-2018.....	50
Table 2-4. Rain energy versus yield regression equations by plot	52
Table 2-5. Silt fence erosion data	52
Table 2-6. Maximum management lengths for the Simonette watershed	53
Table 3-1. Factors contributing to plume length from a review of previous literature	78
Table 3-2. Table of plume dependent and independent variables.....	78
Table 3-3. Fixed and random Monte Carlo plume simulation variables.....	79
Table 3-4. Correlation between plume attributes and predictor variables.....	79
Table 3-5. Plume length and area regressions	80
Table 3-6. Kruskal-Wallis test on residuals for plume length and area regressions	80
Table 4-1. Weighting coefficients for GRAIP erodibility in the Simonette watershed.....	105
Table 4-2. Simulation parameters for READI runs.....	105
Table 4-3. Stream physical parameters, environmental gradients, and road pressure indicators used in this study	106
Table 4-4. Characteristics of study basins.....	107
Table 4-5. Road pressure variables and stream survey results organized by reach.....	108
Table 5-1. Maximum management lengths for roads in the Simonette watershed based on a maximum contributing area of 3500 m ²	127

List of Figures

Figure 1-1. Location of study site in Alberta.	20
Figure 1-2. Theoretical road prism showing features of the road environment, connectivity pathways, and consequences for road erosion.....	21
Figure 1-3. Examples of different types of road cut and fill.	21
Figure 1-4. Examples of road sediment plumes.....	22
Figure 1-5. Severe gullying in ditches, Simonette watershed, Alberta.	22
Figure 1-6. Conceptual model of point source impact to the stream environment	23
Figure 1-7. Environmental gradients in the Simonette watershed	24
Figure 1-8. Climate normals (1981-2010), Simonette weather station	25
Figure 2-1. Location of the Simonette study area in Alberta with mapped surficial geology	54
Figure 2-2. Settling tank plot components	55
Figure 2-3. Typical silt fence erosion plots in the Simonette	55
Figure 2-4. Gullied ditches in the Simonette	56
Figure 2-5. Sediment production rate versus storm energy by settling tank plot.....	56
Figure 2-6. Plot runoff-generating efficiency (left) and peak infiltration rate by plot (right).....	57
Figure 2-7. Sediment yield compared with runoff efficiency for settling tank plots.....	57
Figure 2-8. Comparison of erosion rates estimated from plume extent and thickness from non-gullied road segments (left), and gully surveys (right).....	58
Figure 2-9. Relationship between contributing area and mass for plumes (blue) and gullies (red) showing threshold erosion behaviour for contributing areas greater than 3500 m ²	58
Figure 2-10. Comparison of road sedimentation rates in the Simonette and other areas	59
Figure 3-1. A plume of road sediment deposited in an excavated roadside turnout.....	81
Figure 3-2. Location, natural regions, and surficial geology for the Simonette watershed	82
Figure 3-3. Distribution of categorical variables in the data (out of 62 samples)	83
Figure 3-4. Plume area and length regressions showing overall increase in plume area and length with contributing area (left), and visual examples of outlier points (right).....	83
Figure 3-5. Range of infiltration rates for roads in the Simonette watershed <i>Plots</i>	84
Figure 3-6. Simulation-based parameter estimates from 95 best models	84
Figure 3-7. Predicted versus modelled values for plume area (left) and length (right) using parameter average values and the READI model	85

Figure 4-1. Environmental gradients in the Simonette watershed. (A) Natural subregions (B) Surficial Geology, (C) Bedrock Age, (C) Precipitation.....	110
Figure 4-2. Road density (left), and road crossing density (right) in the Simonette watershed, west-central Alberta	111
Figure 4-3. Map of stream survey sites and watersheds	112
Figure 4-4. Stream physical sampling equipment: counting frame (left); metal freeze-coring device with attached bed substrate material (right)	113
Figure 4-5. Correlations between stream survey variables, natural basin characteristics, and road pressure variables	114
Figure 4-6. Relationship between streambed gravel matrix composition and road pressure variables	115
Figure 5-1. Normalized sediment production (logarithmic axis) versus plot runoff ratio for road plots in the Simonette.....	128
Figure 5-2. Erosion and contributing area relationships for measured sediment plumes (blue), and gullied ditch segments (red).....	129
Figure 5-3. Channelized ditch erosion in the Simonette.....	130
Figure 5-4. Gravel matrix composition compared to road crossing density (#/km), READI values, and road density (km/km ²) from left to right.....	131

1. Introduction

Resource roads are unsealed roads commonly used in agriculture, forestry, oil and gas, and mining. Unsealed resource roads are preferred to paved roads in these industries because they are less expensive to construct, can bear heavy axle loads, and can be more easily repaired after heavy use, rain, or over-loading. In Alberta there are about 173,300 km of unsealed roads (Transport Canada, 2017), many of which are wide, high traffic roads, built to accommodate vehicles and heavy resource production equipment moving at near-highway speeds of 60 – 80 km/hr (Figure 1-1). The construction, repair, and use of resource roads in Alberta is an expensive and complex undertaking involving road leaseholders and paying industrial users. Ten metre-wide double-lane roads cost about \$590,000 per kilometre to construct (Alberta Municipal Affairs & Morrison Hershfeld Ltd., 2008), and routine culvert replacements usually cost several thousands of dollars (Alberta Transportation, 2019). Although they have a central economic importance to Alberta there are many environmental costs associated with resource roads. Impacts include habitat fragmentation and disturbance, and (relevant to this thesis) erosion and instream sedimentation. Resource roads are a major source of sediment pollution in forested watersheds (Bilby, 1985; Cederholm et al., 1980; Elliot, 2013; Hoover, 1952; Lieberman & Hoover, 1948; Megahan & Kidd, 1972; Reid et al., 2016). The contribution of fine sediment from roads is estimated to be second only to wildfire and prescribed burns and can result in stream sediment loads of around two to more than ten times the background erosion rate (Elliot, 2013; Table 1-1, Table 1-2). Affected streams may have a significant portion of suspended sediment load attributed to resource roads (Bilby, 1985; Reid et al., 2016). A better understanding of road erosion and sediment delivery processes is necessary to find ways of locating and mitigating potential sites of road sediment contribution to the stream environment while keeping maintenance costs economically feasible.

1.1 Impact of road fines on fish and fish habitat

The addition of fine-grained sediment from roads can lead to degradation of the instream environment. Sediment-related impacts include high turbidity (Bilby, 1985; Lieberman & Hoover, 1948), reduction in the size of streambed material (Al-Chokhachy et al., 2016; Cederholm et al., 1980), fines accumulation in stream pools (Lisle & Hilton, 1992), and fining of the intragravel matrix (Cederholm et al., 1980; Spillios, 1999). Salmonids, including west-coast salmon species, trout, and grayling, are all sensitive to sediment pollution in the stream environment (Cederholm et al., 1980; Chapman, 1988; Phillips et al., 1975; Reynolds et al., 1990). Road density or percent basin area in

roads are key indicators of habitat degradation for salmonid species, commonly correlated with decreased particle size in streambed gravels (Al-Chokhachy et al., 2016; Cederholm et al., 1980). Unfortunately, road density provides no information about the location of specific sedimentary disturbances in a watershed.

Alberta's Eastslopes watersheds are key habitat for several species of fish in the salmonid family including: Bull Trout, Eastslopes Cutthroat Trout, Athabasca Rainbow Trout, and Arctic Grayling. These watersheds are also a focus for industrial development, with a long history of forestry focused on valuable softwood lumber species, and ongoing exploration in the natural gas and petroleum distillates industries. These industries bring with them a high degree of land disturbance, including clear-cutting, well pad-clearing, and road development. Serious declines in key fish populations have followed industrial development in foothills watersheds (Cahill, 2015; Costello, 2006; Rasmussen & Taylor, 2009; Rodtka et al., 2009; Scrimgeour et al., 2008). Habitat fragmentation and modification from road stream crossings in the Simonette watershed has also been shown to negatively impact fish species richness and diversity (Maitland et al., 2016). Road crossings are also known to contribute fine sediment to gravel matrices in Alberta foothills streams (Spillios, 1999). A present need is for indicators of road sediment pressure that are spatially explicit and help locate specific sites of disturbance in the Alberta foothills.

1.2 Controls on sediment production and delivery in the road environment

Road sediment production is usually related to several overriding variables common to all roads: geometry, construction, materials, traffic, maintenance, and drainage. Geometric issues are related to the size, shape, and slope of road segments, including the running surface, cut-slope, and ditch dimensions (ie. the road prism), construction issues relate to practices involved in road-building, and materials comprise surfacing and subgrade material used to construct the road. Roads with high use (with frequent maintenance schedules) will have different problems than roads which are low use. Drainage of the road surface is an overriding concern, often driven by all the above factors except for traffic. When a segment of road has insufficient drainage, plumes of soil and water from the road surface are able to cross intervening hillslopes and impact the stream environment (Benda et al., 2019; Thompson et al., 2008).

1.2.1 Road geometry, construction, and materials

In order to create a stable running surface for vehicles road-builders must disturb the area containing the road and adjacent right-of-way, also known as the road prism. The road prism

includes the running surface of the road, cuts and fills used to build the running base, and drainage structures designed to convey water away from the road prism and into adjacent terrain (Figure 1-2). Road cut-and-fill strategies commonly employed to accommodate vehicle speed, size, and hauling limitations include filling in topographic low points, such as stream crossings, through-cuts through hummocky terrain or projecting knobs, and cut and fill in side-sloping areas (Figure 1-3). The load-bearing portion of the road prism is comprised of a subgrade of fill and/or native rock and soil compacted to improve load-spreading and water-shedding characteristics. In most roads the compacted subgrade is usually overlain with base and running courses of gravel aggregate or crushed rock to improve the structural bearing capacity of the pavement, to promote drainage, and to prevent erosion of the road surface. Larger roads in Alberta may have the subgrade separated from aggregate courses with geotextile layers. Geotextile separation prevents road subgrade materials from being pumped upward and mixed with base and surface gravel courses during vehicle passes. Roads with gravel or aggregate running surfaces are called gravel roads, whereas roads constructed on prepared native surface material are called native surface roads. Native surface roads generally produce more erosion for a given road segment than roads capped with gravel or other surfacing materials (Brown et al., 2013; Burroughs & King, 1989; Coe, 2006). Because gravel is of limited supply in Alberta, smaller haul roads and local access roads may be more susceptible to erosion than larger trunk roads with better construction and more surfacing material. Because surfacing material is inconsistently applied, the erosion susceptibility of roads in Alberta may be dependent on their underlying geological materials.

A comprehensive comparative study of road erosion found that the erosion susceptibility of roads varied with proportion of water-stable aggregates greater than 2 mm, and that the percentage of water-stable aggregates varied with underlying geology (Packer, 1967). The most susceptible geological types were glacial silt, andesite, and loess, whereas the least susceptible types were hard metasedimentary rock, basalt, and granite. Other studies have found high rates of erosion in weathered granitic bedrock, a fact attributed to rapid *grus* formation (physical and chemical weathering of granite into sand-size particles) on exposed surfaces (Ketcheson & Megahan, 1996; Megahan et al., 1983). Some of the highest road erosion rates are recorded in high-traffic roads underlain by Cenozoic sandstone, greywacke, and siltstone, all of which are soft, sedimentary rocks, susceptible to mechanical breakdown from tire abrasion and grading (Reid & Dunne, 1984). Lower rates of erosion are found where roads are capped with hard volcanic rock (Luce & Black, 2001a). Relatively few studies address relative susceptibility to erosion in glacial terrain (Packer, 1967;

Sugden & Woods, 2007) even though most erosional models rank silty glacial soils, such as those commonly found in west-central Alberta watersheds, as among the most susceptible to erosion (Renard et al., 1997; Wall et al., 2002).

1.2.2 Effects of traffic and maintenance

High traffic roads generally produce more erosion than roads which have little vehicle traffic although the actual difference in erosion rates can vary from approximately two times to more than ten times (Burroughs & King, 1989; Croke et al., 2006; Luce & Black, 2001a; Reid & Dunne, 1984). While grading creates effects that may linger by a year or more (Luce & Black, 2001a), the effects of individual vehicle passes may be more transient. Several studies have found elevated suspended sediment concentrations in road segment outflows that persist for 30 minutes to an hour after vehicle passes. The approximate magnitude of the increase varies from 2 – 3 times (van Meerveld et al., 2014) to about 4 – 5 times (Luce & Black, 2001a). The combination of traffic and regular grading and ditch maintenance, rather than one or the other alone have a multiplicative effect on road erosion susceptibility (Luce & Black, 2001a). This difference is attributed to mobilization of sediment and loss of vegetation cover in ditches, where concentrated flows of water can transport it more efficiently through the road drainage system. Roads in Alberta commonly serve multiple licensees in oil and gas and forestry and have very high traffic levels. As much of Alberta is also located in susceptible glacial terrain, roads are also likely susceptible to accelerated erosion following ditch grading.

1.2.3 Fate of road sediment

Once mobilized, road sediment is transported through the road prism and into downslope areas until it either reaches a waterbody or is infiltrated into the subsurface. Flows of sediment and water are mobilized through all parts of the road prism, from the cutslope which intercepts flow from upslope, along the road surface and ditches, and into adjacent fill-slopes and lower hillslopes through cross-drains and roadside turnouts (Figure 1-4, left). Traces of sediment from flow events on the road surface are known as sediment plumes (Figure 1-4, right). The size of sediment plumes is ultimately related to the amount of flow generated on the road surface, and the ability of the downslope vegetated areas to infiltrate flows of sediment and water from the road. The strength of flow from road surfaces is often correlated with road contributing area (Carson et al., 2018; Coe, 2006; Montgomery, 1994) or culvert spacing (length of undrained road) (Brake et al., 1997; Ketcheson & Megahan, 1996; Packer, 1967). Other factors that have a strong influence on flow

generation include intensity of precipitation input, infiltration capacity of the road surface, and overall slope of the road contributing area. Steeper segments of road generate flows more rapidly than gently-sloping areas (Luce & Black, 1999), and longer segments of road are more likely to develop concentrated rill erosion on the surface and ditches (Packer, 1967; Renard et al., 1997).

The ability of a downslope area to absorb water from the road surface is ultimately controlled by infiltration capacity of adjacent ditches and hillslopes below the right-of-way (Benda et al., 2019; Hairsine et al., 2002). Flows that are dispersed rather than concentrated can spread runoff over a wider area, resulting in shorter sediment plumes. Factors that disperse plumes include obstacle number and spacing below drain points (Brake et al., 1997; Megahan & Ketcheson, 1996; Packer, 1967), and gentler slopes (Brake et al., 1997; Megahan & Ketcheson, 1996).

When there is enough road runoff, flows exiting drain points at the side of the road can create gullies rather than sediment plumes. Sometimes gullies may erode in road ditches (Figure 1-5). The risk of connectivity when downslope areas are gullied is much higher than when road runoff follows dispersive paths (Coe, 2006; Croke et al., 2005). Regardless of whether a road segment is connected, several studies do show that flow dispersion and loss of transporting power downslope results in an exponential decline in sediment delivery with percent of plume length (Megahan & Ketcheson, 1996; Woods et al., 2006). Overall sediment delivery to streams can therefore be thought of as a quantity (or relative intensity) of road erosion, multiplied by percent connectivity to obtain a value for sediment delivery in a catchment or stream reach (Figure 1-6). Not all road segments connected to streams are equally problematic. Those in which most material deposits before reaching streams will be much less problematic than those with a relatively uninterrupted flow of soil and water to a nearby waterbody.

1.3 Assessing and verifying road sedimentation pressure in watersheds

Some road segments are more problematic than others, and watershed managers need reliable tools to identify and remediate road segments with greater sediment delivery potential within a watershed, and to prioritize these segments for remediation. Tools are needed both to identify site-level risks, and watershed-scale hazards. Site-level tools are designed to assess erosion risk of a particular site, whereas watershed-scale tools are designed to stratify road segments into categories of relative sediment contribution risk. Site-level tools include the BC Forest and Range Water Quality Effectiveness Evaluation Protocol (FREP-WQEE) (Carson et al., 2018), the Universal Soil Loss Equation and derivatives (USLE, RUSLE, RUSLE2) (Dissmeyer & Foster, 1980; Renard et

al., 1991), the Washington Road Surface Erosion Model (WARSEM) (Dubé et al., 2004), and site-level inventory functions for the Geomorphic Road Analysis and Inventory Program (GRAIP) (Black et al., 2012). Not all these tools have the same functionality: the USLE does not have factors accounting for traffic or road maintenance, and FREP-WQEE and GRAIP do not account for climatic variability. What these tools have in common is that they use empirical estimates of erosion potential derived from repeated observation of eroding sites (e.g. FREP-WQEE, GRAIP, WARSEM, USLE/RUSLE/RUSLE2). Estimation of connectivity may be verified based on the characteristics of the plume runout area (Black et al., 2012) or contributing area of the road segment (Carson et al., 2018). A weakness of existing tools is that most at present do not accurately account for hydrology either in the contributing area of the road or in downslope receiving areas (Skaugset et al., 2011). A better understanding of actual road surface hydrological performance can result in model improvements (Surfleet et al., 2011).

There have been several attempts to create scaled-up versions of tools designed for site-level analysis. The process-based Watershed Erosion Prediction Program (WEPP) (Nearing et al., 1989) has interfaces that apply its algorithms to estimate road erosion in larger road networks (Elliot et al., 1999), and GRAIP also has a scaled-up version of its database intended to roughly estimate erosion and sediment delivery at the watershed scale from mappable site variables (Nelson et al., 2019). Although techniques of estimating sediment generation and delivery from roads are available, studies of road sediment impact to date have found that road density better predicts overall instream condition (Al-Chokhachy et al., 2016; Cederholm et al., 1980; Scrimgeour et al., 2008). Failures to do so may be related both to weaknesses in the current models, and the way impacts are measured in the stream.

An alternative way to assess watershed impact is to consider connectivity and road segment hydrology first, and then provide relative estimates of road erosion pressure. This approach follows the findings of several studies wherein the majority of road-related sediment is contributed at a relatively limited number of locations (Benda et al., 2019; Skaugset et al., 2011; Takken et al., 2008; Thompson et al., 2009). Benda et al. (2019) found that many of these key drainage segments were in locations where the road ran parallel and close to a stream, and where roads approached streams at crossings. Additional drains in these locations had the effect of reducing delivery of sediment-laden water from road surfaces. These findings indicate that hydrological triage of road segments can provide both the best assessment of likely instream impact, and the best likelihood of properly

targeting limited road maintenance funds. Hydrological models can be supported by high resolution LiDAR surfaces, attributed road network maps, and basic geology and soils map data.

1.4 Fate of sediment in streams

Impacts on the stream environment will vary depending on the geomorphic environment of the stream, its size, and its overall ability to transport differently-sized materials. Small, first-order streams may store gravel-sized road sediment for years to decades only flushing it during large rain events (Bilby et al., 1989), whereas steeper systems calibrated to transport gravel may quickly move it to a more sensitive plane bed or pool-riffle system where it may accumulate (Montgomery & MacDonald, 2002). Montgomery and Macdonald (2002) identified pool-riffle stream systems as being particularly sensitive to disturbance among a division of seven major stream types. These streams are particularly sensitive to inputs of sand-sized material, resulting in changes in gravel composition, and infill of pools. The alternating morphology of side channel bars, riffles, and pools in pool-riffle regimes also creates a heterogeneous flow environment with net water flow into the bed in pool tails and side channel bars, and flow upwelling in riffles (Tonina & Buffington, 2007, 2009). This may result in fine suspended sediment being trapped in gravel interstices in downwelling zones (Rehg et al., 2005). In areas with abundant fine sediment, such as the Alberta foothills, crucial spawning and rearing habitat is likely to be in upwelling zones of gravel-bedded pool-riffle streams.

1.5 Road impacts in Alberta watersheds

Roads in east slopes Rocky Mountain and foothills watersheds are known to impact aquatic habitat (Howard, 2018; Maitland et al., 2016; Scrimgeour et al., 2008; Spillios, 1999). Areas with high road density and industrial disturbance are tied to habitat degradation and population decline of salmonid fish species (Scrimgeour et al., 2008). Road crossings are identified as a particular concern due to their contribution to habitat fragmentation (Maitland et al., 2016), and sediment delivery (Spillios, 1999; Maitland et al., 2016). Culverted crossings may also create micro-habitats, resulting in distinct fish communities upstream and downstream of crossings (Maitland et al., 2016).

Relatively little work has been done to determine erosion susceptibility on roads and vehicle trails in Alberta watersheds. A study of erosion from off-highway vehicle (OHV) trails conducted in a front-range mountain watershed with shale and siltstone bedrock in southern Alberta found that traffic was a strong predictor of erosion rate in natural rainfall plot experiments (Howard, 2018). Subsequent sprinkling experiments found that plot outflow quantity (m^3) and peak intensity (m^3/s)

were greater in high traffic sites than low-traffic sites, indicating that OHV traffic may increase erosion by reducing overall infiltration capacity of trail segments (Howard, 2018). Traffic effects on infiltration capacity are documented for skidding trails in the west-central Alberta foothills (Startsev & McNabb, 2000) with up to six-fold decreases in infiltration capacity following trail use. The findings of the above study also include overall low infiltration rates for forest soils in the region. LiDAR-derived surface roughness has been examined as a possible tool in predicting road surface sediment production and stream connectivity (Huayta Hernani, 2019). Several studies to date on agricultural land suggest that the majority of runoff and sediment production in Alberta may occur during spring snowmelt season (Chanasyk & Woytowich, 1987; Van Vliet & Hall, 1991).

1.6 Unsealed resource roads in the Simonette watershed

The Simonette watershed is approximately 5400 km² in area and is located in central-western Alberta at the transition between the boreal mixedwood and foothills ecoregions (Figure 1-7, upper left). The watershed contains approximately 3010 km of unpaved road. Resource roads in the watershed comprise a network of narrow, low-speed, temporary access roads for forestry, longer-term low-speed oil and gas well-pad access roads, and wide, high-speed trunk roads with overlapping usage agreements between forestry and oil and gas users. Traffic on these roads may include logging equipment, oil and gas rigs, oilfield service vehicles, and numerous crew transport pickup trucks. The northern watershed comprises low-lying mostly flat Cretaceous to Paleogene sandstone, siltstone, and shale bedrock from the Wapiti Formation draped with relatively thick flat-lying Pleistocene glaciolacustrine and stagnant ice deposits (Figure 1-7, upper right & lower left). Higher elevation parts of the watershed are incised into flat-lying Paleogene-aged Paskapoo sandstone and shale covered with a veneer of Cordilleran-origin stony glacial till (Fenton et al., 2013; Prior et al., 2013). Foothills in the Simonette and other watersheds in West-central Alberta are not folded soft Cretaceous bedrock as they are in the south but are instead high-elevation uplands dissected by millions of years of fluvial erosion.

The combination of large roads with high traffic and silty glacial soils means that roads in the west-central Alberta foothills may be a problematic sediment source for aquatic communities. Ongoing declines in Bull Trout and Arctic Grayling are associated with industrial development (including road use and construction) in the west-central Alberta foothills, including the Simonette watershed (Cahill, 2015; Rodtka et al., 2009; Scrimgeour et al., 2008). The climate in west-central Alberta may also influence erosion susceptibility of roads. Precipitation in the Simonette varies

between about 500-700 mm per year, with a pronounced peak during the summer (Figure 1-7, lower right; Figure 1-8). High rates of spring runoff on top of weak, saturated, partially-frozen soil are responsible for significant amounts of erosion in the Prairies (Chanasyk & Woytowich, 1987; McConkey et al., 1997; Van Vliet & Hall, 1991), a relation which is likely to also hold in higher-relief foothills watersheds in west-central Alberta. Resource roads in most parts of Alberta also have a prolonged period of saturation and subgrade weakness following snowmelt when the road is vulnerable to deformation from vehicle traffic. Deformation can lead to the formation of wheel ruts which, if not graded out, can enhance erosion during the subsequent season. Overall, northern foothills environments like the Simonette pose challenges due to their large management areas, overlapping land uses, high traffic rates, and erodible, deformable soils.

1.7 Research contribution and study area

While some work has been done in Southern and Central Alberta looking at road erosion and connectivity (Howard, 2018; Huayta Hernani, 2019), no work has been done in the foothills and boreal ecoregions of west-central Alberta (see Figures 1-1 and 1-6). This region is distinct from the southern Rockies as it is dominated by finer-grained glacial materials, more gently sloping topography, and deeper drainage. To my knowledge only two studies explicitly link estimates of road sediment production with indicators of instream condition, and both of these were only able to link road density (or a similar metric) with degradation of instream conditions, rather than known point-source contributions (Al-Chokhachy et al., 2016; Cederholm et al., 1980).

Sediment pollution from roads is a problem that involves (1) estimating relative or absolute erosion rates, (2) estimating connectivity to streams, and (3) determining how and if road sediment creates a measurable impact in the stream environment, and hence a risk to aquatic life. The thesis is structured in such a way that it addresses each of these problems individually in three distinct chapters (Ch 2,3 &4), and then discusses the result of the work and corresponding management implications in the final chapter.

Chapter 2: Hydrological controls and thresholds for road erosion in the Simonette watershed, west-central Alberta

Chapter 2 is a study of hydrological and qualitative factors in erosion risk in the Simonette watershed. Detailed data is collected on the hydrological response of individual road segments to rain events, and the study is stratified by surficial geology and traffic as I hypothesized that these mappable variables would have a significant impact on road erosion response to rain

events. I also examine hydrological thresholds of enhanced erosion risk from ditch gullyng in the Simonette.

Chapter 3: Road area as a driver of sediment plume size for unsealed roads in west-central Alberta

Chapter 3 examines drivers of sediment plume geometry in the Simonette watershed. I hypothesized that the geometry of sediment plumes represents the hydrological area required to absorb flows from road surfaces – the larger the flow, the larger the plume. The effect of other factors such as presence of obstructions, slope, aspect, and concavity or convexity of the plume runout area on plume geometry were also considered. The primary focus on hydrological or geometric relationships for this study is justified as such a finding would justify the use of readily available hydrological modelling software in modelling road segment connectivity.

Chapter 4: Impacts of road sediment from road-stream crossings on stream gravel matrix in foothills watersheds, Simonette watershed, west-central Alberta

Chapter 4 tests several road impact assessment metrics against standard measures of instream sediment pressure such as pool width and depth, surface grain counts, and subsurface fines intrusion. A key question of the study is if road density is a good indicator of instream condition, or whether some other variable would be a better indicator. It is hypothesized that the effects of disturbance at the reach scale will be dependent on the type of reach receiving the sediment load, and the caliber of sediment received. Fine sediment from the road environment is likely to intrude in zones where water inflows into the bed. The results of the study indicate that the amount of fines in the streambed gravel matrix is likely related to upstream siltation pressure from roads, and that this forcing is related to road crossings and not road density.

Chapter 5: Lessons of scale and scope: how studies in the Simonette watershed can inform challenges ahead in resource management

This chapter provides an overview of the results of the research and its application to future watershed management challenges in Alberta and elsewhere. A main contribution of the research was an increased understanding of local road segment hydrology necessary to triage and assess erosion risks in large, sparsely-managed watersheds. The particular concern of scale in watershed management in the Alberta foothills was also addressed, and therefore the need

to create tools that are appropriately scoped to deal with large-scale watershed management issues which may be better-managed in smaller, more intensively-used watersheds.

1.8 References

- Al-Chokhachy, R., Black, T. A., Thomas, C., Luce, C. H., Rieman, B., Cissel, R., et al. (2016). Linkages between unpaved forest roads and streambed sediment: why context matters in directing road restoration. *Restoration Ecology*, 24(5), 589–598.
<https://doi.org/10.1111/rec.12365>
- Alberta Municipal Affairs & Morrison Hershfeld Ltd. (2008). *Guidelines on Valuation of Tangible Assets for PSAB 3150*. Edmonton. Retrieved from
http://www.municipalaffairs.gov.ab.ca/documents/ms/AIV_TCA_manual_on_guidelines_on_valuations.pdf
- Alberta Transportation. (2019). *Unit Price Averages Reports*.
- Benda, L. E., James, C., Miller, D. J., & Andras, K. (2019). Road Erosion and Delivery Index (READI): A Model for Evaluating Unpaved Road Erosion and Stream Sediment Delivery. *Journal of the American Water Resources Association*, 55(2), 459–484.
<https://doi.org/10.1111/1752-1688.12729>
- Bilby, R. E. (1985). Contributions of road surface sediment to a western Washington stream. *Forest Science*, 31(4), 827–838.
- Bilby, R. E., Sullivan, K., & Duncan, S. H. (1989). The generation and fate of road-surface sediment in forested watersheds in southwestern Washington. *Forest Science*, 35(2), 453–468.
- Black, T. A., Cissel, R. M., & Luce, C. H. (2012). *The Geomorphic Road Analysis and Inventory Package (GRAIP) Volume I: Data Collection Method* (General Technical Report No. RMRS-GTR-280WWW). Rocky Mountain Research Station General Technical Report. Fort Collins, CO. <https://doi.org/10.2737/RMRS-GTR-280>
- Brake, D., Molnau, M., & King, J. G. (1997). *Sediment transport distances and culvert spacings on logging roads within the Oregon coast mountain range. 1997 Annual International Meeting, ASAE*. Minneapolis, MN.
- Brown, K. R., Aust, W. M., & McGuire, K. J. (2013). Sediment delivery from bare and graveled forest road stream crossing approaches in the Virginia Piedmont. *Forest Ecology and Management*, 310, 836–846. <https://doi.org/10.1016/j.foreco.2013.09.031>
- Burroughs, E. R., & King, J. G. (1989). *Reduction of Soil Erosion on Forest Roads*. Ogden, UT.

- Cahill, C. L. (2015). *Status of the Arctic Grayling (Thymallus arcticus) in Alberta: Update 2015*. Alberta Wildlife Status Report No. 57. Edmonton, Alberta. Retrieved from <https://open.alberta.ca/publications/9781460134528>
- Carson, B., Maloney, D., Chatwin, S., Carver, M., & Beaudry, P. G. (2018). *Protocol for Evaluating the Potential Impact of Forestry and Range Use on Water Quality (Water Quality Effectiveness Evaluation)*. Forest and Range Evaluations Program. Victoria, BC. Retrieved from https://www.for.gov.bc.ca/hfp/frep/site_files/Indicators/Indicators-WaterQuality-Protocol-2009.pdf
- Cederholm, C. J., Reid, L. M., & Salo, E. O. (1980). Cumulative effects of logging road sediment on salmonid populations in the Clearwater River, Jefferson County, Washington. In *Salmon-Spawning Gravel: A Renewable Resource in the Pacific Northwest?* (pp. 1-35). Seattle, WA. Retrieved from <https://www.fs.fed.us/psw/publications/reid/Cederholm.pdf>
- Chanasyk, D. S., & Woytowich, C. P. (1987). *A Study of Water Erosion in the Peace Region*. Edmonton, Alberta.
- Chapman, D. W. (1988). Critical review of variables used to define effects of fines in redds of large salmonids. *Transactions of the American Fisheries Society*, 117(1), 1-21. [https://doi.org/10.1577/1548-8659\(1988\)117<0001](https://doi.org/10.1577/1548-8659(1988)117<0001)
- Coe, D. B. R. (2006). *Sediment Production and Delivery From Forest Roads in the Sierra Nevada, California*. Colorado State University.
- Costello, A. B. (2006). *Status of the Westslope Cutthroat Trout (Oncorhynchus clarkii lewisii) in Alberta* (Alberta Wildlife Status Report No. 61). Retrieved from <https://open.alberta.ca/publications/0778518694>
- Croke, J. C., Mockler, S. P., Fogarty, P., & Takken, I. (2005). Sediment concentration changes in runoff pathways from a forest road network and the resultant spatial pattern of catchment connectivity. *Geomorphology*, 68(3-4), 257-268. <https://doi.org/10.1016/j.geomorph.2004.11.020>
- Croke, J. C., Mockler, S. P., Hairsine, P. B., & Fogarty, P. (2006). Relative contributions of runoff and sediment sources within a road prism and implications for total sediment delivery. *Earth Surface Processes and Landforms*, 31(4), 457-468. <https://doi.org/10.1002/esp.1279>

- Dinno, A. (2017). dunn.test. Retrieved from <https://cran.r-project.org/package=dunn.test>
- Dissmeyer, G. E., & Foster, G. R. (1980). *A Guide For Predicting Sheet and Rill Erosion on Forest Land* (Technical Reports No. SA-TP II). Atlanta, GA.
- Dubé, K., Megahan, W. F., & McCalmon, M. (2004). Washington Road Surface Erosion Model (WARSEM) Manual. State of Washington Department of Natural Resources. Retrieved from http://file.dnr.wa.gov/publications/fp_data_warsem_manual.pdf
- Elliot, W. J. (2013). Erosion processes and prediction with WEPP technology in forests in the Northwestern U.S. *Transactions of the ASABE*, 56(2), 563–579.
- Elliot, W. J., Hall, D. E., & Scheele, D. L. (1999). FS-WEPP: Forest Service Interfaces for the Water Erosion Prediction Project Computer Model. Moscow, ID: USDA Forest Service, Rocky Mountain Research Station. Retrieved from <https://forest.moscowfs.wsu.edu/fswpp/>
- Fenton, M. M., Waters, E. J., Pawley, S. M., Atkinson, N., Utting, D. J., & McKay, K. (2013). Surficial Geology of Alberta. *Alberta Geological Survey Map 601*.
- Hairsine, P. B., Croke, J. C., Mathews, H., Fogarty, P., & Mockler, S. P. (2002). Modelling plumes of overland flow from logging tracks. *Hydrological Processes*, 16(12), 2311–2327.
<https://doi.org/10.1002/hyp.1002>
- Hoover, M. D. (1952). Water and Timber Management. *Journal of Soil and Water Conservation*, (April 1952), 75–78.
- Howard, M. J. (2018). *Erosion and Erodibility from Off-Highway Vehicle Trails in Alberta's Southern Rocky Mountains*. University of Alberta.
<https://doi.org/https://doi.org/10.7939/R3SX64R9F>
- Huayta Hernani, L. F. (2019). *Application of LiDAR DEM Metrics to Estimate Road-stream Sediment Connectivity in Alberta Eastslopes Salmonid Habitats*. University of Alberta.
<https://doi.org/https://doi.org/10.7939/r3-lxrm-wj37>
- Ketcheson, G. L., & Megahan, W. F. (1996). *Sediment Production and Downslope Sediment Transport from Forest Roads in Granitic Watersheds* (Research Paper No. INT-RP-486). Ogden, UT.
- Kidd, W.J., Megahan, W.F. (1972). Effects of logging and logging roads on erosion and sediment deposition from steep terrain. *Journal of Forestry*, March 1972, 136-141

- Lieberman, J. A., & Hoover, M. D. (1948). The Effect of Uncontrolled Logging on Stream Turbidity. *Water and Sewage Works*, (July 1948).
- Lisle, T. E., & Hilton, S. (1992). The Volume of Fine Sediment in Pools: an Index of Sediment Supply in Gravel-Bed Streams. *JAWRA Journal of the American Water Resources Association*, 28(2), 371–383. <https://doi.org/10.1111/j.1752-1688.1992.tb04003.x>
- Luce, C. H., & Black, T. A. (1999). Sediment production from forest roads in western Oregon. *Water Resources Research*, 35(8), 2561–2570. <https://doi.org/10.1029/1999WR900135>
- Luce, C. H., & Black, T. A. (2001a). Effects of traffic and ditch maintenance on forest road sediment production. In *Proceedings of the Seventh Federal Interagency Sedimentation Conference* (pp. 67–74). Retrieved from <http://www.treesearch.fs.fed.us/pubs/23963>
- Maitland, B. M., Poesch, M., Anderson, A. E., & Pandit, S. N. (2016). Industrial road crossings drive changes in community structure and instream habitat for freshwater fishes in the boreal forest. *Freshwater Biology*, 61(1), 1–18. <https://doi.org/10.1111/fwb.12671>
- McConkey, B. G., Nicholaichuk, W., Steppuhn, H., & Reimer, C. D. (1997). Sediment yield and seasonal soil erodibility for semiarid cropland in western Canada. *Canadian Journal of Soil Science*, 77(1), 33–40. <https://doi.org/10.4141/S95-060>
- van Meerveld, H. J., Baird, E. J., & Floyd, W. C. (2014). Controls on sediment production from an unpaved resource road in a Pacific maritime watershed. *Water Resources Research*, 50(6), 4803–4820. <https://doi.org/10.1002/2013WR014605>
- Megahan, W. F., & Ketcheson, G. L. (1996). Predicting downslope travel of granitic sediments from forest roads in Idaho. *Water Resources Bulletin*, 32(2), 371–382. Retrieved from files
- Megahan, W. F., & Kidd, W. J. (1972). Effects of logging and logging roads on erosion and sediment deposition from steep terrain. *Journal of Forestry*, (March), 136–141.
- Megahan, W. F., Seyedbagheri, K. A., & Dodson, P. C. (1983). Long-term erosion on granitic roadcuts based on exposed tree roots. *Earth Surface Processes and Landforms*, 8(1), 19–28. <https://doi.org/10.1002/esp.3290080103>
- Montgomery, D. R. (1994). Road surface drainage, channel initiation, and slope instability. *Water Resources Research*, 30(6), 1925–1932. <https://doi.org/10.1029/94WR00538>
- Montgomery, D. R., & MacDonald, L. H. (2002). Diagnostic Approach to Stream Channel

- Assessment and Monitoring. *Journal Of The American Water Resources Association*, 38(1).
- Nearing, M. A., Foster, G. R., Lane, L., & Finkner, S. (1989). A process - based soil erosion model for USDA - water erosion prediction project technology. *Transactions of the American Society of Agricultural Engineers*, 32(5), 1587–1593. <https://doi.org/10.13031/2013.31195>.
- Nelson, N. A., Luce, C. H., & Black, T. A. (2019). *GRAIP_Lite : A System for Road Impact Assessment*. Boise, ID.
- Packer, P. E. (1967). Criteria for Designing and Locating Logging Roads to Control Sediment. *Forest Science*, 13(1), 2–18. <https://doi.org/10.1093/forestscience/13.1.2>
- Phillips, R. W., Lantz, R. L., Claire, E. W., & Moring, J. R. (1975). Some Effects of Gravel Mixtures on Emergence of Coho Salmon and Steelhead Trout Fry. *Transactions of the American Fisheries Society*, 104(3), 461–466. [https://doi.org/10.1577/1548-8659\(1975\)104<461:SEOGMO>2.0.CO;2](https://doi.org/10.1577/1548-8659(1975)104<461:SEOGMO>2.0.CO;2)
- Prior, G. J., Hathway, B., Glombick, P. M., Pana, D. I., Banks, C. J., Hay, D. C., et al. (2013). *Map 600 Bedrock Geology of Alberta* (Vol. 2479). Edmonton, Alberta.
- Rasmussen, J. B., & Taylor, E. B. (2009). *Status of the Athabasca Rainbow Trout (Oncorhynchus mykiss) in Alberta* (Alberta Wildlife Status Report No. 66). *Alberta Wildlife Status Report*. Edmonton, Alberta. <https://doi.org/10.5962/bhl.title.114290>
- Rehg, K. J., Packman, A. I., & Ren, J. (2005). Effects of suspended sediment characteristics and bed sediment transport on streambed clogging. *Hydrological Processes*, 19(2), 413–427. <https://doi.org/10.1002/hyp.5540>
- Reid, D. A., Hassan, M. A., & Floyd, W. C. (2016). Reach-scale contributions of road-surface sediment to the Honna River, Haida Gwaii, BC. *Hydrological Processes*, 30(19), 3450–3465. <https://doi.org/10.1002/hyp.10874>
- Reid, L. M., & Dunne, T. (1984). Sediment Production from Forest Road Surfaces. *Water Resources Research*, 20(11), 1753–1761.
- Renard, K. G., Foster, G. R., Weesies, G. A., & Porter, J. P. (1991). RUSLE: Revised Universal Soil Loss Equation. *J. Soil Water Conserv*, 46, 30–33. Retrieved from www.swcs.org
- Renard, K. G., Foster, G. R., Weesies, G. A., McCool, D. K., & Yoder, D. C. (1997). *Predicting Soil Erosion by Water: A guide to conservation planning with the Revised Universal Soil Loss*

- Equation (RUSLE)* (Agriculture Handbook No. 703). Washington, D.C.
- Reynolds, J. B., Simmons, R. C., & Burkholder, A. R. (1990). Effects of Placer Mining Discharge on Health and Food of Arctic Grayling. *Water Resources Bulletin*, 25(3), 625–635.
- Rodtka, M., Johnston, F. D., & Post, J. R. (2009). *Status of the Bull Trout (Salvelinus confluentus) in Alberta: Update 2009. Wildlife Status Report No. 39*. Edmonton. Retrieved from <https://open.alberta.ca/publications/9780778591788>
- Scrimgeour, G. J., Hvenegaard, P. J., & Tchir, J. (2008). Cumulative industrial activity alters lotic fish assemblages in two boreal forest watersheds of Alberta, Canada. *Environmental Management*, 42(6), 957–970. <https://doi.org/10.1007/s00267-008-9207-2>
- Skaugset, A. E., Surfleet, C. G., Meadows, M. W., & Amann, J. (2011). Evaluation of Erosion Prediction Models for Forest Roads. *Transportation Research Record: Journal of the Transportation Research Board*, 2203, 3–12. <https://doi.org/10.3141/2203-01>
- Spillios, L. C. (1999). *Sediment intrusion and deposition near road crossings in small foothill streams in West Central Alberta*. University of Alberta.
- Startsev, A. D., & McNabb, D. H. (2000). Effects of skidding on forest soil infiltration in west-central Alberta. *Canadian Journal of Soil Science*, 80(4), 617–624. <https://doi.org/10.4141/s99-092>
- Sugden, B. D., & Woods, S. W. (2007). Sediment Production From Forest Roads in Western Montana. *JAWRA Journal of the American Water Resources Association*, 43(1), 193–206. <https://doi.org/10.1111/j.1752-1688.2007.00016.x>
- Surfleet, C. G., Skaugset, A. E., & Meadows, M. W. (2011). Road runoff and sediment sampling for determining road sediment yield at the watershed scale. *Canadian Journal of Forest Research*, 41(10), 1970–1980. <https://doi.org/10.1139/x11-104>
- Takken, I., Croke, J. C., & Lane, P. N. J. (2008). A methodology to assess the delivery of road runoff in forestry environments. *Hydrological Processes*, 22(November 2008), 254–264. <https://doi.org/10.1002/hyp.6581>
- Thompson, C. J., Takken, I., & Croke, J. C. (2008). Hydrological and sedimentological connectivity of unsealed roads. In J. Schmidt, T. Cochrane, C. Phillips, S. Elliott, T. Davies, & L. Basher (Eds.), *Sediment Dynamics in Changing Environments* (pp. 524–531). Christchurch,

NZ: IAHS Press.

- Thompson, C. J., Barry, S., & Takken, I. (2009). A model for optimizing forest road drain spacing. In R. S. Anderssen, R. D. Braddock, & L. T. H. Newham (Eds.), *18th World IMACS Conference and MODSIM09 International Congress on Modelling and Simulation* (pp. 4093–4099). Cairns, Australia: Modelling and Simulation Society of Australia and New Zealand and International Association for Mathematics and Computers in Simulation. Retrieved from <http://www.mssanz.org.au/modsim09/I15/thompson.pdf>
- Tonina, D., & Buffington, J. M. (2007). Hyporheic exchange in gravel bed rivers with pool-riffle morphology: Laboratory experiments and three-dimensional modeling. *Water Resources Research*, 43(1), 1–16. <https://doi.org/10.1029/2005WR004328>
- Tonina, D., & Buffington, J. M. (2009). Hyporheic exchange in mountain rivers I: Mechanics and environmental effects. *Geography Compass*, 3(3), 1063–1086. <https://doi.org/10.1111/j.1749-8198.2009.00226.x>
- Transport Canada. (2017). Transport in Canada: 2017: Statistical Addendum. <https://www.tc.gc.ca/eng/policy/transportation-canada-2017.html#annexb>
- Van Vliet, L. J. P., & Hall, J. W. (1991). Effects of two crop rotations on seasonal runoff and soil loss in the Peace River region. *Canadian Journal of Soil Science*, 71, 533–543. <https://doi.org/10.4141/cjss91-051>
- Wall, G. J., Coote, D. R., Pringle, E. A., & Shelton, I. J. (2002). *RUSLEFAC - Revised Universal Soil Loss Equation for Application in Canada: A Handbook for Estimating Soil Loss from Water Erosion in Canada*. Ottawa, Canada.
- Woods, S. W., Sugden, B. D., & Parker, B. (2006). Sediment Travel Distances below Drivable Drain Dips in Western Montana. In W. Chung & H. S. Han (Eds.), *29th Council on Forest Engineering Conference* (pp. 251–263). Coeur d'Alene, Idaho: Council on Forest Engineering.

1.9 Tables

Table 1-1. Estimates of road-based sedimentation compared to other sources of sediment in forested watersheds (from Elliot, 2013)

Source	Sediment Delivery Rate (t/km² yr)
Undisturbed forest	0 – 8
Low traffic roads	0.5 – 7
High traffic roads	1.8 – 100
Timber harvest	0 – 13
Prescribed fire	0 – 110
Wildfire	0 – 2450

Table 1-2. Relative magnitude of road erosion in selected studies

Study	Metric	Magnitude
Kidd and Megahan, 1972	Logging sedimentation	0.6 x background
	Jammer roads	750 x background
Cederholm et al, 1980	Total road erosion	2.6 – 4.4 x background
	Road surface erosion	0.47 – 1.12 x background
Bilby, 1985	% Reach sediment	21
Reid et al. 2016	% Reach sediment	18 ± 6

1.10 Figures

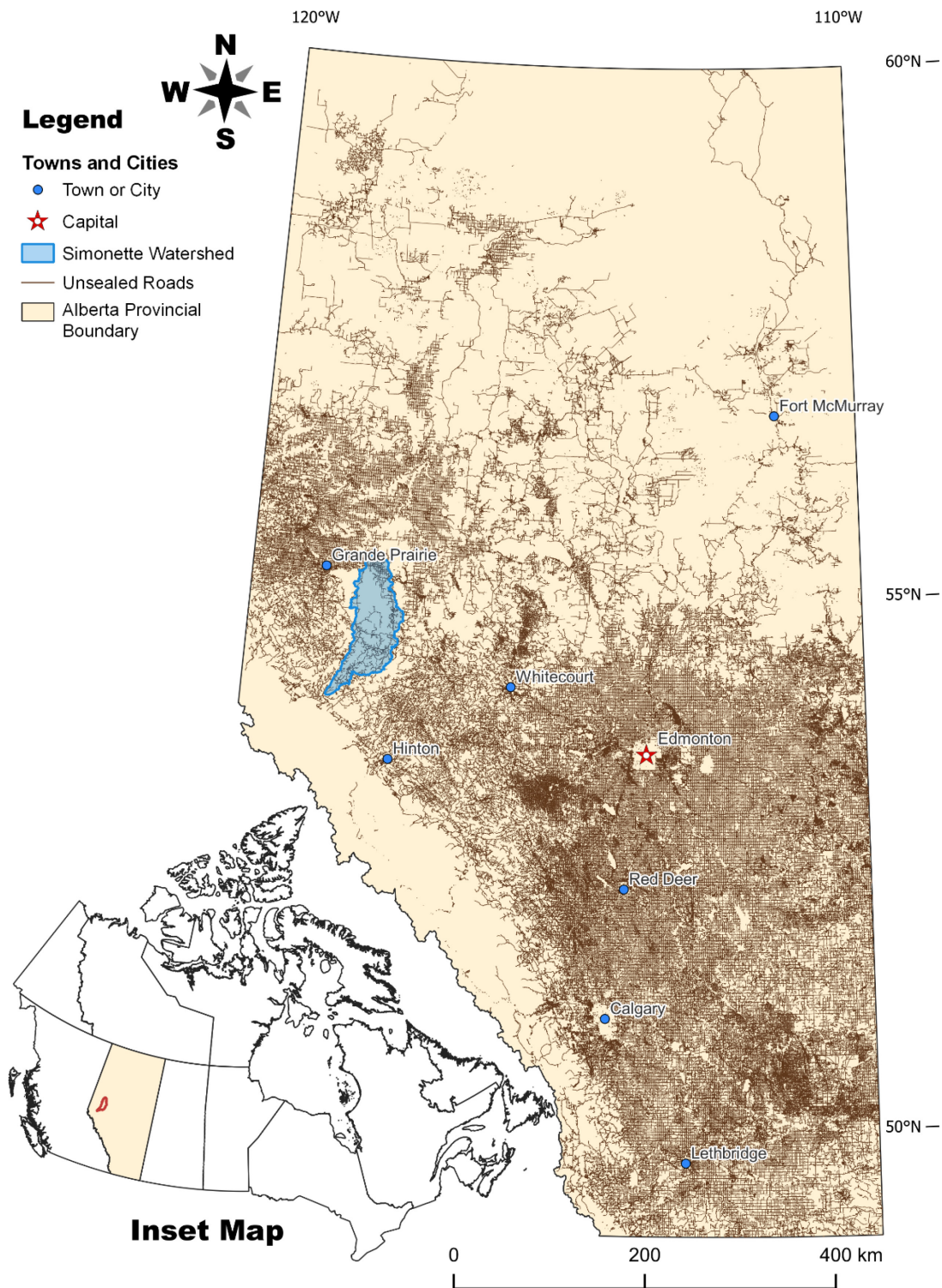


Figure I-1. Location of study site in Alberta.

Unsealed road network shown as thin brown lines. Location of Alberta in Canada is shown in inset map.

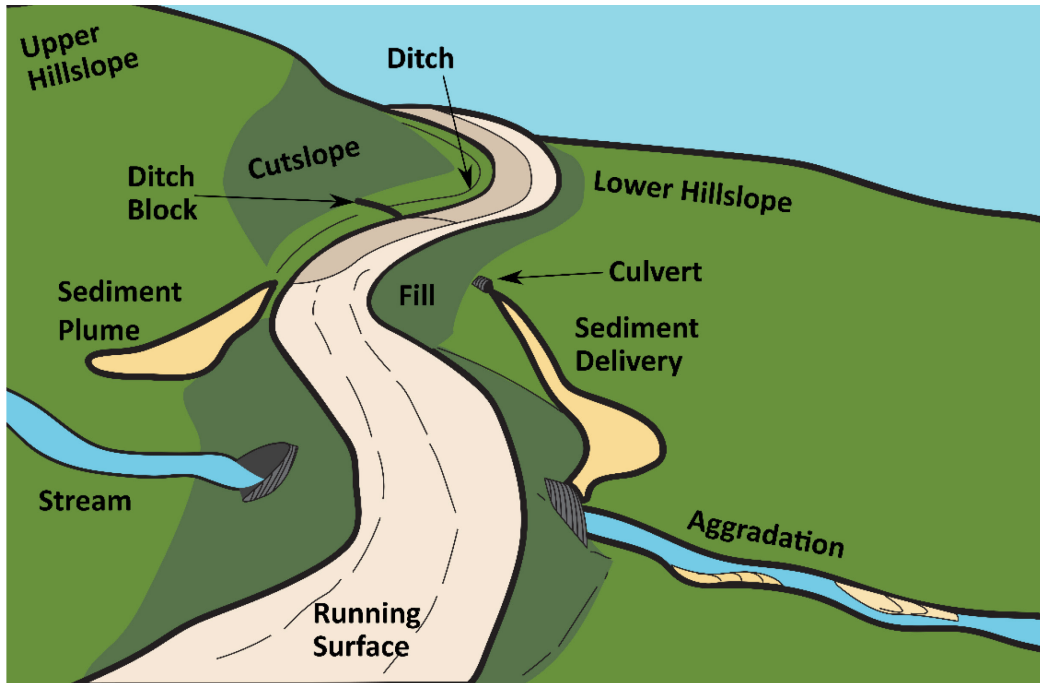


Figure I-2. Theoretical road prism showing features of the road environment, connectivity pathways, and consequences for road erosion

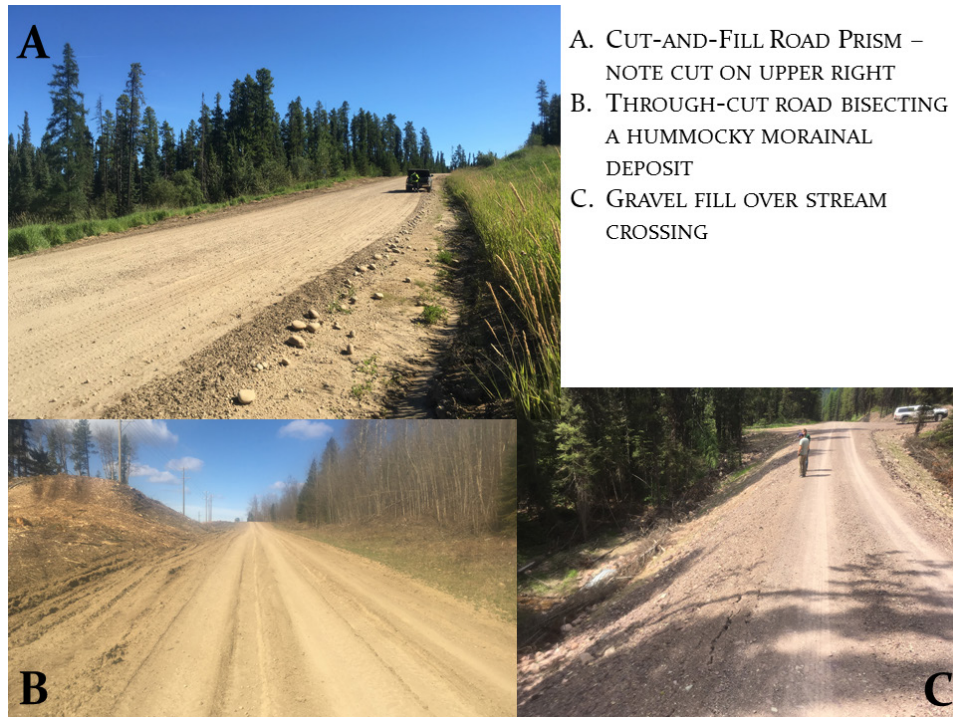


Figure I-3. Examples of different types of road cut and fill.



Figure 1-4. Examples of road sediment plumes: a sediment plume filling a roadside turnout (left), and a large road sediment plume connected to a stream channel (right).



Figure 1-5. Severe gully erosion in ditches, Simonette watershed, Alberta.

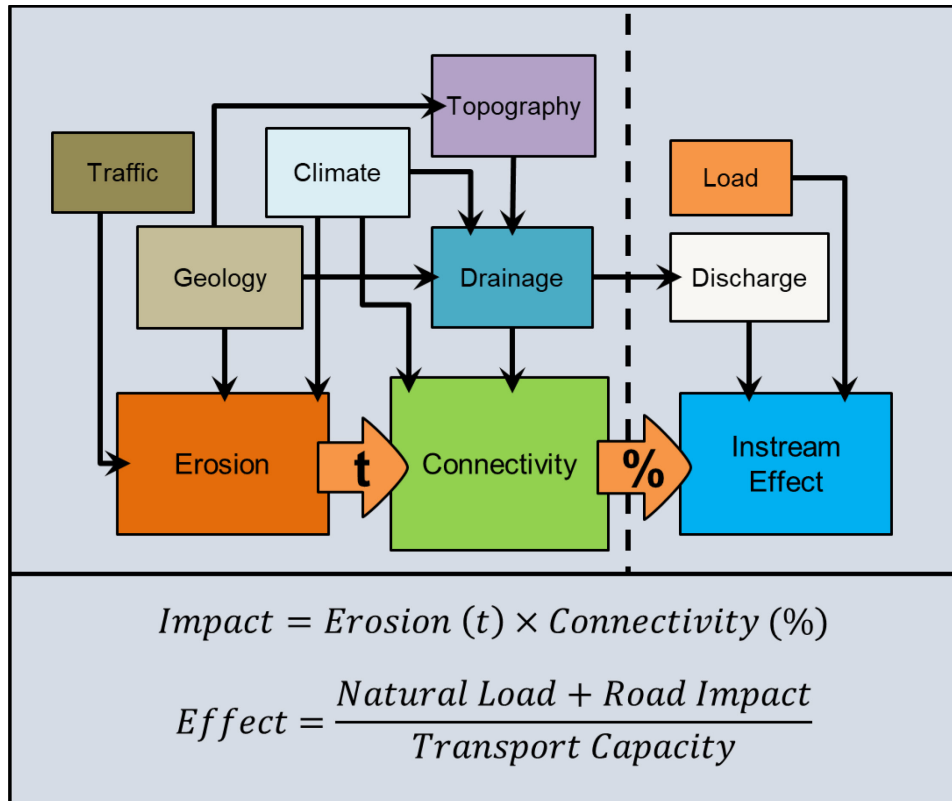


Figure I-6. Conceptual model of point source impact to the stream environment.

Equations below are not necessarily literal but are conceptual in nature. Impact effects could be measured in tons or in an appropriate index variable.

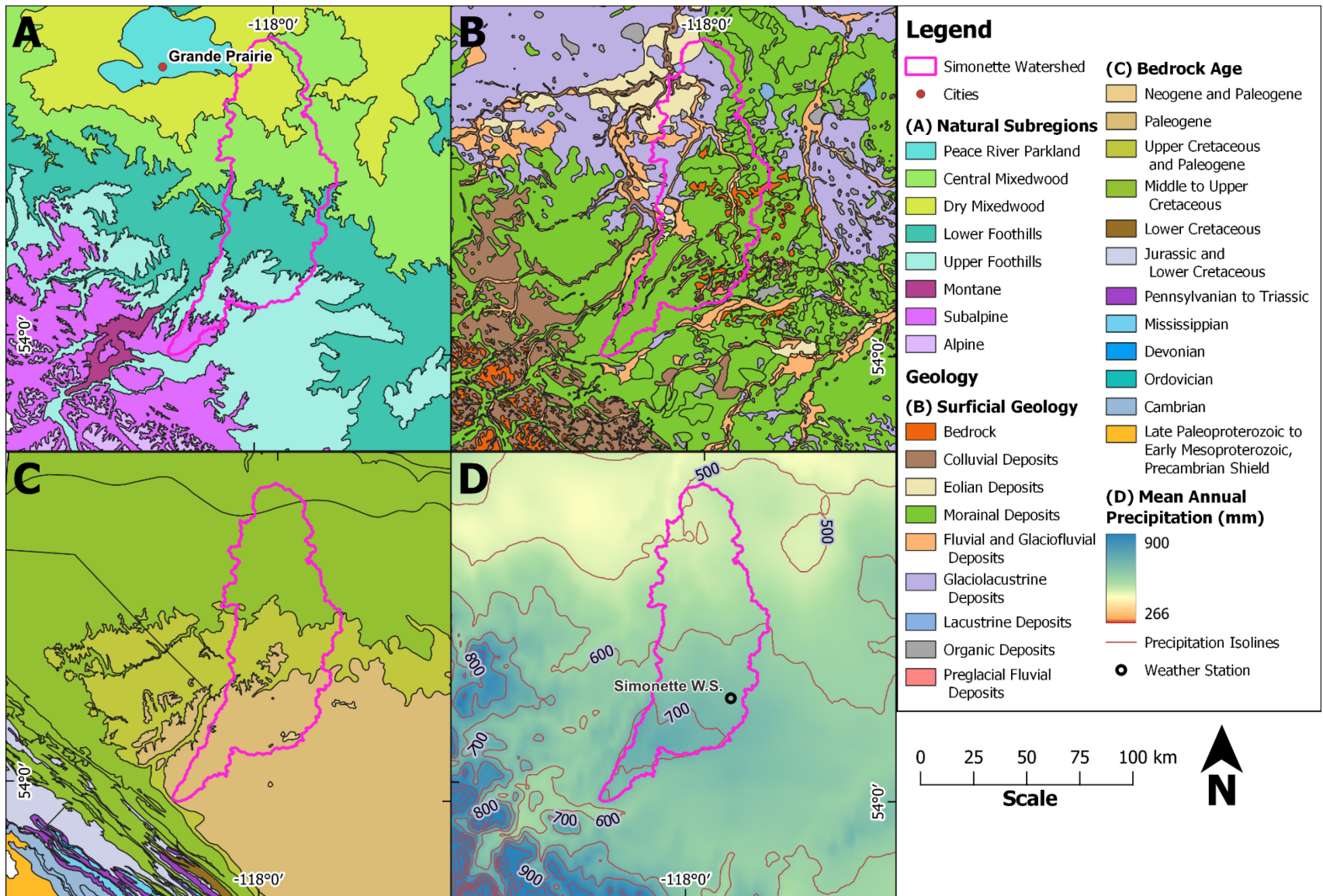
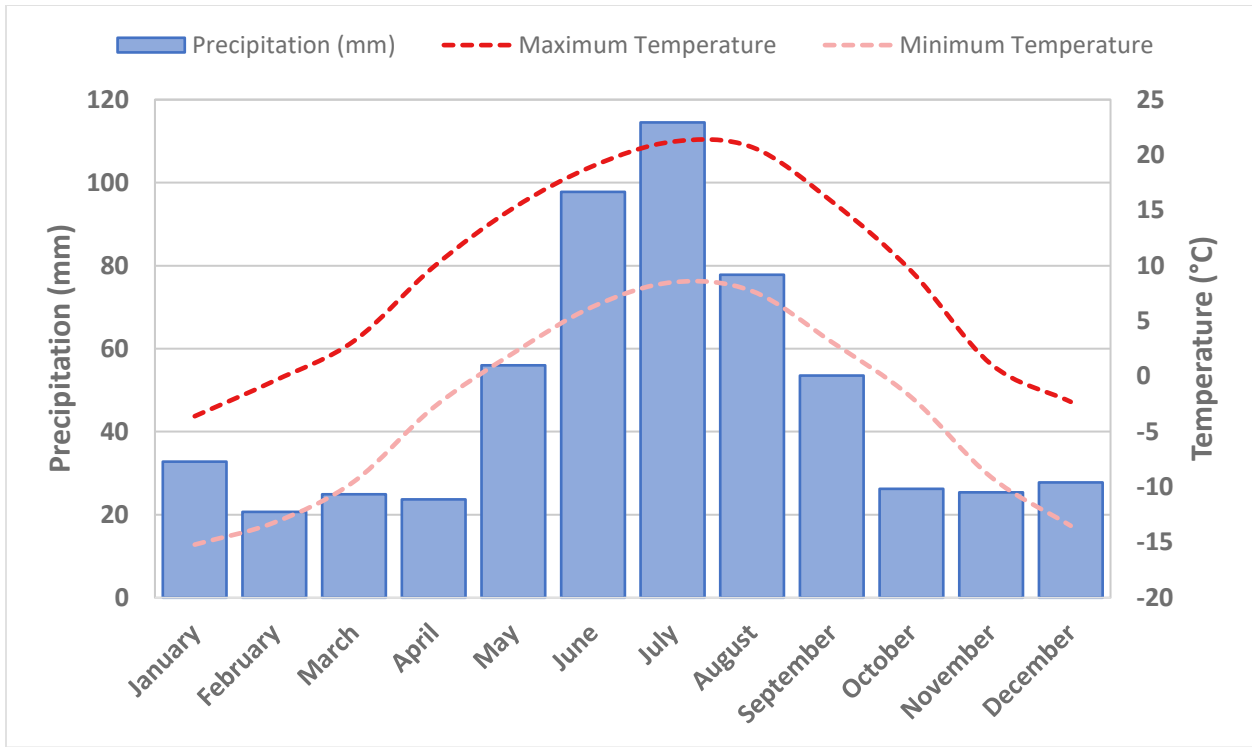


Figure I-7. Environmental gradients in the Simonette watershed.

(A) Natural Subregion, (B) Surficial Geology, (C) Bedrock Age, and (D) Precipitation



9

Figure 1-8. Climate normals (1981-2010), Simonette weather station.

Location: 54°25' N, 117°44' W, 883.9 m asl (shown on Figure 1-7)

2 Hydrological Controls and Thresholds for Road Erosion in a Foothills Watershed, West-Central Alberta

2.1 Introduction

Resource access roads are one of the largest anthropogenic contributors to stream sediment budgets in forested watersheds: only human-caused wildfires are estimated to contribute more sediment (Elliot, 2013). Road surface erosion has been found to increase sediment loading in affected streams by approximately two to ten times the background rate (Elliot et al., 2013). Dense and poorly planned road networks in erodible terrain can cause erosion up to 750 times background rates (Megahan & Kidd, 1972). Streams on the west coast of North America may have between 18-21% of the total sediment sourced from road erosion (Bilby, 1985; Bilby et al., 1989; Reid et al., 2016; Reid et al., 1981). Sediment contribution from road surface erosion is predominantly sand-sized and finer (Reid & Dunne, 1984). Much of this sediment impacts streams, lowering overall bed particle size (Al-Chokhachy et al., 2016), and reducing habitat suitability for salmonid fish (Cederholm et al., 1980; Phillips et al., 1975; Tonina & Buffington, 2009).

Several studies have found significant links between road erosion rate and rainfall amount or intensity (Coe, 2006; van Meerveld et al., 2014; Sugden & Woods, 2007; Welsh, 2008). Other researchers have shown that erosion is a factor of the depth (mm) or intensity (m^3/s) of overland flow generation from the road (Reid & Dunne, 1984; Surfleet et al., 2011). Apart from climate and hydrology, road erosion rates are controlled by the availability of fine, erodible material on the road surface (Brown et al., 2015; Coe, 2006; Luce & Black, 2001a; Packer, 1967; Reid & Dunne, 1984; Sugden & Woods, 2007; Welsh, 2008). Traffic increases sediment availability by breaking down road surfacing aggregates and by pumping fine-grained material from the road subgrade into the running surface (Bilby et al., 1989; Reid & Dunne, 1984). Road erosion responds both to the relative amount of traffic (Reid & Dunne, 1984; Sugden & Woods, 2007) and number of passes during or before a rain event (Bilby et al., 1989; van Meerveld et al., 2014). Road grading also has a significant influence on road erosion rates, in some cases playing a far larger role than other variables (Luce & Black, 2001a). Roads constructed in hard, erosion-resistant geological material usually have lower erosion rates than those constructed in areas with glacial silt or non-resistant sedimentary rock (Bilby et al., 1989; Packer, 1967; Reid & Dunne, 1984; Sugden & Woods, 2007). Roads capped with free-draining gravel or mulches also have lower erosion rates (Brown et al., 2013; Coe, 2006; Sosa-

Pérez & MacDonald, 2017). Road geometric relationships, including area, length and slope have hydrological consequences, also impacting sediment production (Coe, 2006; Luce & Black, 1999; Sugden & Woods, 2007).

In the Alberta foothills energy and forest industries have created large, multi-lane unpaved roads commonly built wider than 10 m to accommodate many heavily-loaded vehicles travelling at near-highway speeds (60-80 km/hr). Lower-use roads are usually about 5 m wide, typically graded once per year and built to service individual forestry cutblocks or well-pads. The landscape is gently sloping, with commonly thick (often 20 m or more) layers of fine-grained glacial material draped over permeable sedimentary bedrock (Atkinson & Hartman, 2017; Atkinson & Lyster, 2010; Prior et al., 2013). Rainfall is moderate (500-800 mm), but soils, particularly in more flat-lying areas, can be slow-draining (Startsev & McNabb, 2000). Soils in a Canadian climate have enhanced susceptibility to erosion during spring, when meltwater flows on weak, thawing soil (Van Vliet & Hall, 1991; Wall et al., 1988). Roads in west-central Alberta are likely to be highly susceptible to erosion because they are large, with high traffic-usage rates, and are constructed on poorly-drained silty to clayey glacial deposits or soft, shale- and siltstone-dominated bedrock. Relatively little work has been done investigating erosion potential in Alberta (Howard, 2018; Huayta Hernani, 2019), and what exists was mostly done in the southern Rocky Mountains and foothills, which have different structural, geological, and climatic characteristics than those in west-central and northern Alberta. There is therefore an incomplete understanding of erosion processes across the entire Foothills region.

In this chapter I describe hydrological and site-level factors that influence road erosion rates in the Simonette watershed in west-central Alberta. The Simonette watershed represents a large management area, so it is useful to determine whether mappable factors like surficial geology and road classification control road erosion, and hence, risk. Furthermore, I also seek to determine how the hydrological characteristics, including road hydrological response, and geometry of individual road segments control sediment production. To achieve this objective, I have used a number of investigation methods: instrumented road plots capturing sediment and water outflow, silt fences, and field measurements of road erosion and deposition features. Sites are classified by mapped geology and relative traffic level in order to facilitate discussion and interpretation of the role these factors may play controlling erosion rates in the Simonette.

2.2 Methods and materials

2.2.1 Study site

The Simonette watershed straddles the foothills and boreal plains of west-central Alberta, Canada, south of the city of Grande Prairie, and west of the towns of Valleyview and Fox Creek (Figure 2-1). The area of the watershed is about 5400 km². The watershed contains about 3010 km of active road as of 2015, of which about 2530 km is gravelled and about 480 km has a natural surface. Average road density for the watershed is about 0.67 km/km². The southern headwaters of the watershed are located 1600 m above mean sea level (amsl), whereas the mouth, at the confluence with the Smoky River, is located at about 500 m amsl. The river forms a deeply-incised valley through glacial lake sediments for about 30 km from its confluence with the Smoky River and most of the rest of the mainstem and branches flow through a kettled till plain (Andriashek, 2001; Fenton et al., 2013; Pawley & Atkinson, 2013). Glaciofluvial delta sediments form on the contact between the till plain and the glacial lake near the headwaters of the tributary Latornell River (Andriashek, 2001). The southern portion of the watershed flows through largely gravel-capped benchlands incised in horizontally-layered soft Paleogene bedrock with morainal veneers (Andriashek, 2001; Fenton et al., 2013; Prior et al., 2013). The front ranges of the Rocky Mountains are located about 20 km southwest of the headwaters of the watershed.

Average annual precipitation varies from 581 mm at the Simonette weather station in the centre of the watershed to 445 mm at the Grande Prairie Airport 110 km north-west (Environment and Climate Change Canada 2019, Table 2-1). The majority of precipitation occurs during the summer months of June, July and August, often falling in short, intense thunderstorms. Less frequent large frontal systems have been known to deliver 90-110 mm of precipitation over a period of one to several days. Significant erosion is also likely tied to snowmelt: Freeze-thaw conditions during the spring and fall months may loosen soil aggregates, and persistent soil saturation lowers effective shear resistance of soils and lowers overland flow thresholds. This period of weak soil conditions, colloquially termed “spring break-up” persists in much of Alberta from the beginning of the snowmelt season into late June or early July (Alberta Transportation, 2020). Road surfacing materials are easily worked into the fine-grained road subgrade by repeated truck passes, compromising the running surface. Traffic and grading on main roads are frequent, as the roads are used for both oil and gas and forest resource development. Topography is commonly gentle to rolling, and roads are often poorly or sparsely-drained as a result.

Land-use in the Simonette is dominated by forestry and oil and gas extraction. A small amount (370 km²) in the northeast is cleared for agricultural land and used for cattle grazing and row crop cultivation. Dominant land-use type in an area affects disturbance patterns, road densities and road types. Permanent main haul roads are usually about 10-12 m wide, and heavily-used. The Canfor Main haul road which runs west-to-east approximately through the centre of the watershed has 187 heavy truck passes per day from June through October. Pickup traffic is unrecorded, but estimated at 4/5 of all traffic (about 930-940 total passes)(Pers. Communication, Canfor Operations Staff, September 5, 2019). The 4000 Main, a moderate-sized haul road accessing remote southern portions of the watershed receives about 100 passes per day, 37 of which are heavy truck traffic from June – October (Pers. Communication, Canfor Operations Staff, September 5, 2019). Main roads are typically constructed on a prepared subgrade of silt or clay which is compacted with sheep's-foot rollers. Geotextile fabric or plastic grids are used to segregate the subgrade from the road surface materials and to provide lateral shear resistance on otherwise highly plastic soils. Base and surface courses of gravel are imported and spread on the roads to improve running characteristics and stability.

Forestry roads used to access cutblocks are commonly native surface winter access roads which are deactivated within 3 years of use (Government of Alberta, 2016). Oil and gas well service roads are used throughout the service life of a well, typically years to decades, and have infrequent heavy use by large oilfield service vehicles, and daily or weekly pickup or ATV use by wellsite production operators. Persistence of oil and gas roads means that areas of intense oil and gas exploration activity account for the highest road densities in the Simonette watershed. Agricultural land zones in the northeastern portion of the Simonette have a dense, rectilinear network of township and range roads although the impacts of these rural roads are not considered in this study.

2.2.2 Road surface sedimentation and data collection

Multiple methods of investigation were used in this study: settling tank sites with integrated plot outflow monitoring and local precipitation monitoring (Black & Luce, 2013), silt fences with precipitation monitoring (Robichaud & Brown, 2002), and surveyed road sediment plumes and sections of road with rilled or gullied ditches. These different techniques allowed for concomitant collection of preliminary erosion data via silt fences, detailed erosion data with hydrologic inputs and outputs from settling tanks, and survey-level information about base road erosion rates and the potential contribution of gullying and rilling to sediment budgets in the Simonette. Plot

sediment production is known to vary with road geometric characteristics (Coe, 2006; Luce & Black, 1999). All silt fence and settling tank plot sediment yields per square metre were corrected by applying standard correction coefficients for the slope-length product as used in the Revised Universal Soil Loss Equation (McCool et al., 1989).

2.2.2.1 Settling tank plots

Site selection for settling tanks was stratified by surficial geology and road type by overlaying surficial geology polygons on attributed road linear features (Table 2-1). Surficial geology was generalized into three categories: sandy sites in glaciofluvial or aeolian terrain, fine-grained lacustrine sites, and mixed to fines-dominated sites corresponding to lodgement and melt-out tills or colluvium. Mapped road sites were then visited to determine suitability for instrumentation. Suitable sites had fill-slopes or shoulders below the road grade which could accommodate the size of the settling tank (about 1.3m high) and had drainage ditches, or sections of road with sufficient slope which could easily be bermed by hand excavation to confine water running off the road surface and prevent it running off the sides. There were two replicates of each surficial geology type: one each in large feeder roads (high traffic) and small well-pad access roads (low traffic), for a total of six settling tank erosion plots. Hand-excavated test pits were used to determine if the soil characteristics at the site corresponded to expected type based on surficial geology mapping. General site characteristics are shown in Table 2-2 and more detailed site descriptions are included in Appendix A of this thesis.

Plots were comprised of drainage diverters, settling tanks, tipping bucket and sub-sampling apparatus, and rain gauges. Plot drainage was isolated at the top and bottom by open-top drainage culverts excavated into the road surface. Culverts were constructed of 2x6" rough-cut timber reinforced with bolted-in galvanized pipe spacers (Figure 2-2A). Plot width was defined by the distance between the road crown and shoulders, length was the distance between culverts, and area was the product of road length and width. Settling tanks were installed in hand-excavated benches dug into the road shoulder. One tank (P286) was excavated vertically into flat ground because the grade separation between the road and ground surface was insufficient. Sediment-charged water was directed along road-side ditches or berms and from the bottom drainage culvert into a polyvinyl chloride (PVC) pipe emptying into a settling tank constructed out of a plastic intermediate bulk container (IBC) mounted on a pallet. Outlets were drilled into the top of every settling tank and connected to a tipping bucket and flow splitter (Figure 2-2B). Tipping buckets

were calibrated in the lab by adjusting stops on the buckets until tip volumes on each side were approximately equal and measuring the resultant tip volume. Calibrations under field conditions were performed by pouring 2-3 18.9 L buckets into a plot inlet and dividing the amount of water by the number of tips on the tip counter. Field-calibrated tip volumes were 1.1 to 1.5 times estimated lab values and this paper uses an average of the lab and field calibrations in presenting runoff volumes. A flow splitter diverted subsamples of sediment-charged water from every second tip to an 18.9 L plastic pail.

Precipitation gauges were located within 5-10 m of the settling tank with the exception of the rain gauge for P4107B which is located in a wide pipeline right-of-way about 800 m east of the site near a silt fence site (P4107A). Precipitation data were collected using lab-calibrated Texas Electronics TB-525 or Davis Instruments Rain Collector II tipping bucket rain gauges with wedge-style rain gauges (Edwards Manufacturing Co.) acting as checks and backups. Station failures were compensated for by filling precipitation data using either distance-weighted averages if there were relatively few events in common, or using statistical similarity between nearby gauges (Ahrens, 2006) if there were many events in common. Rainfall energy intensity (EI30) was summarized using the Rainfall Intensity Summarization Tool (RIST) developed by the USDA (Dabney, 2019). Missing rainfall energy values were estimated from a network of 21 weather stations in west-central Alberta using inverse distance weighting interpolation in ArcGIS (Shepard, 1968) (Appendix B). Infiltration at each plot was recorded by subtracting plot output in millimetres from the measured precipitation for each recorded rain event. Plot records with relatively even precipitation were selected, and infiltration was calculated from the beginning of the precipitation pulse that initiated outflow up to the end of plot outflow.

The settling tanks were weighed twice in Summer 2017 (early August and late September), and approximately every two weeks from early June to late August 2018, with a final weighing in October 2018. Precipitation and tipping bucket logs were downloaded at each visit, and 500 mL sub-samples were taken from the flow-splitter collection bucket after agitation for total suspended sediment concentration. Samples were later analyzed in the lab for suspended sediment concentration using the evaporation method (ASTM D3977-97). Before weighing, tank water levels were checked by comparing with a marked fill line and topped up as needed. Errors in water-level reading, where present, would result in occasional negative sediment weight readings. Tanks were weighed by suspension from a winch mounted on a custom-built steel weighing frame and

connected to a load cell (Optima OP-926-5000, Figure 2-2C). Masses were recorded to the nearest 0.2 kg, and temperature of the water was recorded. Where the temperature of the water was not recorded, an average of the past day's temperature recorded by the rain gauge was used. Tanks that collected more than 400 kg of sediment were cleaned out, filled with stream or pond water and weighed to a new tare value. Subsamples of tank sediment for particle density analysis were collected using bags or bottles during cleanings and fall site deactivation. Particle density was calculated in the lab with a volumetric flask using the method outlined in the Encyclopedia of Soil Science (Blake, 2008). Wildlife damage and equipment malfunctions in 2017 resulted in data gaps for several stations; all stations produced data during the 2018 season.

2.2.2.2 *Silt fences*

Silt fences were used to provide supplementary erosion data to the settling tanks (Robichaud & Brown, 2002). Six silt fences were installed during the summer of 2016 and spring of 2017, mostly located along the 4000 road, a medium- to high-use road in the central Simonette (Table 2-2, a site is shown in Figure 2-3). Sites farther west (4106, 4107, 4108, 4111) contained glaciofluvial geology, and a site located farther to the east (4126) was located in ground moraine. Underlying soil texture of plots was usually similar to textures that would be expected from geologic mapping, although soils near P4111, which were mapped in glaciofluvial terrain were silty-clayey soils with bright white, dense, clay illuviation horizons. P7131 (coincident with the settling tank plot) was installed on a connector road branching off the 4000 road and located in a stagnant ice moraine.

Slit-woven geotextile silt fences (Nilex SIL-2130 WS, 0.6 mm aperture) were installed at dips and at freshly excavated turnouts below cross-drain culverts to capture water draining from a specific road section using a modified version of the method presented by Robichaud & Brown (2002). Contributing length of plots was estimated by walking or surveying the section of road upslope of the outlet until the nearest cross-drain was found or until the road slope was negligible. The width of road plots was estimated based on the total width of the road and the proportion sloping into ditches connected to the drain point. Lengths and areas of ditches and cut-slopes contributing to the drain point were also added to the road area. The roads monitored were generally 10-12 m wide with high traffic levels and a large amount of sediment deposition was expected. Rather than digging and weighing sediment, an irregular grid (1-2 m longitudinally and 1 m laterally) of survey stakes was used to measure the accumulated depth of sediment (+/- 0.5 cm)

at each visit. Stake heights were interpolated into 3-dimensional surfaces using Kriging in ArcGIS. Each surface was subtracted from the bare surface and the results were subtracted from previous volumes to obtain changes in volume of accumulated sediment. The first measurement was subtracted from baseline station surveys for 4108, 4111, and 4126 and sediment volumes were calculated using the end-area method throughout the gridded station extent. Stake depths were subtracted from a lidar bare earth model for P7131, and from total station (Nikon DTM-522) measurements at Sites 4107 and 4106, and sediment volumes were integrated using kriging and cut-and-fill analysis in a geographic information system (ArcGIS). To estimate sediment masses from volumes four bulk density samples were collected from a silt fence site in the study area (P4107) using a standardized plastic container to determine volume, and volume and wet and dry weights were recorded (the last after drying for 24 hours in an oven at 105°C). Two silt fences (P4107A and P4108) were undermined over the course of the study. In each case the fence was repaired and the surface behind the fence was recorded to facilitate measurement of the accumulation volume in the next measurement period; measurements for the undermined period were omitted from the analysis.

2.2.2.3 Sedimentation plume survey data

Erosion data were collected by measuring plumes of sediment deposited at road drainage points in the Simonette watershed. The data were collected as part of a survey of road-stream connectivity in the watershed. Plumes were surveyed by hand using fibreglass measuring tape for distances, compasses (Silva, Brunton, or Suunto) for bearing, and clinometers (Brunton or Suunto) for inclination, or by using a corrected GNSS controller (Trimble Geo 7x) with an external antenna (Trimble Zephyr 2), and depths of the plumes were recorded every 1-2 m along the longitudinal transect of the plume body by digging or coring through the plume surface to reach a matted rooting horizon. Depths in plumes were usually recorded as the average of 2 or more pits or cores located transverse to the centreline, and plume volumes were estimated as the incremental area multiplied by the average depth at a cross section.

Road sections with significant ditch rilling or gullying were also observed and surveyed (Figure 2-4): Gully cross sections were measured at 3-5 metre intervals with one or more depth measurements per cross section depending on whether the cross section was deemed to be roughly rectangular or triangular (1 measurement), or trapezoidal (more measurements). Volumes were integrated as the average of two end areas multiplied by the interval. Some of the larger gullies,

particularly those encountered in the first year of the study, were measured at only a few sections with length estimated either using a laser rangefinder (Nikon Forestry Pro) or as the distance between GPS points located using the Trimble receiver or a Garmin GPSMap 64st GNSS receiver. Volumes were estimated as triangular prisms for these gullies. Masses were estimated by multiplying plume or gully volumes by bulk densities from samples collected at a silt fence in the study area (P4107), although actual bulk densities of removed in-situ materials were likely higher. The masses of sediment found in road plumes and roads with gullied ditches were compared with the total upslope contributing area to the drainage point, which included contributing segments of road, ditches, and cutslopes to the drain point calculated using the same method as for silt fences.

2.3 Results

2.3.1 Settling tank sedimentation plots

Hydrological and sediment output for the settling tank plots organized by surficial geology and road traffic use are shown in Table 2-3. Sediment yield for the morainal high-traffic plot (P7131) was consistently the highest among all plots for 2018 (6.28 kg/m²), and sediment yield for the low-traffic morainal (P4128) and sandy/aeolian (P295) plots was moderate (1.36 and 1.42 kg/m²). Lower sediment yields were found for the lacustrine plots (M270 and P286) and for the high-traffic sandy/aeolian (P4107B) plot (0.07 to 0.57 kg/m²). The year 2017 is not included as a comparison because wildlife damage resulted in not all plots recording sediment yield that year. The plots that produced the most water from rain events were the morainal high and low-traffic plots, and the sandy high-traffic plot. The lacustrine plots and the sandy low-traffic plot were least effective at generating water from rain events. Regular suspended sediment concentrations for the morainal and sandy high and low-traffic plots ranged between 0.5 and 44.7 g/L. Flow-splitter connection failures and overall lower water production from the lacustrine plots limited the collection of suspended sediment data at these plots, but the high-traffic lacustrine plot produced suspended sediment concentrations similar to the morainal and sandy plots (1.1 to 48.2 g/L), and the low-traffic lacustrine plot produced very low suspended sediment amounts (0.5 to 1.1 g/L). The three highest suspended sediment concentrations were produced during the Fall 2017 and 2018 collection periods following early season snowstorms.

The overall amount of rain energy calculated from the site precipitation gauges and from the longer-term weather stations used to interpolate missing values was consistently greater than published estimates of yearly erosivity for the Canadian Prairies (Wall et al., 2002). The estimated

rain energy (E_{I30}) was plotted against sediment yield normalized by USLE length and slope coefficients, and lines of best fit were derived for each sediment plot (Figure 2-5, Table 2-4). The high-traffic morainal and lacustrine plots produced the most sediment with respect to rain energy (1×10^{-3} (kg/m²)/ E_{I30} and 7×10^{-4} (kg/m²)/ E_{I30}), the low-traffic lacustrine plot produced very little sediment regardless of the amount of rain energy (5×10^{-5} (kg/m²)/ E_{I30}), and the other plots produced similar amounts of sediment to each other with respect to rain energy (between 3.7×10^{-4} and 4.9×10^{-4} (kg/m²)/ E_{I30}).

Plot hydrologic outflow was compared with precipitation depth to determine overall plot efficiency and infiltration capacity for individual rain events and is summarized in Figure 2-6. There is a wide variation in plot efficiency, as the amount of water produced is dependent both on the intensity of the rain event and the infiltration capacity of the road subgrade, but the morainal plots (P7131 and P4128) were overall the most efficient at producing water, and the lacustrine plots were the least efficient (P286, and M270). The two glaciofluvial/aeolian plots (P4107B and P295) were more efficient at producing water than anticipated. Estimated average infiltration rates from rain events reflected the overall water production efficiency (Figure 2-6, right). Average infiltration rate was highest for the low-traffic glaciolacustrine plot (3.7 mm/hr, P286), and lowest for the morainal plots (1.2 and 1.3 mm/hr for P4128 and P7131, respectively). Infiltration rates for the high-traffic lacustrine plot, and for the low- and high-traffic aeolian/glaciofluvial plots were 1.9, 1.9, and 1.6 mm/hr, respectively. When normalized sediment production values were plotted against water production efficiency for the measurement period, we observed an overall positive exponential relationship that held across the different types of plots (Figure 2-7). Plots with lower hydrological efficiency tended to cluster at the left end of the figure, and those with higher efficiency showed a variety of responses to different intensity rain events and produced more sediment overall.

2.3.2 Silt fences

Silt fences generally yielded more sediment than settling tanks with the exception of the high-traffic morainal plot (P7131) (Table 2-5). When plot geometric attributes were accounted for in sediment yield and divided by rain energy (E_{I30}), the sediment yield relationships were somewhat higher than the slopes of the rain energy plots for the settling tanks. Two plots (P4107A and P4108) were installed in freshly excavated turnouts in road segments with recent ditch maintenance. Normalized sediment production with respect to erosivity at P4107 decreased by a factor of 2.7 between 2016 and 2017, and by a factor of 4.9 between 2017 and 2018, a 13-fold reduction in

sediment production through the monitoring period. At P4108 normalized sediment yield over erosivity decreased by 10 times between 2017 and 2018. Two silt fence plots (P4106 and P4126) produced negligible amounts of sediment. The non-producing plots have site-specific characteristics that may have limited sediment production: P4106 has rock baffles and a sump installed by road maintenance crews above the plot, and P4126 is a gently sloping plot (3-4%) located just above a natural dip of the road.

2.3.3 Gullies and sediment plumes

Road plumes in un-gullied sections of road produced about 7.6 kg per m² contributing area, and calculated ditch removal in gullied sections was 18 kg/m². Bar charts of plume and gully sediment yields are shown in Figure 2-8. The data were insufficient to make meaningful comparisons for gully and road surface erosion with respect to traffic or surficial geology classification, however simple geometric relationships provided useful insights into erosional behaviour. When sediment yields were plotted against contributing area, gullied and un-gullied road segments produced near identical sediment yields (~7.1 kg/m²) up to a contributing area of 3500 m², but yields increased drastically (~38.4 kg/m²) above that threshold (Figure 2-9). Roads with contributing areas greater than about 3500 m² may be expected to produce sediment at around 5 ½ times the rate of roads below the threshold. This value is likely to vary depending on site level differences in soil drainage, and temporal year-over-year climatic variation.

2.4 Discussion

2.4.1 Hydrological behaviour and erosion risk

The hydrology of road segments is complex, affected by slope, length, and overall size of the contributing road segment, infiltration capacity of road materials, and road construction practices. Contributing area thresholds for severe gully behaviour in the Simonette (Figure 2-9) are implicitly hydrological in nature. Previous research on gully thresholds has found that the area-slope relationship is a good predictor of hillslope incision and mass-wasting (Majhi et al., 2021; Montgomery, 1994; Montgomery & Dietrich, 1992). Slope is viewed as an analogue for runoff speed, and contributing area is considered a proxy for runoff volume (Patton & Schumm, 1975). Similar area or length thresholds exist for gully behaviour in hillslopes below road drainage points (Coe, 2006; Croke & Mockler, 2001), whereas this may be the first study discussing gully thresholds in roadside ditches, an indicator of the severity of the problem in the study area. The responsiveness of a road segment to a particular rain event also determines the amount of erosion that is likely to

be generated. This behaviour likely forms a continuum (Figure 2-7), where greater plot efficiencies are a function of the intensity of the rain event and water loss through the road surface or off the sides. More-or-less native surface roads confined by through-cuts in silty or clayey soil (ie. P7131 and P4128) have the highest plot efficiencies and sediment loads. Roads with permeable bases (P298) or with elevated surfaces in well-drained, uncompacted soils will have lower plot efficiencies and less sediment production.

Soils in the Simonette are dominantly fine-grained, with laterally-isolated veneers of fluvial sand, and local deeper lacustrine sand deposits. Infiltration rates in disturbed road environments are more likely to be reflective of underlying fine-grained geology, typically 1.2 – 1.9 mm/hr, although pockets of deep, well-drained sands (rare in this area) may have infiltration rates of 3.7 mm/hr or more. Road infiltration rates in previous studies ranged from less than 1 mm/hr (Reid & Dunne, 1984) to over 20 mm/hr (Croke et al., 2006; Soon et al., 2000) (See Appendix C). The cumulative effect of road infiltration over a low-intensity, long-duration storm is substantial: A 44 mm storm falling over a period of 24 hours, a 1 in 2 year event in Whitecourt Alberta (Environment Canada, 2019), may only have an average precipitation rate of around 1.8 mm/hr. An average infiltration rate of 1.5 mm/hr operating over this time period would infiltrate around 83% of the rain input from this storm. Relatively low total storm runoff ratios for plots in the Simonette suggest that infiltration plays a substantial role in these losses. The findings of this study support those that describe site sediment production in terms of road segment water yield or flow intensity rather than rain inputs (Howard, 2018; Reid & Dunne, 1984; Surfleet et al., 2011). If rain erosivity is used in modelling erosion for roads in the foothills, practitioners should use local climate data as mapped annual estimates (Wall et al., 2002) appear low compared to the data presented in this study.

2.4.2 Effects of traffic and geology

Contrary to the findings of other studies, higher-use and more-frequently maintained roads in the Simonette watershed do not necessarily have higher erosion rates (see Figure 2.5). The Simonette is a predominantly fine-grained watershed, with spatially-limited distribution of coarse-grained deposits. Aeolian or glaciofluvial deposits are often mapped as thin surficial deposits overlying deeper fine-grained till and glaciolacustrine deposits. Thicker deposits of gravel are found in localized glaciolacustrine beach deposits, glacial outwash deltas, and preglacial terraces. It is notable that the road with the lowest erosion rate and lowest amount of water production was a low-use road situated in deep glaciolacustrine sand deposits (P286). When thin surficial covers of

aeolian or glaciofluvial sand are stripped off during road construction, the road surface takes on the characteristics of the fine-grained material underneath. This is particularly evident in the low-traffic glaciofluvial plot (P295) which runs right through a glaciofluvial contact with underlying fine-grained material. Stripping and homogenization of subgrade material is even more pronounced in high-use roads, and likewise, gravel application is also more frequent on these roads. Gravel application and geotextile separation of subgrade material from base and running courses on higher-use roads limits the ability of vehicle passes to pump predominantly fine-grained subgrade materials into the running surface. Essentially, road construction practices and gravelling on higher-use roads counteracts the expected higher erodibility from greater vehicle traffic and acts to smooth out expected differences related to mapped surficial geology.

Similar contradictory results between sediment production and traffic level were found in Washington where secondary haul roads had greater response to individual vehicle passes than heavily-used main roads. This difference was attributed to the buffering effect of disturbed sediment on high-traffic roads, and also to greater piping of fines through the road bed in the less well-gravelled secondary roads (Bilby et al., 1989). Elevated suspended sediment values for fall samples collected at stations M270, P295 and P7131 may reflect conditions with frequent traffic and slow release of snow meltwater on the road surface. Sediment concentration may also occur from gravity settling of coarser fines when sample buckets overflow. However, since not all of these samples were collected under these conditions, it is plausible that elevated sediment concentrations are the result of the interaction of traffic and saturated road conditions. Further work is needed to determine how traffic, geology, and road construction practices influence erosion rates in Alberta.

2.4.3 Effect of road and ditch maintenance

This study found that periodic ditch maintenance increased road erosion rates in several monitored sections (see Table 2-5), whereas road reconstruction that incorporated practices improving drainage and subgrade stability reduced road erosion susceptibility (see Table 2-3, site 4017B). Two sites (P4107A and P4108) were located road sections with fresh ditch maintenance and were monitored for several years. Erosion from ditches and bare sides of the turnouts contributed a large amount of sediment to these plots in the first year of their operation. As the plots revegetated in subsequent years, sediment yields decreased so that normalized estimates of production relative to rainfall energy in the silt fence in P4107 were comparable to or less than production for the nearby settling tank in summer 2018 (Table 2-5). These results are similar to those found in the

Coast Range of Oregon (Luce & Black, 2001b). In contrast, the high traffic glaciofluvial settling tank (P4107B) underwent complete road reconstruction and showed a *decrease* in sediment yield (Table 2-3). The road was reconstructed on a carefully prepared native glaciofluvial subgrade separated from the base and running courses by geotextile. The prepared road surface was then sprayed with calcium chloride dust suppressant. The road is well-drained, fines are isolated from the running surface, and the running surface has been treated with a chemical binder.

2.4.4 Erosion rates in the Simonette compared to other studies

Road erosion rates in the Simonette watershed are moderate to high, comparable with erosion rates in steeper, wetter terrain on the west coast of North America (Figure 2-8, Appendix D). Gullied road segments are a particular concern, as they represent the second-highest erosion rate among the studies. A road erosion study conducted in the Olympic Peninsula, Western Washington reported comparable peak erosion rates to this study (Reid & Dunne, 1984). Geology comprised soft, relatively young sedimentary rock (Reid & Dunne, 1984) and roads were paved with glaciofluvial gravel. Traffic on the high-use roads in that study was comparable to that in the Simonette watershed, but the climate was much wetter (3900 mm/year precipitation) than the Simonette. Considerable sediment production was attributed to breakdown of the surfacing gravels, and vehicle traffic pumping fines from the road base into the running surface. The Washington state study also showed that, when stratified by relative traffic level, road sediment production was well-correlated to both culvert discharge and storm precipitation, and thus the overall high erosion levels may be attributed to precipitation, traffic, and erodible geological and surfacing materials. Another study in Western Washington with similar traffic levels, but greater precipitation, and hard andesite gravel over glacial materials had similar erosion rates to the high-traffic silt fence and settling tank sites in the present study (Bilby et al., 1989). Studies with lower-use roads and resistant surfacing material (Luce & Black, 2001a; Sugden & Woods, 2007) generally show lower erosion rates, whereas sites in soils with high erosion potential have relatively high erosion rates notwithstanding lower traffic rates and a drier climate similar to Alberta (Welsh, 2008).

Roads in the Simonette watershed are commonly constructed on a base of glaciolacustrine or morainal silt and clay: materials with poor drainage, low resistance to lateral shear, and relatively weak erosion resistance. Although overall precipitation is much lower in the Simonette watershed compared to the West Coast, spring melt and multi-day storm systems can create prolonged soft road conditions which promote pumping of fine-grained subgrade material into the road surface.

Gravel is commonly sourced from isolated preglacial uplands or buried valley systems, and tends to be applied conservatively, usually on main roads. Thin and inconsistent gravel application promotes working of subgrade materials into the road surface, as does the lateral deformability of silt-clay soil mixtures. Although grading is relatively frequent on roads in the Simonette watershed, heavy vehicle traffic during soft conditions flattens out the road structure, impeding drainage away from the road. Impeded road drainage and grading mistakes may compound existing drainage problems on roads in the Simonette watershed, allowing ditches to form rills and gullies. All these factors have been shown in previous studies to promote increased rates of road erosion in watersheds. Hence, overall high erosion rates of roads in the Simonette watershed are probably a result of inconsistent road water management, soil conditions, and a climate where freeze thaw processes occur.

2.4.5 Management and modelling implications

Modelling sediment delivery from roads is a key concern for natural resources managers. Part of the sediment delivery equation is the amount of sediment generated; the other consideration is how much sediment reaches receptors. This study highlights the importance of road hydrology in determining the amount of sediment generated on road surfaces. Hydrological road models are also useful insofar as they can provide continuum modelling of runoff generation and fate in the watershed. Such models should ideally include terms for water abstraction in the road, ditches, and downslope areas (ie. Surfleet et al. 2011; Benda et al. 2019). Proper model use and calibration can assist in finding potential road sedimentation hotspots.

The results of the study indicate that proper water management is key to minimizing erosion, particularly threshold-based processes like gullying. Long sections of road with inadequate drainage hamper proper management efforts. Road segments with contributing areas $>3500 \text{ m}^2$ eroded faster than road segments with a smaller contributing area, as water flowing in ditches and along the sides of roads exceeded threshold shear stress values for incision (see Patton and Schumm 1975). This kind of erosion was usually associated with poor maintenance practices such as failed culverts or grader-berming along ditches. Road sections that confine water and do not allow it to flow into adjacent forest floor areas thus become chronic sediment producers. Further neglect of chronic sediment-producing road sections may lead to compounded failures. If one culvert is undermined, then other downstream drainage structures in a segment of road could also be undermined. If one of these structures is designed to redirect water away from a stream crossing,

then substantial sediment delivery can result. Moreover, the relative magnitude of the erosion problem associated with road gullying in this study is on par with some of the highest sediment generation rates found in the literature (Reid & Dunne, 1984). Recommended minimum inspection lengths of roads with several different geometries corresponding to the threshold contributing area (3500 m²) are provided in Table 2-6. This suggests that undrained, uninspected road segments should have maximum lengths between 117 and 350 m depending on road confinement characteristics, after which best management practice actions must be taken for a given road segment.

2.5 Conclusion

This study corroborates findings from other studies that erosion from road surfaces is strongly related to the hydrological response of the road surface (Howard, 2018; Reid & Dunne, 1984; Surfleet et al., 2011). Well-drained sites which produce little runoff also produce less sediment. There is some evidence from this study that factors such as traffic and geology may affect road surface hydrology; however, the hydrological effects of traffic and surficial geology are not easily disentangled from traffic-related supply processes (Bilby et al., 1989; van Meerveld et al., 2014; Reid & Dunne, 1984), and differential erodibility of road surface and subgrade materials (Dubé et al., 2004; Packer, 1967; Sugden & Woods, 2007). Hydrological thresholds also influence road erosion. The risk of gullying in the road increases with uncontrolled drainage along ditches, partly from poor traffic control and grading practices, and from poor construction techniques. Future road research in Alberta watersheds should be geared towards better understanding the main drivers of the demonstrated enhanced erosional response in Alberta watersheds. Topics of consideration may include the interactive effects of traffic and soils, spring melt processes, and better characterization of northern foothills climate and its impact on soil erosion.

2.6 References

- Ahrens, B. (2006). Distance in spatial interpolation of daily rain gauge data. *Hydrology and Earth System Sciences*, 10(2), 197–208. <https://doi.org/10.5194/hess-10-197-2006>
- Al-Chokhachy, R., Black, T. A., Thomas, C., Luce, C. H., Rieman, B., Cissel, R., et al. (2016). Linkages between unpaved forest roads and streambed sediment: why context matters in directing road restoration. *Restoration Ecology*, 24(5), 589–598. <https://doi.org/10.1111/rec.12365>
- Alberta Transportation. (2020). Historical Seasonal Weight Changes. Retrieved January 16, 2021, from <http://www.transportation.alberta.ca/content/doctype260/production/trans-historical-seasonal-weight-changes.pdf>
- Andriashek, L. D. (2001). *Surficial Geology of Wapiti Area, NTS 83L* (No. Map 239). Edmonton, Alberta.
- ASTM. (2014). *ASTM D3977-97(2013) - Standard Test Methods for Determining Sediment Concentration in Water Samples. ASTM Book of Standards* (Vol. 90). West Conshohocken, PA: ASTM International. <https://doi.org/10.1520/D3977-97R13E01.2>
- Atkinson, N., & Hartman, G. M. D. (2017). *West-Central Alberta Regional Stratigraphic Model - Sediment Thickness* (Digital Data No. DIG 2017-0016). Edmonton, Alberta.
- Atkinson, N., & Lyster, S. (2010). *Thickness and Distribution of Quaternary and Neogene Sediment in Alberta, Canada* (Digital Data No. DIG 2010-0036). Edmonton, Alberta: Alberta Geological Survey.
- Baptiste, A. (2017). gridExtra: Miscellaneous Functions for “Grid” Graphics. Retrieved from <https://cran.r-project.org/package=gridExtra>
- Benda, L. E., James, C., Miller, D. J., & Andras, K. (2019). Road Erosion and Delivery Index (READI): A Model for Evaluating Unpaved Road Erosion and Stream Sediment Delivery. *Journal of the American Water Resources Association*, 55(2), 459–484. <https://doi.org/10.1111/1752-1688.12729>
- Bilby, R. E. (1985). Contributions of road surface sediment to a western Washington stream. *Forest Science*, 31(4), 827–838.
- Bilby, R. E., Sullivan, K., & Duncan, S. H. (1989). The generation and fate of road-surface sediment in forested watersheds in southwestern Washington. *Forest Science*, 35(2), 453–468.
- Black, T. A., & Luce, C. H. (2013). Measuring Water and Sediment Discharge From a Road Plot With a Settling Basin and Tipping Bucket, (June), 38.

- Blake, G. R. (2008). Particle Density. In W. Chesworth (Ed.), *Encyclopedia of Soil Science*. Dordrecht: Springer Netherlands. <https://doi.org/10.1007/978-1-4020-3995-9>
- Brown, K. R., Aust, W. M., & McGuire, K. J. (2013). Sediment delivery from bare and graveled forest road stream crossing approaches in the Virginia Piedmont. *Forest Ecology and Management*, *310*, 836–846. <https://doi.org/10.1016/j.foreco.2013.09.031>
- Brown, K. R., McGuire, K. J., Hession, W. C., & Aust, W. M. (2015). Can the Water Erosion Prediction Project Model be used to estimate best management practice effectiveness from forest roads? *Journal of Forestry*, *114*(January 2015), 17–26. <https://doi.org/10.5849/jof.14-101>
- Cederholm, C. J., Reid, L. M., & Salo, E. O. (1980). Cumulative effects of logging road sediment on salmonid populations in the Clearwater River, Jefferson County, Washington. In *Salmon-Spawning Gravel: A Renewable Resource in the Pacific Northwest?* (pp. 1–35). Seattle, WA. Retrieved from <https://www.fs.fed.us/psw/publications/reid/Cederholm.pdf>
- Coe, D. B. R. (2006). *Sediment Production and Delivery From Forest Roads in the Sierra Nevada, California*. Colorado State University.
- Croke, J. C., & Mockler, S. P. (2001). Gully initiation and road-to-stream linkage in a forested catchment southeastern Australia. *Earth Surface Processes and Landforms*, *26*(2), 205–217. [https://doi.org/10.1002/1096-9837\(200102\)26:2<205::AID-ESPI68>3.0.CO;2-G](https://doi.org/10.1002/1096-9837(200102)26:2<205::AID-ESPI68>3.0.CO;2-G)
- Croke, J. C., Mockler, S. P., Hairsine, P. B., & Fogarty, P. (2006). Relative contributions of runoff and sediment sources within a road prism and implications for total sediment delivery. *Earth Surface Processes and Landforms*, *31*(4), 457–468. <https://doi.org/10.1002/esp.1279>
- Dabney, S. (National S. L. (2019). RIST (Rainfall Intensity Summarization Tool). Oxford, Mississippi: USDA National Sedimentation Laboratory. Retrieved from <https://www.ars.usda.gov/southeast-area/oxford-ms/national-sedimentation-laboratory/watershed-physical-processes-research/research/rist/rist-rainfall-intensity-summarization-tool/>
- Dubé, K., Megahan, W. F., & McCalmon, M. (2004). Washington Road Surface Erosion Model (WARSEM) Manual. State of Washington Department of Natural Resources. Retrieved from http://file.dnr.wa.gov/publications/fp_data_warsem_manual.pdf
- Elliot, W. J. (2013). Erosion processes and prediction with WEPP technology in forests in the Northwestern U.S. *Transactions of the ASABE*, *56*(2), 563–579.
- Environment and Climate Change Canada. (2019). Canadian Climate Normals and Averages 1981-2010. Retrieved July 7, 2020, from

- https://climate.weather.gc.ca/climate_normals/index_e.html
- Environment Canada. (2019). Short-Duration Rainfall Intensity-Duration-Frequency Data. Ottawa, Canada: Government of Canada. Retrieved from https://climate.weather.gc.ca/prods_servs/engineering_e.html
- Fenton, M. M., Waters, E. J., Pawley, S. M., Atkinson, N., Utting, D. J., & Mckay, K. (2013). Surficial Geology of Alberta. *Alberta Geological Survey Map 601*.
- Fox, J., & Weisberg, S. (2019). *An {R} Companion to Applied Regression* (Third Edit). Thousand Oaks, CA: Sage. Retrieved from <https://socialsciences.mcmaster.ca/jfox/Books/Companion/>
- Government of Alberta. Alberta Timber Harvest Planning and Operating Ground Rules Framework for Renewal (2016). Retrieved from [https://www1.agric.gov.ab.ca/\\$department/deptdocs.nsf/all/formain15749/\\$FILE/TimberHarvestPlanning-OperatingGroundRulesFramework-Dec2016.pdf](https://www1.agric.gov.ab.ca/$department/deptdocs.nsf/all/formain15749/$FILE/TimberHarvestPlanning-OperatingGroundRulesFramework-Dec2016.pdf) - section II.1.2
- Hlavac, M. (2018). stargazer: Well-formatted Regression and Summary Statistics Tables. Retrieved from <https://cran.r-project.org/package=stargazer>
- Howard, M. J. (2018). *Erosion and Erodibility from Off-Highway Vehicle Trails in Alberta's Southern Rocky Mountains*. University of Alberta. <https://doi.org/https://doi.org/10.7939/R3SX64R9F>
- Huayta Hernani, L. F. (2019). *Application of LiDAR DEM Metrics to Estimate Road-stream Sediment Connectivity in Alberta Eastslopes Salmonid Habitats*. University of Alberta. <https://doi.org/https://doi.org/10.7939/r3-1xrm-wj37>
- Luce, C. H., & Black, T. a. (1999). Sediment production from forest roads in western Oregon. *Water Resources Research*, 35(8), 2561–2570. <https://doi.org/10.1029/1999WR900135>
- Luce, C. H., & Black, T. A. (2001a). Effects of traffic and ditch maintenance on forest road sediment production. In *Proceedings of the Seventh Federal Interagency Sedimentation Conference* (pp. 67–74). Retrieved from <http://www.treesearch.fs.fed.us/pubs/23963>
- Luce, C. H., & Black, T. A. (2001b). Spatial and Temporal Patterns in Erosion from Forest Roads. In M. S. Wigmosta & S. J. Burges (Eds.), *Influence of Urban and Forest land Uses on the Hydrologic-Geomorphic Responses of Watersheds* (pp. 165–178). Washington, D.C.: American Geophysical Union. <https://doi.org/2>
- Majhi, A., Nyssen, J., & Verdoodt, A. (2021). What is the best technique to estimate topographic thresholds of gully erosion? Insights from a case study on the permanent gullies of Rarh plain, India. *Geomorphology*, 375, 107547. <https://doi.org/10.1016/j.geomorph.2020.107547>

- McCool, D. K., Foster, G. R., Mutchler, C. K., & Meyer, L. D. (1989). Revised Slope Length Factor for the Universal Soil Loss Equation. *Transactions of the American Society of Agricultural Engineers*, 32(5), 1571–1576.
- van Meerveld, H. J., Baird, E. J., & Floyd, W. C. (2014). Controls on sediment production from an unpaved resource road in a Pacific maritime watershed. *Water Resources Research*, 50(6), 4803–4820. <https://doi.org/10.1002/2013WR014605>
- Megahan, W. F., & Kidd, W. J. (1972). Effects of logging and logging roads on erosion and sediment deposition from steep terrain. *Journal of Forestry*, (March), 136–141.
- Montgomery, D. R. (1994). Road surface drainage, channel initiation, and slope instability. *Water Resources Research*, 30(6), 1925–1932. <https://doi.org/10.1029/94WR00538>
- Montgomery, D. R., & Dietrich, W. E. (1992). Channel Initiation and the Problem of Landscape Scale. *Science*, 255(5046), 826–830.
- Packer, P. E. (1967). Criteria for Designing and Locating Logging Roads to Control Sediment. *Forest Science*, 13(1), 2–18. <https://doi.org/10.1093/forestscience/13.1.2>
- Patton, P. C., & Schumm, S. A. (1975). Gully Erosion, Northwestern Colorado: A Threshold Phenomenon. *Geology*, 3(2), 88–90.
- Pawley, S. M., & Atkinson, N. (2013). *Surficial Geology of the Little Smoky Area (NTS 83K/NW)* (No. Map 564). Edmonton, Alberta.
- Phillips, R. W., Lantz, R. L., Claire, E. W., & Moring, J. R. (1975). Some Effects of Gravel Mixtures on Emergence of Coho Salmon and Steelhead Trout Fry. *Transactions of the American Fisheries Society*, 104(3), 461–466. [https://doi.org/10.1577/1548-8659\(1975\)104<461:SEOGMO>2.0.CO;2](https://doi.org/10.1577/1548-8659(1975)104<461:SEOGMO>2.0.CO;2)
- Prior, G. J., Hathway, B., Glombick, P. M., Pana, D. I., Banks, C. J., Hay, D. C., et al. (2013). *Map 600 Bedrock Geology of Alberta* (Vol. 2479). Edmonton, Alberta.
- R Core Team. (2019). R: A language and environment for statistical computing. Vienna, Austria: R Foundation for Statistical Computing. Retrieved from <https://www.r-project.org/>
- Reid, D. A., Hassan, M. A., & Floyd, W. C. (2016). Reach-scale contributions of road-surface sediment to the Honna River, Haida Gwaii, BC. *Hydrological Processes*, 30(19), 3450–3465. <https://doi.org/10.1002/hyp.10874>
- Reid, L. M., & Dunne, T. (1984). Sediment Production from Forest Road Surfaces. *Water Resources Research*, 20(11), 1753–1761.
- Reid, L. M., Dunne, T., & Cederholm, C. J. (1981). Application of sediment budget studies to the

- evaluation of logging road impact. *Journal of Hydrology*, 49–62. Retrieved from http://www.wou.edu/las/physci/taylor/andrews_forest/refs/reid_etal_198x.pdf
- Robichaud, P. R., & Brown, R. E. (2002). *Silt Fences : An Economical Technique for Measuring Hillslope Soil Erosion* (General Technical Reprint No. RMRS-GTR-94). *General Technical Report*. Fort Collins, CO. Retrieved from http://www.fs.fed.us/rm/pubs/rmrs_gtr94.pdf
- Shepard, D. (1968). A two-dimensional interpolation function for irregularly-spaced data. In *Proceedings of the 1968 23rd ACM National Conference, ACM 1968* (pp. 517–524). Association for Computing Machinery, Inc. <https://doi.org/10.1145/800186.810616>
- Soon, Y. K., Arshad, M. A., Rice, W. A., & Mills, P. (2000). Recovery of chemical and physical properties of boreal plain soils impacted by pipeline burial. *Canadian Journal of Soil Science*, 80(3), 489–497. <https://doi.org/10.4141/S99-097>
- Sosa-Pérez, G., & MacDonald, L. H. (2017). Effects of closed roads, traffic, and road decommissioning on infiltration and sediment production: A comparative study using rainfall simulations. *Catena*, (159), 93–105. <https://doi.org/10.1016/j.catena.2017.08.004>
- Startsev, A. D., & McNabb, D. H. (2000). Effects of skidding on forest soil infiltration in west-central Alberta. *Canadian Journal of Soil Science*, 80(4), 617–624. <https://doi.org/10.4141/s99-092>
- Sugden, B. D., & Woods, S. W. (2007). Sediment Production From Forest Roads in Western Montana. *JAWRA Journal of the American Water Resources Association*, 43(1), 193–206. <https://doi.org/10.1111/j.1752-1688.2007.00016.x>
- Surfleet, C. G., Skaugset, A. E., & Meadows, M. W. (2011). Road runoff and sediment sampling for determining road sediment yield at the watershed scale. *Canadian Journal of Forest Research*, 41(10), 1970–1980. <https://doi.org/10.1139/x11-104>
- Tonina, D., & Buffington, J. M. (2009). Hyporheic exchange in mountain rivers I: Mechanics and environmental effects. *Geography Compass*, 3(3), 1063–1086. <https://doi.org/10.1111/j.1749-8198.2009.00226.x>
- Van Vliet, L. J. P., & Hall, J. W. (1991). Effects of two crop rotations on seasonal runoff and soil loss in the Peace River region. *Canadian Journal of Soil Science*, 71, 533–543. <https://doi.org/10.4141/cjss91-051>
- Wall, G. J., Dickinson, W. T., Rudra, R. P., & Coote, D. R. (1988). Seasonal Soil Erodibility Variation in Southwestern Ontario. *Canadian Journal of Soil Science*, 68, 417–424. <https://doi.org/10.4141/cjss88-038>

Wall, G. J., Coote, D. R., Pringle, E. A., & Shelton, I. J. (2002). *RUSLEFAC - Revised Universal Soil Loss Equation for Application in Canada: A Handbook for Estimating Soil Loss from Water Erosion in Canada*. Ottawa, Canada.

Welsh, M. J. (2008). *Sediment Production and Delivery from Forest Roads and Off-Highway Vehicle Trails in the Upper South Platte River Watershed, Colorado*. Colorado State University.

Wickham, H. (2016). *ggplot2: Elegant Graphics for Data Analysis*. New York: Springer-Verlag.
Retrieved from <https://ggplot2.tidyverse.org>

Wickham, H., Romain, F., Henry, L., & Müller, K. (2021). *dplyr: A Grammar of Data Manipulation*.
Retrieved from <https://cran.r-project.org/package=dplyr>

2.7 Tables

Table 2-1. Climate variability in and near the Simonette watershed (Canadian Climate Normals 1981-2010)

Variable	Station		
	Valleyview	Grande Prairie	Simonette
Latitude	55°04'00" N	55°10'47" N	54°25'29" N
Longitude	117°16'00" W	118°53'06" W	117°44'28" W
Elevation	762.0 m	669.0 m	883.9 m
Daily Mean Temperature (°C)	3.2	2.2	3
Precipitation (mm)	504.8	445.1	581.2
Extreme Daily Precipitation (mm)	91.1	90	115
	07/14/1982	08/05/1994	07/31/1987
Highest 2 Months Precipitation (mm)	92.4 (July)	76.1 (July)	114.5 (July)
	79.4 (June)	75.9 (June)	97.8 (June)

Table 2-2. Location and description of settling tank and silt fence sites

Sites are colour-coded by traffic and surficial geology classification using a scheme that is consistent across this chapter: Blue = glaciolacustrine, orange = glaciofluvial, and green = morainal. Dark colours = high traffic and light colours are low traffic.

	Site	Geology	Offset Soil Pits	Road Surface	Traffic	Plot Area (m ²)	Plot Length (m)	Slope (%)
Se	M270	Glacio-lacustrine (silty)	Silty clay loam	Gravel worked into fill of glaciolacustrine sand and clay	HIGH	480/ 700**	80/ 194 **	5
	P286-SP	Glacio-lacustrine (sandy)	Sandy loam	Winnowed gravel, some sand	LOW	320	80	9
	P4107B	Aeolian	Organic bog deposits	Well-gravelled surface over fill	HIGH	361	56.5	8
	P295-SP	Glaciofluvial/aeolian veneer overlying stagnant ice moraine	Loamy sand to sandy clay	Thin gravel worked into native surface	LOW	531	88.5	7
	P7131	Stagnant ice moraine	Silty clay	Gravel mixed into till subgrade. Through-cut in morainal knob.	HIGH	388	80	7
	P4128-SP	Stony ground moraine	Silty clay loam	Thin cobbly gravel layer applied to stony till, mostly through-cut in study section.	LOW	381	79	6
Si	P4106*	Glaciofluvial	-	Well-gravelled surface	HIGH	1100	107	6.5
	P4107A	Glaciofluvial	Sand veneer over clay	Well-gravelled surface	HIGH	2368	250	10
	P4108	Glaciofluvial	-	Well-gravelled surface overlaying sand subgrade	HIGH	470	55.5	3.5
	P4111	Glaciofluvial	Silty-sandy clay, elluviated clay hardpan	Thin gravel partially worked into native soil	HIGH	300	60	5
	P7131	Stagnant ice moraine	See above	See above	HIGH	338	83.5	7
	P4126*	Moraine	-	Gravel partially worked into native surface	HIGH	690	114	2.5

*Non-producing plots

**Compromised upper culvert in Fall 2017 resulted in length extension of 114m, or 194m total. Total estimated plot area for Fall 2017 is 700m².

Table 2-3. Precipitation, rain energy, water yield, settling tank masses, and fines estimates: settling tank plots, 2017-2018

Missing values are shown with asterisks (*); underlined precipitation values are interpolated from nearby station records; **bolded values are seasonal totals**; colour scheme follows Table 2-2. For each plot the four columns on the left are precipitation and water discharge variables, and the four columns on the right are sediment production variables. EI30 is a shortened form of (MJ-mm)/(ha-h).

Collection Dates	Morainal, High Traffic (P7131)				Area 388				Morainal, Low Traffic (P4128)				Area 381			
	Precip (mm)	EI ₃₀	Disch. (L)	Eff (%)	SSC (g/L)	Fines (kg)	Tank (kg)	Av. (kg/m ²)	Precip (mm)	EI ₃₀	Disch. (L)	Eff (%)	SSC (g/L)	Fines (kg)	Tank (kg)	Av. (kg/m ²)
Aug 15 – 16, 2017	67.3	296	2019	7.7	8.2	16.5	356.9	0.96	*	*	*	*	*	*	*	*
Sept 26 – 29, 2017	134.1	101	*	*	* c	*	122.6	0.32	*	*	*	*	*	*	*	*
Total	201.4	397	2019	2.6	-	16.5	479.4	1.28								
Jun 9 – 10, 2018	11.8	66	267	5.8	14.3	3.8	104.6	0.28	11.2	6	382	9	*	*	24.3	0.06
23-Jun-18	18	60	1253	17.9	12.3	15.5	10.8	0.07	31.2	83	3476	29.3	6.2	21.4	-17.4 ^d	0.01
Jul 7 – 8, 2018	109	156	23855	56.4	6.2	147.8	393.8	1.40	148.8	280	20172 ^d	35.6	7.6	153.6	155.2	0.81
Jul 24 – 25, 2018	129	520	13832	27.6	19.6	271.2	499.3	1.99	<u>161</u>	<u>550</u>	11868	19.3	*	*	143.6	0.38
Aug 4, 2018 ^a	*	*	*	*	*	*	*	*	*	*	*	*	*	*	*	*
Aug 18 – 19, 2018	25.1	23	1260	12.9	3.0	3.8	16	0.05	16.6	12	1470	23.3	1.5	2.2	-32.9 ^d	-0.08
Oct 13 – 14, 2018	129.1	68	23470	46.9	40.1	901.1	165.5	2.75	158.7	102	4837	8	2.3	11.0	56.8	0.18
Total	421.9	892	63937	39.1	-	1245.0	1189.9	6.28	527.4	1032	42206	21	-	188.1	329.7	1.36
Collection Dates	Sandy/Aeolian, High Traffic (P4107B)				Area 361				Sandy/Aeolian, Low Traffic (P295)				Area 531			
	Precip (mm)	EI ₃₀	Disch. (L)	Eff (%)	SSC (g/L)	Fines (kg)	Tank (kg)	Av. (kg/m ²)	Precip (mm)	EI ₃₀	Disch. (L)	Eff (%)	SSC (g/L)	Fines (kg)	Tank (kg)	Av. (kg/m ²)
Aug 15 – 16, 2017	36	<u>80</u>	19	0.1	3.7	0.1	12.2	0.03	29.3	20	109	0.7	2.0	0.2	23.6	0.04
Sept 26 – 29, 2017	<u>128</u>	<u>320</u>	20235 ^e	43.8	6.5	122.5	98.2	0.61	160	375	755	0.9	44.7	33.8	82.9	0.22
Total	164	400	18533	31.3	-	120.3	122.9	0.67	189.3	395	864	0.9	-	34.1	106.5	0.26
Jun 9 – 10, 2018	13.92	15	503	10	5.0	2.5	1.8	0.01	12.5	16	684	10.3	1.8	1.2	54.7	0.11
23-Jun-18	12.27	6.6	947	21.4	1.9	1.8	28.5	0.08	8.4	5	354	8	0.5	0.2	-15.5 ^d	-0.03
Jul 7 – 8, 2018	119.2	178	13153	30.6	1.9	25.5	5.2	0.08	78	96	8949	21.6	4.7 ^c	42.5	99.7	0.27
Jul 24 – 25, 2018	132.9	550	12362	25.8	3.2	39.3	38.9	0.22	<u>152</u>	<u>680</u>	15843	19.6	13.1	207.2	266.9	0.89
Aug 4, 2018 ^a	*	*	*	*	*	*	*	*	*	*	*	*	*	*	*	*
Aug 18 – 19, 2018	19.12	8	0	0	*	0.0	-10.3 ^d	-0.03	<u>32</u>	<u>60</u>	651	3.8	4.1	2.7	-0.5 ^d	0.00
Oct 13 – 14, 2018	114.5	63	7044	17	2.0	14.4	58.8	0.20	<u>100</u>	<u>65</u>	7789	14.7	5.2	40.2	55.7	0.18
Total	411.8	821	34010	22.9	-	83.5	122.9	0.57	382.8	922	34270	17	-	294.0	461	1.42

Table 2-3 (continued). Precipitation, rain energy, settling tank masses, and fines estimates: settling tank plots, 2017-2018

Collection Dates	Lacustrine, High Traffic (M270)								Lacustrine, Low Traffic (P286)									
	Precip (mm)	El ₃₀	Disch. (L)	Eff (%)	SSC (g/L)	Fines (kg)	Tank (kg)	Av. (kg/m ²)	Area 470 ^b	Precip (mm)	El ₃₀	Disch. (L)	Eff (%)	SSC (g/L)	Fines (kg)	Tank (kg)	Av. (kg/m ²)	Area 320
Aug 15 – 16, 2017	*	*	*	*	*	*	*	0.00		*	*	*	*	*	*	*	*	
Sept 26 – 29, 2017	245.5	613	1486	1.3	48.2 ^c	71.6	817.0	1.85		159.9	399	6793	13.3	1.1	7.1	90.2	0.30	
Total	245.5	613	1486	1.3	-	72.0	817.0	1.27^b		159.9	399	6793	13	-	7.1	90.2	0.30	
Jun 9 – 10, 2018	25.2	58	0	0	*	0.0	-7.0 ^d	-0.01		*	*	*	*	*	*	*	*	
23-Jun-18	*	*	*	*	*	*	*	*		*	*	*	*	*	*	*	*	
Jul 7 – 8, 2018	96.8	126	10148	21.8	*	*	133.6	0.28		147.9	272	1114	2.4	0.5	0.6	17.8	0.06	
Jul 24 – 25, 2018	141.7	502	4346	6.4	*	*	2.1	0.00		168.8	906	6293	11.6	0.7	4.3	16.4	0.06	
Aug 4, 2018 ^a	*	*	*	*	*	*	*	*		18.98	131	314	5.2	*	0.0	-8.1 ^d	-0.03	
Aug 18 – 19, 2018	21.9	7	195	1.9	1.1	0.2	12.9	0.03		16.05	14	0	0	*	0.0	9.9	0.03	
Oct 13 – 14, 2018	95.3	43	9498	20.8	4.0	37.5	63.1	0.21		68.98	66	*	*	*	*	-16.9 ^d	-0.05	
Total	380.8	736	24188	12.8	-	37.7	205.0	0.51		420.7	1389	7720	5.7	-	4.8	19.2	0.07	

Table Footnotes:

^aVery little precipitation during this period. Only one plot responded significantly to rain.

^bUpper plot boundary compromised during this period. Total contributing area estimated 700 m²

^cSub-sample bucket over-filled

^dFalse negative values caused by water level measurement errors. IBC Tote dimensions are: 114.3 x 101.6 cm (45 by 40 in.) such that a 1 cm reading error propagates to a about 11.6 kg weighing error.

^eLogger memory filled, tips under-counted

Table 2-4. Rain energy versus yield regression equations by plot

Plot	Intercept		Slope (kg/m ²)/(MJ·mm/ha-hr)*		Formulas	R ²
	2.50%	97.50%	2.50%	97.50%		
P7131	0.09	0.93	-0.0008	0.0054	0.00115*EI30+0.2436	0.19
P4128	-0.13	0.42	-0.0014	0.0053	0.00049*EI30+0.0279	0.41
P4107B	-0.12	0.37	-0.0015	0.0046	0.00037*EI30+0.0302	0.3
P295	-0.14	0.32	-0.0015	0.0044	0.00044*EI30+0.0106	0.83
M270	-0.14	0.17	-0.0012	0.0026	0.0007*EI30+0.0127	0.43
P286	-0.15	0.34	-0.0019	0.0040	0.00005*EI30+0.0081	0.13

*RUSLE K-values are equivalent to ten times slope

Table 2-5. Silt fence erosion data

Bolded values are seasonal totals; prod/EI30 is equivalent to RUSLE-K factor. Values are normalized for plot length and slope (Table 2-2) using, RUSLE LS relationships.

Plot	Date	El ₃₀	Mass (kg)	Area (m ²)	Av. Prod. (kg/m ²)	Norm. Prod. (kg/m ²)	Prod/EI ₃₀ (kg/m ²)/(MJ·mm/ha-hr)
P7131 (silt fence)	17/09/2016	564	809	338	2.39	1.01	1.8x10 ⁻³
	07/08/2016	56	2457	2368	1.04	0.10	1.9x10 ⁻³
	25/08/2016	163	3096	2368	1.31	0.13	8.0x10 ⁻⁴
	17/09/2016	21	341	2368	0.14	0.01	6.9x10 ⁻⁴
P4107A (2016)	Total	240	5893	2368	2.49	0.25	1.0x10⁻³
P4107A (2017)	10/06/2017	74	1278	2368	0.54	0.05	7.3x10 ⁻⁴
	07/07/2017	117	1690	2368	0.71	0.07	6.1x10 ⁻⁴
	24/07/2017	18	1747	2368	0.74	0.07	4.1x10 ⁻³
	29/09/2017	391	866	2368	0.37	0.04	9.0x10 ⁻⁵
P4107A (2017)	Total	600	5581	2368	2.36	0.24	3.9x10⁻⁴
P4107A (2018)	08/07/2018	396	682	2368	0.29	0.03	7.0x10 ⁻⁵
	25/07/2018	1136	2201	2368	0.93	0.09	8.0x10 ⁻⁵
	Total	1532	2883	2368	1.22	0.12	8.0x10⁻⁵
P4108 (2017)	10/06/2017	74	781	470	1.66	1.74	2.4x10 ⁻²
	07/07/2017	117	703	470	1.50	1.57	1.3x10 ⁻²
	24/07/2017	18	714	470	1.52	1.59	8.8x10 ⁻²
	26/09/2017	391	35	470	0.07	0.08	2.0x10 ⁻⁴
P4108 (2017)	Total	600	2233	470	4.75	4.98	8.3x10⁻³
P4108 (2018)	08/07/2018	396	156	470	0.33	0.35	8.8x10 ⁻⁴
	25/07/2018	1136	398	470	0.85	0.89	7.8x10 ⁻⁴
	Total	1532	554	470	1.18	1.24	8.1x10⁻⁴
P4111	10/06/2017	74	363	300	1.21	0.90	1.2x10 ⁻²
	07/07/2017	118	255	300	0.85	0.63	5.4x10 ⁻³
	24/07/2017	18	390	300	1.30	0.97	5.4x10 ⁻²
	26/09/2017	391	29	300	0.10	0.07	1.9x10 ⁻⁴
P4111	Total	601	1038	300	3.46	2.58	4.3x10⁻³

Table 2-6. Maximum management lengths for the Simonette watershed

Maximum Management Area (m ²)		3500			
Road segment type	Camber	Ditch Width (m)	Cutslope (m)	Contributing Roadway (m)	Max. Length (m)
Raised, well-drained road segment	Crowned	5	N	5	350
	Insloping	5	N	10	233
Cut-and fill segment	Crowned	5	5	5	233
	Insloping	5	5	10	175
Through-cut or wind-rowed	Either	5	5	10	117

2.8 Figures

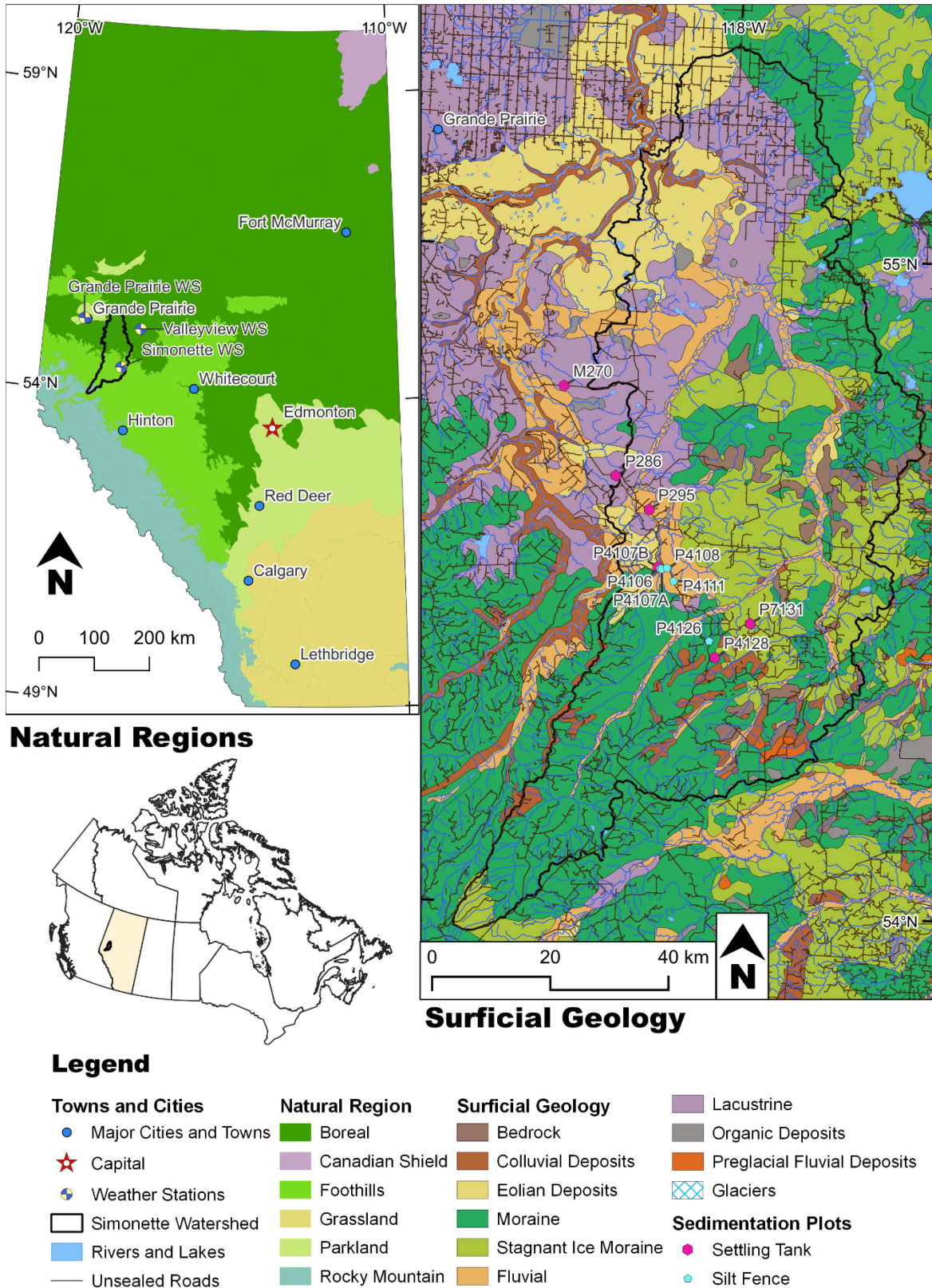


Figure 2-1. Location of the Simonette study area in Alberta with mapped surficial geology



Figure 2-2. Settling tank plot components (A) open top wooden culverts draining a road segment, (B) tipping bucket mechanism, (C) weighing frame with battery-operated winch



Figure 2-3. Typical silt fence erosion plots in the Simonette
The left shows a silt fence under dry conditions, the right shows ponding during a rain event.



Figure 2-4. Gullied ditches in the Simonette

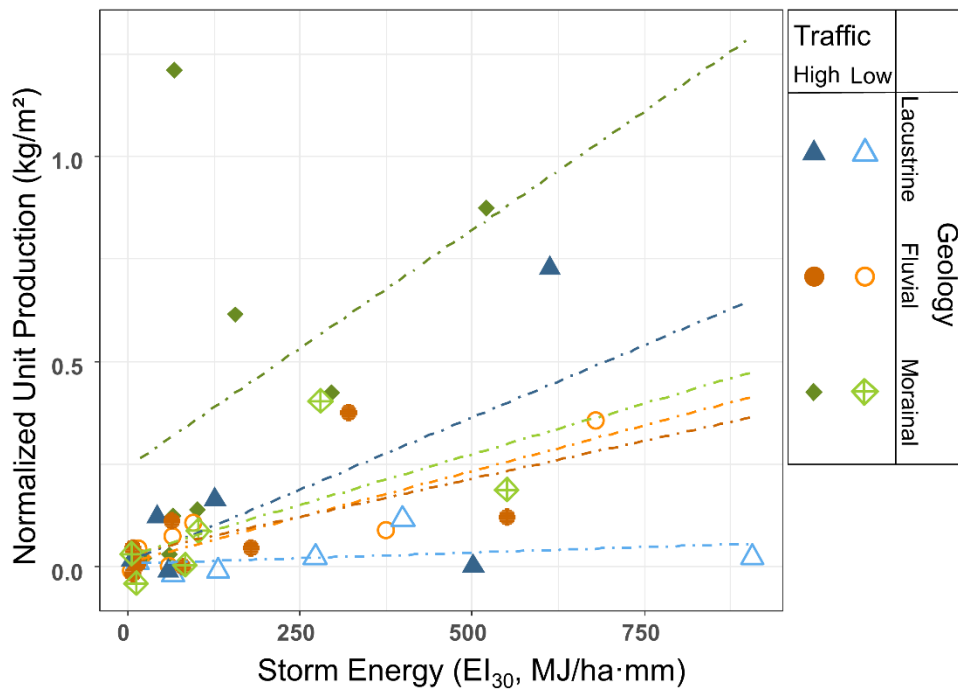


Figure 2-5. Sediment production rate versus storm energy by settling tank plot

Blue plots are in glaciolacustrine sediment, orange plots are glaciofluvial, green plots are morainal. Darker-shaded plots are on high-traffic roads, and lighter-shaded plots are on low-traffic roads. The large outlier in the high-traffic morainal plot was collected following a large, early fall snowstorm, with persistent, low-intensity flow and regular vehicular disturbance during snowmelt.

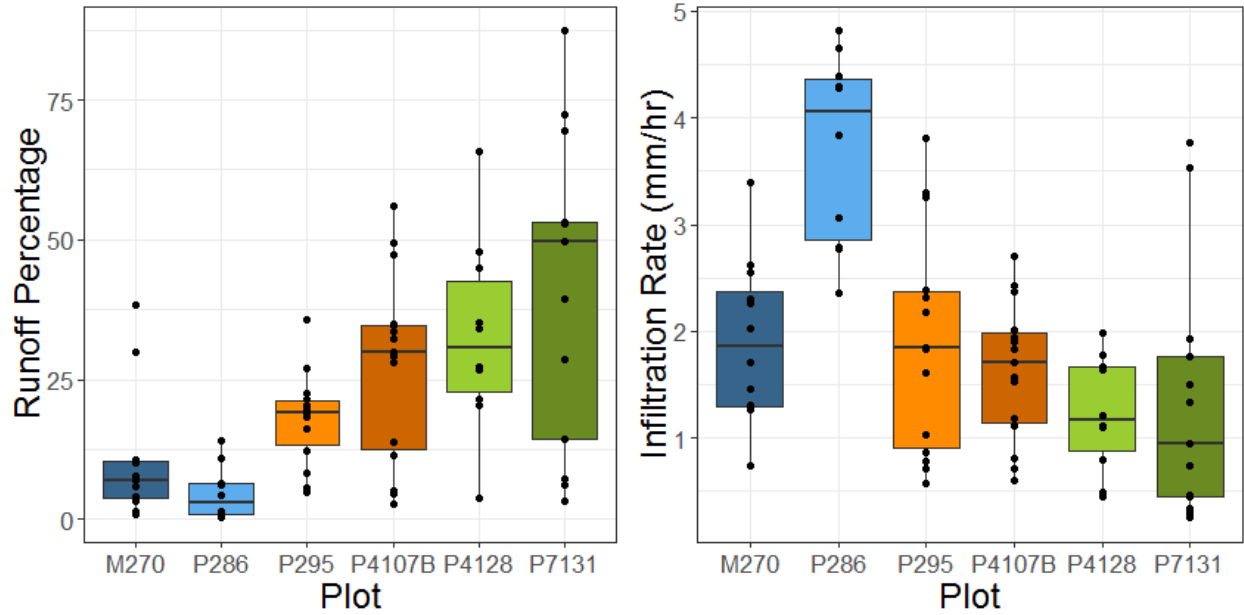


Figure 2-6. Plot runoff-generating efficiency (left) and peak infiltration rate by plot (right)
Plot colours represent traffic and surficial geology, with blue representing lacustrine sediment, orange fluvial sediment, and green morainal sediment, lighter shades represent low traffic, and darker shades high traffic.

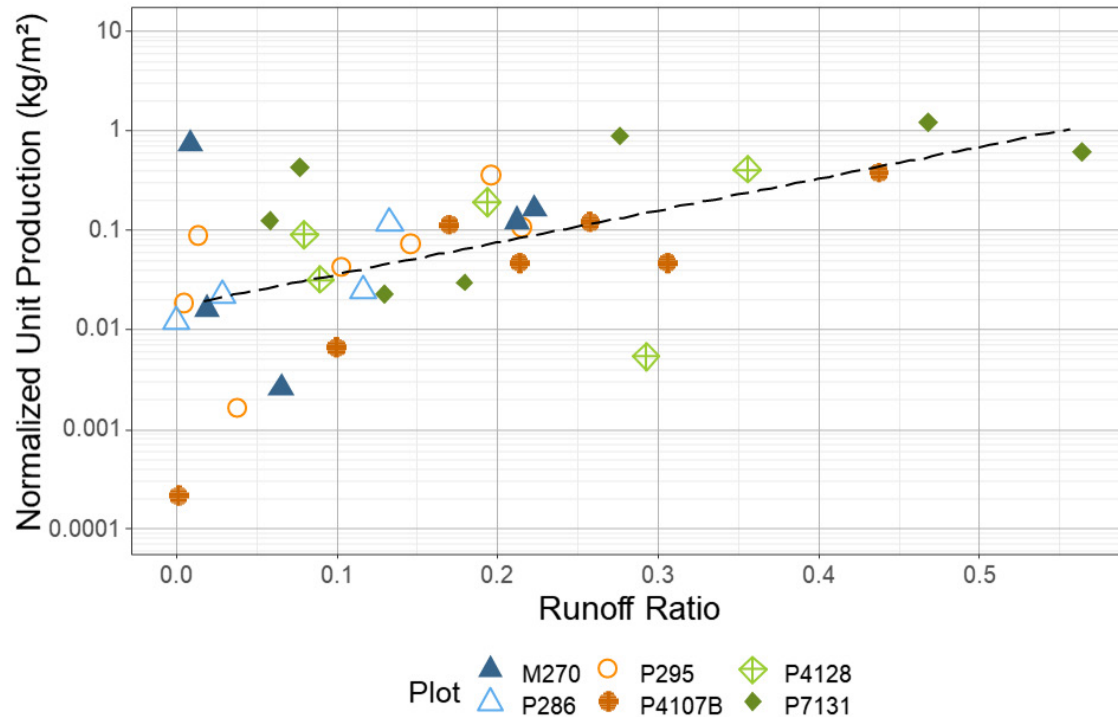


Figure 2-7. Sediment yield compared with runoff efficiency for settling tank plots.
Vertical scale is logarithmic. Note that sediment production generally increases with runoff ratio and rate of increase is non-linear.

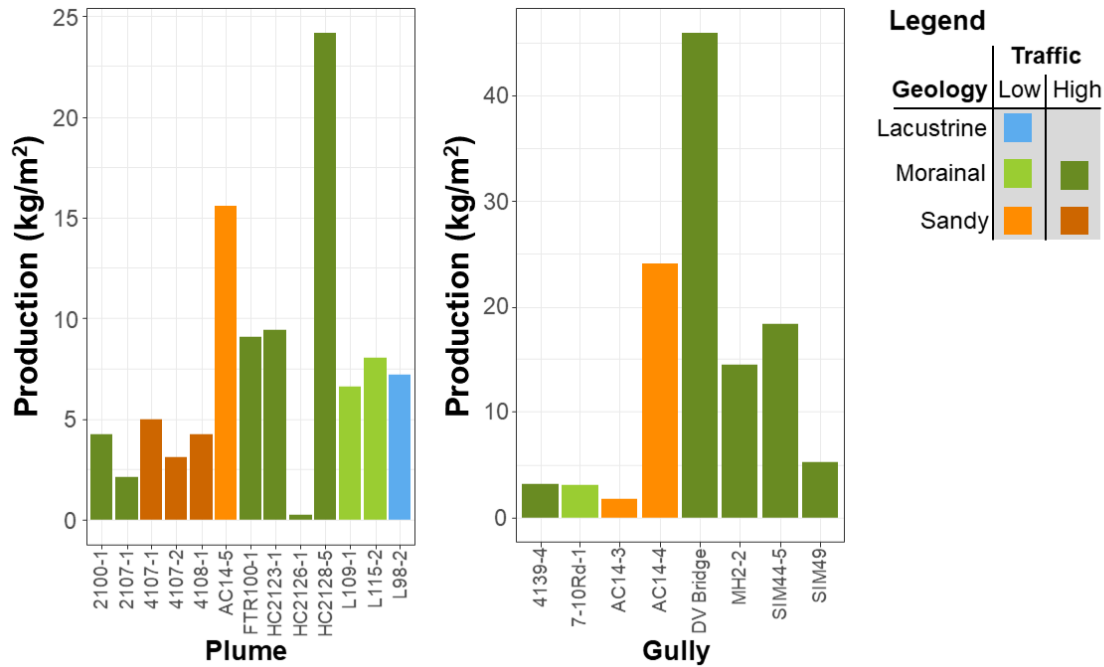


Figure 2-8. Comparison of erosion rates estimated from plume extent and thickness from non-gullied road segments (left), and gully surveys (right)

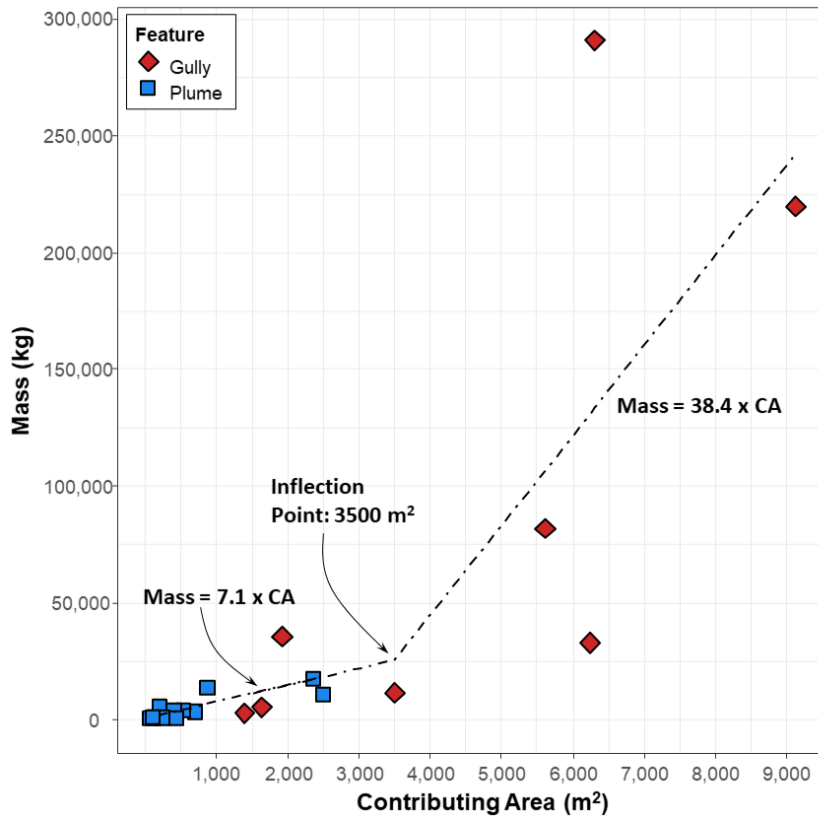


Figure 2-9. Relationship between contributing area and mass for plumes (blue) and gullies (red) showing threshold erosion behaviour for contributing areas greater than 3500 m²

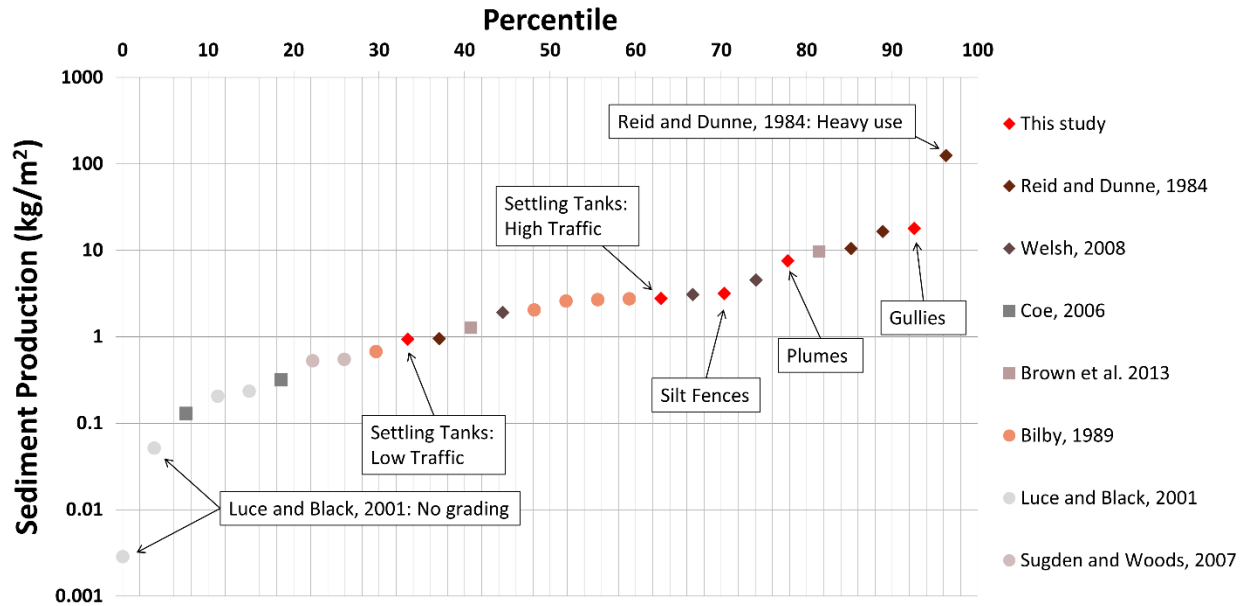


Figure 2-10. Comparison of road sedimentation rates in the Simonette and other areas.

Annualized erosion rates in the Simonette were obtained by dividing the seasonal erosion estimate by the fraction of total seasonal precipitation captured during the measurement period (seasonal precipitation being defined as any precipitation falling during the period of year with average temperatures above 0°C). These sedimentation rates are visually compared with other studies in North America in (a corresponding table is included in the Appendices) (Bilby et al., 1989; Brown et al., 2013; Coe, 2006; Luce & Black, 2001b; Reid & Dunne, 1984; Sugden & Woods, 2007; Welsh, 2008). Studies are ranked according to sediment production from lowest to highest. Rates from this study range from just under the 50th percentile to over the 90th percentile of the studies mentioned. Gullying and large plumes account for a higher erosion risk than plots with limited areal extent.

3 Road-Related Contributing Area as a Driver of Sediment Plume Size for Unsealed Roads In West-Central Alberta, Canada

3.1 Introduction

Unsealed gravel or native surface roads are a key part of resource extraction infrastructure in remote regions, and are used by rural municipalities, and mining, oil and gas, and forestry companies. Unpaved roads also come with an environmental cost: a number of studies show that unpaved resource roads contribute the majority of anthropogenic sedimentation to streams in forested watersheds (Cederholm et al., 1980; Elliot, 2013; Megahan & Kidd, 1972). In some cases road segments draining into streams contribute between 18-21% of reach sediment (Bilby, 1985; Reid et al., 2016). Sediment delivery stops when roads are hydrologically disconnected from the stream network (Bilby et al., 1989; Hairsine et al., 2002). Both industrial and academic stakeholders therefore have an interest in understanding the processes responsible for connecting roads to streams and what management practices can minimize this connection.

3.1.1 Factors influencing road sediment connectivity

The most commonly studied indicator of road connection potential to the stream network is a trace of the overland flow of sediment and water from a road drainage point known as a sediment plume (Figure 3-1). Sediment plumes can provide direct evidence of road connection to the stream network and show the likely range of sediment travel lengths that can be expected for roads in a particular region. Expected sediment plume travel lengths can be compared with mapped hillslope buffer distance between road segments and streams to predict connectivity. Road sediment plume studies have found that plume runout behaviour is controlled by a number of landscape factors which may vary from region to region (ie. Brake et al., 1997; Coe, 2006; Megahan & Ketcheson, 1996; Packer, 1967). Table 3-1 shows published landscape factors and their influence on plume length. A major conceptual driver of models predicting sediment plume size is the amount of water generated on the road surface; therefore it is not surprising that the length of sediment plumes has been reported to be positively correlated with contributing area, road length, and sediment volume in the plume (Brake et al., 1997; Coe, 2006; Megahan & Ketcheson, 1996; Rivenbark & Jackson, 2004; Woods et al., 2006). Length-slope or contributing area-slope relationships are often related to the speed and intensity of overland flow development on road segments or hillslopes, influencing slope erosional processes and rates and have been shown in the

past to contribute to sediment plume length (Coe, 2006; Dietrich et al., 1992; McCool et al., 1989; Montgomery, 1994). Road network connectivity can also increase from regions with lower to higher rainfall intensity and duration (Al-Chokhachy et al., 2016; Benda et al., 2019; Bilby, 1985; Cederholm et al., 1980; Coe, 2006; Croke et al., 2005; Sidle et al., 2004). Once a flow of water and soil is generated on a road surface, it must either infiltrate into a receiving hillslope or break through into a stream. The infiltration capacity of roadside drainage ditches or the hillslope below the road outlet is therefore one of the main factors affecting sediment plume size (Bilby et al., 1989; Croke et al., 2005; Elliot & Tysdal, 1999; Hairsine et al., 2002; Takken et al., 2008). Underlying geological materials influence the size of surfacing aggregates and drainage of receiving slopes, which may drive variation in plume length in areas with different underlying geology (Coe, 2006; Packer, 1967; Woods et al., 2006). Roads with heavier vehicle traffic also generally have higher erosion rates, which leads to longer plumes (Coe, 2006). Type and frequency of drainage is also a key factor in sediment plume propagation. Plumes from culverts are longer than those from road fills and rock drains, both of which allow for more diffuse and more frequent road drainage (Megahan & Ketcheson, 1996). Factors that influence the confinement and velocity of the water flowing on the receiving slope also affect the sediment plume length, and include obstruction spacing and type (Brake et al., 1997; Packer, 1967), hillslope roughness, forest floor slope below the culvert (Brake et al., 1997), and dispersive versus gullied hillslope flow paths (Coe, 2006; Croke & Mockler, 2001; Rivenbark & Jackson, 2004).

3.1.2 Conceptual model of plume formation

Studies in Australia have sought to provide a hydrological model of plume runout behaviour. Hairsine et al. (2002) proposed that road sediment plumes utilize forest floor hydrological storage as they break through a buffer zone, thus requiring a certain amount of water to travel a set distance through a buffer. Plume advance is therefore a non-equilibrium storage process. This volume-to-breakthrough approach assumes that no significant infiltration occurs in the body of the plume once it has advanced, an assumption which may not hold in all situations (Thompson et al., 2008). Benda et al., (2019) presented an alternative model which assumes that road sediment plumes are propagated when the water input exceeds the equilibrium infiltration capacity of the receiving slopes. The model generates overland flow on unpaved road surfaces and ditches using equation 1, and estimates the length of the plume from the drainage point using equation 2:

$$(1) \quad Q_{DRAIN} = L_R W_{RCA} * P + L_R W_D (P - i_D)$$

$$(2) \quad L_P = \frac{Q_{DRAIN}}{W_P * (i_S - P)}$$

The effective discharge at the drain (Q_{DRAIN}) is equal to the length of road (L_R) multiplied by the effective contributing road width (W_{RCA}), and precipitation rate (P) added to the ditch width and length (W_D, L_R) multiplied by effective precipitation ($P-i_D$). The length of the plume is equal to Q_{DRAIN} divided by plume width (W_P) and effective infiltration in the receiving slope ($i_S - P$). Roads may in fact infiltrate a considerable quantity of rain during rainstorms (Croke et al., 2006; Hairsine et al., 2002; and see Chapter 2 of this thesis) and therefore a road infiltration term (i_R) is added for this study in equation 1:

$$(1b) \quad Q_{DRAIN} = L_R W_{RCA} * (P - i_R) + L_R W_D (P - i_D)$$

Water is routed down the road surface using a sheet-flow kinematic wave function (Overton & Meadows, 1976; Welle & Woodward, 1986), off the road surface into ditches, and then onto hillslopes as overland flow. The sheet-flow kinematic wave equation is:

$$(3) \quad T_{CR} = \alpha \frac{n L_R^{0.6}}{P_E^{0.4} S^{0.3}}$$

where T_{CR} is time of concentration in minutes, α is a unit conversion factor dependent on units of length and time used in analysis, n is the Manning constant, L is the length of the road, and P_E is effective precipitation ($P-i_R$). The time of concentration for the plume T_{CP} has the same form as equation 3, although the length of plume from equation 2, is substituted for L_R , and (i_S-P) is substituted for effective precipitation. If the model (Benda et al., 2019) is an appropriate representation of reality, then the relationship between sediment plume area and the road contributing area should be related to the proportional difference in effective precipitation (Equations 5 and 6, from Dan Miller, pers. comment):

$$(5) \quad A_P * (i_P - P) = A_{CA} * (P - i_{CA})$$

$$(6) \quad \frac{A_P}{A_{CA}} = \frac{P - i_{CA}}{i_P - P}$$

where A_P is the area of the sediment plume, and A_{CA} is the total area contributing to the plume, P is the rainfall input in mm/hr, and i_{CA} and i_P are the infiltration rates in the contributing area and plume respectively. Equation (6) should hold in a region that has distinct rainfall intensity and duration, road infiltration, and hillslope soils. This is to say, averaged over a number of years, the area relationships of plumes in a watershed should be related to regional watershed constants,

particularly the relationship between precipitation intensity and frequency. Factors such as road slope, hillslope shape, and confinement may influence the shape of the sediment plume, driving a robust length derivation from modelled plume area.

3.1.3 Research objectives

This study examines road sediment connectivity in the boreal plains and foothills of west-central Alberta. The region of study is sparsely populated, and resource companies have expansive road networks to manage, and limited funds available to direct towards road remediation. Efforts to mitigate road-stream sediment connectivity in this region need to be tailored toward landscape features that can be easily obtained via remote sensing or consultation of high-level geographic data, such as road shapefiles, LiDAR coverage, and soils or surficial mapping.

In this study the key parameters that determine road sediment plume size and runout distance were examined. It was hypothesized that empirical relationships between sediment plumes and landscape features have an explicit hydrological meaning. The hydrological area index of plume area versus contributing area was predicted to represent a contrast in infiltration between the weighted average contributing area and the target hillslope that varies with mapped surficial geology type and possibly traffic level on roads. The hydrological behaviour of plume runout was examined using hydrological modelling software to estimate runout length and area for plumes with known geometrical characteristics.

3.2 Study area and methods

3.2.1 Study area

The Simonette watershed straddles the foothills and boreal plains natural regions of Alberta, south of the city of Grande Prairie (Figure 3-2). The area of the watershed is about 5400 km². The watershed contains about 3010 km of active road as of 2015, of which about 2530 km is gravelled and about 480 km has a natural surface. Average road density for the watershed is about 0.67 km/km². Elevation varies from about 1500 m in the southern headwaters of the watershed to around 530 m near the mouth. The river forms a deeply-incised valley through flat-lying glacial lake sediments for about 30 km from its confluence with the Smoky River. The remainder of the mainstem and tributaries flow through a hummocky to undulating kettled till plain. Glaciofluvial delta sediments form on the contact between the till deposits and the glacial lake near the headwaters of the tributary Latornell River. The southern portion of the watershed flows through

moderately-sloping bedrock-controlled foothills. The front ranges of the Rocky Mountains are located about 20 km southwest of the headwaters of the watershed.

Measured annual precipitation varies from 581 mm at the Simonette weather station in the centre of the watershed to 445 mm at the Grande Prairie Airport 110 km north-west (Canadian Climate Normals, 1980-2010). Precipitation during the summer often falls in short, intense thunderstorms in June, July, and August. The most powerful storms are large frontal systems that may deliver 90-110 mm of precipitation over a period of one to several days. Soil drainage is slow enough that unpaved roads may remain in a partially-saturated state through the beginning of the snowmelt season, and into late June or early July.

Land-use in the Simonette is dominated by forestry and oil and gas extraction. A small portion (6.8 km²) in the northeast is agricultural land used for cattle grazing and row crop cultivation. The dominant land-use type in an area affects disturbance patterns, road densities, and road types. Permanent main haul roads are usually 10-12 m wide and heavily-used. The Canfor Main haul road has on average 187 recorded passes per day from June through October, almost all of which are heavy trucks. Smaller, non-commercial pickup traffic is not recorded but is approximately five times greater than commercial traffic. The 4000 Main, a moderate-sized haul road accessing a remote southern portion of the watershed has about 100 passes per day, of which 18 are heavy truck traffic from June through October (Pers. Communication, Canfor Operations Staff). Main roads are typically constructed on a prepared subgrade of glacial clay which is compacted with sheep's-foot rollers. Geotextile fabric or plastic grids are often used on main roads to separate the subgrade from the road surface materials and to provide lateral shear resistance on otherwise highly plastic soils. Base and surface courses of gravel are imported and spread on the roads to improve running characteristics and stability, however, the roads rapidly form potholes during wet spring conditions. Smaller roads are designed to access forestry cutblocks or oil and gas wells and are usually a cleared trail in native material with the required cuts, and sometimes a thin layer of gravel surfacing. Roads used for forestry are usually deactivated as soon as winter hauling is complete, or at most within three years (Government of Alberta, 2016). Temporary roads are deactivated by pulling back the native soil layer, and scarifying the surface or placing coarse woody debris, both of which encourage rapid revegetation of the right-of-way. Oil and gas well service roads are used for years to decades and have infrequent heavy use by large oilfield service vehicles, and periodic ATV or pickup use by wellsite production operators. Areas of intense oil and gas

exploration activity therefore account for the highest road densities in the Simonette watershed. Agricultural land use in the northeastern portion of the Simonette watershed accounts for a much higher rate of disturbance, with a dense, rectilinear network of township and range roads, and fields of annual dryland row crops.

3.2.2 Field data collection

3.2.2.1 Site selection

To obtain a broad representation of sediment plumes and possible factors controlling the sediment plume dimensions, data on sediment plumes were collected in three phases, and then aggregated for analysis. A reconnaissance survey and measurement of 26 plumes throughout the watershed was conducted in late summer of 2016. During the reconnaissance it was observed that a number of larger, more visible plumes were mapped in sandy glaciofluvial terrain. It was hypothesized that plume extent may be related to surficial geology and traffic and roads were stratified in the Simonette watershed accordingly. To test the hypothesized influence of surficial geology on plume extent, the roads were stratified by three levels of geology (lacustrine, fluvial, and morainal), and two levels of traffic (high and low, for a total of six stratification categories. Each road was divided into 1 km segments (transects) and 27 randomly selected road transects from each category were measured in 2017. If a transect was inaccessible, then the next-ordered transect was investigated. Investigated transects were walked or driven and sediment plumes encountered in the 1 km transect were measured. In 2018 another 28 sediment plumes were measured to refine estimates of sediment contribution in a portion of 24 sub-watersheds (10-20 km²) selected for a study of geomorphic consequences of roads in the Simonette watershed (Chapter 4 of this thesis). Sites measured in 2018 were organized to follow the requirements of a geomorphic stream survey, which described stream reaches in watersheds stratified by road density (high, medium, and low) and by ecological region. Plumes were investigated in individual watersheds over several weeks through June and early July 2018.

3.2.2.2 Sediment plume data collection

Data were collected using standardized field cards with the variables listed in Table 3-2. Dependent variables were related to plume geometry and connectivity, and independent variables were related to the geometry of the contributing area, underlying environmental parameters, and design elements like traffic and maintenance levels. The geographic location of each plume and its relative location in the road network were also recorded using GNSS receivers (Garmin GPSMap or

Trimble Geo7x with a Zephyr 2 antenna). Plumes were named according to the nearest kilometre posting with a hyphenated number denoting the plume number in that road section (ie. 4107-1).

3.2.2.3 *Sediment plume area calculations*

Plume and road geometric characteristics were measured and mapped using the most practical tools available. In the 2018 field season, where there was good satellite coverage and open canopy, plume geometry was collected using a sub-meter resolution GNSS (Trimble Geo7x) collector with L1 frequency band enabled. GNSS-collected plume outlines were post-processed and edited in ArcGIS. Prior to obtaining the GNSS data collector, and in areas with heavy forest cover or precise detail which limited usability of the GNSS collector, plume mapping was carried out by hand using closure, offset, or grid methods with compass, clinometer (Brunton or Silva, accurate to ± 0.5 percent), and a fibreglass tape-measure. In practice, the closure method with the tools available produced unacceptable errors, and so most plumes were mapped by taking perpendicular offsets along traverse lines following the plume centreline. For some larger, and more complicated plumes the best field method was to lay out a 5 x 5 m grid over the sediment plume and delineate the outer contours of the plume relative to the grid. Hand-surveyed plume notes were digitized into outlines and areas using COGO tools in ArcGIS. Where plume volumes were desired, average depth was measured by digging through sediment plumes with a spade or coring with a soil-corer, usually by taking 2-3 depth measurements along a plume offset location or, for plumes measured using the grid method, at measured grid points. Offset depths were either integrated using the end area average method for prism volumes, or for gridded plumes, depth measurements were input into GIS software and kriged over the measured plume extent to provide an estimate of depths.

3.2.3 **Statistical methods**

The relative influence of predictor variables was assessed using random forest modelling in the RandomForest package in R (Liaw & Weiner, 2002; R Core Team, 2019). Continuous response and predictor variables were further analysed using pairs plots and correlation charts with the ggPlot package in R (Wickham, 2016). Predictor variables which were well-correlated (collinear) were excluded from analysis, and linear step models were run to determine the best combination of linear prediction variables for sediment plume length and width. We tested qualitative differences in road and runout area conditions by analyzing the residuals of the best linear models using Kruskal-Wallis tests with Dunn comparisons (dunn.test package, Dinno, 2017).

3.2.4 Steady-state plume hydrological model calibration

Plume geometric relationships, and data from a previous study of road hydrology and erosion (Chapter 2) were used to calibrate a hydrological model of plume development (Benda et al., 2019), using Microsoft Excel. Hydrological input values included: storm precipitation rate and duration, length, area, and infiltration rates of the road section, Manning's roughness (n), and grade of plume and contributing areas. Monte Carlo simulations were used to estimate most probable ranges of infiltration rates for roads and contributing areas given a range of probable precipitation intensities using a random number generator (Table 3-3). The results of each trial were investigated using Nash-Sutcliffe efficiency statistics, root mean square errors of the simulated variable versus the field estimate, and visual comparison of each model run with the 1:1 line.

The range of road infiltration and precipitation values was derived from one and a half summers' worth of erosion plot monitoring in the Simonette watershed. The events used to estimate road infiltration were a subset of the precipitation and infiltration dataset with relatively long periods of even precipitation, and a well-defined response on the plot hydrograph. Plume area infiltration was unknown, but the potential limits were estimated by using equation 6 with the bootstrapped 95% confidence interval of the slope of a zero-intercept univariate regression between plume area and contributing area (Fox & Weisberg, 2019). The upper limit of precipitation for the model is slightly outside of the observed range of maximum 1 hour precipitation intensity at the Simonette weather station, and corresponds to an approximately 1 in 100 year event in Whitecourt, and a greater than 1 in 100 year event in Grande Prairie, the two nearest weather stations with IDF curves (Environment Canada, 2019). Table 3-3 shows the fixed and randomized input variables in the plume hydrological model, and the ranges of their values.

3.3 Results

3.3.1 Empirical relationships

3.3.1.1 Data summary and primary correlations

Of the 78 mapped and described plumes in the Simonette watershed, 62 plumes did not deliver sediment to streams. These 62 plumes and were selected for further analysis, as some water from the connected plumes reached the stream and did not infiltrate. The plumes were mostly concentrated in a belt from east to west in the central portion of the watershed (Figure 3-2). The distribution of categorical variables in the data is shown in Figure 3-3, including plume aspect, slope

topography, soil type, road maintenance and traffic variables, surfacing, and type of drain point or outlet causing the plume. Although data collection was stratified to attempt to achieve a balanced sample, the resulting data did not equally represent all types of sediment plumes. Sediment plumes were generally more prevalent on high or moderate traffic roads, and in mixed or coarse terrain. Sediment plumes were less prevalent on lower traffic roads and in glaciolacustrine areas in flat topography, likely because water typically collected in poorly-drained low spots or ran off the sides of the road into ditches rather than travelling down the running surface. Some variables, such as aspect, outlet type, topography, and surfacing, were not controlled for in the sampling strategy.

Random Forest models of plume geometric attributes identified that the most consistently influential predictors of plume area and length were road length, road contributing area, and total contributing area with ditches and cutslopes included. Qualitative variables such as geology type, traffic, and outlet type were of secondary importance. A correlation grid of plume geometric measurements versus contributing area geometric attributes indicated that good predictors of plume area and length were either road area or total contributing area (Table 3-4). Length-slope and contributing area-slope interactions were also considered. Plume analysis in this study was done using an area-slope interaction product as it was more robust than a length-slope interaction ($r = 0.54$ plume length; $r = 0.84$ plume area). Since road length and road contributing area are collinear variables ($r = 0.85$), and total contributing area was also collinear with both road length ($r = 0.71$) and area ($r = 0.85$), regressions were limited to only using the most correlated non-collinear variables.

3.3.1.2 Plume length and area relationships, and outlier analysis

Plume length and area show an overall increasing relationship with respect to contributing area (Figure 3-4, left) with most sediment plumes plotting close to the lines of best fit. Some points do not follow the trends, including two extremely long (233 and 86 m) plumes relative to contributing area were confined in long, narrow, artificial drainage ditches or swales (Figure 3-4, upper right). Two other plumes originated from a culvert failure. The shorter plume deposited until the culvert filled up with sand, and the water overtopped a nearby ditch block and caused gully erosion in the ditch below (Figure 3-4, lower right). Both plumes were shorter and smaller than the general trend of the plume area regression but combining the two results in a larger plume close to the central regression line (Figure 3-4, shown in red). The largest plume in the dataset (852 m²) has a gullied ditchline, and tall cutslopes which extended part way up a hill, so the contributing area

may have been underestimated. Another large plume (612 m²) flowed into a relatively wet site and may have propagated farther than expected due to poor drainage. Two other larger-than-expected plumes were likely a result of measurement error from using the closure method to estimate shape and extent during summer 2017. Site level variations like these may in part explain the difference between area outliers. Regressions described in this chapter exclude the two large plumes from summer 2017, which were likely to be measurement errors, and merged the two plumes related to the culvert overflow as they represent different parts of the same event.

3.3.1.3 *Sediment plume empirical model selection*

The road length, road area and total contributing area were collinear predictor variables (Table 3-4), so only contributing area, road grade, and plume slope were used for multivariable regression analysis. Multivariable regressions used the following continuous variables: contributing area, road grade, and plume slope. Interactions of plume slope and road grade with contributing area were also represented. The best plume length regression model ($R^2 = 0.43$, $RSE = 28.29$ m) only included contributing area (Table 3-5, Model 1), whereas the best plume area regression model ($R^2 = 0.77$, $RSE = 80.7$ m²) is a the product of contributing area and road grade (Table 3-5, Model 2).

Nonparametric tests were used to determine which categorical variables were likely to produce plumes larger or smaller, longer or shorter than the regression mean. Table 3-6 presents the results of a Kruskal-Wallis test of residuals with respect to qualitative plume attributes. The only significant difference between plume geometry was a difference in the plume area residual ($p = 0.04$) with respect to slope aspect. A post-hoc Dunn's test on the residuals suggests that west-facing slopes may have smaller plumes than north-facing slopes.

3.3.2 **Road infiltration modelling**

Contributing areas include sections of road, ditches, and cutslopes, and therefore the slope of the regression line may represent the ratio of average infiltration rate in contributing areas versus infiltration rate in the plume runout area (Figure 3-4, top). Road infiltration data were available from a previous study of road infiltration and sediment production in Chapter 2 of this thesis, however, ditch and cutslope infiltration rates were unknown. Estimated ranges of road infiltration rate from analysis of road runoff data in the Simonette watershed are shown in Figure 3-5 (left) with a table of averages to the right of the figure. For the analyses we excluded hydrographs which had uneven precipitation patterns, large peaks, and likely loss off the sides of the road, although it

should be noted that even including large or uneven events did not substantially change the *average* steady-state estimates of infiltration rates shown to the right of the figure. Most roads had infiltration rates of 1-2 mm/hr under even precipitation conditions except for one road, P286, on a sandy glaciolacustrine terrace, which had infiltration rate of 3.7 mm/hr. The limits for road infiltration were therefore varied between about 3.2 and 1.2 mm/hr (Table 3-3).

The equation of best fit for a univariate regression of plume area versus contributing area had a 95% bootstrapped confidence interval of:

$$Area = (0.085 \pm 0.015) \times Contributing Area$$

Using the confidence limits above, and solving equation 6 for plume infiltration (i_p) provided the following upper and lower limits for estimated plume infiltration rate: 1) for a steady rain of about 7 mm/hr over four hours (240 minutes), the upper and lower estimates of plume infiltration using the road infiltration limits of 1.2 – 3.7 mm/hr were about 47 – 96 mm/hr, and 2) for a heavy rain of 16 mm/hr over four hours, the upper and lower estimates of plume infiltration were 137 – 225 mm/hr. The estimates of plume infiltration for an extreme (16 mm/hr) event are not likely in any setting, let alone a till-dominated post-glacial landscape, so modelled infiltration was capped below 120 mm/hr. The estimates are also likely somewhat high because some contributing areas include areas of ditches and cutslopes

The READI model had high equifinality and simulations did not converge on a narrow range of parameter estimates; instead, increases in one variable were cancelled out by decreases in another. As a result the underlying statistical distributions for all variables except precipitation and infiltration were flat to randomly multimodal (Figure 3-6). Because of the scalar influence of precipitation and plume infiltration, the results of the simulation were dominated by these two variables, and cutslope, ditch, and road infiltration all interact with each other in making up the difference in water balance. There can therefore, be no central tendency for any of these values.

The relative accuracy of the model was much lower than empirical results. Predicted versus measured values for sediment plume area and length are depicted in Figure 3-7. The model consistently over predicted sediment plume length and tended to underpredict measured sediment plume area for larger plumes. The residual standard errors of the model run depicted in Figure 3-7 were 58 m and 136 m² for length and area respectively. Essentially, the length error was about one and a half times the standard deviation of the raw data (37.7 m), and the area residual was similar to the raw data (166.8 m²). Conversely, the residual standard errors for the empirical models in

Table 3-5 are 28.3 m and 80.7 m² for length and area, respectively. Although the model proposed by Benda et al. (2019) is theoretically applicable over a wider range of site conditions, when implemented in this study it predicted plume lengths and areas for a known sample of plumes with roughly twice as much uncertainty as the empirical model, and the same or greater uncertainty than the raw data.

3.4 Discussion

In road connectivity studies, the three most common factors tending towards longer plumes are obstruction spacing and/or density, length or area of contributing road drainage, and lower hillslope gradient (see Table 3-1). Road length and gradient interactions are also important, although they are more commonly associated with soil erosion potential (Coe, 2006; Luce & Black, 1999; Woods et al., 2006). This study shows an overwhelming influence of road-related drainage area on sediment plume development characteristics. The influence of other features such as obstructions and downhill slope was much lower. Obstructions were not a notable influence on plume length and were in fact omitted from this study because they were often not present or had a small diameter. Likewise, the gently undulating to rolling topography of the study area meant that the influence of forest floor slope was unlikely to show any effect on plume length, except possibly near steep incised stream crossings. The small sample size hampered investigation of some of the finer qualitative details that a more exhaustive study of road drainage would reveal, and which would help guide road drainage best management practices. Based on only a few observations, however, one might infer that long, confined drainage swales above stream crossings may not be a good strategy of reducing sediment delivery. Instead, they can increase erosion downslope (Coe, 2006; Croke & Mockler, 2001) and, more often than not, simply move the problem farther downslope (Elliot & Tysdal, 1999).

This study shows that road-related drainage area is a significant driver of downslope drainage problems. Other studies have presented similar results, as road drainage area modification thresholds (Montgomery, 1994), or as a relative source strength related to road area, soil infiltration, and precipitation intensity (Croke et al., 2005; Hairsine et al., 2002). Furthermore, the interaction of contributing area and gradient indicates that strength of runoff response from the road segment is an important factor in plume development. More steeply-sloping roads reach hydrological saturation sooner, and divert less water off the shoulders and into more permeable ditches and are therefore more important hydrological source areas.

The steady-state hydrological model used to model road runoff generation and plume development was not as reliable at estimating the length and area of road runoff plumes as the empirical relationships. One reason for this could be that the road runoff is not a steady-state or equilibrium process. Rain is very rarely steady: the most intense parts of storms tend to be short-lived relative to the total storm duration, so that an overland flow event may be better modelled as a pulse of rain. When modelled this way, it is possible that not all road segments will reach full saturation, but this ignores the potential of longer-duration, lower-intensity portions of the rainfall event to contribute to total and peak discharge. Neither is infiltration a steady process over time (Horton, 1945). Instead, forest soils have a certain amount of unsaturated storage that may be used up before water begins to infiltrate at a considerably lower, more steady state. This is the inherent assumption of the volume-to-breakthrough model proposed by Hairsine et al. (2002). These caveats need to be considered when implementing the hydrological model used above. It should be noted, for example, that the Benda et al. (2019) model can be run at steady or non-steady-state configurations. We chose to implement the model at a steady state in order to test a hypothesis about plume propagation. As this provides inadequate predictions, it may be more constructive to implement the model using typical storm lengths and infiltration rates for a watershed so that some road segments do not reach hydrological saturation.

3.5 Conclusion

This study found that road segments and associated contributing areas in ditches and cut-slopes were a good predictor of sediment plume runoff potential from the road segments. The area of sediment plumes was well-predicted by the product of the contributing area of a road segment and its grade, and the lengths of sediment plumes were moderately well-predicted by contributing area of the road segment. These relationships were hypothesized to have hydrologic meaning, with the ratio between sediment plume area and road contributing area being the inverse of infiltration rate in vegetated receiving slopes versus infiltration rate in the road-related contributing areas given a probable peak precipitation rate in a watershed. When this relationship was tested, using a hydrological model run at steady-state, there was poor agreement with measured plume extents. Given the highly significant interaction between contributing area and slope in predicting plume area, it was posited that sediment plume propagation is not well-modelled as a steady-state process. Other findings of the study included the observation that long, confined drainages such as those commonly produced to direct water away from stream crossings

may have actually allowed water to propagate farther downslope as reported in other studies (ie. (Elliot & Tysdal, 1999)).

3.6 References

- Al-Chokhachy, R., Black, T. A., Thomas, C., Luce, C. H., Rieman, B., Cissel, R., Carlson, A., Hendrickson, S., Archer, E. K., & Kershner, J. L. (2016). Linkages between unpaved forest roads and streambed sediment: why context matters in directing road restoration. *Restoration Ecology*, 24(5), 589–598. <https://doi.org/10.1111/rec.12365>
- Benda, L., James, C., Miller, D., & Andras, K. (2019). Road Erosion and Delivery Index (READI): A Model for Evaluating Unpaved Road Erosion and Stream Sediment Delivery. *Journal of the American Water Resources Association*, 55(2), 459–484. <https://doi.org/10.1111/1752-1688.12729>
- Bilby, R. E. (1985). Contributions of road surface sediment to a western Washington stream. *Forest Science*, 31(4), 827–838.
- Bilby, R. E., Sullivan, K., & Duncan, S. H. (1989). The generation and fate of road-surface sediment in forested watersheds in southwestern Washington. *Forest Science*, 35(2), 453–468.
- Brake, D., Molnau, M., & King, J. G. (1997). Sediment transport distances and culvert spacings on logging roads within the Oregon coast mountain range (Paper No. IM-975018) [Conference Presentation]. Presented at 1997 Annual International Meeting, ASAE, August 10-14, 1997, Minneapolis, MN. 12 pp.
- Burroughs, E. R., & King, J. G. (1989). *Reduction of Soil Erosion on Forest Roads* (General Technical Report INT-264). USDA Forest Service, Intermountain Research Station, July 1989, 21 pp.
- Cederholm, C. J., Reid, L. M., & Salo, E. O. (1980). Cumulative effects of logging road sediment on salmonid populations in the Clearwater River, Jefferson County, Washington. In *Salmon-Spawning Gravel: A Renewable Resource in the Pacific Northwest?* October 6-7, 1980, Seattle, WA. (pp. 1-35) . Retrieved from <https://www.fs.fed.us/psw/publications/reid/Cederholm.pdf>
- Coe, Drew Bailey Rogers. (2006). *Sediment Production and Delivery From Forest Roads in the Sierra Nevada, California* (Master's Thesis). Colorado State University, 110 pp.
- Croke, J., & Mockler, S. (2001). Gully initiation and road-to-stream linkage in a forested catchment southeastern Australia. *Earth Surface Processes and Landforms*, 26(2), 205–217. [https://doi.org/10.1002/1096-9837\(200102\)26:2<205::AID-ESPI68>3.0.CO;2-G](https://doi.org/10.1002/1096-9837(200102)26:2<205::AID-ESPI68>3.0.CO;2-G)

- Croke, J., Mockler, S., Fogarty, P., & Takken, I. (2005). Sediment concentration changes in runoff pathways from a forest road network and the resultant spatial pattern of catchment connectivity. *Geomorphology*, 68(3–4), 257–268.
<https://doi.org/10.1016/j.geomorph.2004.11.020>
- Croke, J., Mockler, S., Hairsine, P., & Fogarty, P. (2006). Relative contributions of runoff and sediment sources within a road prism and implications for total sediment delivery. *Earth Surface Processes and Landforms*, 31(4), 457–468. <https://doi.org/10.1002/esp.1279>
- Dietrich, W. E., Wilson, C. J., Montgomery, D. R., McKean, J., & Bauer, R. (1992). Erosion thresholds and land surface morphology. *Geology*. [https://doi.org/10.1130/0091-7613\(1992\)020<0675:ETALSM>2.3.CO;2](https://doi.org/10.1130/0091-7613(1992)020<0675:ETALSM>2.3.CO;2)
- Dinno, A. (2017). dunn.test (1.3.5) [Computer Program]. <https://cran.r-project.org/package=dunn.test>
- Elliot, W. J. (2013). Erosion processes and prediction with WEPP technology in forests in the Northwestern U.S. *Transactions of the ASABE*, 56(2), 563–579.
- Elliot, W. J., & Tysdal, L. M. (1999). Understanding and reducing erosion from insloping roads. *Journal of Forestry*, August 1999, 30–34.
- Environment and Climate Change Canada. (2019). Canadian Climate Normals and Averages 1981-2010. Retrieved July 7, 2020, from https://climate.weather.gc.ca/climate_normals/index_e.html
- Environment Canada. (2019). Short-Duration Rainfall Intensity-Duration-Frequency Data. Ottawa, Canada: Government of Canada. Retrieved from https://climate.weather.gc.ca/prods_servs/engineering_e.html
- Fox, J., & Weisberg, S. (2019). *An {R} Companion to Applied Regression* (3rd Ed.). Sage. <https://socialsciences.mcmaster.ca/jfox/Books/Companion/>
- Government of Alberta. Alberta Timber Harvest Planning and Operating Ground Rules Framework for Renewal (2016). Retrieved from [https://www1.agric.gov.ab.ca/\\$department/deptdocs.nsf/all/formain15749/\\$FILE/TimberHarvestPlanning-OperatingGroundRulesFramework-Dec2016.pdf](https://www1.agric.gov.ab.ca/$department/deptdocs.nsf/all/formain15749/$FILE/TimberHarvestPlanning-OperatingGroundRulesFramework-Dec2016.pdf) - section 11.1.2

- Hairsine, P. B., Croke, J. C., Mathews, H., Fogarty, P., & Mockler, S. P. (2002). Modelling plumes of overland flow from logging tracks. *Hydrological Processes*, *16*(12), 2311–2327. <https://doi.org/10.1002/hyp.1002>
- Horton, R. E. (1945). Erosional Development of Streams and their Drainage Basins. *Bulletin of the Geological Society of America*, *56*, 275–370. [https://doi.org/http://dx.doi.org/10.1130/0016-7606\(1945\)56\[275:EDOSAT\]2.0.CO;2](https://doi.org/http://dx.doi.org/10.1130/0016-7606(1945)56[275:EDOSAT]2.0.CO;2)
- Liaw, A., & Weiner, M. (2002). Classification and Regression by randomForest. *R News*, *2*(3), 18–22. <https://cran.r-project.org/doc/Rnews/>
- Luce, C. H., & Black, T. a. (1999). Sediment production from forest roads in western Oregon. *Water Resources Research*, *35*(8), 2561. <https://doi.org/10.1029/1999WR900135>
- McCool, D. K., Foster, G. R., Mutchler, C. K., & Meyer, L. D. (1989). Revised Slope Length Factor for the Universal Soil Loss Equation. *Transactions of the American Society of Agricultural Engineers*, *32*(5), 1571–1576.
- Megahan, W. F., & Ketcheson, G. L. (1996). Predicting downslope travel of granitic sediments from forest roads in Idaho. *Water Resources Bulletin*, *32*(2), 371–382. files
- Megahan, W. F., & Kidd, W. J. (1972). Effects of logging and logging roads on erosion and sediment deposition from steep terrain. *Journal of Forestry*, March 1972, 136–141.
- Montgomery, D. R. (1994). Road surface drainage, channel initiation, and slope instability. *Water Resources Research*, *30*(6), 1925–1932. <https://doi.org/10.1029/94WR00538>
- Overton, D., & Meadows, M. (1976). *Stormwater Modelling*. Academic Press.
- Packer, P. E. (1967). Criteria for Designing and Locating Logging Roads to Control Sediment. *Forest Science*, *13*(1), 2–18. <https://doi.org/10.1093/forestscience/13.1.2>
- R Core Team. (2019). R: A language and environment for statistical computing (3.6.2-- "Dark and Stormy Night") [Computer Program]. R Foundation for Statistical Computing. <https://www.r-project.org/>
- Reid, D. A., Hassan, M. A., & Floyd, W. (2016). Reach-scale contributions of road-surface sediment to the Honna River, Haida Gwaii, BC. *Hydrological Processes*, *30*(19), 3450–3465. <https://doi.org/10.1002/hyp.10874>

- Rivenbark, B. L., & Jackson, C. R. (2004). Concentrated flow breakthroughs moving through silvicultural streamside management zones: southeastern peidmont, USA. *Journal of the American Water Resources Association*, 40(4), 1043–1052. <https://doi.org/10.1111/j.1752-1688.2004.tb01065.x>
- Sidle, R. C., Sasaki, S., Otsuki, M., Noguchi, S., & Abdul Rahim, N. (2004). Sediment pathways in a tropical forest: Effects of logging roads and skid trails. *Hydrological Processes*, 18(4), 703–720. <https://doi.org/10.1002/hyp.1364>
- Takken, I., Croke, J., & Lane, P. N. J. (2008). A methodology to assess the delivery of road runoff in forestry environments. *Hydrological Processes*, 22 (November 2008), 254–264. <https://doi.org/10.1002/hyp.6581>
- Thompson, C. J., Takken, I., & Croke, J. (2008). Hydrological and sedimentological connectivity of unsealed roads. In J. Schmidt, T. Cochrane, C. Phillips, S. Elliott, T. Davies, L. Basher (Eds.) *Sediment Dynamics in Changing Environments* (Proceedings of a Symposium held in Christchurch, NZ). IAHS-AISH Publication 325, 524–531.
- Welle, P. I., & Woodward, D. (1986). *Time of Concentration* (Technical Note No. 4). U.S. Department of Agriculture Soil Conservation Service.
- Wickham, H. (2016). *ggplot2: Elegant Graphics for Data Analysis*. Springer-Verlag. <https://ggplot2.tidyverse.org>
- Woods, S. W., Sugden, B., & Parker, B. (2006). Sediment Travel Distances below Drivable Drain Dips in Western Montana. In W. Chung & H. S. Han (Eds.), *29th Council on Forest Engineering Conference Proceedings*, July 22-Aug 2, 2006, Coeur d’Alene, Idaho (pp. 251–263). Council on Forest Engineering.

3.7 Tables

Table 3-1. Factors contributing to plume length from a review of previous literature

Factor	Tendency	Studies mentioning factor
Obstruction density	(-)	Packer (1967); Burroughs & King (1989); Megahan and Ketcheson (1996); Brake et al. (1997)
Sediment volume	(+)	Megahan and Ketcheson (1996); Woods et al. (2006)
Hillslope cover density	(-)	Packer (1967); Brake et al. (1997)
Gradient of lower hillslope	(+)	Megahan and Ketcheson (1996); Brake et al. (1997); Rivenbark and Jackson (2004)
Contributing road length or area	(+)	Packer (1967); Megahan and Ketcheson (1996); Brake et al. (1997); Coe (2006); Rivenbark and Jackson (2004)
Traffic	(+)	Coe (2006)
Fillslope erodibility	(+)	Coe (2006)
Particle size of surface material	(-)	Packer (1967); Coe (2006); Woods et al. (2006)
Gullying	(+)	Croke et al. (2005); Coe (2006); Rivenbark and Jackson (2004)

Table 3-2. Table of plume dependent and independent variables.

*Connectivity class is defined as (1) Connected: Delivering sand and fines; (2) Connected: Fines only; (3) Incomplete: Water only; (4) Not connected: >5m to stream

Dependent variables	Independent variables	
- Connectivity class (CC)* - Sediment travel distance below outlet (m) - Plume Area (m ²) - Plume width (m) - Average depth (cm)	- Road segment gradient (%) - Road surface area (m ²) (Road CA) - Road Length (m) - Road Width (m) - Hillslope gradient (%) - Cutslope height (m) - Cutslope length (m) - Cutslope gradient (%) - Left and right ditch width (m) - Soil classification - Mapped lithology	- Road camber: insloped, outsloped, crowned, flat -Outlet: dip, diffuse, culvert, grader berm, push-out - Presence and type of obstructions - Presence of gullying in ditch or fillslope - Ground vegetation type - Downslope topography: concave, convex, hummocky, planar - Slope Aspect: N, S, E, W - Road surfacing and condition - Traffic: high, medium, low - Maintenance: high, medium, low

Table 3-5. Plume length and area regressions

Model					
1) Plume Length with Outliers Removed (m)					
Coefficients		Estimate	Std. Error	t-statistic	Pr.
Intercept		10.2	4.62	2.21	0.031
Total Contributing Area (m ²)		0.0162	0.0024	6.73	9.1E-9
RSE	28.4	Model R ²	0.44	Model P	9.1E-9
2) Plume Area with Outliers Removed (m ²)					
Coefficients		Estimate	Std. Error	t-statistic	Pr.
Intercept		-1.35	12.5	-0.018	0.92
Contr. Area (m ²) X Grade		1.75	0.127	13.8	<2.2E-16
RSE	80.7	Model R ²	0.77	Model P	<2.2E-16

Table 3-6. Kruskal-Wallis test on residuals for plume length and area regressions

Factor	Probability of significant group difference in residual	
	Length	Area
Outlet Type	0.19	0.71
Maintenance	0.13	0.74
Traffic	0.68	0.07
Surface	0.42	0.16
Mapped Surficial Geology	0.11	0.19
Topography	0.91	0.17
Aspect	0.2	0.04*

**Denotes a significant relationship*

3.8 Figures



Figure 3-1. A plume or road sediment deposited in an excavated roadside turnout

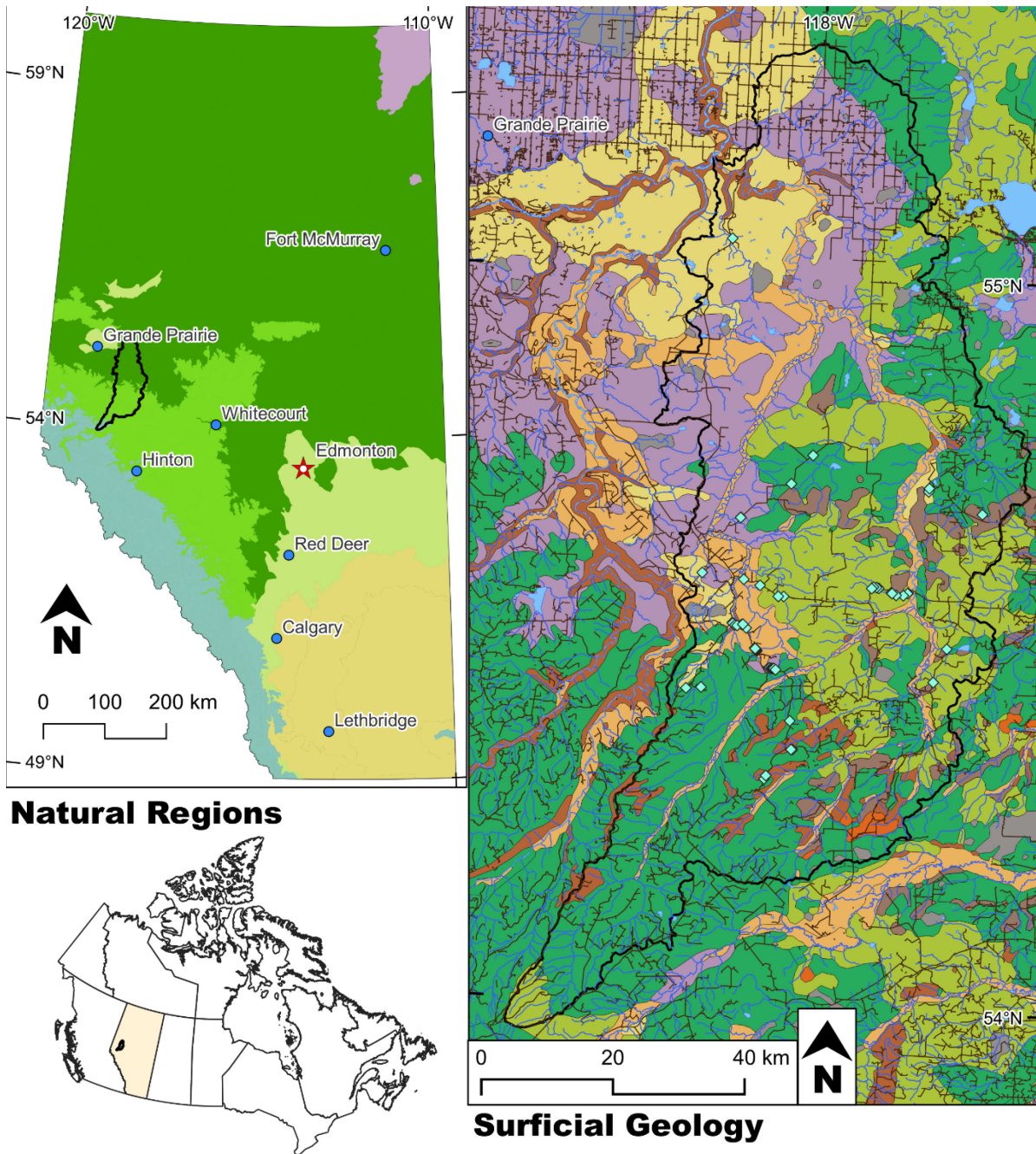


Figure 3-2. Location, natural regions, and surficial geology for the Simonette watershed
Sediment plumes mapped in this study are shown as light blue diamonds.

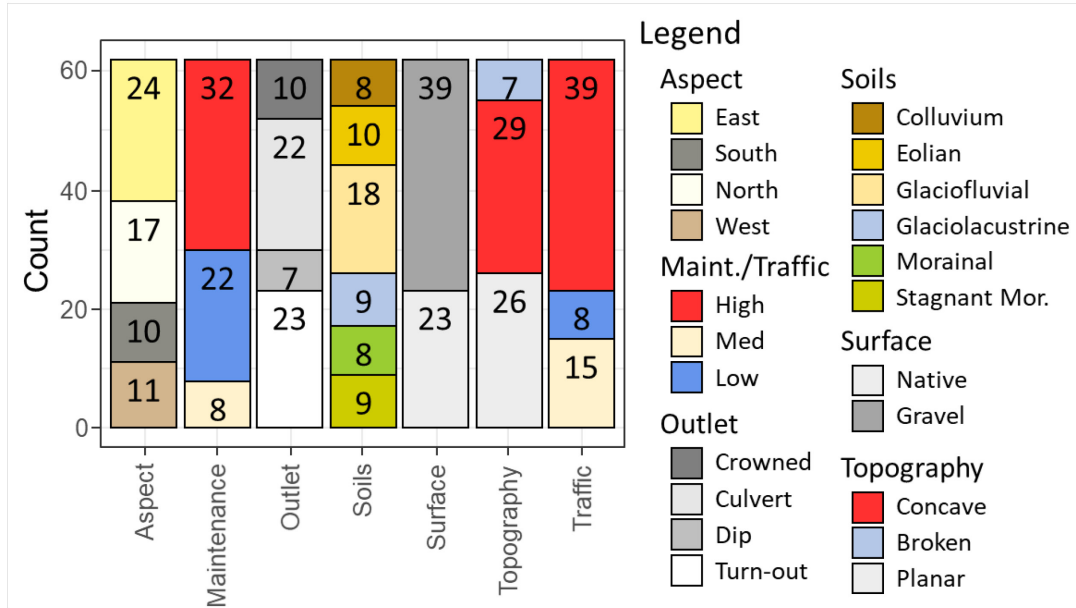


Figure 3-3. Distribution of categorical variables in the data (out of 62 samples)
 Larger category breaks are shown along the x-axis, and subcategory breaks are differentiated in the legend.

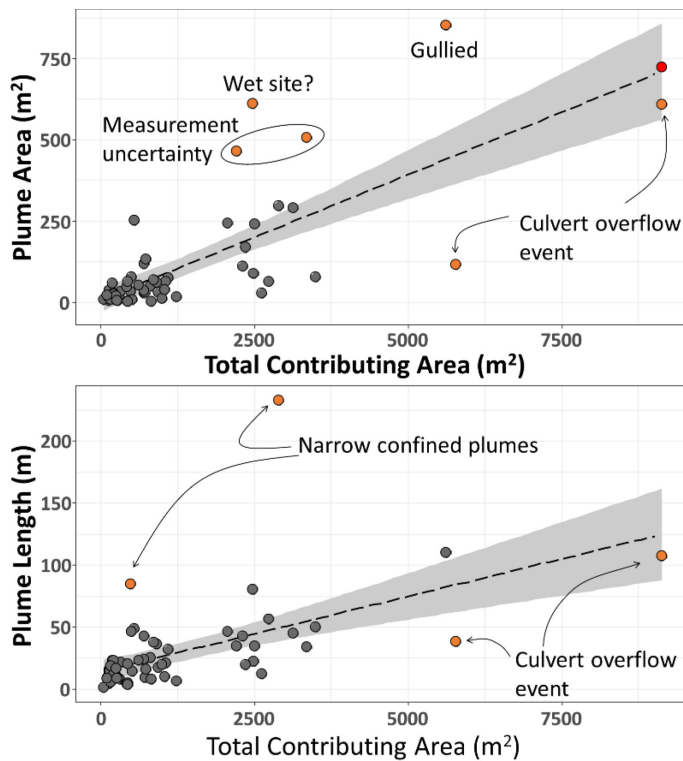


Figure 3-4. Plume area and length regressions showing overall increase in plume area and length with contributing area (left), and visual examples of outlier points (right)

A narrow, confined, 230 m-long plume is shown in the top right, and the results of the culvert overflow event and subsequent gully are shown in the lower right. The red point in the top graph is the combined culvert overflow event.

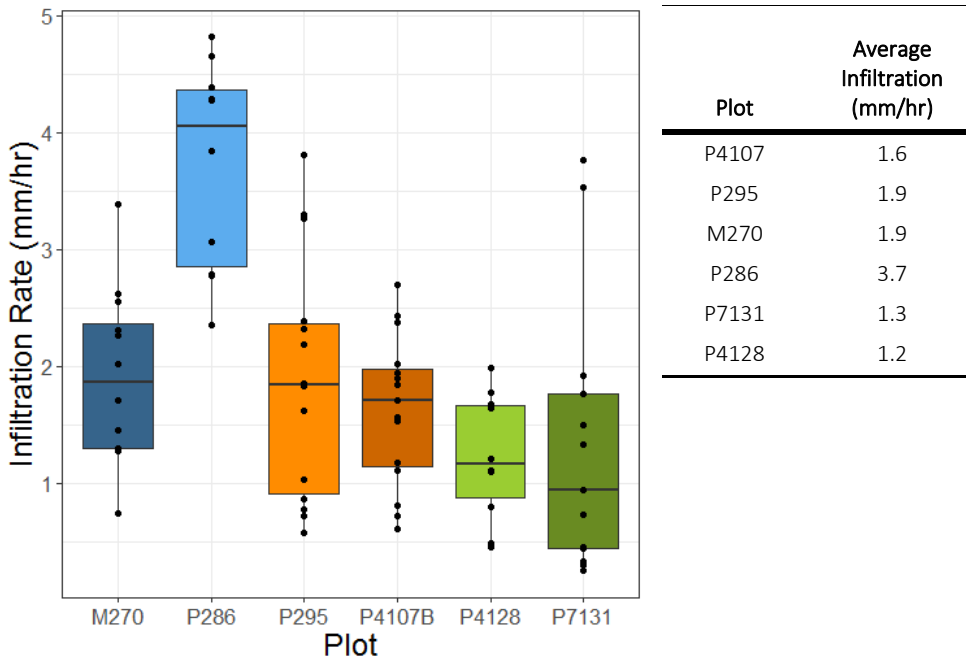


Figure 3-5. Range of infiltration rates for roads in the Simonette watershed

Plots are colour-coded according to geological type and traffic (traffic: light shade = light traffic, dark shade = high traffic; geology: blue = glaciolacustrine, orange/brown = glaciofluvial or fluvial, green = morainal).

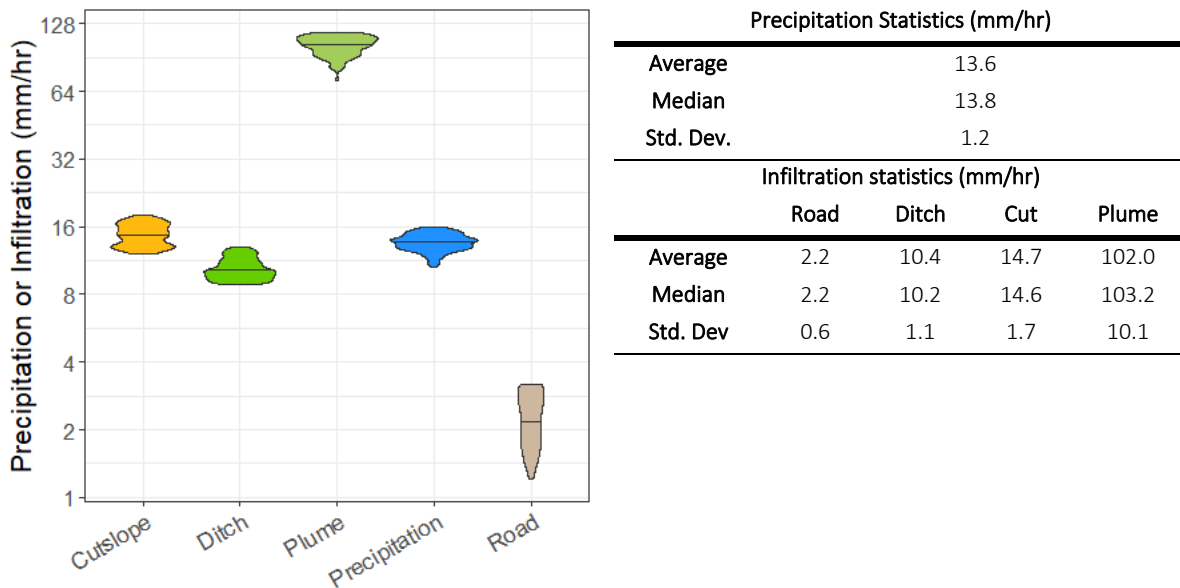


Figure 3-6. Simulation-based parameter estimates from 95 best models

Statistical distributions of the parameter estimates are shown to the left, numerical results are shown to the right. Note that the precipitation is represented as a base 2 logarithm.

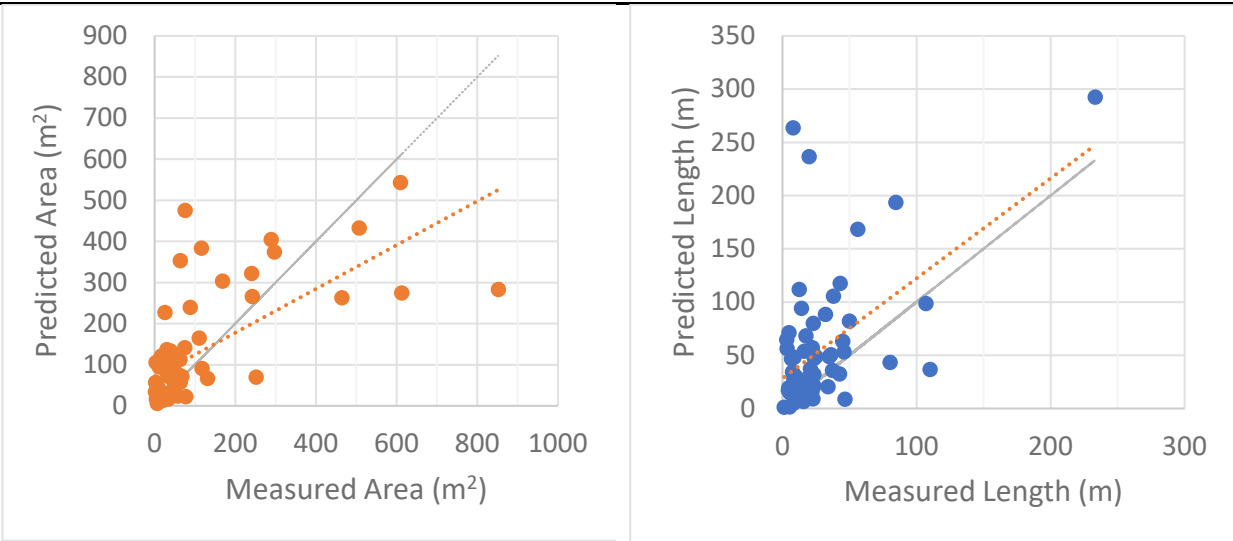


Figure 3-7. Predicted versus modelled values for plume area (left) and length (right) using parameter average values and the READI model. 1:1 line is plotted in grey. Values above the 1:1 line are over-predictions, and values below the line are under-predictions. Red dashed lines are the trend lines of the prediction.

4 Sediment Contributions from Road-Stream Crossings Cause Downstream Gravel Matrix-Fining in a Foothills Watershed in Alberta, Canada

4.1 Introduction

Resource roads are well-known contributors of fine sediment to streams (Bilby, 1985; Cederholm et al., 1980; Elliot, 2013; Reid et al., 2016), but tracing the location of instream impacts from contributing sites is not a trivial task. Road sedimentation impact studies are not always capable of linking the location and magnitude of road sediment contributions with a measurable impact on the stream sedimentary environment. Bilby (1985) found that 21% of reach suspended sediment in a stream in Western Washington came from a nearby upstream road crossing; however, there was little impact on surface gravel composition. A later study (Bilby et al., 1989) found that road sediment transport was related to stream order: lower-order streams tended to act as temporary reservoirs of gravel and sand because sediment supply tended to overwhelm the transport capacity. In larger-order streams in trunk valleys, there was little evidence that logging-related fines were retained. Investigations of a stream in Haida Gwaii (Reid et al., 2016) found that 18% of suspended sediment was traceable to a nearby logging road. Percentage of road-related sediment varied from 0.5-15% during the dry season (April – September) to 5-70% during the wet season (October – March), but there was no evidence of in-reach storage of this sediment.

Sediment contributions from logging activities can cause decreases in the sediment calibre of streambed gravels. The findings of a study in Western Washington indicated that when a higher percentage of basin area was covered by logging roads, there were more fines in salmon spawning gravels in downstream areas (Cederholm et al., 1980). The same study found that road-related erosion in the area was 2.6 – 4.3 times greater than erosion in an undisturbed basin. Researchers studying low-gradient depositional stream reaches in Western Montana found that median surface particle size decreased with increasing road density (Al-Chokhachy et al., 2016). The authors of the study also produced an estimate of road erosion using the US Forest Service GRAIP algorithm, but this could not be dependably linked to stream impact measures. Lisle and Hilton (1992) used a non-dimensional measure of fines accumulation in pools (V^*) to link increased logging-related stream disturbance with greater fines accumulation in pools in California. Careful measures of fines in

streambed gravel or of bed particle size can therefore be used to detect the influence of logging roads, although these might not be tied to specific measures of sedimentation.

4.1.1 Selection of appropriate indicators

Although the results of the above studies are useful, road sedimentation impact is represented variously by using road density-related metrics (Cederholm et al., 1980; Al-Chokhachy et al., 2016), some form of ad-hoc road pressure indicator (Lisle and Hilton, 1992), or a site-level assessment of sedimentation pressure from a limited number of road segments (Bilby, 1985; Reid et al., 2016). Road density is commonly used as an indicator of overall watershed disturbance and has been shown to predict sedimentation pressure in some studies (Cederholm et al., 1980; Al-Chokhachy et al., 2016). A problem with using road density is that it cannot be used to tier sedimentation impacts in a road network or to predict the most likely locations of road sediment delivery. Some have suggested that using road crossings is more appropriate because roads deliver most sediment at road crossings and near stream-parallel road segments (Benda et al., 2019).

Sediment delivery from roads is primarily composed of fine-grained sediment fractions. The term as used in biological literature usually refers to material that is sand-sized and finer, or fine-grained relative to the gravelly stream beds inhabited by salmonids (Cederholm et al., 1980; Lisle and Hilton, 1992). Sand-sized sediment may preferentially accumulate in low-velocity areas of a stream reach, such as in pools, or on the lee side of gravel bars. Silt and clay-sized fine-grained material may enter interstices of the streambed gravel matrix in zones of downwelling flow, such as pool tails or side-channel bars (Tonina & Buffington, 2007; 2009; Rehg et al., 2005).

Stream impact assessments can be improved by a careful consideration of context. Some of these contexts may be historical in nature (Al-Chokhachy et al., 2016), such as whether or not a watershed has a history of severe disturbance followed by longer-term low-level disturbance. Another element of context may be whether a particular stream response variable is likely to be driven by acute or chronic disturbance. Surface gravel composition may be an example of a lagging indicator of severe disturbance because it is only periodically mobilized during high-magnitude low-frequency flow events and may take decades to move downstream from an area of impact. In contrast, zones of fines deposition in the stream environment may represent chronic disturbance, as fines will be reworked into the water column and flushed out of the system during the same low frequency high magnitude flow events that rework channel gravel. Analysis of silt and clay fractions

within the grave matrix may be a better indicator of basin-scale road sedimentation than surface gravel composition.

4.1.2 Erosion and sedimentation modelling and indicators

Understanding the impact of road erosion on the stream environment is aided by the use of modelling and assessment tools to estimate the magnitude of impact on a portion of a stream network. Tools used to manage permanent road networks should be designed in such a way that they accurately locate the most likely source areas of road impact. Assessors should know which road segments are most likely to contribute sediment, and what role proximity to stream environment plays in determining if a road segment will contribute sediment (Benda et al., 2019; Thompson et al., 2009; Hairsine et al., 2002). This information helps assessors determine where to direct limited road and drainage repair budgets (Benda et al., 2019).

A number of road management tools have been developed in the past few decades to help direct road and drainage repair efforts and to assist natural resource users in managing their land base. The oldest and most widely-used erosion management tool is the universal soil loss equation (USLE) (Wischmeier & Smith, 1978) and its modernized descendant the revised universal soil loss equation (RUSLE, RUSLE2) (Renard et al., 1991). These tools, however, were designed specifically to manage agricultural erosion from cropland and are less reliable at estimating erosion losses and sediment delivery from road networks. The Washington Road Surface Erosion Model (WARSEM) (Dubé et al., 2004) uses factor-based empirical erosion equations similar to USLE. The Water Erosion Prediction Program (WEPP) (Nearing et al., 1989) is a process-based model with interfaces for forestry use (Elliot et al., 1999). Practical use of these computer programs is currently hindered by limited applicability and transferability to new management settings (Skaugset et al., 2011). Other models presently being developed and evaluated include the Geomorphic Road Analysis and Inventory Package (GRAIP) (N. A. Nelson et al., 2019; Tarboton, 2014) and the Road Erosion and Sediment Delivery Index (READI) (Benda et al., 2019). Ongoing challenges for many road erosion software packages include accurately determining the magnitude of sedimentation and representing likelihood of sediment delivery. More importantly, these erosion tools need to be assessed against measures of instream impact.

4.1.3 Objective

The objective of this study was to compare several different stream impact assessment metrics against a series of disturbance metrics in a sample of small (approx. 10-20 km²) watersheds

to determine (A) which stream disturbance metrics are useful for capturing a long-term, chronic disturbance signal, and (B) which assessment metrics are meaningful for targeting problematic locations of stream sediment delivery from roads. A main question with respect to stream disturbance metrics was to determine if surface grain counts or estimates of fines infiltration were better for capturing a chronic disturbance signal. A second key question was whether a metric tied to road sediment delivery would improve the assessment of sediment delivery from roads compared to the more commonly used metric of road density, and if road crossing density was also an appropriate stream metric.

4.2 Study site

The Simonette watershed has an area of 5400 km² and is located in west-central Alberta (Figure 4-1). The watershed is approximately 150 km long from north to south, and up to 50 km wide. The Simonette River is a Strahler seventh-order stream at its junction with the Smoky River (Alberta Environment and Parks, 2018). Elevations in the watershed vary between 1500 m in the southern headwaters, to approximately 530 m near the confluence with the Smoky River in the north. Average annual precipitation varies from around 445 mm at the Grande Prairie Airport, north of the watershed, to upward of 600 mm in the southern headwaters (Figure 4-1D). Mean annual air temperature varies from 2.3 °C in the North, to about 1.8 °C in the south (Wang, 2020; Wang et al., 2016). Average open-water season (March 1st – October 31st) runoff at the mouth of the Simonette River is about 143 mm (Environment Canada, 2021 & Alberta Environment, 2021). The expected peak daily discharge for any given year is about 350 m³/s, which is the median value of a 52-year record of discharge. The largest daily discharge was 3170 m³/s on August 3, 1987.

Due to its size and location, the Simonette watershed occurs within several distinct eco-climatic zones: the central and dry mixed-wood in the north, the lower and upper foothills in the central and southern portions of the watershed, and subalpine in the extreme southern portion of the watershed (Natural Regions Committee, 2006, Figure 4-1A). These regions are characterized by distinct gradients in elevation, average annual air temperature, and precipitation, which combined with surficial geology result in different stream types.

Flat-lying glaciolacustrine and glaciofluvial deposits are located in the northern portion of the watershed coincident with the Central Mixedwood ecozone. Hummocky moraine, local glaciolacustrine deposits, and glaciofluvial deposits comprise much of the terrain in a wide belt through the middle of the watershed in the Lower Foothills. Morainal mantles and veneers over

rolling, moderately-sloping Paleogene bedrock are found in the Upper Foothills and Subalpine ecoregions in the southern portion of the watershed (Figure 4-1B, C).

Much of the watershed is developed for oil and gas extraction and forestry, with the most intense resource-use zones being located on the Simonette mainstem south of Latornell River, and in the Deep Valley watershed. Most land in the northeastern portion of the watershed is used for agriculture. Roads in the watershed are generally one of three types: heavy-use main haul roads at least 10-12 m wide, narrow, long-term light use oil and gas lease access roads, and temporary forest access roads which are constructed, used, and deactivated within 1-3 years. Portions of the watershed with the highest road and stream crossing densities (Figure 4-2) are areas with both extensive short-term forestry roads, and dense networks of semi-permanent oil and gas roads. Road network density in the watershed typically varies from about 0.3 to 1.2 km/km². Road crossings per kilometre-squared of watershed varies between 0.6 to 1.8/km².

4.2.1 Sample design: sub-watershed selection

Road disturbance effects were investigated in small 10-20 km² watersheds within the Simonette (Table 4-4). The size reflects watersheds that are large enough to have significant particle transport, and small enough to reflect a local disturbance signal. Stream linework with associated basin attributes was provided by TerrainWorks as part of a data package for the Simonette watershed. Stream segments with basin areas greater than 10 km² and less than 20 km² were selected using geographic information system software (ArcGIS). Endpoints of the selected stream reaches were then used to create watersheds in ArcGIS from high-resolution topographic map data (1m LiDAR DEM) of larger sub-basins within the Simonette. Road density was calculated for each 10-20 km² sub-watershed using the road linework provided by Canfor and a road density algorithm within NetMap. Watersheds were binned into four classes of relative road density risk (<0.3, 0.3-0.6, 0.6-0.85, >0.85 km/km²) and overlaid on a map of Alberta ecoregions (Figure 4-3). Watersheds within the Central Mixedwood, Lower Foothills and Upper Foothills ecoregions (Natural Regions Committee, 2006) were examined in this study. The study was designed to have two replicates for each category of relative road risk density risk (4 categories), and natural subregion (3 categories), a total of 24 watersheds. Based on anecdotal observations, the actual road access on mapped roads was not always good, and therefore watersheds were randomly ranked and stratified by relative density risk and natural subregion with the intention of visiting the next-ranked watershed if a particular watershed proved inaccessible.

4.2.2 Erosion simulations

This study compares two computer simulated road erosion indices with coarser, regional estimates of road pressure (road density and road crossing density). The two road erosion indexes are GRAIP_Lite, a variant of the Geomorphic Roads Analysis and Inventory Program (GRAIP) developed by the US Forest Service (N. A. Nelson et al., 2019; Tarboton, 2014), and the Road Erosion and Sediment Delivery Index (READI) developed by Terrainworks (Benda et al., 2019). These indices were chosen because they are currently being developed and improved, and because they represent different approaches to determining road erosion: a simple process-based hydrological model (READI), and an empirical model (GRAIP).

4.2.2.1 GRAIP_Lite simulation

GRAIP_Lite can use field-calibrated estimates of road erosion potential coupled with probabilistic sediment delivery curves developed for different classes of contributing road length to determine the likely mass of sediment (kg) contributed to streams over all road segments in a watershed. GRAIP erosion estimates are not explicitly related to the intensity of a particular storm event, but are averaged over a number of years, and assumed to represent a base or chronic level of sedimentation pressure in a watershed. The basic GRAIP road erosion equation is:

$$E = BRSV \tag{1}$$

Where E is the total erosion (kg), B is the geological base rate in kilograms per metre of road decline, R is the calculated elevation difference over the road segment (m), S is the surfacing type modifier, and V is the vegetation factor. Vegetation condition of roads in the Simonette watershed is unknown, although it could possibly be estimated for closed or small access roads based on state (active or deactivated), and time since deactivation (years). This information was not readily available so we weighted erosion measurements calculated from summer 2017 and 2018 (*Chapter 2 in this thesis*) on the basis of geological material and the surfacing (S) factor in order to determine appropriate base rates for the Simonette watershed. The GRAIP surfacing factor varies from approximately 20 on high traffic native surface roads, to 1 for low-use roads with crushed rock surfacing (N. A. Nelson et al., 2019). Almost all roads in the watershed have at least some aggregate surfacing, with high-use trunk roads receiving more frequent applications of higher quality gravel than wellsite access roads or small forestry haul roads. Road subgrade material in the watershed is variable, although it is commonly compacted glaciolacustrine clay or till. These materials are extremely weak during saturated spring conditions and thus readily mix with road base and surface

gravel courses. Actual road properties for local forestry and oil and gas roads are therefore likely close to that of native surface roads elsewhere. Table 4-1 presents calculated GRAIP base rates for roads in the Simonette watershed. In this simulation we used base erosion rates of 46 kg/m for roads with sandy subgrade, 69 kg/m for roads with glacial silt and clay subgrades, and 99 kg/m for roads with a till subgrade. A significant driver of the erosion difference is likely the relative permeability of these subgrade materials, and therefore, the ease with which they generate overland flow during rain events (*see Chapter 2, this thesis*). The numerical contrast variable between high and low traffic roads was set at 4.

4.2.2.2 READI simulations

The READI algorithm simulates road erosion in response to a storm event of particular intensity (I , m/hr) and duration (hr). The READI erosion equation is of the form:

$$E = c_3 * (c_1 + c_2 * I), \text{ for } t < T_{pulse} (\sim 0.5 \text{ hour}) \quad (2)$$

Where E is the erosion produced (in this case a unitless contrast variable), c_1 and c_2 are coefficients related to road surfacing and materials, and c_3 is a coefficient related to sediment generation from traffic and maintenance. As the exact level of traffic response was not known from our previous studies in the watershed we weighted separate equations using c_1 and c_2 to account for roads in different types of surficial materials, and with qualitatively different levels of traffic (LOW versus HIGH/MEDIUM). Erosion in the READI model can be specifically tied to USLE soil loss values, although it is typically input as an ordinal contrast variable, and hence provides relative weighting for sediment delivery from road segments, not absolute amounts of sedimentation. Instead of using a distribution function to calculate sediment runout from a road segment, READI calculates the amount of water likely to be generated on a road surface from a given rain event and uses a hillslope infiltration equation to calculate the likely length of a sediment delivery plume. Percent delivery of the plume is then calculated using an exponential decay relationship based on the percent of expected plume length relative to available hillslope (Megahan & Ketcheson, 1996). READI simulations were performed using relative contrast variables for different road segments, and two storms with different recurrence intervals: a 1:2 year event, and a 1:25 year event based on the Environment Canada intensity-duration-frequency curves for Whitecourt, the closest weather station with a foothills climate similar to the Simonette watershed (Environment Canada, 2019). Road erodibility contrast variables are derived from the relative slope difference in rain energy versus erosion regression lines from road erosion data we collected in the summers of 2017/2018,

but should not be construed as absolute differences in erodibility as they represent a best guess of actual erodibility contrasts across the watershed based on limited data. The model run parameters are summarized in Table 4-2. Both READI and GRAIP impact estimates are represented as basin-averaged impacts (ie. Sediment delivery per km² basin area).

4.2.3 Stream physical attribute study

Streams were surveyed for dimensional attributes: length, width, depth, and gradient, surface grain size distribution, percent fines in pool ends or side-bars, and subsurface matrix composition. Reaches were pre-selected according to the stratification scheme described previously, and individual reaches were surveyed and photographed. Three stream reaches were surveyed in each 10 – 20 km² basin selected for analysis. Length, width, and depth were also measured for each pool, riffle and/or run in the study reach. Length attributes were measured using fibreglass measuring tapes in the field, depth was measured using a fibreglass composite folding engineering ruler (Rhino Rulers), and gradient was field-estimated with a Brunton Clinometer (accurate to ~0.5%), and later more precisely estimated using stream thalweg locations in a GIS shapefile, and 1 m resolution LiDAR elevation included in the NetMap dataset (LiDAR coverage date prior to 2015). Surface grain counts were performed using a gridded sampling frame with a design similar to that in Bunte and Abt (2001) as shown in Figure 4-4, left, putting grains in one of four sediment size classes (<2, 2-16, 16-64, and >64 mm). The grain size class was determined based on the median of three perpendicular semi-major axis measurements obtained with either a caliper or a folding fibreglass ruler.

Subsurface grain samples were collected using a purpose-fabricated metal freeze corer which used propane as the refrigerant (Figure 4-4, right). The design of the corer was the same as that used in studies of intruded fines in the southern Alberta Rocky Mountains (Hawthorn, 2014; Spillios, 1999). Refrigeration was initially tested using 5 or 20 lb propane tanks, however, the propane was not stored at sufficient pressure to produce the refrigeration effect needed, so pre-filled 1 lb propane bottles were used instead. Although freeze cores were initially collected using one bottle per sample with two samples per reach, it was quickly discovered that the most consistent sediment freeze cores were collected using two bottles at one location per reach. Samples were therefore collected using two bottles after completing surveys of the first few streams. Frozen samples were dislodged from the freeze corer using a geological hammer and stored in double Ziploc freezer bags. Additional fines were washed into the Ziploc bags using sample wash bottles

filled with clean stream water. Samples were stored out of sunlight in plastic tote boxes and transferred to a freezer at the end of every week-long field visit.

4.2.4 Lab analysis of freeze core samples

Samples were pre-treated prior to being analyzed for grain size at the Natural Resources Analytical Laboratory at the University of Alberta. Frozen samples were removed from plastic Ziploc bags and put in aluminum baking tins. Fines adhering to the surfaces of the bags were washed into the tins with distilled water, and samples were oven dried for 24 hours at 105°C to remove all moisture. Following drying, hardened samples were broken apart with a rubber mallet, and clay aggregates were broken apart with a wooden mortar and pestle. Samples were sieved through a 2 mm sieve and the gravel and sand fractions were separated and weighed. The freeze core sample technique did not collect enough coarse gravel for an effective size determination, so gravels were set aside, and material that passed the 2 mm sieve was sub-sampled using a vibrating riffler (Gilson SP-230), and grain size was determined using a Beckman Coulter LS13 320 laser diffraction instrument. The reported grain size is the average of two sub-samples. Samples which failed a quality control check were run again, and grain size was reported as the closest 2/3 samples measured.

4.2.5 Statistical analysis of stream physical parameters and road pressure variables

R statistical software was used to examine the relationships between stream physical variables, environmental gradients, and calculated road pressure variables (R Core Team, 2019). Stream road pressure variables were obtained by extracting simulated stream sedimentation impacts produced in ArcGIS from study reaches on the basis of their location in space (a spatial join operation). The variables analysed in this study are listed in Table 4-3. Figures of correlations and linear relationships between stream physical response variables, environmental gradients and road pressure variables were plotted using third-party packages in R (Schloerke et al., 2018; Wickham, 2016). Correlations described in the study are made using Spearman correlation coefficients which can capture both linear and non-linear correlations between variables.

4.3 Results

Physical and land-use characteristics of sampled watersheds are summarized in Table 4-4, and the results of the stream physical attribute surveys are compared with calculated road pressure variables in Table 4-5. Detailed graphs of particle size distribution for the matrix sediment are

presented in Appendix E. Although differences in road density and stream matrix composition were expected to vary by natural subregion, preliminary regression analyses using this grouping indicated that streams followed a similar trend regardless of grouping. Stream analysis was therefore lumped. Results were grouped by stream and include average width and depth of pool segments in each reach, surface grain size counts in pools, matrix composition from freeze core samples, and area-averaged road pressure variables. The amount of sand in freeze core samples generally decreased in stream reaches with greater upstream road crossing density (number of crossings per km² of basin area). The percentage of sand also generally decreased as the READI road sediment delivery index increased. The correlations between stream physical response variables (stream geometry, surface sediment composition, and gravel matrix composition), basin physical characteristics, and road pressure variables are shown in Figure 4-5. Road density, a common indicator of stream condition was not correlated with sampled surface counts, or with sub-surface gravel matrix composition. In contrast, both 1:2-year READI sediment delivery index, and road crossing density were moderately correlated ($r = \pm 0.4$ and ± 0.5) with gravel matrix composition (% sand, silt, and clay in freeze-core samples). Sediment loading predicted by the GRAIP algorithm was not correlated ($r = \pm 0.1$) with either surface or sub-surface grain size characteristics. Of the two READI runs, the typical (1:2 year) run was more correlated with gravel matrix composition than the higher-intensity lower-frequency (1:25 year) run. Linear regression relationships between road pressure indicators (road crossing density, 1:2 year READI index, road density) and gravel matrix composition averaged over study reaches are shown in Figure 4-6. Although significant, only weak relationships were observed between road crossing density and percentages of sand, silt, and clay in the gravel matrix ($R^2 = 0.19 - 0.3$; $p = 1.4 \times 10^{-3} - 4 \times 10^{-5}$), and between 1:2 year READI index and gravel matrix composition ($R^2 = 0.17 - 0.23$; $p = 4 \times 10^{-4} - 2.3 \times 10^{-3}$). The correlation between road density and streambed composition was very low ($R^2 = 0.048 - 0.06$; $p = 0.053 - 0.075$).

4.4 Discussion

This study provides evidence that chronic inputs of fines into a stream through road crossings can create measurable differences in substrate matrix composition. Past studies in the Simonette (Maitland et al., 2016; Scrimgeour et al., 2008) have shown direct physical impacts on stream fish assemblages from road-related development and crossing structures. Maitland et al. (2016) found significant differences in streambed composition related to crossing type, with culverts having significantly more fines upstream of the crossing than downstream, and bridges having more fines

downstream than upstream, and both having somewhat more fines than reference streams. This and other contrasting environmental gradients related to stream crossings caused differences in fish species assemblages upstream and downstream of crossings. Differences in species composition were also attributed to habitat fragmentation related to culverted crossings. A study of fish assemblages in the Kakwa and Simonette Rivers (Scrimgeour et al., 2008) found significant differences in fish species presence in streams based on percent disturbance and road density. Environmentally sensitive fish such as Bull Trout and Mountain Whitefish were less likely in reaches with greater upstream road density.

Our study did not find strong relationships between surface grain counts and proposed disturbance metrics. One reason for this may be that our grain counts were binned too coarsely. Using binning instead of providing raw grain-size measurements may have masked subtle but significant differences in average grain size in the streambed. The methodology was similar to that used in Scrimgeour et al. (2008) and it is notable that they also did not find a significant difference between disturbed and reference reaches in the Simonette watershed. This is similar to findings by Bilby (1985), and Reid et al. (2016), while other authors (Al-Chokhachy et al., 2016; Cederholm et al., 1980; Lane & Sheridan, 2002; Lisle & Hilton, 1992) have found evidence of accumulation of gravel in streambeds downstream of impacted sites. Another potential reason for the lack of significant differences in surface grain size composition with disturbance matrices is that stream reaches directly downstream of road crossings were not considered in this study. The aim of the present study was to determine whether local disturbance at crossings may leave a visible disturbance signal in surficial material some distance downstream. Other studies had observed that depositional context may be important in determining where and why particular stream reaches are impacted (Al-Chokhachy et al., 2016). No evidence of disturbance farther downstream from road crossings was observed in this study. This may be because roads generally contribute more fine material to stream crossings than they do coarse material, and because gravel is only transported periodically during high flow events. Al-Chokhachy et al. (2016) observed that they were unable to correlate road sedimentation rates and contributions estimated through GRAIP with instream sediment size distribution because the streams may in fact be recording disturbance signals from past infrastructure or from periodic large-scale disturbance from mass-wasting. Others have observed that large-scale disturbances in the sedimentary environment, for example from placer gold mining, may take many decades to move through a system (A. D. Nelson & Church, 2012). The context of sediment inputs matters, but so does the behaviour of individual streams, and

the material being assessed. The location and type of assessment parameter depends on the type of disturbance (acute or chronic), the history of disturbance (whether it occurred over a period of years or nearly instantaneously), and the transport regime of the receiving streams (whether large material will become trapped or gradually move through the system). Surface grain counts may be better suited for measuring impacts in streams with known and significant inputs of anthropogenic gravel and sand. These impacts are more likely to be measured in stream reaches directly downstream of the impact site (Lane & Sheridan, 2002) or in stream reaches which are transitional between transporting predominantly gravel and predominantly sand (Al-Chokhachy et al., 2016; Montgomery, 1999; A. D. Nelson & Church, 2012).

Although there was no evidence of a change in grain size composition of surface sediments in this study, the relationships between subsurface matrix composition and road pressure were significant. The relatively low coefficients of determination suggest that road pressure is not the only factor driving matrix composition, but that it is still influential in determining overall matrix composition. Some variation in road density and sediment properties due to landform differences was expected with different ecoregions, however, preliminary analysis indicated similar trends across ecoregions with respect to road density and grain size. Therefore, the best explanation of the variation in matrix grain size at present is also the simplest one: that higher contributions of fine sediment from roads cause silt and clay to preferentially infiltrate into gravel matrices rather than sand. This change in matrix composition is also ecologically important, as it is associated with zones of hyporheic inflow. Infiltration of clay and silt into the matrix in side-channel bars and pool tails has been shown to reduce the strength of hyporheic mixing in these zones in sand bed flume studies (Rehg et al., 2005). This is problematic, because salmonids preferentially use sites of hyporheic upwelling downstream of inflow areas for nest-building (Tonina & Buffington, 2007). This study indicates that fines derived from roads may affect the streambed precisely where they can do the most damage to fish nesting sites. Management strategies should focus on finding and remediating sites of fine sediment contribution in the stream environment. Road density thresholds may not have any meaningful bearing on this objective. Road crossings, however, seem to be a common sediment delivery location (Maitland et al., 2015; Benda et al., 2019).

Computer models that predict physical connections between streams and roads are likely to provide estimates of sedimentation pressure that agree with actual instream conditions. READI, which uses a simple mass-balance and kinematic wave model to predict peak discharge from road

segments and probable plume length, provides a useful measure of instream impact, whereas GRAIP, which relies on sediment plume exceedance-probability curves, does not. A study in the Flathead watershed in western Montana also did not find strong linkage between GRAIP-derived sediment yield in stream segments and in-stream habitat quality (Al-Chokhachy et al., 2016). As the authors noted, this may be because streams in that watershed are still responding to legacy harvesting pressures. Given the substantial impact of fine sediment on the stream environment, its relative mobility within the stream system, and the fact that it will preferentially infiltrate in areas of sensitive fish habitat, it would seem that a road pressure indicator that can provide a meaningful assessment of the impact of present road usage in the stream environment is needed. The results of this study indicate that an urgent area for fisheries research is on the overlap between road sedimentation models and instream fines infiltration. Freeze-coring is a relatively cheap and effective way of assessing stream gravel matrix composition, however, there are other meaningful types of instrumentation that may provide useful reach-level assessment of the condition of the stream hyporheic zone in water downwelling zones.

4.5 Conclusion

In this study the best measure of road-related disturbance was infiltration of fines into the gravel substrate, and the best measure of road impact was road crossing density, rather than road density, suggesting that the most likely source areas for excess fine sediment are stream crossings. The READI index for a 1 in 2 year event was the best road sedimentation model. It performed better than the same index for a 1 in 25 year event, indicating that the quality of stream habitat is responding to common flow conditions with chronic input of fine sediment rather than extreme events. The GRAIP_Lite road sedimentation model were not correlated with instream condition parameters. This suggests that the READI model, while an imperfect representation of reality, captures some of the hydrological drivers of connection between roads and streams and warrants future use and study.

Measuring fines intrusion is a reasonably cost- and time-effective way of assessing downstream impact from roads. The location of measurement should have physical meaning: fines intrusion is more likely to be significant in locations where water flows into the stream bed, such as pool tails or channel side bars. This technique is well-suited to monitoring the regional or sub-basin scale impacts of road sedimentation, particularly because the majority of road-contributed sediment in impacted watersheds comprises fine material. In conclusion, as others have indicated

in the past (Al-Chokhachy et al., 2016), landscape, climate, and disturbance regime contexts matter in assessing the impacts of stream disturbance in a watershed, locating probable sites of impact, and in assessing the type of impact.

4.6 References

- Alberta Environment and Parks (2021). Alberta River Basins [web app]. Retrieved May 24, 2021 from <https://rivers.alberta.ca/>
- Alberta Environment and Parks (2018). Base Watersheds – Simplified Hydrography [GIS features]. Retrieved October 2, 2021 from: <https://geodiscover.alberta.ca/geoportal/rest/metadata/item/e4197d5f6b3043be8cbf9e7f8b49c4fe/html>
- Al-Chokhachy, R., Black, T. A., Thomas, C., Luce, C. H., Rieman, B., Cissel, R., Carlson, A., Hendrickson, S., Archer, E. K., & Kershner, J. L. (2016). Linkages between unpaved forest roads and streambed sediment: why context matters in directing road restoration. *Restoration Ecology*, 24(5), 589–598. <https://doi.org/10.1111/rec.12365>
- Benda, L., James, C., Miller, D., & Andras, K. (2019). Road Erosion and Delivery Index (READI): A Model for Evaluating Unpaved Road Erosion and Stream Sediment Delivery. *Journal of the American Water Resources Association*, 55(2), 459–484. <https://doi.org/10.1111/1752-1688.12729>
- Bilby, R. E. (1985). Contributions of road surface sediment to a western Washington stream. *Forest Science*, 31(4), 827–838.
- Bilby, R. E., Sullivan, K., & Duncan, S. H. (1989). The generation and fate of road-surface sediment in forested watersheds in southwestern Washington. *Forest Science*, 35(2), 453–468.
- Bunte, K., & Abt, S. R. (2001). Sampling frame for improving pebble count accuracy in coarse gravel-bed streams. *JAWRA (Journal of the American Water Resources Association)*, 37(4), 1001–1014. <https://doi.org/10.1111/j.1752-1688.2001.tb05528.x>
- Cederholm, C. J., Reid, L. M., & Salo, E. O. (1980). Cumulative effects of logging road sediment on salmonid populations in the Clearwater River, Jefferson County, Washington. In *Salmon-Spawning Gravel: A Renewable Resource in the Pacific Northwest?* Seattle, WA. October 6-7, 1980, 1-35. Retrieved from <https://www.fs.fed.us/psw/publications/reid/Cederholm.pdf>
- Dube, K., Megahan, W., & McCalmon, M. (2004). *Washington Road Surface Erosion Model (WARSEM) Manual*, State of Washington Department of Natural Resources. 189 pp. Retrieved from: http://dnr.wa.gov/Publications/fp_data_warsem_manual.pdf

- Elliot, W. J. (2013). Erosion processes and prediction with WEPP technology in forests in the Northwestern U.S. *Transactions of the ASABE*, 56(2), 563–579.
- Elliot, W. J., Hall, D. E., & Scheele, D. L. (1999). FS-WEPP: Forest Service Interfaces for the Water Erosion Prediction Project Computer Model [Web Application]. USDA Forest Service, Rocky Mountain Research Station. <https://forest.moscowfsl.wsu.edu/fswepp/>
- Environment Canada (2021). Historical Hydrometric Data. Retrieved May 24, 2020, from https://wateroffice.ec.gc.ca/mainmenu/historical_data_index_e.html
- Environment and Climate Change Canada (2019). Short-Duration Rainfall Intensity-Duration-Frequency Data, Version 3.00 [Engineering Climate Dataset]. Retrieved March 9, 2020, from https://climate.weather.gc.ca/prods_servs/engineering_e.html
- Hairsine, P. B., Croke, J. C., Mathews, H., Fogarty, P., & Mockler, S. P. (2002). Modelling plumes of overland flow from logging tracks. *Hydrological Processes*, 16(12), 2311–2327. <https://doi.org/10.1002/hyp.1002>
- Hawthorn, K. F. (2014). *The role of fine sediment in phosphorous dynamics and stream productivity in Rocky Mountain headwater streams: Possible long-term effects of extensive logging* (Master's Thesis). 116 pp. Retrieved from <https://era.library.ualberta.ca/>
- Lane, P. N. J., & Sheridan, G. J. (2002). Impact of an unsealed forest road stream crossing: Water quality and sediment sources. *Hydrological Processes*, 16(13), 2599–2612. <https://doi.org/10.1002/hyp.1050>
- Lisle, T. E., & Hilton, S. (1992). The Volume of Fine Sediment in Pools: an Index of Sediment Supply in Gravel-Bed Streams. *Journal of the American Water Resources Association*, 28(2), 371–383. <https://doi.org/10.1111/j.1752-1688.1992.tb04003.x>
- Maitland, B. M., Poesch, M., Anderson, A. E., & Pandit, S. N. (2016). Industrial road crossings drive changes in community structure and instream habitat for freshwater fishes in the boreal forest. *Freshwater Biology*, 61(1), 1–18. <https://doi.org/10.1111/fwb.12671>
- Megahan, W. F., & Ketcheson, G. L. (1996). Predicting downslope travel of granitic sediments from forest roads in Idaho. *Water Resources Bulletin*, 32(2), 371–382. files
- Montgomery, D. R. (1999). Process Domains and the River Continuum. *JAWRA (Journal of the American Water Resources Association)*, 35(2), 397–410. <https://doi.org/10.1111/j.1752-1688>

- Montgomery, D. R., & Buffington, J. M. (1997). Channel-reach morphology in mountain drainage basins. *Bulletin of the Geological Society of America*, 109(5), 596–611.
[https://doi.org/10.1130/0016-7606\(1997\)109<0596:CRMIMD>2.3.CO](https://doi.org/10.1130/0016-7606(1997)109<0596:CRMIMD>2.3.CO)
- Natural Regions Committee. (2006). *Natural regions and subregions of Alberta* (Pub. No. T/852). Compiled by D. J. Downing & W. W. Pettapiece (Eds). Government of Alberta.
<https://doi.org/10.5962/bhl.title.115367>
- Nearing, M., Foster, G., Lane, L., & Finkner, S. (1989). A process - based soil erosion model for USDA - water erosion prediction project technology. *Transactions of the American Society of Agricultural Engineers*, 32(5), 1587–1593. <https://doi.org/10.13031/2013.31195>.
- Nelson, A. D., & Church, M. (2012). Placer mining along the Fraser River, British Columbia: The geomorphic impact. *Bulletin of the Geological Society of America*, 124(7–8), 1212–1228.
<https://doi.org/10.1130/B30575.1>
- Nelson, N., Luce, C., & Black, T. (2019). *GRAIP_Lite: A System for Road Impact Assessment* [Working Paper]. U.S.D.A. Forest Service.
- R Core Team. (2019). R: A language and environment for statistical computing (3.6.2-- "Dark and Stormy Night") [Computer Program]. R Foundation for Statistical Computing. <https://www.r-project.org/>
- Rehg, K. J., Packman, A. I., & Ren, J. (2005). Effects of suspended sediment characteristics and bed sediment transport on streambed clogging. *Hydrological Processes*, 19(2), 413–427.
<https://doi.org/10.1002/hyp.5540>
- Reid, D. A., Hassan, M. A., & Floyd, W. (2016). Reach-scale contributions of road-surface sediment to the Honna River, Haida Gwaii, BC. *Hydrological Processes*, 30(19), 3450–3465.
<https://doi.org/10.1002/hyp.10874>
- Renard, K., Foster, G. R., Weesies, G. A., & Porter, J. P. (1991). RUSLE: Revised Universal Soil Loss Equation. *Journal of Soil and Water Conservation*, 46, 30–33. www.swcs.org
- Schloerke, B., Crowley, J., Cook, D., Briatte, F., Marbach, M., Thoen, E., Elberg, A., & Larmarange, J. (2018). GGally: Extension to “ggplot2” (1.4.0) [Computer Program]. <https://cran.r-project.org/package=GGally>

- Scrimgeour, G. J., Hvenegaard, P. J., & Tchir, J. (2008). Cumulative industrial activity alters lotic fish assemblages in two boreal forest watersheds of Alberta, Canada. *Environmental Management*, 42(6), 957–970. <https://doi.org/10.1007/s00267-008-9207-2>
- Skaugset, A. E., Surfleet, C. G., Meadows, M. W., & Amann, J. (2011). Evaluation of Erosion Prediction Models for Forest Roads. *Transportation Research Record: Journal of the Transportation Research Board*, 2203, 3–12. <https://doi.org/10.3141/2203-01>
- Spillios, L. C. (1999). *Sediment intrusion and deposition near road crossings in small foothill streams in West Central Alberta* (Master's Thesis). Retrieved from: <https://era.library.ualberta.ca/>
- Tarboton, D. G. (2014). Geomorphologic Road Analysis and Inventory Package (GRAIP) (1.0.10) [Computer Program]. Utah State University. <http://hydrology.usu.edu/dtarb/graip/>
- Thompson, C. J., Barry, S., & Takken, I. (2009). A model for optimizing forest road drain spacing. In R. S. Anderssen, R. D. Braddock, & L. T. H. Newham (Eds.), *18th World IMACS Conference and MODSIM09 International Congress on Modelling and Simulation* (pp. 4093–4099). Cairns, Australia: Modelling and Simulation Society of Australia and New Zealand and International Association for Mathematics and Computers in Simulation. Retrieved from <http://www.mssanz.org.au/modsim09/115/thompson.pdf>
- Tonina, D., & Buffington, J. M. (2007). Hyporheic exchange in gravel bed rivers with pool-riffle morphology: Laboratory experiments and three-dimensional modeling. *Water Resources Research*, 43(1), 1–16. <https://doi.org/10.1029/2005WR004328>
- Tonina, D., & Buffington, J. M. (2009). Hyporheic exchange in mountain rivers I: Mechanics and environmental effects. *Geography Compass*, 3(3), 1063–1086. <https://doi.org/10.1111/j.1749-8198.2009.00226.x>
- Wang, T. (2020). ClimateWNA_Map [Web Page]. <http://www.climatewna.com/ClimateWNA.aspx>
- Wang, T., Hamann, A., Spittlehouse, D., & Carroll, C. (2016). Locally downscaled and spatially customizable climate data for historical and future periods for North America. *PLoS ONE*, 11(6). <https://doi.org/10.1371/journal.pone.0156720>

Wickham, H. (2016). *ggplot2: Elegant Graphics for Data Analysis*. Springer-Verlag.
<https://ggplot2.tidyverse.org>

Wischmeier, W. H., & Smith, D. D. (1978). *Predicting rainfall erosion losses - a guide to conservation planning* (Agriculture Handbook Number 537). Washington, D.C. Retrieved from <https://naldc-legacy.nal.usda.gov/catalog/CAT79706928>

4.7 Tables

Table 4-1. Weighting coefficients for GRAIP erodibility in the Simonette watershed

Traffic	Geology	R (kg/m)	S (Emp)	Surf	S (Sugg.)	R-rev (kg/m)
High	Clay/Mixed	413	4.2	AGG	4	99
Low	Clay/Mixed	99	1	AGG	1	99
High	Sandy	182	20.2	AGG	4	46
Low	Sandy*	9	1	AGG	1	46
High	Silty/Loamy	277*	7.7	AGG	4	69
Low	Sandy-Silty	36	1	AGG	1	69

*Lacustrine plots P286 (sandy), M270 (silty/loamy)

Table 4-2. Simulation parameters for READI runs

Variable	Fixed/ Varied	Values	GIS Field
60-Minute Storm Intensity (m/hr)	Varied	0.014 (1 in 2 year event) 0.032 (1 in 25 year event)	-
Ditch Infiltration Rate (m/hr)	Fixed	0.018	DitchInfil
Soil Infiltration Rate (m/hr)	Fixed	0.097	-
Ditch Width (m)	Varied	Calculated in GIS: $f \text{ (Avail. Rd. ROW} - \text{Rd. Width)}/2$	DitchWidth
Runoff Plume Width (m)	Fixed	4	-
Slope Exponent	Fixed	1	-
Outslope Proportion	Fixed	0.5	Outslope_P
Road Width (m)	Varied	Between 6-10 m	Width_M
Erodibility (c_1)	Varies (geol)	Between 1 and 2: 1 for well-drained fines and sand 2 for poorly-drained fines	Erodibil
Storm Erodibility (c_2)	Varies (geol and traffic)	Geology: 1 sandy soils 2 well-drained fines 3 poorly-drained fines Traffic intensity multiplier: 1 low and medium traffic 2 high traffic	E_Intsty
Pulse Erodibility (c_3)	Fixed	Set at 1 (<i>included in c_2</i>)	E_Pulse
Pulse Duration	Fixed	Set at 0	T_Pulse

Table 4-3. Stream physical parameters, environmental gradients, and road pressure indicators used in this study

Stream Response	Environmental Gradients	Road Pressure Indicators
Average pool width and depth (m)	Basin area (km ²)	GRAIP (cumulative)
% Pool tail fines	Elevation (m asl)	GRAIP (area-averaged)
% Surface grain counts in <2 mm, 2 – 16 mm, 16 – 64 mm, > 64 mm size classes	Stream Gradient (GIS calculated)	READI (1:2 year, area-averaged)
% Sand, silt, and clay in freeze core gravel matrix	Stream Order (ordinal)	READI (1:25 year, area-averaged)
	Mean annual precipitation (mm)	Road Density (km/km ²)
		Rd. Crossing Density (#/km ²)

Table 4-4. Characteristics of study basins*Most stream names are specific to this study except for those with an asterisk (*) at the end*

Basin	Lat.	Long.	Elev. (m)	Strahler Order	MAP (mm)	Basin Area (km ²)	Xing Dens. (#/km ²)	Road Dens. (km/km ²)	NSR Name	Geology (Dom/Sub)
7-10 Stream	54.437	-118.228	914	4	576	14.13	1.06	1.03	Lower Foothills	Moraine
Frying Pan Creek*	54.464	-118.232	894	4	576	19.40	0.67	0.70	Lower Foothills	Moraine/Eolian
Peyto FTR 130	54.200	-118.358	1136	3	603	10.22	1.47	1.03	Upper Foothills	Moraine
Sun Valley SP7	54.246	-118.014	1171	3	627	18.80	0.37	0.28	Upper Foothills	Moraine
4139 Stream	54.317	-118.064	1126	3	631	13.79	0.80	0.76	Upper Foothills	Moraine
Boulder Creek 4133	54.361	-118.016	1083	4	624	16.24	1.23	0.51	Upper Foothills	Moraine
Carol Creek 4122	54.448	-118.007	893	2	619	5.62	1.42	1.12	Lower Foothills	Moraine
Hennigar Creek 7140	54.414	-117.791	867	3	599	15.81	1.01	0.77	Lower Foothills	Moraine
Bremner Creek AC8	54.696	-117.656	753	2	555	13.25	1.81	0.79	Central Mixedwood	Moraine/Colluvial
Ante Creek* East	54.713	-117.617	743	3	537	18.91	2.80	1.00	Central Mixedwood	Moraine/Colluvial
Ante Creek* South	54.641	-117.613	804	2	540	11.30	1.33	0.77	Central Mixedwood	Moraine
Hodgins Creek* 2123	54.581	-117.830	841	3	568	14.32	0.14	0.07	Lower Foothills	Moraine
Beaverdam Creek DV7	54.388	-117.682	881	2	592	8.86	0.79	0.30	Lower Foothills	Moraine/Colluvial
Resthaven 6-3	54.245	-118.365	1159	3	604	8.75	1.83	0.66	Upper Foothills	Moraine
Paralator Creek	54.337	-118.300	1131	3	629	12.17	0.99	1.00	Upper Foothills	Moraine
Smulin Creek	54.630	-118.248	801	3	584	25.85	1.08	0.66	Lower Foothills	Eolian/Glaciofluvial

Table 4-5. Road pressure variables and stream survey results organized by reach

Road pressure variables include basin-averaged sediment loading (GRAIP and READI), road density, and road crossing density. Variables that are posited to respond to road pressure include average pool width and depth, surface grain size, and composition of subsurface gravel matrix. Note: * READI sediment loading is unitless and is expressed per square kilometre of basin area.

Stream	Reach	Road Pressure Variables					Reach Av. Geom. (m)		Surface Grain Size (%)					Matrix Comp. (%)		
		GRAIP (kg/km ²)	READI* (1:2)	READI* (1:25)	Rd. Dens (km/km ²)	Rd. X Dens (#/km)	Width	Depth	Pool Tail Fines	<2 mm	2-16 mm	16-64 mm	>64 mm	Clay	Silt	Sand
4139 Stream	1	1982	273	324	0.76	0.80	3.8	0.2	0.0	0.0	4.7	57.0	38.4	24.7	45.2	30.1
	2	1976	272	324	0.76	0.80	4.3	0.3	2.7	1.9	8.3	56.5	33.3	20.1	30.6	49.3
	3	1976	272	324	0.76	0.80	3.8	0.3	0.7	0.0	7.2	58.6	34.2	26.5	51.1	22.3
Boulder Creek 4133	1	427	310	384	0.51	1.23	3.8	0.4	14.0	0.7	0.7	62.2	36.4	21.5	31.0	47.5
	2	427	310	384	0.51	1.23	3.5	0.3	15.3	0.0	2.4	79.2	18.4	15.1	22.1	62.7
	3	427	310	384	0.51	1.23	4.2	0.4	34.7	34.3	0.0	34.3	31.5	21.7	27.4	50.8
Frying Pan Creek	1	2005	363	579	0.70	0.67	3.3	0.5	83.3	100.0	0.0	0.0	0.0	11.6	18.0	70.4
	2	2005	363	579	0.70	0.67	4.1	0.5	49.3	56.0	28.0	16.0	0.0	3.2	4.2	92.6
	3	2006	363	579	0.70	0.67	3.5	0.5	28.0	4.0	36.0	60.0	0.0	2.0	3.3	94.8
Beaverdam Creek DV7	1	1138	87	92	0.30	0.79	1.9	0.2	28.0	29.3	8.6	49.3	12.9	7.4	10.0	82.6
	2	1138	87	92	0.30	0.79	2.5	0.4	80.0	95.8	0.0	2.8	1.4	11.7	20.0	68.4
	3	1137	87	91	0.30	0.79	1.6	0.2	18.7	15.2	6.1	58.3	20.5	6.2	9.6	84.2
Smulin Creek	1	722	61	88	0.66	1.08	3.1	0.3	13.3	0.0	19.7	56.3	23.9	16.5	18.3	65.2
	2	722	61	88	0.66	1.08	3.8	0.3	5.3	62.8	12.4	22.1	2.8	35.8	35.6	28.6
	3	722	61	88	0.66	1.08	3.4	0.3	38.0	44.6	20.0	28.0	7.4	22.4	33.9	43.7
7-10 Stream	1	2810	209	374	1.02	0.99	2.6	0.4	52.0	7.4	59.1	32.9	0.7	4.4	5.2	90.4
	2	2810	209	374	1.02	0.99	2.8	0.2	72.7	86.0	8.0	5.3	0.7	8.4	11.7	79.8
	3	2810	209	374	1.02	0.99	3.8	0.3	48.0	81.6	8.2	6.1	4.1	3.2	3.9	92.9
Peyto FTR 130	1	1121	439	650	1.03	1.47	2.6	0.6	59.3	68.5	2.2	28.3	1.1	11.5	20.4	68.1
	2	1121	439	650	1.03	1.47	1.8	0.6	34.0	35.6	8.9	53.4	2.1	16.3	24.0	59.7
	3	1121	439	650	1.03	1.47	1.3	0.7	30.0	65.7	5.6	25.2	3.5	3.8	6.9	89.3
Sun Valley SP7	1	397	49	57	0.28	0.37	5.5	0.4	8.0	1.4	2.8	85.4	10.4	6.7	11.3	82.1
	2	397	49	57	0.28	0.37	3.6	0.4	41.3	28.1	0.0	60.4	11.5	4.9	6.7	88.4
	3	397	49	57	0.28	0.37	4.5	0.6	64.0	18.6	3.2	59.7	18.6	4.6	5.9	89.6

Stream	Road Pressure Variables						Reach Av. Geom. (m)		Surface Grain Size (%)					Matrix Comp. (%)		
	Reach	GRAIP (kg/km ²)	READI* (1:2)	READI* (1:25)	Rd. Dens (km/km ²)	Rd. X Dens (#/km)	Width	Depth	Pool Tail Fines	<2 mm	2-16 mm	16-64 mm	>64 mm	Clay	Silt	Sand
Carol Creek 4122	1	1807	640	1034	1.12	1.42	2.7	0.3	26.0	16.4	0.0	66.4	17.2	-	-	-
	2	1807	640	1034	1.12	1.42	3.0	0.1	2.7	0.0	6.4	75.2	18.4	30.1	39.7	30.2
	3	1807	640	1034	1.12	1.42	3.1	0.1	13.3	7.4	14.7	58.1	19.9	24.3	33.2	42.5
Resthaven 6-3	1	1036	854	903	0.66	1.83	3.9	0.3	28.0	43.8	9.7	41.1	5.4	26.5	49.5	24.1
	2	1036	854	903	0.66	1.83	2.8	0.5	50.7	48.5	6.8	31.8	12.9	23.5	34.4	42.1
	3	967	795	840	0.63	1.70	3.0	0.3	22.0	4.6	8.2	50.0	37.3	29.1	46.4	24.4
Paralator Creek	1	760	260	384	1.00	0.99	5.5	0.4	0.7	6.3	1.8	52.3	39.6	9.7	15.2	75.1
	2	760	260	384	1.00	0.99	5.5	0.3	22.5	2.9	7.6	73.7	15.8	14.1	22.0	63.9
	3	760	260	384	1.00	0.99	3.1	0.6	49.3	29.4	2.8	51.1	16.8	17.4	27.6	54.9
Hennigar Creek 7140	1	429	250	371	0.77	1.01	5.2	0.5	92.0	99.0	1.0	0.0	0.0	4.9	6.6	88.4
	2	428	250	370	0.77	1.01	3.5	0.4	58.7	78.0	6.0	16.0	0.0	7.5	9.4	83.1
	3	429	250	371	0.77	1.01	4.6	0.3	60.7	77.1	9.9	8.9	4.2	14.0	22.0	63.9
Bremner Creek AC8	1	730	157	203	0.79	1.81	2.3	0.3	18.0	37.8	12.2	43.9	6.1	14.6	28.1	57.4
	2	730	157	203	0.79	1.81	1.9	0.3	46.7	15.7	24.4	32.2	27.8	29.9	39.2	30.9
	3	730	156	203	0.79	1.81	2.0	0.3	24.0	28.7	37.3	28.1	6.0	17.6	23.5	58.8
Ante Creek East	1	1101	485	548	1.00	2.80	1.3	0.1	25.3	24.1	5.0	62.4	8.5	38.4	39.5	22.1
	2	1101	485	548	1.00	2.80	2.7	0.4	68.0	50.9	0.0	28.2	20.9	5.8	5.9	88.3
	3	1101	485	548	1.00	2.80	1.8	0.1	17.3	13.7	14.5	42.7	29.0	43.0	42.3	14.7
Ante Creek South	1	474	205	272	0.77	1.33	3.4	0.2	66.7	41.3	14.7	44.0	0.0	2.0	2.5	95.5
	2	474	205	272	0.77	1.33	3.5	0.1	45.3	26.2	14.8	45.1	13.9	15.2	18.1	66.7
	3	474	205	272	0.77	1.33	2.2	0.2	11.3	13.6	9.3	47.5	29.7	7.0	8.0	85.0
Hodgins Creek 2123	1	0	34	55	0.07	0.14	2.3	0.3	46.0	46.0	11.5	34.5	7.9	9.7	11.3	79.0
	2	0	34	55	0.07	0.14	2.2	0.1	16.7	21.9	11.7	54.0	12.4	5.5	6.3	88.2
	3	0	34	55	0.07	0.14	1.8	0.2	21.3	33.6	7.4	53.0	6.0	3.3	3.7	93.1

4.8 Figures

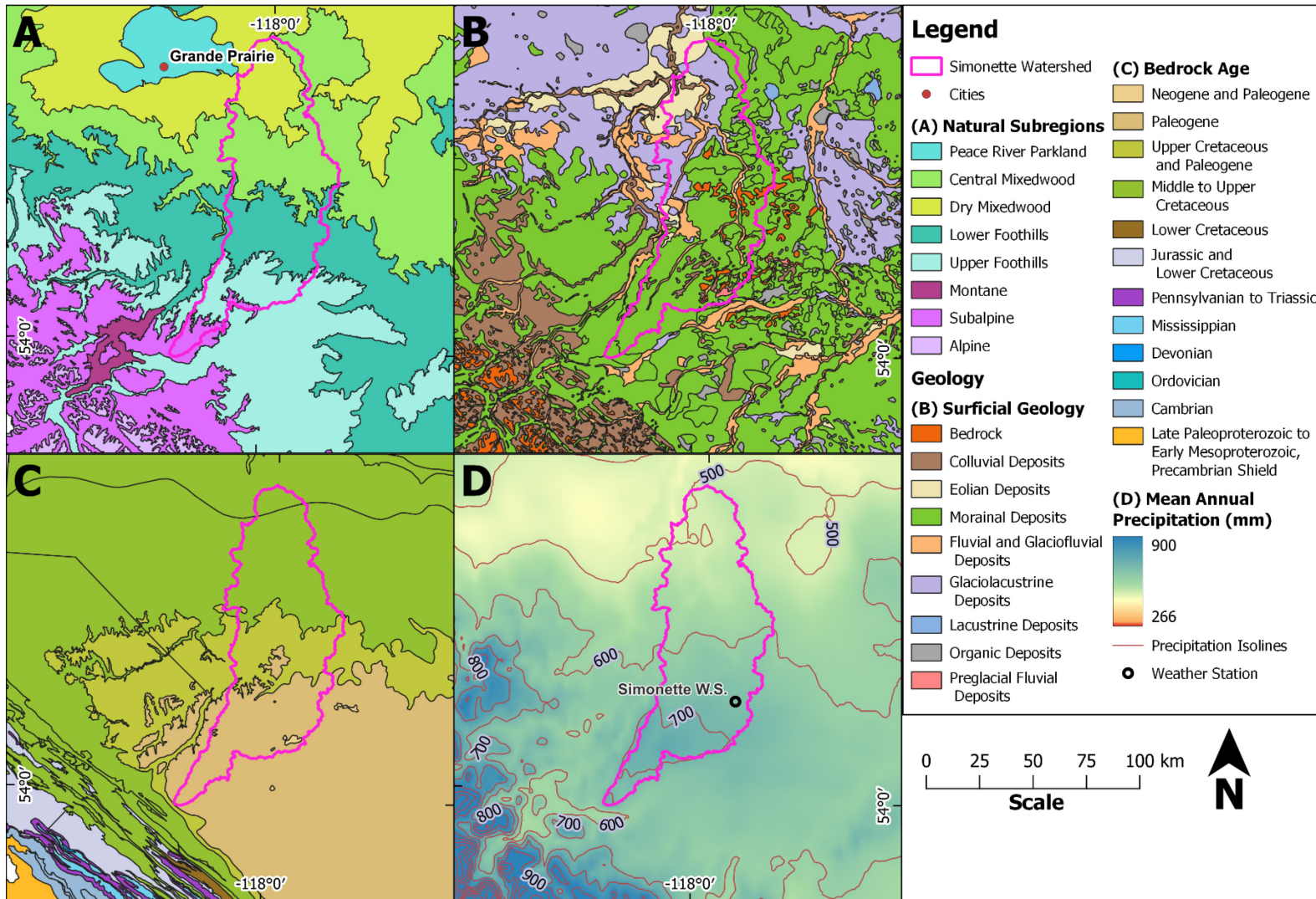


Figure 4-1. Environmental gradients in the Simonette watershed. (A) Natural subregions (B) Surficial Geology, (C) Bedrock Age, (C) Precipitation

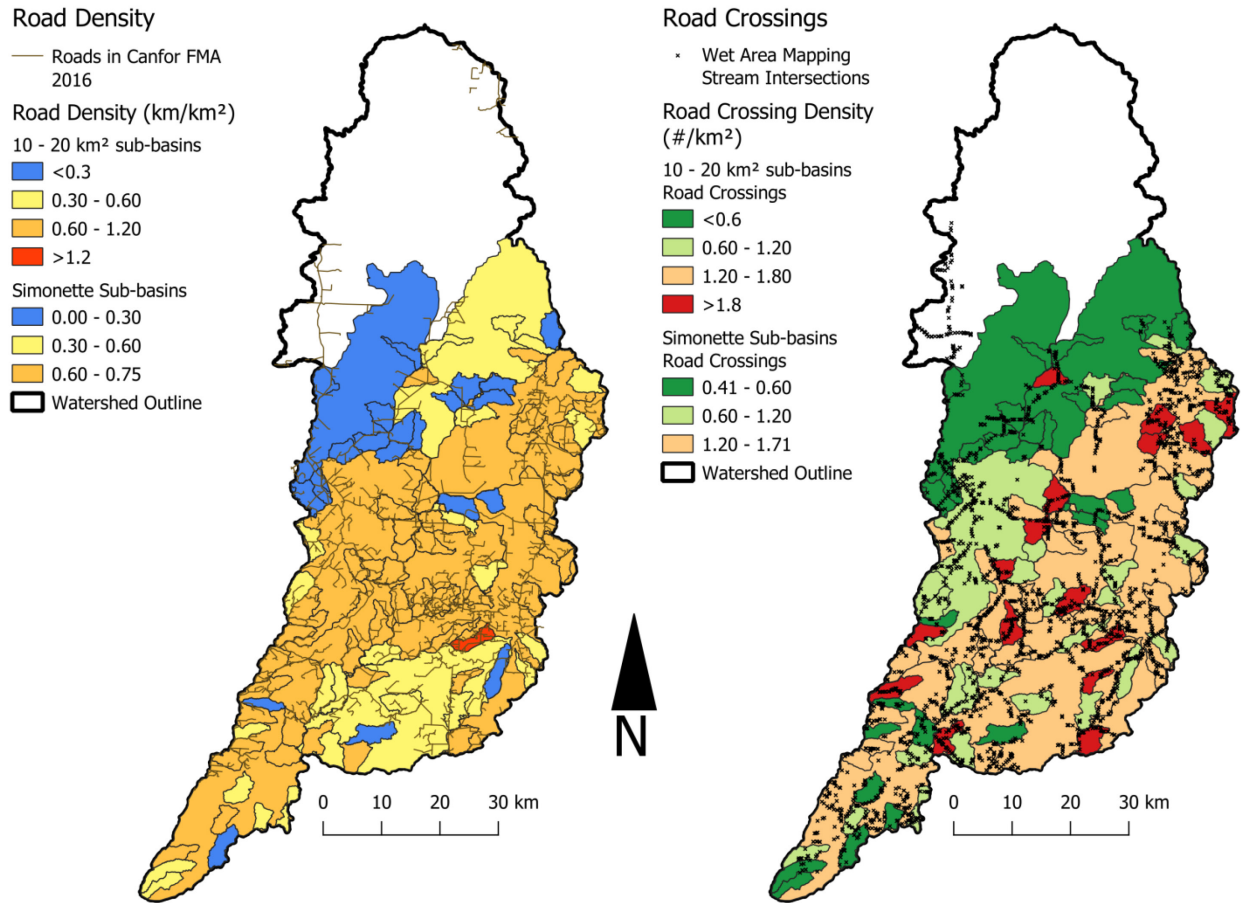


Figure 4-2. Road density (left), and road crossing density (right) in the Simonette watershed, west-central Alberta

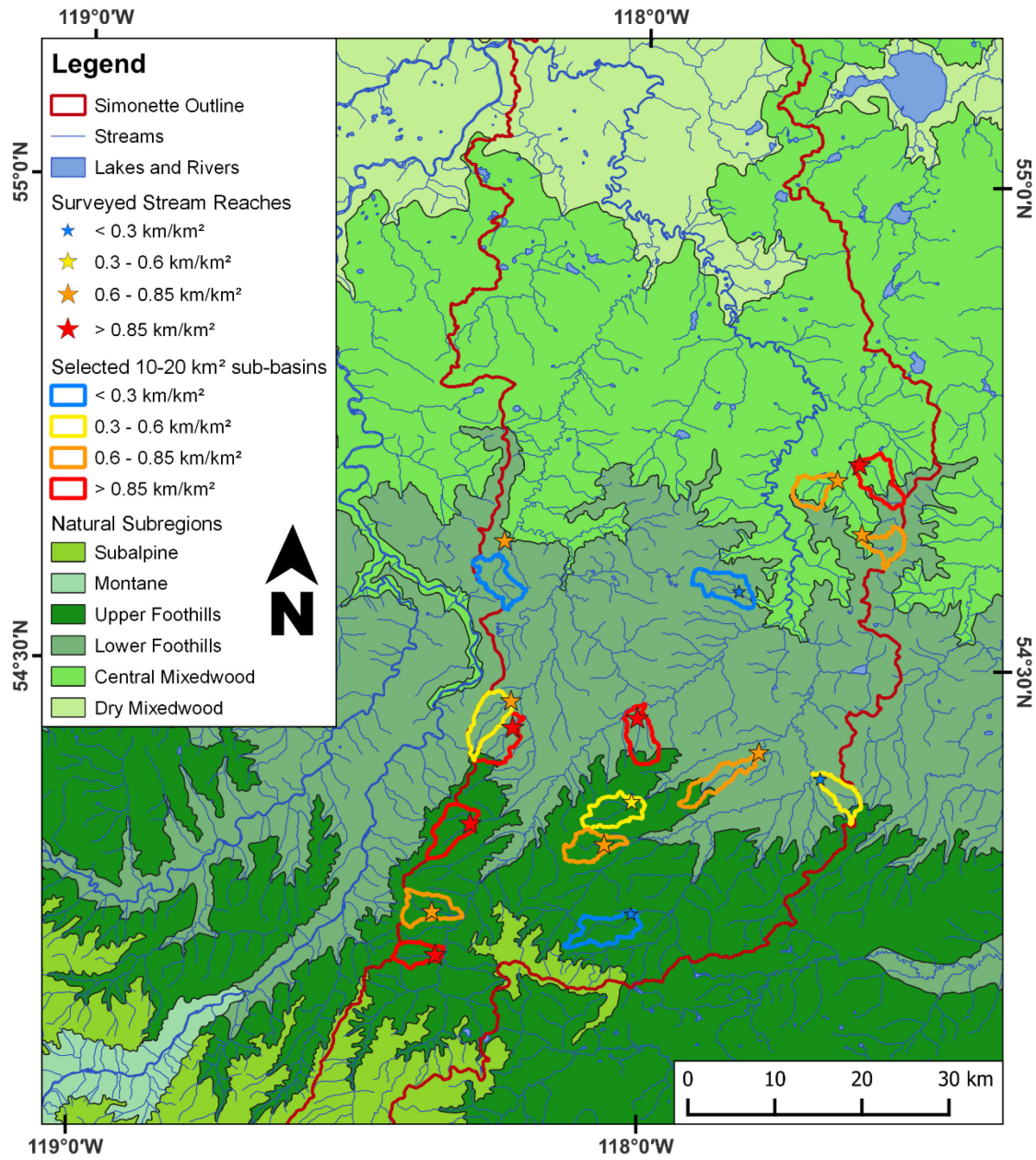


Figure 4-3. Map of stream survey sites and watersheds



Figure 4-4. Stream physical sampling equipment: counting frame (left); metal freezing device with attached bed substrate material (right)

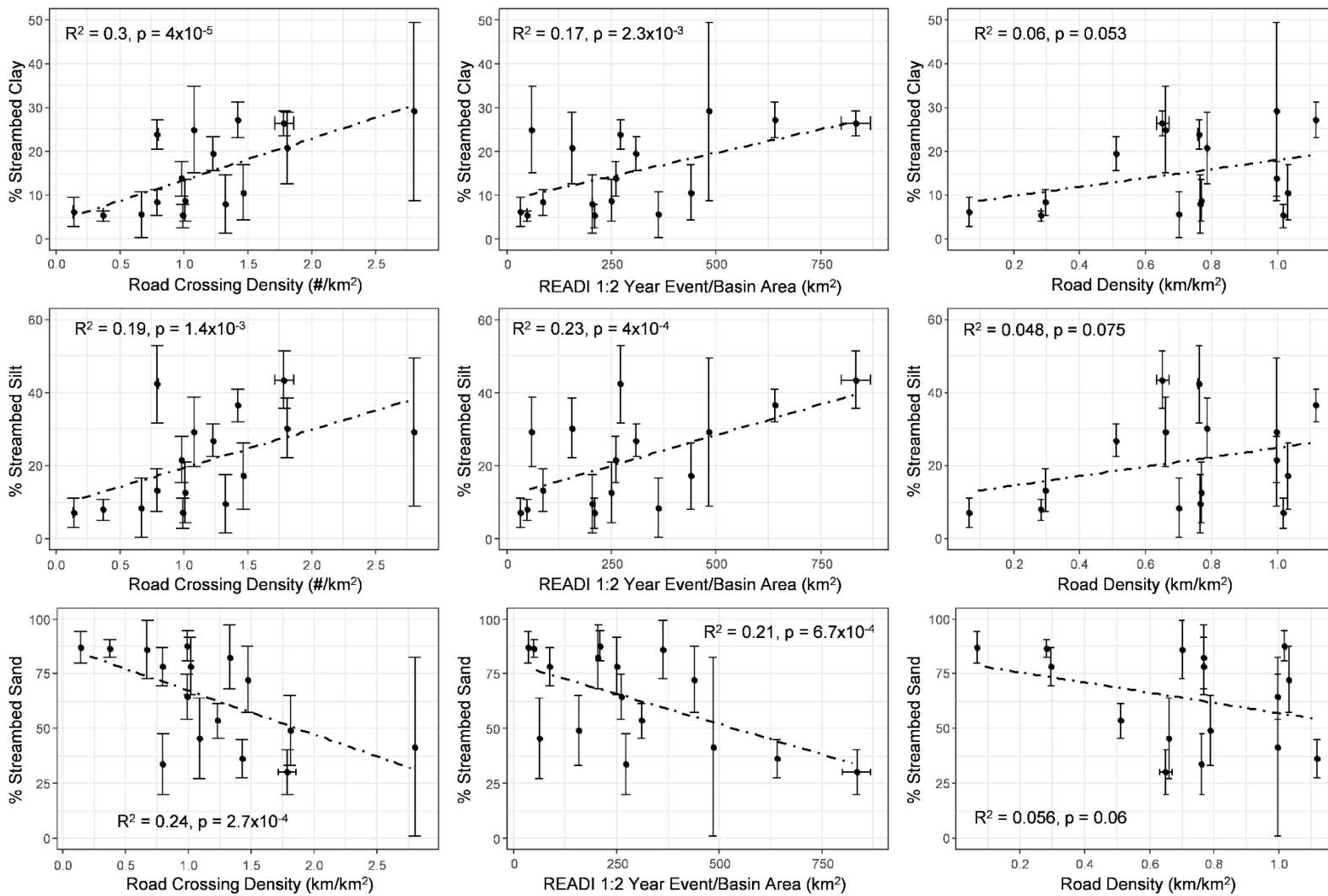


Figure 4-6. Relationship between streambed gravel matrix composition and road pressure variables, showing increased silt and clay percentage with higher road crossing density (#/km²) and READI indexed sediment loading per km² basin area. Road density does not significantly predict streambed gravel matrix composition.

5 Lessons learned: How studies in the Simonette watershed inform resource management

5.1 Introduction

Watershed management challenges in the Simonette watershed in west-central Alberta are similar to those in other industrial watersheds in western Canada. Continued improvement of linear infrastructure management in Alberta's foothills and boreal forests must acknowledge several ongoing issues which are peculiar to watersheds in Alberta. In this chapter I highlight several findings from this research, and how these findings may apply to management and future research in Alberta. These challenges include very high and heavy traffic levels on significant portions of Alberta's unsealed road network and a present ad-hoc regime of linear infrastructure management with significant unknowns over vast areas. Lessons learned include practical and scientific understanding of the importance of road hydrology in road management plans, the need to understand process thresholds in road erosion and deposition, the need to focus on road crossings as a significant contributor of environmentally-damaging sediment, and finally, that monitoring and anticipating consequence needs to be done with a clear understanding of how excess fine sediment actually propagates through impacted stream systems. Given the scope of the problem and the lessons learned, stakeholders in Alberta also need practical tools to assess and manage watershed development risks, and they also need an adaptive and collaborative "continuous improvement" mindset.

5.2 Research and infrastructure challenges in Alberta foothills watersheds

Resource roads in Alberta watersheds are often subject to heavy use from multiple resource operators. Roads must sustain heavy loads not only from logging trucks, but from cranes, drill rigs, and completion equipment. Intense road usage creates logistical hurdles to overcome in obtaining stakeholder assent to research plans and places operational limitations on the kinds of research infrastructure that can be installed, and for how long. A substantial consideration for this study was how long road sediment monitoring stations could be installed in the road precisely because they were viewed as logistical impairments by road operators, and how robust they would need to be to sustain high levels of traffic.

Alberta operational watersheds are very large relative to their discharge due to the broad, flat-lying to rolling topography of the lower foothills and boreal plains. Despite their vast size,

Alberta watersheds have lower drainage density than more mountainous regions where road impact studies have traditionally been carried out (ie. Al-Chokhachy et al., 2016; Bilby, 1985; Bilby et al., 1989; Reid & Dunne, 1984). Because the terrain is gentler, roads can often be built somewhat more cheaply than in more adverse mountainous settings, and because drainage density is lower, there is less emphasis on precise placement of drainage structures and maintenance of existing structures. Unfortunately, the relative flatness of the Alberta environment and the softness of underlying soils means that proper drainage management may be just as necessary in Alberta as elsewhere. Failure to properly channel and control water flows from the road surface can cause deterioration of the road subgrade, and washouts along ditches and other drainage structures.

Because of the size of the management area and the scope of the management issues it seemed prudent not to focus on inventorying roads or performing detailed process measurements which would not advance a clear understanding of the main drivers of erosion in the Simonette watershed. Instead, I focused on some of the suspected main drivers of erosion and sediment delivery in the watershed, which included: traffic and surficial geology, contributing area of road segments, and hydrological response of road segments to precipitation events. This study has several useful lessons that are related to the science and practical matters of watershed management. A main finding is that any watershed assessment approach should be governed by the scope of the problem. If problem areas are unknown and need to be localized, as they surely are in much of Alberta, then the primary watershed assessment must be broad in scale, focused on ranking problem areas for further investigation, and determining overall level of impact. As a watershed becomes better understood and managed, and with the increasing use of best management practices (BMPs), a study can become more detailed, with more focus on examining site-level factors and processes responsible for sediment delivery.

5.3 Road segment hydrology

Road segment hydrology is a key driver of erosion in unsealed road networks. Numerous studies have found that unsealed roads infiltrate water at least to some degree (Croke et al., 2006; Luce & Cundy, 1994; Skaugset et al., 2011; Surfleet et al., 2011). Comparison of road surface runoff with event depth and intensity showed that road erosion was closely linked to the efficiency of hydrological response of a segment to a particular storm (Figure 5-1). Road surfaces did not have constant runoff ratios: instead, runoff ratio varied with the intensity and duration of the storm, although more hydrologically confined road segments in less permeable materials generally had

higher runoff ratios than those which were less confined and in more permeable materials. Road surfaces with the lowest average runoff ratios had the lowest sediment production. A reasonable outcome of this finding is that sediment production needs to be considered on a whole storm time-frame, and the timing and the amount of precipitation should be considered in modelling.

5.4 Contributing area thresholds in the road prism

A consideration when modelling natural systems is whether there are inherent hydrological thresholds, which once crossed, change the behaviour of the system. One of the first systematic studies of forest road erosion by Packer, (1967) defined factors that would increase or decrease the length of road required to incise a rill 1 inch deep on the road surface. Later studies of land surface morphology suggested there were distinct area per contour length thresholds for slope channelization and mass-wasting dependent on large scale landform morphology (Dietrich et al., 1992). Road systems may alter naturally existing slope thresholds by redirecting water or by decreasing permeability of the surface and therefore increasing water yields at road drain points (Montgomery, 1994). Contributing area thresholds were described in chapter 2 of this thesis for uncontrolled channelized erosion in road ditches. Erosion increased moderately up to a contributing area threshold of about 3500 m² and increased much more rapidly after that (Figure 5-2). Channelized ditch erosion could be severe in places, creating ditches up to one and a half metres deep, and partly undermining the road prism (Figure 5-3). Channelized erosion has problematic impacts on roads in two ways. First, it requires prompt attention, commonly grading, but in some places, partial or complete road reconstruction (Figure 5-3, left). Secondly, ditch erosion may damage or bypass existing drainage structures, increasing the likelihood that some or all of the material generated will deposit in a watercourse (Figure 5-3, right). In cases like these it is important to include some estimate of severe gullying probability in a road assessment. A simple approach is to create a table based on a contributing area threshold value for severe erosion that road managers can use in determining a minimum management length for roads, above which some form of site verification is needed in a high-level assessment. A more sophisticated approach may consider the contributing area/slope factor and may consider threshold shear stresses and infiltration rates for different surficial materials.

Contributing area also has scalar effects on road sediment connectivity. Around 77% of the variance in plume extent from roads within the Simonette watershed is explained by the product of upslope contributing area and road grade (or a slope-area product). This finding suggests that

relatively simple hydraulic models can and should be used in future to model road sediment connectivity (Takken et al., 2008; Thompson et al., 2009). Hydrology needs to be explicitly considered when assessing road sediment problems.

5.5 Road crossings as impact sites

Forest road crossings have previously been identified as problematic areas for sediment delivery in the Simonette watershed. Road crossings in the watershed have been found to fragment stream habitat and may create warm backwaters upstream of crossings which impact species distributions upstream and downstream of culverts (Maitland et al., 2016). Additional work examining and identifying erosion risks for culverts and other stream crossing structures in the Simonette watershed was also completed in 2003 (Van Geloven et al., 2004). Work in California confirms the notion that road-stream crossings, and sections of road running parallel and close to streams are a high priority for sediment control (Benda et al., 2019). Similar findings were also reported in chapter 4 of this thesis. Fine sediment intrusion into gravel bedforms in streams in the study area was related to stream crossing density upstream of the sampling point. Clay and Silt fractions increased in the stream bed matrix, whereas sand decreased with increasing road crossing density (Figure 5-4, left). Increasing bed matrix fines were also correlated with higher READI index numbers (Figure 5-4, middle). Road density was not a useful indicator of gravel matrix composition (Figure 5-4, right).

5.6 Stream dynamics predict the location of impact

Hydrology predicts the magnitude of road sediment impact based on the runoff relationship of individual road segments. It also defines the additional risk of gullyng in road segments, and connectivity probability, or the likelihood that a plume of sediment-laden road runoff will be delivered to a stream during a rain event. Hydrological processes also underpin where the impact will be felt in the stream system. Location of impact depends on the caliber of sediment, whether a stream is in a transporting or depositional reach (Al-Chokhachy et al., 2016; Montgomery, 1999), as well as the configuration of bedforms within a stream reach (Tonina & Buffington, 2007, 2009). Road erosion contributes fine sediment to stream networks (Bilby, 1985; Brown et al., 2013; Cederholm et al., 1980; Lisle & Hilton, 1992), and fine sediment tends to follow water flow lines as it travels in suspension. Water flows into and out of the streambed in zones of hyporheic exchange, particularly in pool tails along riffles, and through side-channel bars. Fine sediment intrusion into these areas has been shown to form sediment bridges that plug the upper layer of river bedforms

in sand-bedded rivers and prevent further hyporheic inflow (Rehg et al., 2005). Similar dynamics, potentially with deeper fine sediment infiltration, should occur in gravel-bedded rivers. Streambed freeze core sampling in the study area was focused on side-channel bars, pool tails, and other locations where water was likely to flow into the streambed, and this is where evidence of sediment intrusion was found. Further corroboration of these preliminary findings is recommended, as salmonid fish have a tendency to excavate redds and lay eggs in zones of streambed upwelling, typically downstream of pool crests (Tonina & Buffington, 2009). Stream dynamics therefore not only predict what will be deposited, but where it is most likely to be deposited. Stream beds are commonly reworked during high flow events, thus, changes in bed composition are most likely to persist only where there is chronic sedimentation pressure from road segments.

5.7 Road crossing inventories and watershed monitoring

Road network management, particularly management of stream crossings should be placed on a “continuous improvement” footing. Often, drainage in resource road networks is not well-mapped, but considerable data can be calculated by recording road erosion problems when and where they are observed. Field sediment plume surveys in this watershed were carried out mostly using hand-held global-positioning units, widely available field clinometers, and fibreglass tape measures. Part of assessing and repairing road drainage should involve measuring the impact of a specific drainage failure, including depth of road incision, and a quick survey of plume size taken possibly by dividing the plume into oval, rectangular, or triangular sections and estimating length and width of each. More detailed measurements may use a grid or centreline approach. Road contributing area and slope can be estimated in the field and corrected if necessary in the office using GIS software and accurate elevation models and road linework. Repeated observations over time will build into a formidable dataset that road leaseholders can use to better understand connectivity issues and use to build and refine contributing area thresholds for road problems.

This study used relatively expensive and hard-to-maintain road sedimentation plots to estimate road sedimentation rates and hydrological response in the Simonette. The up-front cost of the equipment itself was dwarfed by time required for plot maintenance and site selection, and by the cost of purchasing and using heavy-duty field equipment to maintain the road sediment plots. A less expensive, less intrusive, and more easily-implemented approach for future work would be to monitor individual culverts and their drainage areas in a watershed. Culvert storm flow rate and turbidity can be estimated using depth and turbidity sensors mounted in the pipe calibrated to

different stage heights and augmented by threshold turbidity samples or grab samples (Skaugset et al., 2011). Alternatively, sediment issuing from a culvert can be impounded behind a silt fence, and periodically dug out and measured.

5.8 General recommendations for resource road management

Historically, road erosion models have lacked strong hydrological inputs due to the difficulty of predicting road erosion using process-based models. The use of these models in watershed assessments often has mixed results (Brown et al., 2015; Skaugset et al., 2011; Wade et al., 2012). One thing that most watershed assessment models have in common is an emphasis on modelling road sediment production and an underemphasis on hydrology, whereas even rudimentary hydrological modelling may go a long way toward properly delineating road sediment delivery zones (Benda et al., 2019; Takken et al., 2008; Thompson et al., 2008, 2009).

A better approach for road assessments may be to break down road network management problems by scale and scope – broad, imprecise, coarse-grained analyses to identify significant potential problem areas, followed by site-level investigation and remediation. This is the approach suggested by Dubé et al. (2004) for the Washington Road Surface Erosion Model. More detailed erosion models may be more useful in local site-based assessment of problem areas. This suggests that rather than using one model to describe all aspects of a road network, there is a need for road managers to use broad-scope tools and detailed site analysis tools together. These need not only be GIS or computer-based but could also take the form of surveys which provide additional site-level estimates of sediment delivery (ie. Carson et al., 2018) depending on budget and organizational expertise.

Another use of site-level road hydrological models may be in assessing the effectiveness of best management practice (BMP) installation. One common concern for road managers is the problematic impact of using culverts for drainage. Several studies have found that road sediment plumes from culvert drains are larger than for other drainage features (Megahan & Ketcheson, 1996; Takken et al., 2008). This is because culverts tend to be installed sparingly due to their inherent cost. Alternative management practices and BMP assessments would involve looking at which BMPs can be most cost-effectively installed and maintained to minimize use of culverts. Such assessments may include determining how much road drainage area turnouts can capture, appropriate road camber and speed limit requirements to direct more water away from inboard ditches that need to be relieved by cross drains, appropriate drain-cleaning schedules, and

hydraulic effect of artificially-placed roughness elements such as straw bales, stones, or wattles in drain outlets. Detailed hydrological modelling and analysis can also further refine hydraulic “worry thresholds” for road segment management (ie. Table 5-1).

5.9 Road infrastructure management options to improve watershed health

Although the costs of sedimentation are widely known and acknowledged in industry, academia, and regulatory bodies, there is not always a consistent emphasis on correcting the problem. As noted in the introduction to this thesis, roads are expensive to maintain (Alberta Municipal Affairs & Morrison Hershfeld Ltd., 2008). Prioritizing maintenance, such that the limited dollars available are well-spent is a key objective for lease-holders. Some of the lessons learned from this thesis research can help stakeholders make better decisions. One major lesson is that road crossings and their approaches are the likely locus of sediment contribution, particularly of fine sediment that has been shown to have negative impacts on the streambed environment. Currently, crossings are a focus of remediation efforts due to their fragmentation impacts on resident fish populations, but a well-designed crossing that maximizes fish passage, can also be constructed to minimize erosion both during and after installation. If crossings are already a remediation focus for fish passage, they can be concurrently optimized to minimize sedimentation risk.

Another element of road network management that needs to be considered is overall cost of ownership. Poorly-maintained or undersized stream crossings are likely to be more expensive to maintain, and may need to be replaced more often than well-constructed, properly-sized stream crossings. Well-drained roads leading to these crossings will also have less problems with ditch gullying, erosion, and drainage control, leading to an overall reduction in total road costs. For inactive or deactivated roads, the simplest, cheapest, and most effective tool for drainage management is usually to pull out culverts and replace them with armoured cross ditches.

5.10 References

- Al-Chokhachy, R., Black, T. A., Thomas, C., Luce, C. H., Rieman, B., Cissel, R., Carlson, A., Hendrickson, S., Archer, E. K., & Kershner, J. L. (2016). Linkages between unpaved forest roads and streambed sediment: why context matters in directing road restoration. *Restoration Ecology*, 24(5), 589–598. <https://doi.org/10.1111/rec.12365>
- Alberta Municipal Affairs, & Morrison Hershfeld Ltd. (2008). *Guidelines on Valuation of Tangible Assets for PSAB 3150*, Alberta Municipal Affairs. 35 pp. Retrieved from http://www.municipalaffairs.gov.ab.ca/documents/ms/AIV_TCA_manual_on_guidelines_on_valuations.pdf
- Benda, L., James, C., Miller, D., & Andras, K. (2019). Road Erosion and Delivery Index (READI): A Model for Evaluating Unpaved Road Erosion and Stream Sediment Delivery. *Journal of the American Water Resources Association*, 55(2), 459–484. <https://doi.org/10.1111/1752-1688.12729>
- Bilby, R. E. (1985). Contributions of road surface sediment to a western Washington stream. *Forest Science*, 31(4), 827–838.
- Bilby, R. E., Sullivan, K., & Duncan, S. H. (1989). The generation and fate of road-surface sediment in forested watersheds in southwestern Washington. *Forest Science*, 35(2), 453–468.
- Brown, K R, McGuire, K. J., Hession, W. C., & Aust, W. M. (2015). Can the Water Erosion Prediction Project Model be used to estimate best management practice effectiveness from forest roads? *Journal of Forestry*, 114 (January 2015), 17-26. <https://doi.org/10.5849/jof.14-101>
- Brown, Kristopher R., Michael Aust, W., & McGuire, K. J. (2013). Sediment delivery from bare and graveled forest road stream crossing approaches in the Virginia Piedmont. *Forest Ecology and Management*, 310, 836–846. <https://doi.org/10.1016/j.foreco.2013.09.031>
- Carson, B., Maloney, D., Chatwin, S., Carver, M., & Beaudry, P. (2018). *Protocol for Evaluating the Potential Impact of Forestry and Range Use on Water Quality (Water Quality Effectiveness Evaluation)*. *Forest and Range Evaluations Program*, B.C. Ministry of Forest Range and Natural Resource Operations and B.C. Min. Env. 70 pp. Retrieved from https://www.for.gov.bc.ca/hfp/frep/site_files/Indicators/Indicators-WaterQuality-Protocol-2009.pdf

- Cederholm, C. J., Reid, L. M., & Salo, E. O. (1980). Cumulative effects of logging road sediment on salmonid populations in the Clearwater River, Jefferson County, Washington. In *Salmon-Spawning Gravel: A Renewable Resource in the Pacific Northwest?* Seattle, WA. October 6-7, 1980, 1-35. Retrieved from <https://www.fs.fed.us/psw/publications/reid/Cederholm.pdf>
- Croke, J., Mockler, S., Hairsine, P., & Fogarty, P. (2006). Relative contributions of runoff and sediment sources within a road prism and implications for total sediment delivery. *Earth Surface Processes and Landforms*, 31(4), 457–468. <https://doi.org/10.1002/esp.1279>
- Dubé, K., Megahan, W. F., & McCalmon, M. (2004). Washington Road Surface Erosion Model (WARSEM) Manual. State of Washington Department of Natural Resources. Retrieved from http://file.dnr.wa.gov/publications/fp_data_warsem_manual.pdf
- Dietrich, W. E., Wilson, C. J., Montgomery, D. R., McKean, J., & Bauer, R. (1992). Erosion thresholds and land surface morphology. *Geology*, 20(8), 675–679. [https://doi.org/10.1130/0091-7613\(1992\)020<0675:ETALSM>2.3.CO;2](https://doi.org/10.1130/0091-7613(1992)020<0675:ETALSM>2.3.CO;2)
- Lisle, T. E., & Hilton, S. (1992). The Volume of Fine Sediment in Pools: an Index of Sediment Supply in Gravel-Bed Streams. *Journal of the American Water Resources Association*, 28(2), 371–383. <https://doi.org/10.1111/j.1752-1688.1992.tb04003.x>
- Luce, C. H., & Cundy, T. W. (1994). Parameter identification for a runoff model for forest roads. *Water Resources Research*, 30(4), 1057–1069. <https://doi.org/10.1029/93WR03348>
- Maitland, B. M., Poesch, M., Anderson, A. E., & Pandit, S. N. (2016). Industrial road crossings drive changes in community structure and instream habitat for freshwater fishes in the boreal forest. *Freshwater Biology*, 61(1), 1–18. <https://doi.org/10.1111/fwb.12671>
- Megahan, W. F., & Ketcheson, G. L. (1996). Predicting downslope travel of granitic sediments from forest roads in Idaho. *Water Resources Bulletin*, 32(2), 371–382. files
- Montgomery, D. R. (1994). Road surface drainage, channel initiation, and slope instability. *Water Resources Research*, 30(6), 1925–1932. <https://doi.org/10.1029/94WR00538>
- Montgomery, D. R. (1999). Process Domains and the River Continuum. *Journal of the American Water Resources Association*, 35(2), 397–410. <https://doi.org/10.1111/j.1752-1688>
- Packer, P. E. (1967). Criteria for Designing and Locating Logging Roads to Control Sediment. *Forest Science*, 13(1), 2–18. <https://doi.org/10.1093/forestscience/13.1.2>

- Rehg, K. J., Packman, A. I., & Ren, J. (2005). Effects of suspended sediment characteristics and bed sediment transport on streambed clogging. *Hydrological Processes*, *19*(2), 413–427. <https://doi.org/10.1002/hyp.5540>
- Reid, L., & Dunne, T. (1984). Sediment Production from Forest Road Surfaces. *Water Resources Research*, *20*(11), 1753–1761.
- Skaugset, A. E., Surfleet, C. G., Meadows, M. W., & Amann, J. (2011). Evaluation of Erosion Prediction Models for Forest Roads. *Transportation Research Record: Journal of the Transportation Research Board*, *2203*, 3–12. <https://doi.org/10.3141/2203-01>
- Surfleet, C. G., Skaugset, A. E., & Meadows, M. W. (2011). Road runoff and sediment sampling for determining road sediment yield at the watershed scale. *Canadian Journal of Forest Research*, *41*(10), 1970–1980. <https://doi.org/10.1139/x11-104>
- Takken, I., Croke, J., & Lane, P. N. J. (2008). A methodology to assess the delivery of road runoff in forestry environments. *Hydrological Processes*, *22* (November 2008), 254–264. <https://doi.org/10.1002/hyp.6581>
- Thompson, C., Barry, S., & Takken, I. (2009). A model for optimizing forest road drain spacing. In Anderssen, R.S., R.D. Braddock, and L.T.H. Newham (Eds.) *18th World IMACS Congress and MODSIM09 International Congress on Modelling and Simulation*, July 2009, Cairns, Australia, (pp. 4093–4099). Retrieved from <http://www.mssanz.org.au/modsim09/115/thompson.pdf>
- Thompson, C. J., Takken, I., & Croke, J. (2008). Hydrological and sedimentological connectivity of unsealed roads. In J. Schmidt, T. Cochrane, C. Phillips, S. Elliott, T. Davies, L. Basher (Eds.) *Sediment Dynamics in Changing Environments* (Proceedings of a Symposium held in Christchurch, NZ). IAHS-AISH Publication 325, 524–531.
- Tonina, D., & Buffington, J. M. (2007). Hyporheic exchange in gravel bed rivers with pool-riffle morphology: Laboratory experiments and three-dimensional modeling. *Water Resources Research*, *43*(1), 1–16. <https://doi.org/10.1029/2005WR004328>
- Tonina, D., & Buffington, J. M. (2009). Hyporheic exchange in mountain rivers I: Mechanics and environmental effects. *Geography Compass*, *3*(3), 1063–1086. <https://doi.org/10.1111/j.1749-8198.2009.00226.x>

- Van Geloven, C., Newman, N., & Beaudry, P. G. (2004). *Results of the Stream Crossing Quality Index (SCQI) Survey in FMA 9900037 , 2003 Field Season* [Environmental Monitoring Report], prepared for Canadian Forest Products by P. Beaudry and Assoc. Ltd. 78 pp.
- Wade, C. R., Bolding, M. C., Aust, W. M., Lakel, W. A., & Schilling, E. B. (2012). Comparing sediment trap data with the USLE-Forest, RUSLE2, and WEPP-Road erosion models for evaluation of bladed skid trail BMPs. *Transactions of the ASABE*, 55(2), 403-414.

5.11 Tables

Table 5-1. Maximum management lengths for roads in the Simonette watershed based on a maximum contributing area of 3500 m²

Maximum Management Area (m ²)		3500			
Road segment type	Camber	Ditch Width (m)	Cutslope (m)	Contributing Roadway (m)	Max. Length (m)
Raised, well-drained road segment	Crowned	5	N	5	350.0
	Insloping	5	N	10	233.33
Cut-and fill segment	Crowned	5	5	5	233.33
	Insloping	5	5	10	175.00
Through-cut or wind-rowed	Either	5	5	10	116.67

5.12 Figures

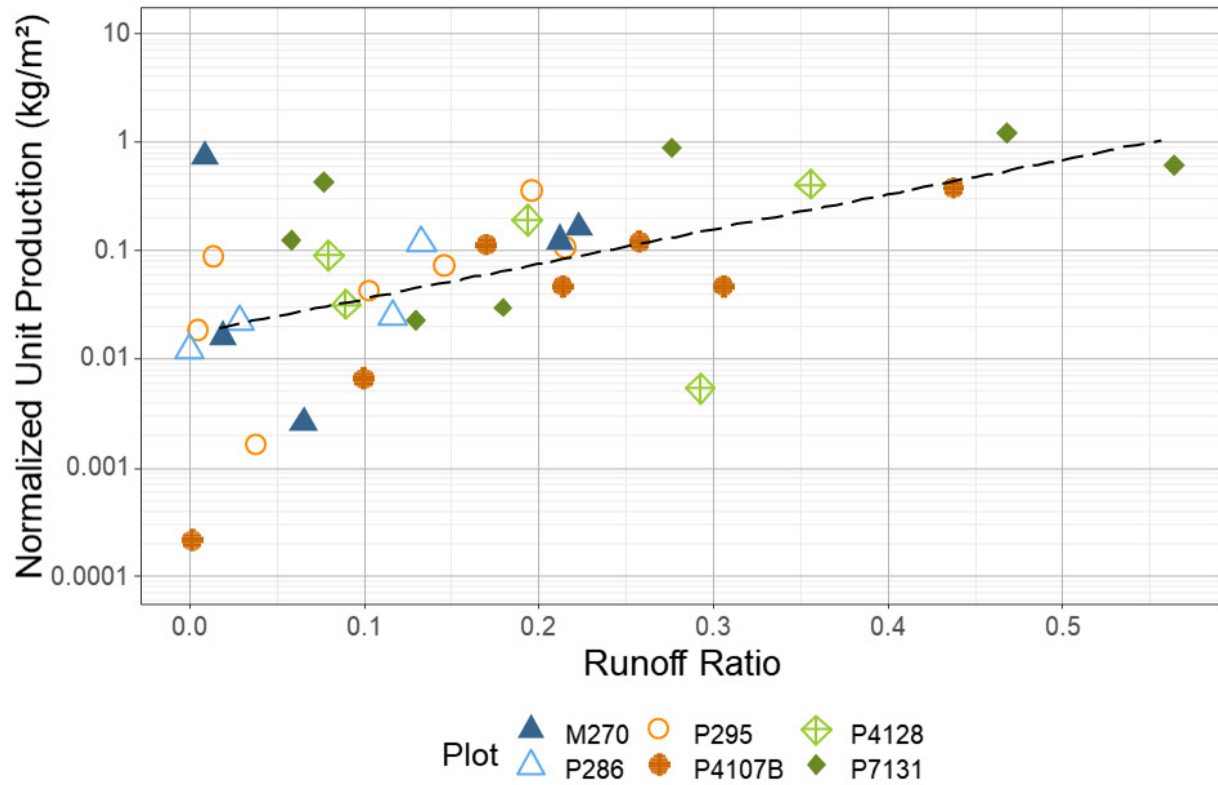


Figure 5-1. Normalized sediment production (logarithmic axis) versus plot runoff ratio for road plots in the Simonette

Colours correspond to geological type (blue = lacustrine; orange = fluvial; green = morainal/mixed), solid points are high and moderate traffic roads, whereas hollow points are low traffic roads.

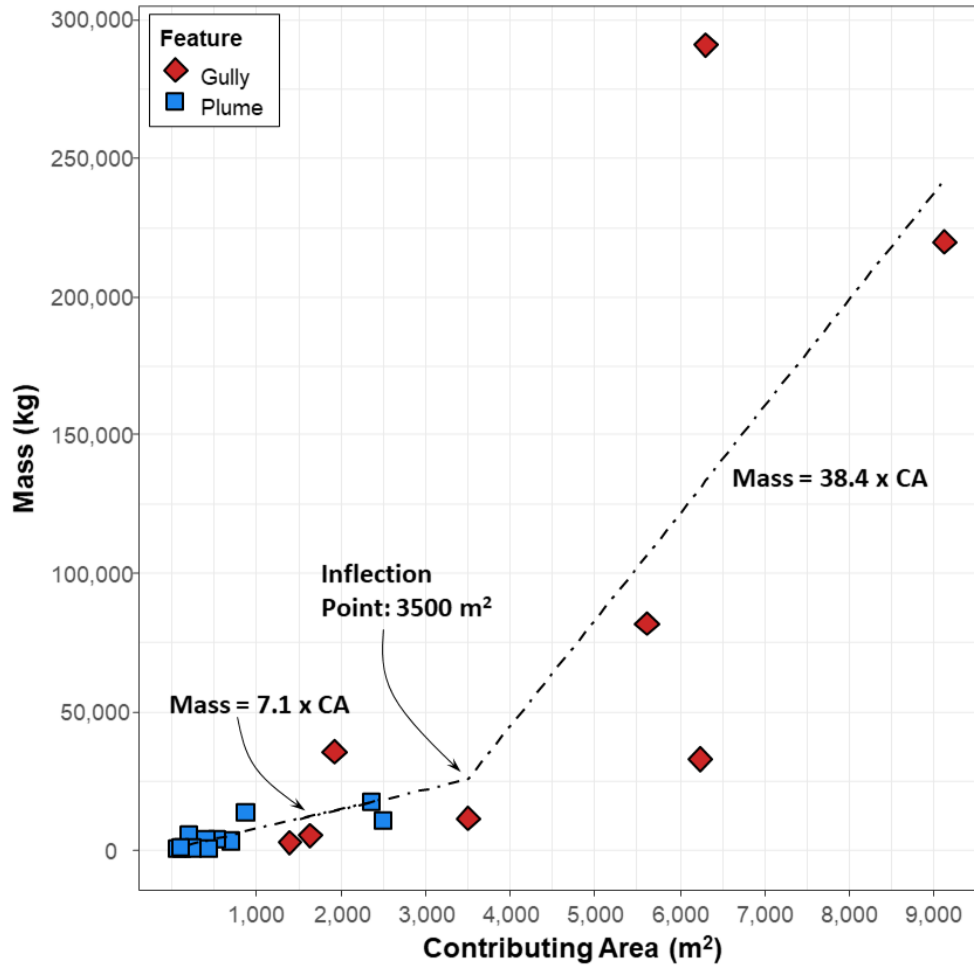


Figure 5-2. Erosion and contributing area relationships for measured sediment plumes (blue), and gullied ditch segments (red). Erosion increases rapidly for sections of road larger than 3500 m²



Figure 5-3. Channelized ditch erosion in the Simonette. Deep erosion with partial undermining of the road prism (left), long, narrow, and deep channel depositing in Deep Valley Creek (right).

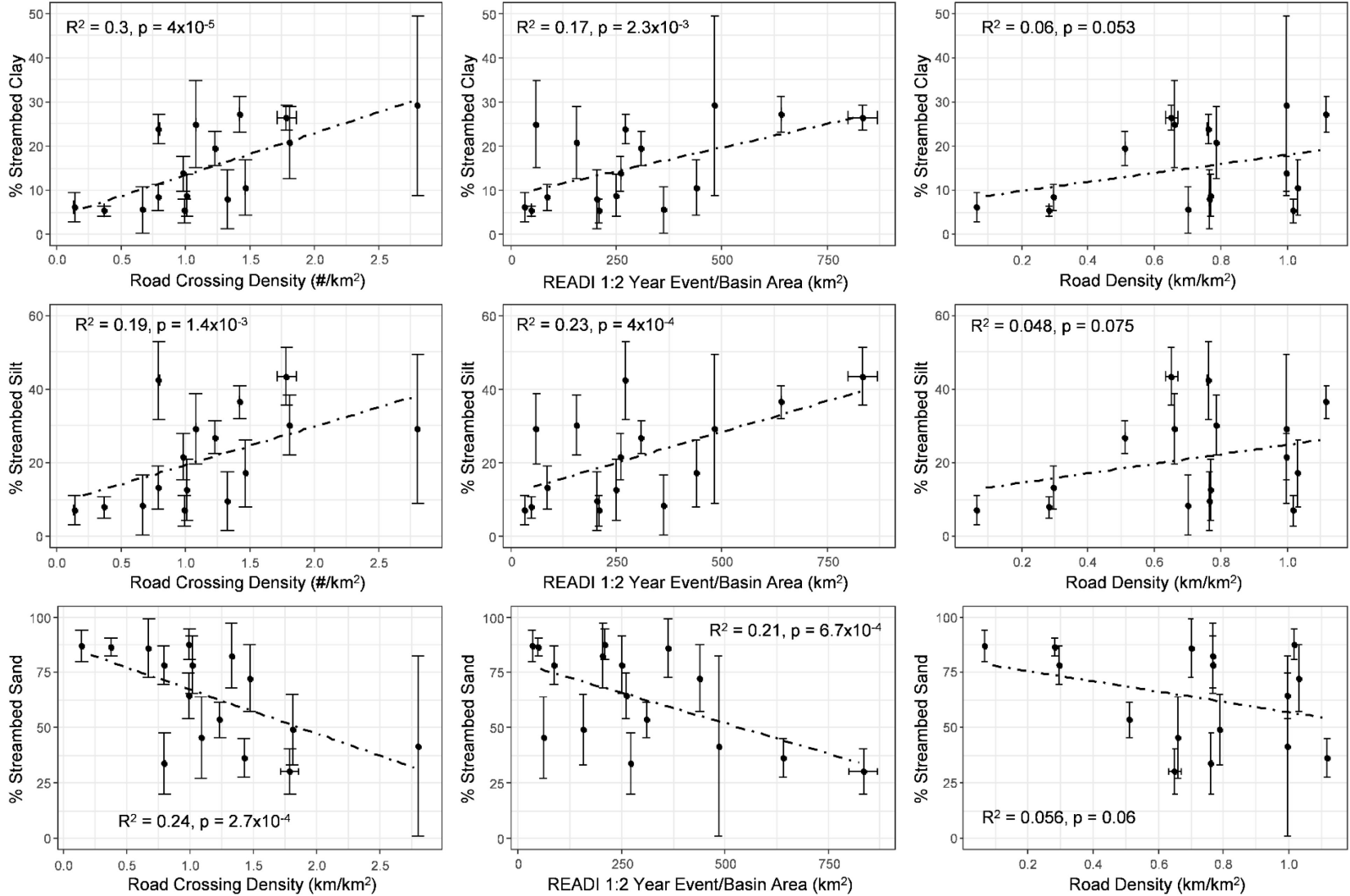


Figure 5-4. Gravel matrix composition compared to road crossing density (#/km), READI values, and road density (km/km²) from left to right. The most significant correlations are between road crossing density and gravel matrix composition, and the least are between road density and gravel matrix composition.

References

- Ahrens, B. (2006). Distance in spatial interpolation of daily rain gauge data. *Hydrology and Earth System Sciences*, 10(2), 197–208. <https://doi.org/10.5194/hess-10-197-2006>
- Al-Chokhachy, R., Black, T. A., Thomas, C., Luce, C. H., Rieman, B., Cissel, R., et al. (2016). Linkages between unpaved forest roads and streambed sediment: why context matters in directing road restoration. *Restoration Ecology*, 24(5), 589–598. <https://doi.org/10.1111/rec.12365>
- Alberta Environment and Parks (2021). Alberta River Basins [web app]. Retrieved May 24, 2021 from <https://rivers.alberta.ca/>
- Alberta Environment and Parks (2018). Base Watersheds – Simplified Hydrography [GIS features]. Retrieved October 2, 2021 from: <https://geodiscover.alberta.ca/geoportal/rest/metadata/item/e4197d5f6b3043be8cbf9e7f8b49c4fe/html>
- Alberta Municipal Affairs, & Morrison Hershfeld Ltd. (2008). *Guidelines on Valuation of Tangible Assets for PSAB 3150*. Edmonton. Retrieved from http://www.municipalaffairs.gov.ab.ca/documents/ms/AIV_TCA_manual_on_guidelines_on_valuations.pdf
- Alberta Transportation. (2019). *Unit Price Averages Reports*.
- Alberta Transportation. (2020). Historical Seasonal Weight Changes. Retrieved January 16, 2021, from <http://www.transportation.alberta.ca/content/doctype260/production/trans-historical-seasonal-weight-changes.pdf>
- Andriashek, L. D. (2001). *Surficial Geology of Wapiti Area, NTS 83L* (No. Map 239). Edmonton, Alberta.
- ASTM. (2014). *ASTM D3977-97(2013) - Standard Test Methods for Determining Sediment Concentration in Water Samples*. *ASTM Book of Standards* (Vol. 90). West Conshohocken, PA: ASTM International. <https://doi.org/10.1520/D3977-97R13E01.2>
- Atkinson, N., & Hartman, G. M. D. (2017). *West-Central Alberta Regional Stratigraphic Model - Sediment Thickness* (Digital Data No. DIG 2017-0016). Edmonton, Alberta.

- Atkinson, N., & Lyster, S. (2010). *Thickness and Distribution of Quaternary and Neogene Sediment in Alberta, Canada* (Digital Data No. DIG 2010-0036). Edmonton, Alberta: Alberta Geological Survey.
- Baptiste, A. (2017). gridExtra: Miscellaneous Functions for “Grid” Graphics. Retrieved from <https://cran.r-project.org/package=gridExtra>
- Benda, L. E., James, C., Miller, D. J., & Andras, K. (2019). Road Erosion and Delivery Index (READI): A Model for Evaluating Unpaved Road Erosion and Stream Sediment Delivery. *Journal of the American Water Resources Association*, 55(2), 459–484. <https://doi.org/10.1111/1752-1688.12729>
- Bilby, R. E. (1985). Contributions of road surface sediment to a western Washington stream. *Forest Science*, 31(4), 827–838.
- Bilby, R. E., Sullivan, K., & Duncan, S. H. (1989). The generation and fate of road-surface sediment in forested watersheds in southwestern Washington. *Forest Science*, 35(2), 453–468.
- Black, T. A., & Luce, C. H. (2013). Measuring Water and Sediment Discharge From a Road Plot With a Settling Basin and Tipping Bucket, (June), 38.
- Black, T. A., Cissel, R. M., & Luce, C. H. (2012). *The Geomorphic Road Analysis and Inventory Package (GRAIP) Volume 1: Data Collection Method* (General Technical Report No. RMRS-GTR-280WWW). Rocky Mountain Research Station General Technical Report. Fort Collins, CO. <https://doi.org/10.2737/RMRS-GTR-280>
- Blake, G. R. (2008). Particle Density. In W. Chesworth (Ed.), *Encyclopedia of Soil Science*. Dordrecht: Springer Netherlands. <https://doi.org/10.1007/978-1-4020-3995-9>
- Brake, D., Molnau, M., & King, J. G. (1997). *Sediment transport distances and culvert spacings on logging roads within the Oregon coast mountain range. 1997 Annual International Meeting, ASAE*. Minneapolis, MN.
- Brown, K. R., Aust, W. M., & McGuire, K. J. (2013). Sediment delivery from bare and graveled forest road stream crossing approaches in the Virginia Piedmont. *Forest Ecology and Management*, 310, 836–846. <https://doi.org/10.1016/j.foreco.2013.09.031>
- Brown, K. R., McGuire, K. J., Hession, W. C., & Aust, W. M. (2015). Can the Water Erosion Prediction Project Model be used to estimate best management practice effectiveness from

- forest roads? *Journal of Forestry*, 114(January 2015), 17–26. <https://doi.org/10.5849/jof.14-101>
- Bunte, K., & Abt, S. R. (2001). SAMPLING FRAME FOR IMPROVING PEBBLE COUNT ACCURACY IN COARSE GRAVEL-BED STREAMS. *JAWRA Journal of the American Water Resources Association*, 37(4), 1001–1014. <https://doi.org/10.1111/j.1752-1688.2001.tb05528.x>
- Burroughs, E. R., & King, J. G. (1989). *Reduction of Soil Erosion on Forest Roads*. Ogden, UT.
- Cahill, C. L. (2015). *Status of the Arctic Grayling (Thymallus arcticus) in Alberta: Update 2015*. Alberta Wildlife Status Report No. 57. Edmonton, Alberta. Retrieved from <https://open.alberta.ca/publications/9781460134528>
- Carson, B., Maloney, D., Chatwin, S., Carver, M., & Beaudry, P. G. (2018). *Protocol for Evaluating the Potential Impact of Forestry and Range Use on Water Quality (Water Quality Effectiveness Evaluation)*. Forest and Range Evaluations Program. Victoria, BC. Retrieved from https://www.for.gov.bc.ca/hfp/frep/site_files/Indicators/Indicators-WaterQuality-Protocol-2009.pdf
- Cederholm, C. J., Reid, L. M., & Salo, E. O. (1980). Cumulative effects of logging road sediment on salmonid populations in the Clearwater River, Jefferson County, Washington. In *Salmon-Spawning Gravel: A Renewable Resource in the Pacific Northwest?* (pp. 1–35). Seattle, WA. Retrieved from <https://www.fs.fed.us/psw/publications/reid/Cederholm.pdf>
- Chanasyk, D. S., & Woytowich, C. P. (1987). *A Study of Water Erosion in the Peace Region*. Edmonton, Alberta.
- Chapman, D. W. (1988). Critical review of variables used to define effects of fines in redds of large salmonids. *Transactions of the American Fisheries Society*, 117(1), 1–21. [https://doi.org/10.1577/1548-8659\(1988\)117<0001](https://doi.org/10.1577/1548-8659(1988)117<0001)
- Coe, D. B. R. (2006). *Sediment Production and Delivery From Forest Roads in the Sierra Nevada, California*. Colorado State University.
- Costello, A. B. (2006). *Status of the Westslope Cutthroat Trout (Oncorhynchus clarkii lewisii) in Alberta* (Alberta Wildlife Status Report No. 61). Retrieved from <https://open.alberta.ca/publications/0778518694>
- Croke, J. C., & Mockler, S. P. (2001). Gully initiation and road-to-stream linkage in a forested catchment southeastern Australia. *Earth Surface Processes and Landforms*, 26(2), 205–217.

[https://doi.org/10.1002/1096-9837\(200102\)26:2<205::AID-ESPI68>3.0.CO;2-G](https://doi.org/10.1002/1096-9837(200102)26:2<205::AID-ESPI68>3.0.CO;2-G)

- Croke, J. C., Mockler, S. P., Fogarty, P., & Takken, I. (2005). Sediment concentration changes in runoff pathways from a forest road network and the resultant spatial pattern of catchment connectivity. *Geomorphology*, 68(3–4), 257–268.
<https://doi.org/10.1016/j.geomorph.2004.11.020>
- Croke, J. C., Mockler, S. P., Hairsine, P. B., & Fogarty, P. (2006). Relative contributions of runoff and sediment sources within a road prism and implications for total sediment delivery. *Earth Surface Processes and Landforms*, 31(4), 457–468. <https://doi.org/10.1002/esp.1279>
- Dabney, S. (National S. L. (2019). RIST (Rainfall Intensity Summarization Tool). Oxford, Mississippi: USDA National Sedimentation Laboratory. Retrieved from <https://www.ars.usda.gov/southeast-area/oxford-ms/national-sedimentation-laboratory/watershed-physical-processes-research/research/rist/rist-rainfall-intensity-summarization-tool/>
- Dietrich, W. E., Wilson, C. J., Montgomery, D. R., McKean, J., & Bauer, R. (1992). Erosion thresholds and land surface morphology. *Geology*. [https://doi.org/10.1130/0091-7613\(1992\)020<0675:ETALSM>2.3.CO;2](https://doi.org/10.1130/0091-7613(1992)020<0675:ETALSM>2.3.CO;2)
- Dinno, A. (2017). dunn.test. Retrieved from <https://cran.r-project.org/package=dunn.test>
- Dissmeyer, G. E., & Foster, G. R. (1980). *A Guide For Predicting Sheet and Rill Erosion on Forest Land* (Technical Reports No. SA-TP 11). Atlanta, GA.
- Dubé, K., Megahan, W. F., & McCalmon, M. (2004). Washington Road Surface Erosion Model (WARSEM) Manual. State of Washington Department of Natural Resources. Retrieved from http://file.dnr.wa.gov/publications/fp_data_warsem_manual.pdf
- Elliot, W. J. (2013). Erosion processes and prediction with WEPP technology in forests in the Northwestern U.S. *Transactions of the ASABE*, 56(2), 563–579.
- Elliot, W. J., & Tysdal, L. M. (1999). Understanding and reducing erosion from insloping roads. *Journal of Forestry*, (August 1999), 30–34.
- Elliot, W. J., Hall, D. E., & Scheele, D. L. (1999). FS-WEPP: Forest Service Interfaces for the Water Erosion Prediction Project Computer Model. Moscow, ID: USDA Forest Service, Rocky Mountain Research Station. Retrieved from <https://forest.moscowfsl.wsu.edu/fswepp/>

- Environment and Climate Change Canada. (2019). Canadian Climate Normals and Averages 1981-2010. Retrieved July 7, 2020, from https://climate.weather.gc.ca/climate_normals/index_e.html
- Environment Canada. (2019). Short-Duration Rainfall Intensity-Duration-Frequency Data. Ottawa, Canada: Government of Canada. Retrieved from https://climate.weather.gc.ca/prods_servs/engineering_e.html
- Fenton, M. M., Waters, E. J., Pawley, S. M., Atkinson, N., Utting, D. J., & McKay, K. (2013). Surficial Geology of Alberta. *Alberta Geological Survey Map 601*.
- Fox, J., & Weisberg, S. (2019). *An {R} Companion to Applied Regression* (Third Edit). Thousand Oaks, CA: Sage. Retrieved from <https://socialsciences.mcmaster.ca/jfox/Books/Companion/>
- Van Geloven, C., Newman, N., & Beaudry, P. G. (2004). *Results of the Stream Crossing Quality Index (SCQI) Survey in FMA 9900037 , 2003 Field Season*. Prince George, BC.
- Government of Alberta. Alberta Timber Harvest Planning and Operating Ground Rules Framework for Renewal (2016). Retrieved from [https://www1.agric.gov.ab.ca/\\$department/deptdocs.nsf/all/formain15749/\\$FILE/TimberHarvestPlanning-OperatingGroundRulesFramework-Dec2016.pdf](https://www1.agric.gov.ab.ca/$department/deptdocs.nsf/all/formain15749/$FILE/TimberHarvestPlanning-OperatingGroundRulesFramework-Dec2016.pdf) - section II.1.2
- Hairsine, P. B., Croke, J. C., Mathews, H., Fogarty, P., & Mockler, S. P. (2002). Modelling plumes of overland flow from logging tracks. *Hydrological Processes*, 16(12), 2311–2327. <https://doi.org/10.1002/hyp.1002>
- Hawthorn, K. F. (2014). *The role of fine sediment in phosphorous dynamics and stream productivity in Rocky Mountain headwater streams: Possible long-term effects of extensive logging*. University of Alberta.
- Hlavac, M. (2018). stargazer: Well-formatted Regression and Summary Statistics Tables. Retrieved from <https://cran.r-project.org/package=stargazer>
- Hoover, M. D. (1952). Water and Timber Management. *Journal of Soil and Water Conservation*, (April 1952), 75–78.
- Horton, R. E. (1945). Erosional Development of Streams and their Drainage Basins. *Bulletin of the Geological Society of America*, 56, 275–370. [https://doi.org/http://dx.doi.org/10.1130/0016-7606\(1945\)56\[275:EDOSAT\]2.0.CO;2](https://doi.org/http://dx.doi.org/10.1130/0016-7606(1945)56[275:EDOSAT]2.0.CO;2)

- Howard, M. J. (2018). *Erosion and Erodibility from Off-Highway Vehicle Trails in Alberta's Southern Rocky Mountains*. University of Alberta.
<https://doi.org/https://doi.org/10.7939/R3SX64R9F>
- Huayta Hernani, L. F. (2019). *Application of LiDAR DEM Metrics to Estimate Road-stream Sediment Connectivity in Alberta Eastslopes Salmonid Habitats*. University of Alberta.
<https://doi.org/https://doi.org/10.7939/r3-lxrm-wj37>
- Ketcheson, G. L., & Megahan, W. F. (1996). *Sediment Production and Downslope Sediment Transport from Forest Roads in Granitic Watersheds* (Research Paper No. INT-RP-486). Ogden, UT.
- Kidd, W.J., Megahan, W.F. (1972). Effects of logging and logging roads on erosion and sediment deposition from steep terrain. *Journal of Forestry*, March 1972, 136-141
- Lane, P. N. J., & Sheridan, G. J. (2002). Impact of an unsealed forest road stream crossing: Water quality and sediment sources. *Hydrological Processes*, 16(13), 2599–2612.
<https://doi.org/10.1002/hyp.1050>
- Liaw, A., & Weiner, M. (2002). Classification and Regression by randomForest. *R News*, 2(3), 18–22. Retrieved from <https://cran.r-project.org/doc/Rnews/>
- Lieberman, J. A., & Hoover, M. D. (1948). The Effect of Uncontrolled Logging on Stream Turbidity. *Water and Sewage Works*, (July 1948).
- Lisle, T. E., & Hilton, S. (1992). The Volume of Fine Sediment in Pools: an Index of Sediment Supply in Gravel-Bed Streams. *JAWRA Journal of the American Water Resources Association*, 28(2), 371–383. <https://doi.org/10.1111/j.1752-1688.1992.tb04003.x>
- Luce, C. H., & Black, T. a. (1999). Sediment production from forest roads in western Oregon. *Water Resources Research*, 35(8), 2561–2570. <https://doi.org/10.1029/1999WR900135>
- Luce, C. H., & Black, T. A. (2001a). Effects of traffic and ditch maintenance on forest road sediment production. In *Proceedings of the Seventh Federal Interagency Sedimentation Conference* (pp. 67–74). Retrieved from <http://www.treesearch.fs.fed.us/pubs/23963>
- Luce, C. H., & Black, T. A. (2001b). Spatial and Temporal Patterns in Erosion from Forest Roads. In M. S. Wigmosta & S. J. Burges (Eds.), *Influence of Urban and Forest land Uses on the Hydrologic-Geomorphic Responses of Watersheds* (pp. 165–178). Washington, D.C.: American

- Geophysical Union. <https://doi.org/2>
- Luce, C. H., & Cundy, T. W. (1994). Parameter identification for a runoff model for forest roads. *Water Resources Research*, 30(4), 1057–1069. <https://doi.org/10.1029/93WR03348>
- Maitland, B. M., Poesch, M., Anderson, A. E., & Pandit, S. N. (2016). Industrial road crossings drive changes in community structure and instream habitat for freshwater fishes in the boreal forest. *Freshwater Biology*, 61(1), 1–18. <https://doi.org/10.1111/fwb.12671>
- Majhi, A., Nyssen, J., & Verdoodt, A. (2021). What is the best technique to estimate topographic thresholds of gully erosion? Insights from a case study on the permanent gullies of Rarh plain, India. *Geomorphology*, 375, 107547. <https://doi.org/10.1016/j.geomorph.2020.107547>
- McConkey, B. G., Nicholaichuk, W., Steppuhn, H., & Reimer, C. D. (1997). Sediment yield and seasonal soil erodibility for semiarid cropland in western Canada. *Canadian Journal of Soil Science*, 77(1), 33–40. <https://doi.org/10.4141/S95-060>
- McCool, D. K., Foster, G. R., Mutchler, C. K., & Meyer, L. D. (1989). Revised Slope Length Factor for the Universal Soil Loss Equation. *Transactions of the American Society of Agricultural Engineers*, 32(5), 1571–1576.
- van Meerveld, H. J., Baird, E. J., & Floyd, W. C. (2014). Controls on sediment production from an unpaved resource road in a Pacific maritime watershed. *Water Resources Research*, 50(6), 4803–4820. <https://doi.org/10.1002/2013WR014605>
- Megahan, W. F., & Ketcheson, G. L. (1996). Predicting downslope travel of granitic sediments from forest roads in Idaho. *Water Resources Bulletin*, 32(2), 371–382. Retrieved from files
- Megahan, W. F., & Kidd, W. J. (1972). Effects of logging and logging roads on erosion and sediment deposition from steep terrain. *Journal of Forestry*, (March), 136–141.
- Megahan, W. F., Seyedbagheri, K. A., & Dodson, P. C. (1983). Long-term erosion on granitic roadcuts based on exposed tree roots. *Earth Surface Processes and Landforms*, 8(1), 19–28. <https://doi.org/10.1002/esp.3290080103>
- Montgomery, D. R. (1994). Road surface drainage, channel initiation, and slope instability. *Water Resources Research*, 30(6), 1925–1932. <https://doi.org/10.1029/94WR00538>
- Montgomery, D. R. (1999). Process Domains and the River Continuum. *Journal Of The American Water Resources Association*, 35(2), 397–410. <https://doi.org/10.1111/j.1752-1688>

- Montgomery, D. R., & Buffington, J. M. (1997). Channel-reach morphology in mountain drainage basins. *Bulletin of the Geological Society of America*, 109(5), 596–611. [https://doi.org/10.1130/0016-7606\(1997\)109<0596:CRMIMD>2.3.CO](https://doi.org/10.1130/0016-7606(1997)109<0596:CRMIMD>2.3.CO)
- Montgomery, D. R., & Dietrich, W. E. (1992). Channel Initiation and the Problem of Landscape Scale. *Science*, 255(5046), 826–830.
- Montgomery, D. R., & MacDonald, L. H. (2002). Diagnostic Approach to Stream Channel Assessment and Monitoring. *Journal Of The American Water Resources Association*, 38(1).
- Natural Regions Committee. (2006). *Natural regions and subregions of Alberta*. (D. J. Downing & W. W. Pettapiece, Eds.). Edmonton, Alberta. <https://doi.org/10.5962/bhl.title.115367>
- Nearing, M. A., Foster, G. R., Lane, L., & Finkner, S. (1989). A process - based soil erosion model for USDA - water erosion prediction project technology. *Transactions of the American Society of Agricultural Engineers*, 32(5), 1587–1593. <https://doi.org/10.13031/2013.31195>.
- Nelson, A. D., & Church, M. (2012). Placer mining along the Fraser River, British Columbia: The geomorphic impact. *Bulletin of the Geological Society of America*, 124(7–8), 1212–1228. <https://doi.org/10.1130/B30575.1>
- Nelson, N. A., Luce, C. H., & Black, T. A. (2019). *GRAIP_Lite : A System for Road Impact Assessment*. Boise, ID.
- Overton, D. E., & Meadows, M. E. (1976). *Stormwater Modelling*. New York: Academic Press.
- Packer, P. E. (1967). Criteria for Designing and Locating Logging Roads to Control Sediment. *Forest Science*, 13(1), 2–18. <https://doi.org/10.1093/forestscience/13.1.2>
- Patton, P. C., & Schumm, S. A. (1975). Gully Erosion, Northwestern Colorado: A Threshold Phenomenon. *Geology*, 3(2), 88–90.
- Pawley, S. M., & Atkinson, N. (2013). *Surficial Geology of the Little Smoky Area (NTS 83K/NW)* (No. Map 564). Edmonton, Alberta.
- Phillips, R. W., Lantz, R. L., Claire, E. W., & Moring, J. R. (1975). Some Effects of Gravel Mixtures on Emergence of Coho Salmon and Steelhead Trout Fry. *Transactions of the American Fisheries Society*, 104(3), 461–466. [https://doi.org/10.1577/1548-8659\(1975\)104<461:SEOGMO>2.0.CO;2](https://doi.org/10.1577/1548-8659(1975)104<461:SEOGMO>2.0.CO;2)

- Prior, G. J., Hathway, B., Glombick, P. M., Pana, D. I., Banks, C. J., Hay, D. C., et al. (2013). *Map 600 Bedrock Geology of Alberta* (Vol. 2479). Edmonton, Alberta.
- R Core Team. (2019). R: A language and environment for statistical computing. Vienna, Austria: R Foundation for Statistical Computing. Retrieved from <https://www.r-project.org/>
- Rasmussen, J. B., & Taylor, E. B. (2009). *Status of the Athabasca Rainbow Trout (Oncorhynchus mykiss) in Alberta* (Alberta Wildlife Status Report No. 66). *Alberta Wildlife Status Report*. Edmonton, Alberta. <https://doi.org/10.5962/bhl.title.114290>
- Rehg, K. J., Packman, A. I., & Ren, J. (2005). Effects of suspended sediment characteristics and bed sediment transport on streambed clogging. *Hydrological Processes*, *19*(2), 413–427. <https://doi.org/10.1002/hyp.5540>
- Reid, D. A., Hassan, M. A., & Floyd, W. C. (2016). Reach-scale contributions of road-surface sediment to the Honna River, Haida Gwaii, BC. *Hydrological Processes*, *30*(19), 3450–3465. <https://doi.org/10.1002/hyp.10874>
- Reid, L. M., & Dunne, T. (1984). Sediment Production from Forest Road Surfaces. *Water Resources Research*, *20*(11), 1753–1761.
- Reid, L. M., Dunne, T., & Cederholm, C. J. (1981). Application of sediment budget studies to the evaluation of logging road impact. *Journal of Hydrology*, 49–62. Retrieved from http://www.wou.edu/las/physci/taylor/andrews_forest/refs/reid_etal_198x.pdf
- Renard, K. G., Foster, G. R., Weesies, G. A., & Porter, J. P. (1991). RUSLE: Revised Universal Soil Loss Equation. *J. Soil Water Conserv*, *46*, 30–33. Retrieved from www.swcs.org
- Renard, K. G., Foster, G. R., Weesies, G. A., McCool, D. K., & Yoder, D. C. (1997). *Predicting Soil Erosion by Water: A guide to conservation planning with the Revised Universal Soil Loss Equation (RUSLE)* (Agriculture Handbook No. 703). Washington, D.C.
- Reynolds, J. B., Simmons, R. C., & Burkholder, A. R. (1990). Effects of Placer Mining Discharge on Health and Food of Arctic Grayling. *Water Resources Bulletin*, *25*(3), 625–635.
- Rivenbark, B. L., & Jackson, C. R. (2004). Concentrated flow breakthroughs moving through silvicultural streamside management zones: southeastern piedmont, USA. *Journal of the American Water Resources Association*, *40*(4), 1043–1052. <https://doi.org/10.1111/j.1752-1688.2004.tb01065.x>

- Robichaud, P. R., & Brown, R. E. (2002). *Silt Fences : An Economical Technique for Measuring Hillslope Soil Erosion* (General Technical Reprint No. RMRS-GTR-94). *General Technical Report*. Fort Collins, CO. Retrieved from http://www.fs.fed.us/rm/pubs/rmrs_gtr94.pdf
- Rodtka, M., Johnston, F. D., & Post, J. R. (2009). *Status of the Bull Trout (Salvelinus confluentus) in Alberta : Update 2009*. *Wildlife Status Report No. 39*. Edmonton. Retrieved from <https://open.alberta.ca/publications/9780778591788>
- Schloerke, B., Crowley, J., Cook, D., Briatte, F., Marbach, M., Thoen, E., et al. (2018). GGally: Extension to “ggplot2.” Retrieved from <https://cran.r-project.org/package=GGally>
- Scrimgeour, G. J., Hvenegaard, P. J., & Tchir, J. (2008). Cumulative industrial activity alters lotic fish assemblages in two boreal forest watersheds of Alberta, Canada. *Environmental Management*, 42(6), 957–970. <https://doi.org/10.1007/s00267-008-9207-2>
- Shepard, D. (1968). A two-dimensional interpolation function for irregularly-spaced data. In *Proceedings of the 1968 23rd ACM National Conference, ACM 1968* (pp. 517–524). Association for Computing Machinery, Inc. <https://doi.org/10.1145/800186.810616>
- Sidle, R. C., Sasaki, S., Otsuki, M., Noguchi, S., & Abdul Rahim, N. (2004). Sediment pathways in a tropical forest: Effects of logging roads and skid trails. *Hydrological Processes*, 18(4), 703–720. <https://doi.org/10.1002/hyp.1364>
- Skaugset, A. E., Surfleet, C. G., Meadows, M. W., & Amann, J. (2011). Evaluation of Erosion Prediction Models for Forest Roads. *Transportation Research Record: Journal of the Transportation Research Board*, 2203, 3–12. <https://doi.org/10.3141/2203-01>
- Soon, Y. K., Arshad, M. A., Rice, W. A., & Mills, P. (2000). Recovery of chemical and physical properties of boreal plain soils impacted by pipeline burial. *Canadian Journal of Soil Science*, 80(3), 489–497. <https://doi.org/10.4141/S99-097>
- Sosa-Pérez, G., & MacDonald, L. H. (2017). Effects of closed roads, traffic, and road decommissioning on infiltration and sediment production: A comparative study using rainfall simulations. *Catena*, (159), 93–105. <https://doi.org/10.1016/j.catena.2017.08.004>
- Spillios, L. C. (1999). *Sediment intrusion and deposition near road crossings in small foothill streams in West Central Alberta*. University of Alberta.
- Startsev, A. D., & McNabb, D. H. (2000). Effects of skidding on forest soil infiltration in west-

- central Alberta. *Canadian Journal of Soil Science*, 80(4), 617–624. <https://doi.org/10.4141/s99-092>
- Sugden, B. D., & Woods, S. W. (2007). Sediment Production From Forest Roads in Western Montana. *JAWRA Journal of the American Water Resources Association*, 43(1), 193–206. <https://doi.org/10.1111/j.1752-1688.2007.00016.x>
- Surfleet, C. G., Skaugset, A. E., & Meadows, M. W. (2011). Road runoff and sediment sampling for determining road sediment yield at the watershed scale. *Canadian Journal of Forest Research*, 41(10), 1970–1980. <https://doi.org/10.1139/x11-104>
- Takken, I., Croke, J. C., & Lane, P. N. J. (2008). A methodology to assess the delivery of road runoff in forestry environments. *Hydrological Processes*, 22(November 2008), 254–264. <https://doi.org/10.1002/hyp.6581>
- Tarboton, D. G. (2014). Geomorphologic Road Analysis and Inventory Package (GRAIP). Logan, UT: Utah State University. Retrieved from <http://hydrology.usu.edu/dtarb/graip/>
- Thompson, C. J., Takken, I., & Croke, J. C. (2008). Hydrological and sedimentological connectivity of unsealed roads. In J. Schmidt, T. Cochrane, C. Phillips, S. Elliott, T. Davies, & L. Basher (Eds.), *Sediment Dynamics in Changing Environments* (pp. 524–531). Christchurch, NZ: IAHS Press.
- Thompson, C. J., Barry, S., & Takken, I. (2009). A model for optimizing forest road drain spacing. In R. S. Anderssen, R. D. Braddock, & L. T. H. Newham (Eds.), *18th World IMACS Conference and MODSIM09 International Congress on Modelling and Simulation* (pp. 4093–4099). Cairns, Australia: Modelling and Simulation Society of Australia and New Zealand and International Association for Mathematics and Computers in Simulation. Retrieved from <http://www.mssanz.org.au/modsim09/115/thompson.pdf>
- Tonina, D., & Buffington, J. M. (2007). Hyporheic exchange in gravel bed rivers with pool-riffle morphology: Laboratory experiments and three-dimensional modeling. *Water Resources Research*, 43(1), 1–16. <https://doi.org/10.1029/2005WR004328>
- Tonina, D., & Buffington, J. M. (2009). Hyporheic exchange in mountain rivers I: Mechanics and environmental effects. *Geography Compass*, 3(3), 1063–1086. <https://doi.org/10.1111/j.1749-8198.2009.00226.x>

- Transport Canada. (2017). Transport in Canada: 2017: Statistical Addendum.
<https://www.tc.gc.ca/eng/policy/transportation-canada-2017.html#annexb>
- Van Vliet, L. J. P., & Hall, J. W. (1991). Effects of two crop rotations on seasonal runoff and soil loss in the Peace River region. *Canadian Journal of Soil Science*, *71*, 533–543.
<https://doi.org/10.4141/cjss91-051>
- Wade, C. R., Bolding, M. C., Aust, W. M., Lakel, W. A., & Schilling, E. B. (2012). Comparing sediment trap data with the USLE-Forest, RUSLE2, and WEPP-Road erosion models for evaluation of bladed skid trail BMPs. *Transactions of the ASABE*, *55*(2), 403–414.
- Wall, G. J., Dickinson, W. T., Rudra, R. P., & Coote, D. R. (1988). Seasonal Soil Erodibility Variation in Southwestern Ontario. *Canadian Journal of Soil Science*, *68*, 417–424.
<https://doi.org/10.4141/cjss88-038>
- Wall, G. J., Coote, D. R., Pringle, E. A., & Shelton, I. J. (2002). *RUSLEFAC - Revised Universal Soil Loss Equation for Application in Canada: A Handbook for Estimating Soil Loss from Water Erosion in Canada*. Ottawa, Canada.
- Wang, T. (2020). ClimateWNA_Map. Retrieved May 18, 2020, from
<http://www.climatewna.com/ClimateWNA.aspx>
- Wang, T., Hamann, A., Spittlehouse, D., & Carroll, C. (2016). Locally downscaled and spatially customizable climate data for historical and future periods for North America. *PLoS ONE*, *11*(6). <https://doi.org/10.1371/journal.pone.0156720>
- Welle, P. I., & Woodward, D. (1986). *Time of Concentration* (U.S. Department of Agriculture Soil Conservation Service Technical Note No. 4).
- Welsh, M. J. (2008). *Sediment Production and Delivery from Forest Roads and Off-Highway Vehicle Trails in the Upper South Platte River Watershed, Colorado*. Colorado State University.
- Wickham, H. (2016). *ggplot2: Elegant Graphics for Data Analysis*. New York: Springer-Verlag.
Retrieved from <https://ggplot2.tidyverse.org>
- Wickham, H., Romain, F., Henry, L., & Müller, K. (2021). *dplyr: A Grammar of Data Manipulation*. Retrieved from <https://cran.r-project.org/package=dplyr>

Wischmeier, W. H., & Smith, D. D. (1978). *Predicting rainfall erosion losses - a guide to conservation planning* (Agriculture Handbook Number 537). Washington, D.C. Retrieved from <https://naldc-legacy.nal.usda.gov/catalog/CAT79706928>

Woods, S. W., Sugden, B. D., & Parker, B. (2006). Sediment Travel Distances below Drivable Drain Dips in Western Montana. In W. Chung & H. S. Han (Eds.), *29th Council on Forest Engineering Conference* (pp. 251-263). Coeur d'Alene, Idaho: Council on Forest Engineering.

Appendices

Appendix A. Detailed site descriptions

Settling tank and silt fence site details and site selection rationale

Settling tanks were the primary means of obtaining high quality sedimentation information from instrumented road sections in the Simonette. The main aim of installing the settling tanks was to capture as much road erosion information as possible from each site by estimating flow from the plot and sub-sampling fine sediments collected during flow events. Details of plot installation and monitoring techniques are found in the methodology for Chapter 2 and need not be recounted here. The following appendix provides additional details about the instrumented plots. Table A1 below shows the basic plot location and stratification details, and Figure A1 shows the location of silt fence and settling tank plots in the watershed. Site maps for settling tanks, and photos for all instrumented sites are included below.

Table A1. Settling tank locations and general plot parameters

	Site	Latitude	Longitude	Geology	Traffic	Plot Area (m ²)	Plot Length (m)	Av. Plot Width (m)	Slope (%)
S	M270	54°47'50"N	118°25'43"W	Glacio-lacustrine (silty)	HIGH	480/700**	80/194**	6	5
	P286-SP	54°39'30"N	118°16'51"W	Glacio-lacustrine (sandy)	LOW	320	80	4	9
	P4107B	54°31'21"N	118°09'37"W	Aeolian	HIGH	361	56.5	6.4	8
	P295-SP	54°36'30"N	118°11'26"W	Aeolian overlying stagnant ice moraine	LOW	531	88.5	6	7
	P7131	54°26'36"N	117°54'45"W	Stagnant Ice Moraine	HIGH	388	80	4.9	7
	P4128-SP	54°23'17"N	118°00'04"W	Stony ground moraine	LOW	381	79	4.8	6
Si	P4106*	54°31'11"N	118°9'15"W	Glaciofluvial	HIGH	1100	107		6.5
	P4107A	54°31'10"N	54°31'10"N	Glaciofluvial	HIGH	2368	250	~9.5	10
	P4108	54°31'18"N	118°8'11"W	Glaciofluvial	HIGH	470	55.5	8.5	3.5
	P4111	54°30'06"N	118°07'02"W	Glaciofluvial	HIGH	300	60	5	5
	P7131	54°26'36"N	117°54'45"W	Stagnant Ice Moraine	HIGH	338	83.5	4	7
	P4126*	54°24'47"N	118°01'05"W	Moraine	HIGH	690	114	6	2.5

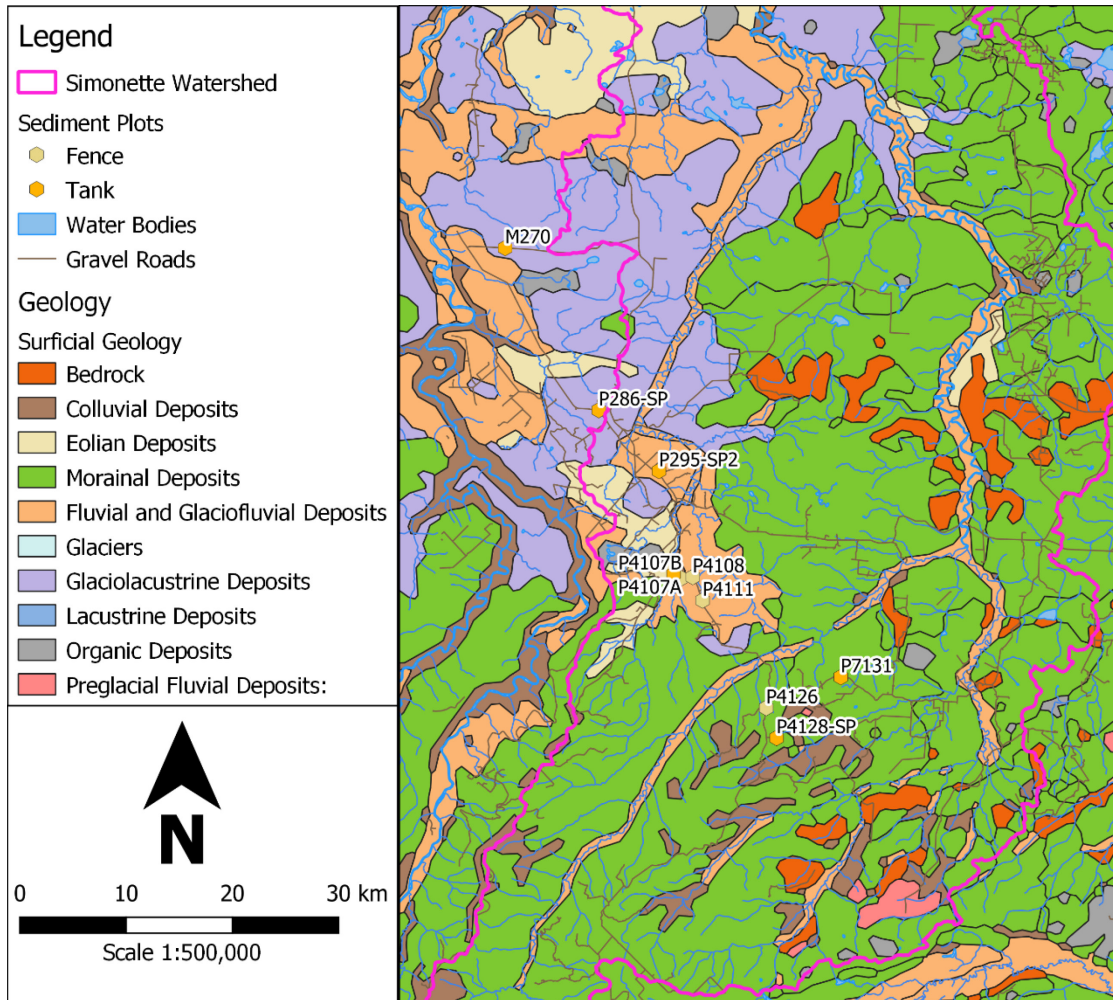


Figure A1. Map of the study area showing spatial distribution of settling basin points

Station maps and site photos

P4107B

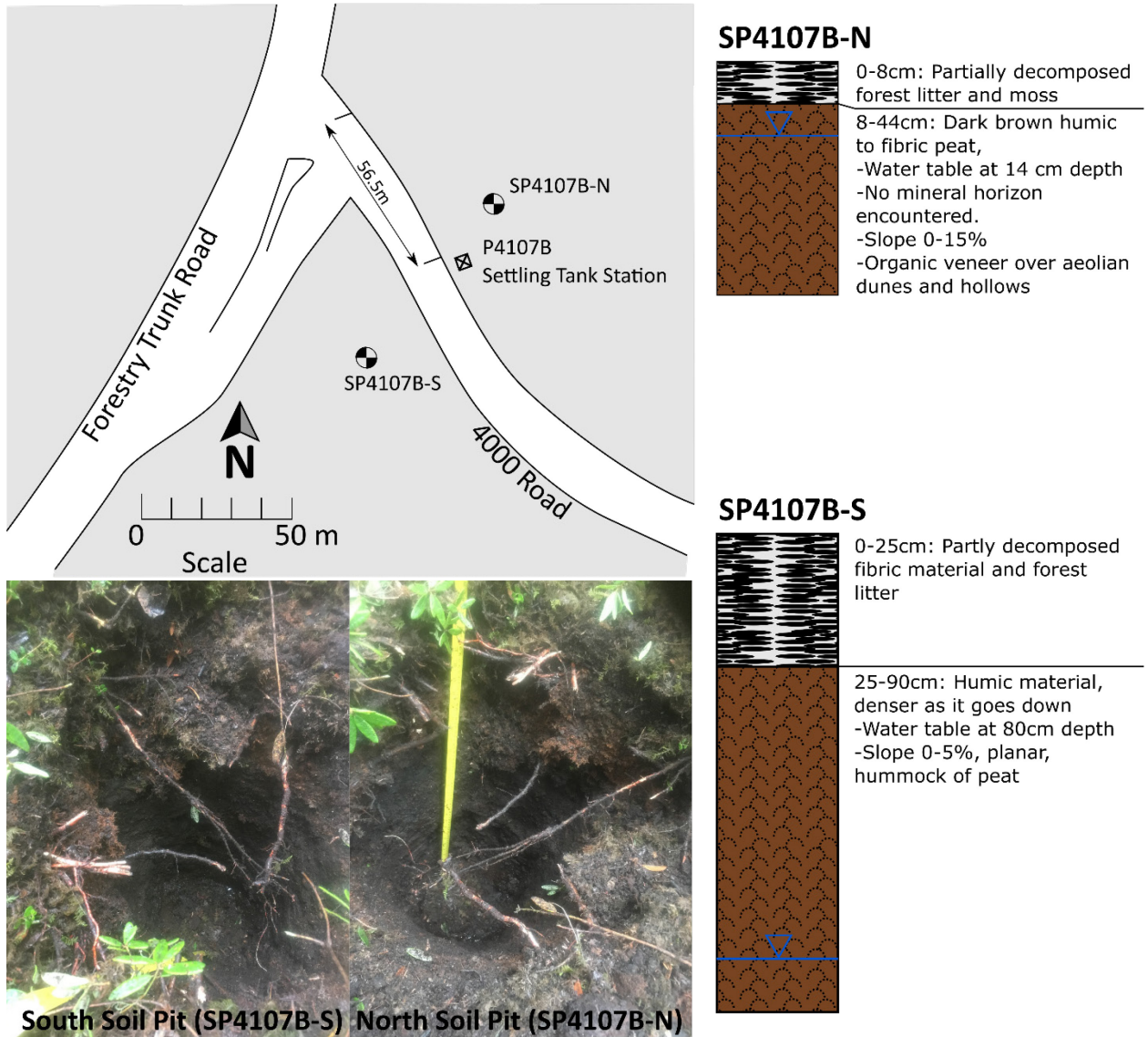


Figure A2. P4107B site map and soil pits. Soil pits show that the road was built out of imported sandy fill material used to cross a deep organic bog. Alternating bog and sand-hill deposits are common in aeolian terrain.



Figure A3. P4107B pictures of road surface: (top left) upper culvert installation, (top right) bottom of plot, (bottom) overview of road showing thick, well-gravelled fill

P295

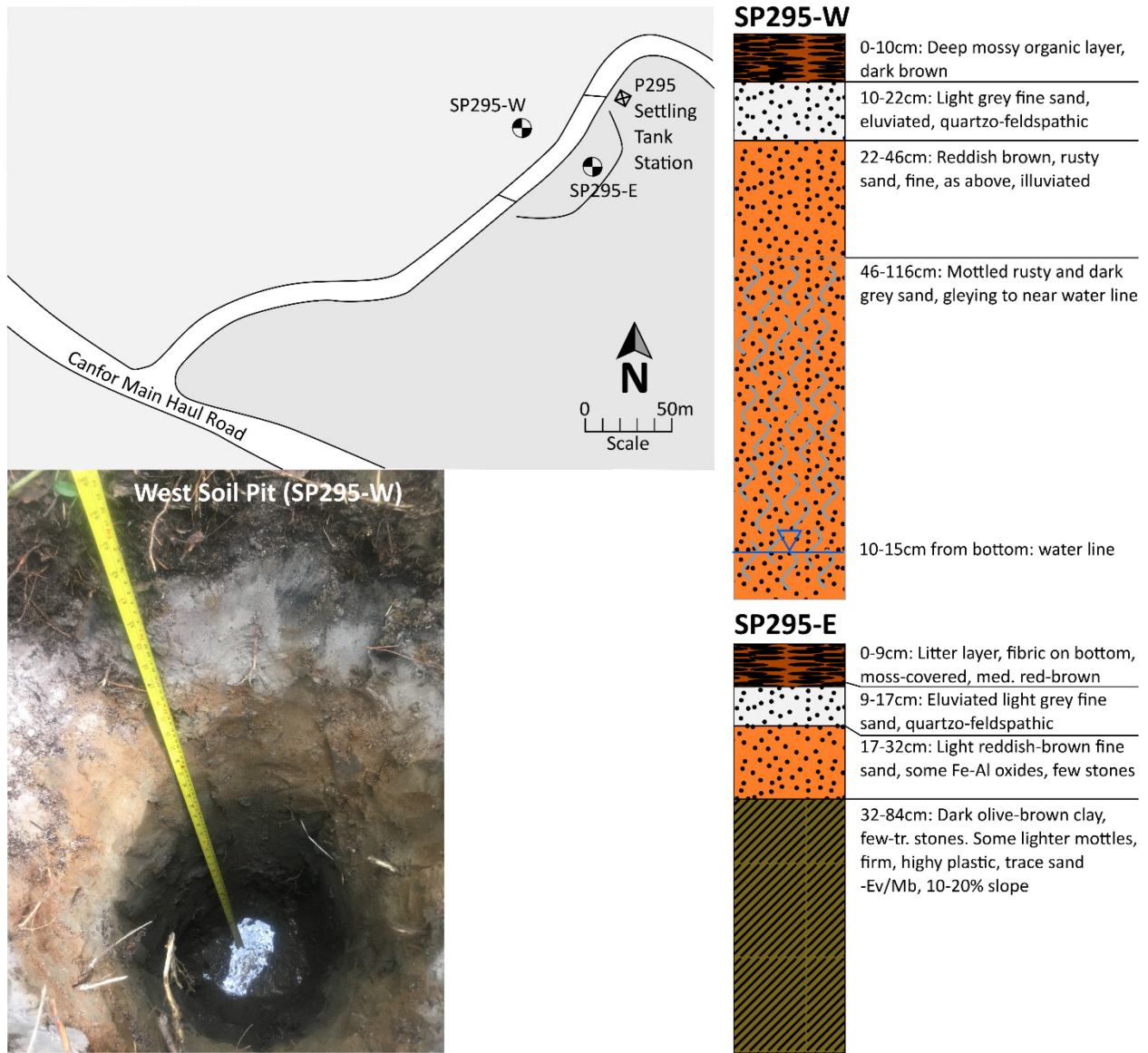


Figure A4. P295 site map and soil pits. Water table encountered at bottom of west soil pit. Thin, relatively well-drained sand over firm (compact) poorly-drained glacial clay.



Figure A5. Pictures of P295, bare plot (upper left), plot with culvert installed (upper right), road site in saturated fall conditions, showing intrusion of underlying fine-grained material (bottom).

M270

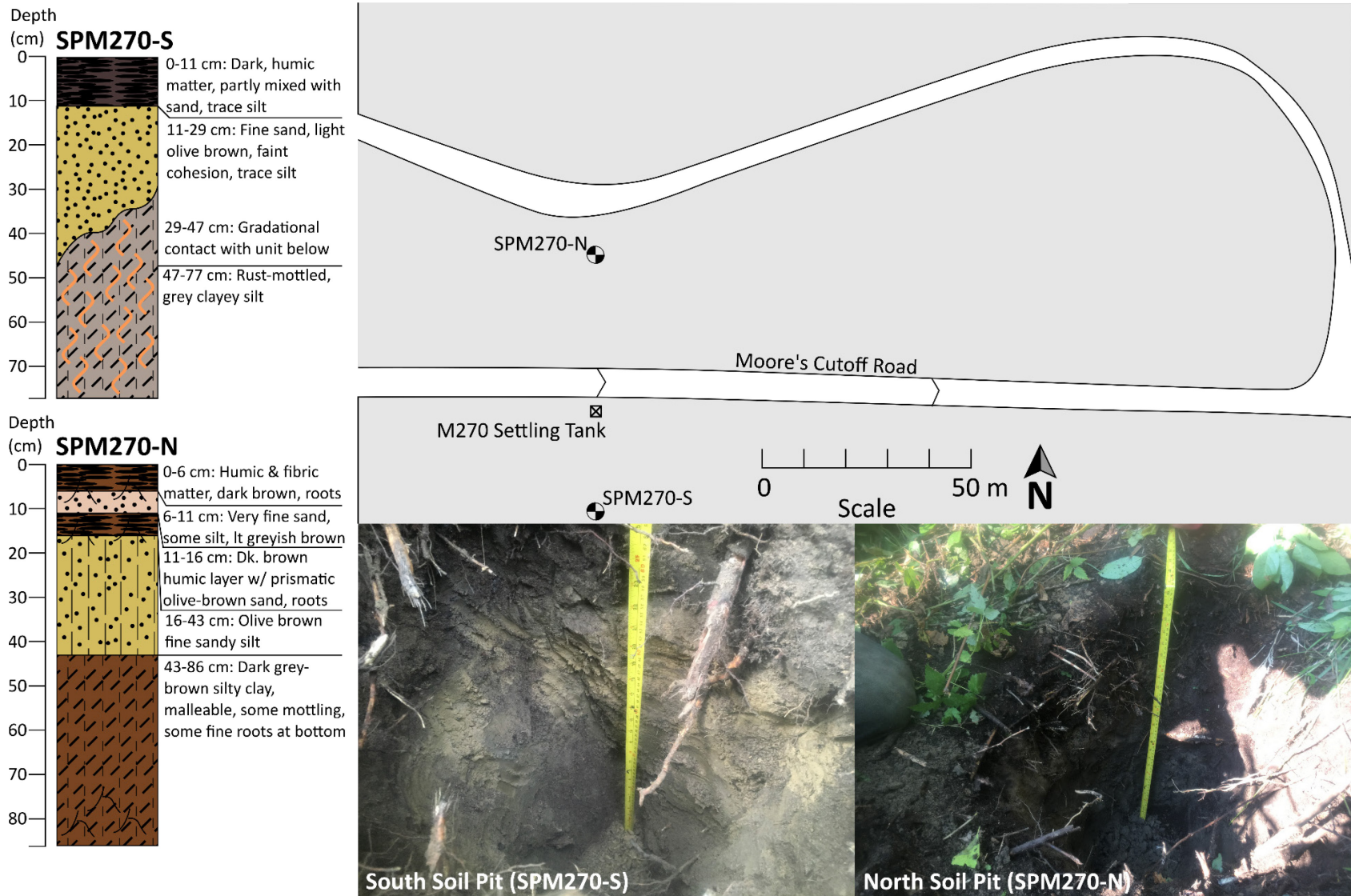


Figure A7. M270 site map and soil pits. This site had well-drained soil not overcompacted by glacial overriding.



Figure A6. M270 culvert bounding lower edge of plot (upper left); settling tank (upper right); detail of road surface showing gravel mixed in with silty fill material (bottom).

P286

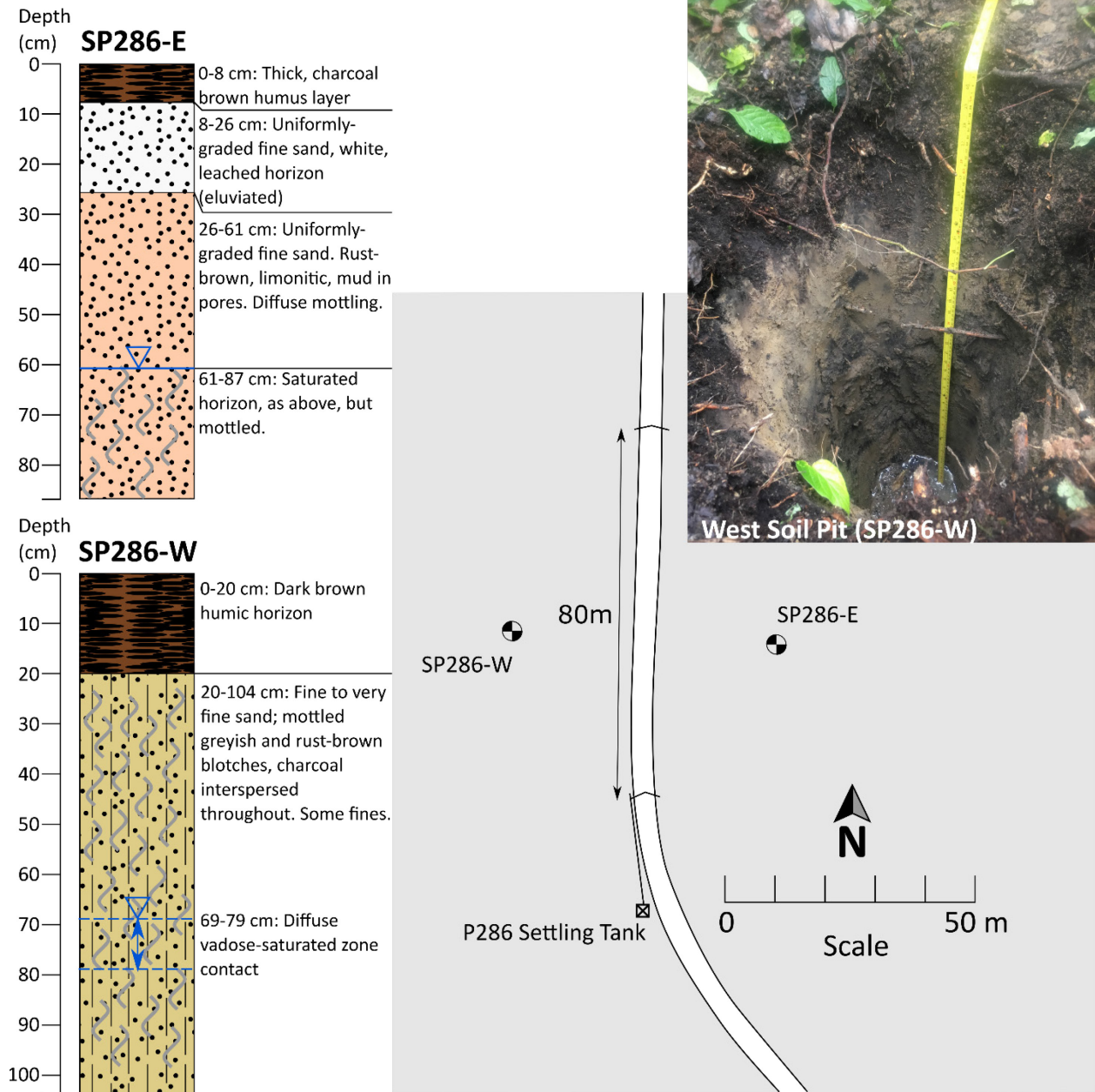


Figure A8. P286 site diagram and soil pits. This was the sandiest and best-drained site encountered in the study.



Figure A9. P286 site photograph showing well-gravelled sandy surface texture (top); bottom culvert and tank set-up (bottom left); tank set-up looking upslope (bottom right)

P7131

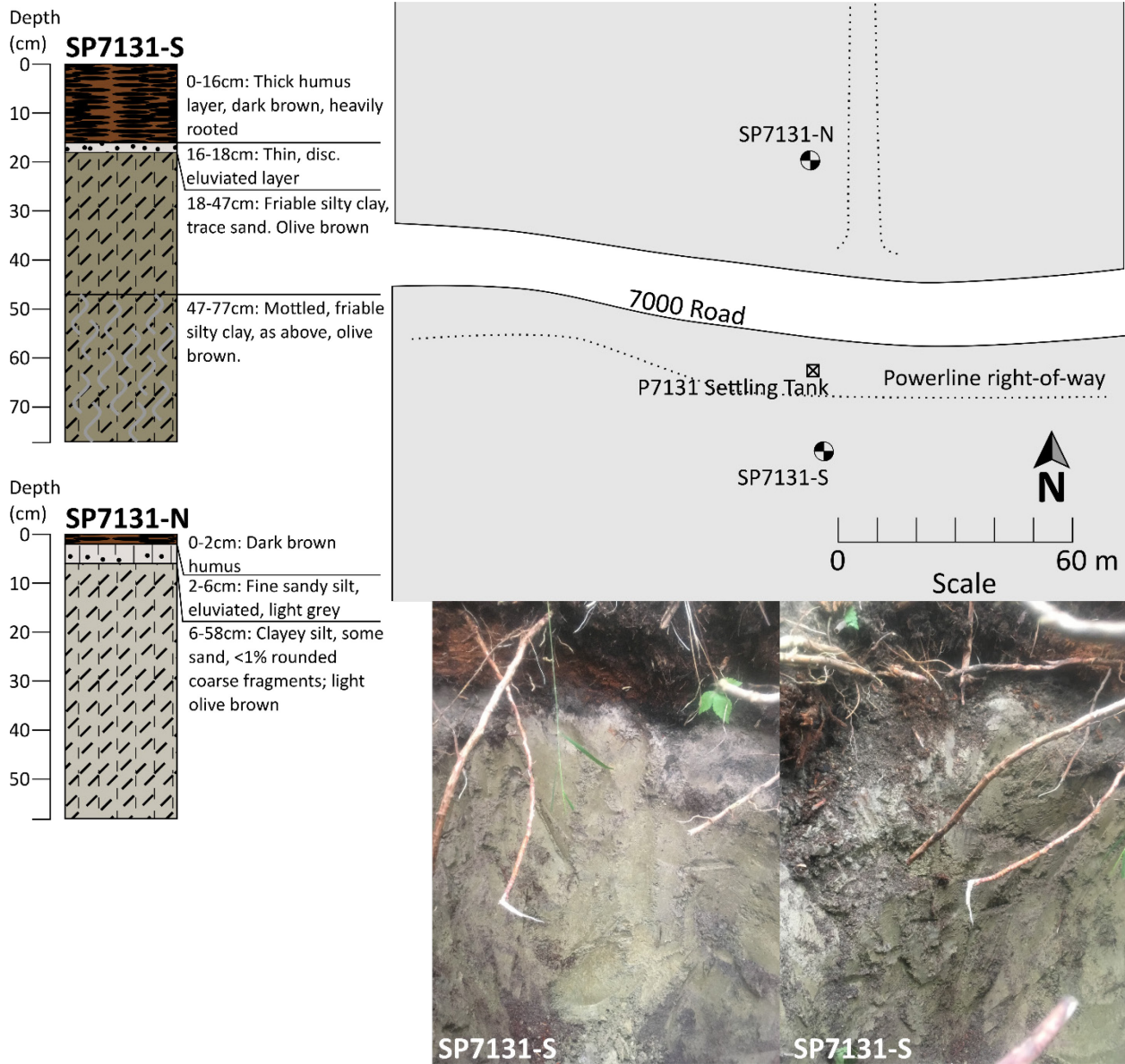


Figure A10. P7131 site map with soil pits showing compact silty clay with a few coarse fragments. Olive-brown to greyish colours with mottling indicate site is imperfectly-drained. Thin eluviated horizons in both soil pits.



Figure A10. P7B1 site photos, road with steel trough culvert, showing worn clay surface (top left), settling tank intake (top right), road surface in wet conditions showing plastic deformation.

P4128

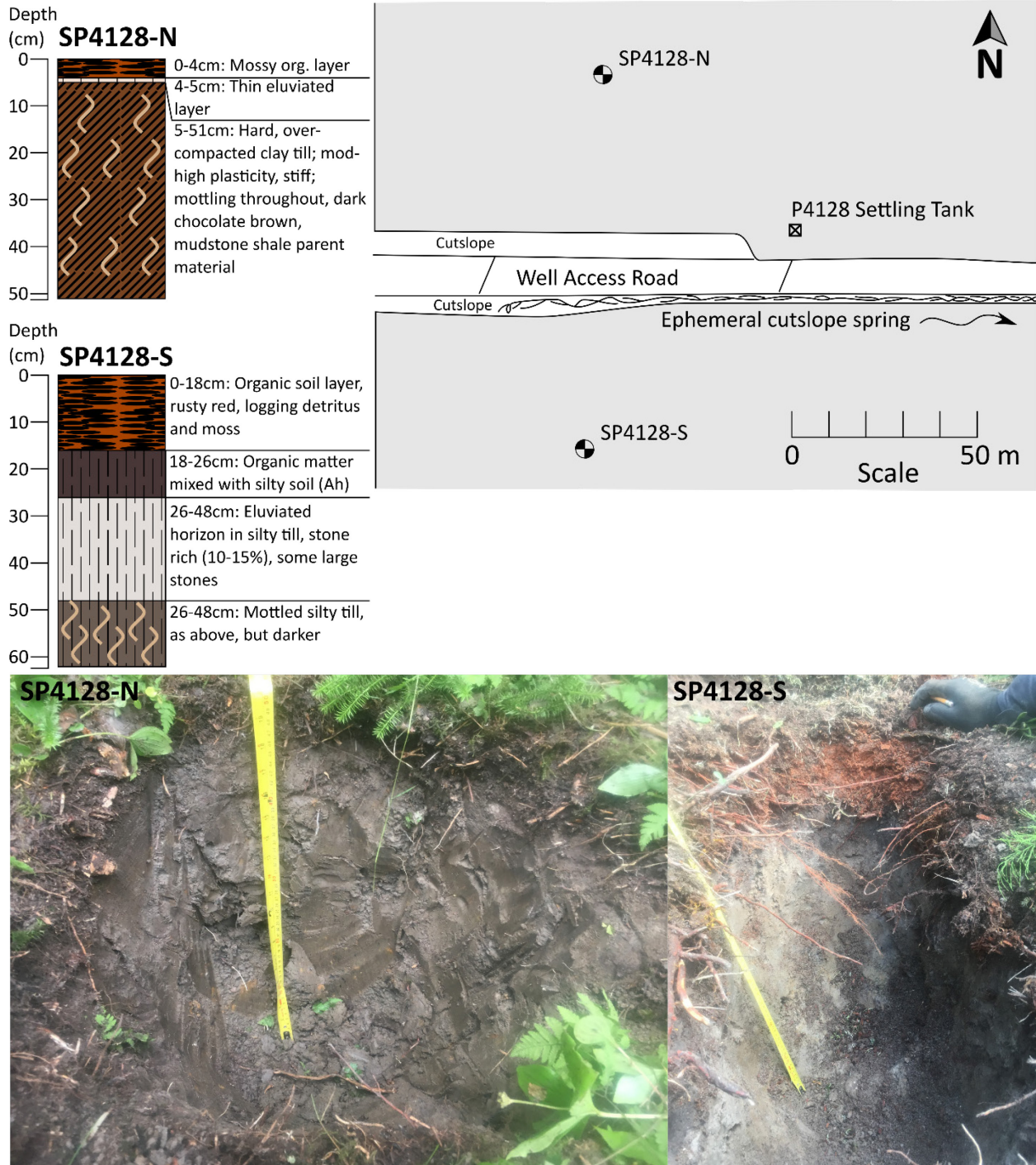


Figure A12. P4128 plot diagram and soil pits showing compact, silt and clay-rich morainal soil.



Figure A11. P4128 site photos, freshly-installed top culvert in dry conditions showing mixed stony soil with silt (top left), lower plot boundary after rain (top right), marked lower plot boundary in spring in moist soil conditions (bottom).

Silt Fence Sites

P4107A



Figure A13. Photos of P4107 silt fence plot, from top left: outflow of culvert in front of settling fence (out of view), road in dry conditions, well-gravelled sandy road surface after a summer rainstorm.

P4108



Figure A14. P4108 plot photos (clockwise from top left): (1) Oblique view of plot set up with centreline and boundary flags, and labelled silt marker stakes. (2) Centerline view of plot. (3) Section of road downslope of plot prior to fence installation. Culvert failure in 2016 or earlier caused rilling of the ditchline and deposition of a major plume at the road drain point.

P4111



Figure A15. P4111 Site Photos: (top) looking downslope from P4111 drain point. Road has more silty material in this area and nearby soil pits are clayey luvisols with an illuviated clay hardpan. Plot outlet (bottom) showing flagging and plot delineation. This was a relatively small plot overall.

P4106



Figure A16. Site photos of P4106. Top: Repaired culvert with rocks around intake (rocks are also at the outlet). Bottom: Silt fence with thin mud layer after a storm. While there was some deposition at the site, it was very difficult to measure with the stakes, probably not more than 0.5-1cm.

P4126



Figure AI7. Site photos of P4126. Site was installed in a low-gradient (2.5°) segment of road (top), and a turnout berm was hand-excavated just up-gradient of a previous settling location with some sediment in it (bottom). Overall low slope and possible bypass may have compromised the ability of this plot to produce a meaningful sediment signature.

Appendix B. Rainfall energy summarization for stations in west-central Alberta

The following table provides more-or-less unfiltered rain energy calculations for stations in and around the Simonette used to create a Kriging map of rainfall energy to fill missing rain gauge data. Results from this table should be used judiciously: Intervals where a gap in data has been identified which may result in an artificial rainfall energy peak are shaded grey with red text.

Date	Lat	Long	Station	Depth	EI30	Dur	I30	Start Time	Peak Delay
Y-M-D	DD	DD		mm	MJ*mm/ha*hr	hr	mm/hr	hr	hr
2016-08-20	54.442	-117.911	P7131	66.70	503.43	40.18	39.60	19.29	21.83
2016-08-27	54.442	-117.911	P7131	7.83	5.93	4.95	5.10	1.68	3.85
2016-08-27	54.442	-117.911	P7131	21.99	59.57	19.01	13.69	13.02	3.25
2016-08-31	54.442	-117.911	P7131	5.14	3.73	8.76	5.02	23.21	6.60
2016-09-02	54.442	-117.911	P7131	5.68	5.96	6.78	6.80	18.07	1.78
2016-09-08	54.442	-117.911	P7131	8.98	19.71	12.80	11.54	15.43	0.42
2017-07-23	54.442	-117.911	P7131	9.47	14.06	6.88	8.72	23.89	4.77
2017-07-29	54.442	-117.911	P7131	25.13	244.77	8.25	36.78	18.42	4.57
2017-08-03	54.442	-117.911	P7131	4.98	4.46	2.28	5.86	16.59	1.22
2017-08-06	54.442	-117.911	P7131	13.19	32.42	9.26	13.04	22.10	7.20
2017-09-08	54.442	-117.911	P7131	4.10	2.55	3.24	3.92	10.12	0.35
2017-09-08	54.442	-117.911	P7131	12.34	15.83	3.79	7.94	21.75	1.52
2017-09-12	54.442	-117.911	P7131	5.52	3.19	5.23	3.83	22.21	3.60
2017-09-13	54.442	-117.911	P7131	2.95	2.30	7.79	4.25	9.69	3.53
2017-09-18	54.442	-117.911	P7131	7.59	2.75	8.22	2.76	12.38	0.42
2017-09-19	54.442	-117.911	P7131	61.97	65.86	40.74	7.16	3.63	33.95
2017-09-21	54.442	-117.911	P7131	16.83	8.46	5.81	3.79	9.51	3.70
2018-05-16	54.442	-117.911	P7131	9.29	3.03	12.62	2.51	22.63	7.00
2018-05-25	54.442	-117.911	P7131	11.55	35.28	9.94	14.15	13.41	7.88
2018-06-01	54.442	-117.911	P7131	11.38	66.08	5.11	21.54	13.85	4.97
2018-06-25	54.442	-117.911	P7131	8.91	12.78	2.20	8.20	11.19	0.43
2018-07-02	54.442	-117.911	P7131	88.60	156.12	51.16	11.29	1.20	44.75
2018-08-01	54.442	-117.911	P7131	7.96	11.88	3.74	7.60	17.32	0.35
2018-08-04	54.442	-117.911	P7131	2.85	1.57	1.13	3.66	21.55	0.73
2018-08-12	54.442	-117.911	P7131	10.64	9.12	11.39	5.79	0.08	10.40
2018-08-26	54.442	-117.911	P7131	14.31	15.58	22.80	6.65	1.33	18.28
2018-08-28	54.442	-117.911	P7131	7.83	13.17	14.91	7.90	15.31	2.43
2018-08-30	54.442	-117.911	P7131	6.63	2.90	15.96	3.11	1.74	10.88
2018-09-11	54.442	-117.911	P7131	10.84	6.62	13.79	4.16	8.22	9.12
2018-09-16	54.442	-117.911	P7131	17.10	9.07	12.15	3.24	14.37	1.35
2018-09-26	54.442	-117.911	P7131	24.73	16.82	38.23	4.86	2.63	12.42
2018-10-03	54.442	-117.911	P7131	5.90	3.56	6.20	4.35	11.73	1.15
2018-06-03	54.609	-118.190	P295	12.45	15.98	6.50	7.92	20.05	5.82
2018-06-10	54.609	-118.190	P295	8.39	4.59	10.19	3.59	20.74	0.35

Date	Lat	Long	Station	Depth	EI30	Dur	I30	Start Time	Peak Delay
Y-M-D	DD	DD		mm	MJ*mm/ha*hr	hr	mm/hr	hr	hr
2018-06-25	54.609	-118.190	P295	9.34	10.75	2.53	6.90	11.23	0.55
2018-07-02	54.609	-118.190	P295	55.59	85.66	51.79	9.31	0.38	45.67
2018-07-19	54.609	-118.190	P295	31.80	70.31	32.27	12.70	18.68	1.07
2018-07-22	54.609	-118.190	P295	5.02	12.47	0.37	10.04	15.16	0.19
2018-08-26	54.609	-118.190	P295	12.66	29.18	23.42	12.18	0.24	19.23
2018-08-30	54.609	-118.190	P295	7.94	6.27	6.32	5.16	9.77	3.00
2017-08-06	54.658	-118.281	P286	4.49	2.94	7.67	4.38	22.49	1.05
2017-08-22	54.658	-118.281	P286	6.45	8.33	3.61	7.29	21.35	3.05
2017-08-23	54.658	-118.281	P286	22.85	155.87	2.46	25.69	22.94	0.35
2017-08-24	54.658	-118.281	P286	5.46	4.32	1.93	5.31	12.45	1.68
2017-09-02	54.658	-118.281	P286	9.67	3.72	9.91	2.61	5.76	3.28
2017-09-08	54.658	-118.281	P286	5.86	4.36	3.06	4.95	9.81	0.57
2017-09-08	54.658	-118.281	P286	16.49	96.53	2.81	24.55	22.50	1.87
2017-09-18	54.658	-118.281	P286	8.33	4.46	7.56	3.71	12.24	2.25
2017-09-19	54.658	-118.281	P286	80.33	118.41	45.05	9.46	5.97	11.37
2018-06-03	54.658	-118.281	P286	14.03	19.26	6.03	8.20	20.31	5.30
2018-06-10	54.658	-118.281	P286	8.64	5.81	10.31	4.15	20.56	0.37
2018-06-25	54.658	-118.281	P286	10.27	9.24	2.82	5.84	11.19	1.40
2018-07-01	54.658	-118.281	P286	45.68	57.50	21.77	7.56	19.16	15.42
2018-07-03	54.658	-118.281	P286	40.26	177.87	22.10	23.47	2.24	20.02
2018-07-06	54.658	-118.281	P286	2.18	2.35	0.16	4.36	14.60	0.08
2018-07-19	54.658	-118.281	P286	92.37	467.44	52.24	24.88	16.59	51.30
2018-07-22	54.658	-118.281	P286	71.88	427.89	31.72	30.07	5.48	15.85
2018-07-23	54.658	-118.281	P286	4.57	10.73	0.45	9.14	19.96	0.22
2018-08-01	54.658	-118.281	P286	18.98	130.95	1.95	28.65	16.69	0.42
2018-08-12	54.658	-118.281	P286	16.05	14.41	10.99	5.34	0.41	7.20
2018-08-26	54.658	-118.281	P286	7.80	14.26	4.39	9.11	19.01	0.42
2018-08-30	54.658	-118.281	P286	10.72	9.09	6.17	5.42	9.89	2.72
2018-09-11	54.658	-118.281	P286	7.69	9.44	16.21	6.96	5.38	12.13
2018-09-16	54.658	-118.281	P286	8.18	3.37	12.78	2.69	11.98	1.72
2018-09-26	54.658	-118.281	P286	16.36	18.64	28.25	6.65	4.19	10.38
2018-10-11	54.658	-118.281	P286	10.94	6.59	19.11	3.84	22.71	10.85
2018-10-13	54.658	-118.281	P286	7.29	4.50	4.76	3.95	11.59	0.85
2017-07-27	54.791	-118.429	M270	4.10	1.98	6.17	3.08	7.19	4.17
2017-07-29	54.791	-118.429	M270	5.22	4.58	7.12	4.41	20.03	2.75
2017-08-03	54.791	-118.429	M270	4.98	5.95	1.81	6.06	16.56	0.35
2017-08-06	54.791	-118.429	M270	4.15	2.27	7.23	3.70	22.46	6.62
2017-08-22	54.791	-118.429	M270	4.03	3.66	4.85	5.14	23.78	0.35
2017-08-23	54.791	-118.429	M270	43.57	283.55	19.43	26.60	19.21	4.20
2017-09-02	54.791	-118.429	M270	11.92	5.21	9.66	2.96	5.73	4.78
2017-09-08	54.791	-118.429	M270	7.92	6.23	5.01	5.26	6.95	3.30
2017-09-08	54.791	-118.429	M270	14.43	83.09	1.87	23.53	23.57	1.18

Date	Lat	Long	Station	Depth	EI30	Dur	I30	Start Time	Peak Delay
Y-M-D	DD	DD		mm	MJ*mm/ha*hr	hr	mm/hr	hr	hr
2017-09-09	54.791	-118.429	M270	20.36	125.71	16.08	26.64	18.11	0.38
2017-09-18	54.791	-118.429	M270	11.87	7.70	8.80	4.33	12.73	1.72
2017-09-19	54.791	-118.429	M270	81.64	95.28	44.15	7.58	6.57	11.23
2018-05-20	54.791	-118.429	M270	7.62	9.95	1.56	7.83	16.15	1.22
2018-05-25	54.791	-118.429	M270	7.82	7.35	3.87	5.91	19.45	2.88
2018-06-03	54.791	-118.429	M270	21.90	58.49	6.53	14.79	20.22	5.03
2018-06-14	54.791	-118.429	M270	6.10	7.47	7.49	7.51	9.37	7.22
2018-06-25	54.791	-118.429	M270	10.27	8.82	2.90	5.72	11.37	1.62
2018-07-01	54.791	-118.429	M270	26.85	26.59	15.73	6.39	23.25	6.42
2018-07-03	54.791	-118.429	M270	36.14	83.43	26.36	13.06	0.16	23.82
2018-07-19	54.791	-118.429	M270	39.65	299.29	15.16	35.09	17.31	4.70
2018-07-20	54.791	-118.429	M270	32.80	75.57	11.67	13.17	16.38	5.85
2018-07-21	54.791	-118.429	M270	12.77	48.04	7.81	15.42	14.95	4.37
2018-07-22	54.791	-118.429	M270	40.36	78.79	26.57	11.32	9.19	25.32
2018-08-12	54.791	-118.429	M270	12.43	6.61	8.50	3.57	0.99	4.45
2018-08-26	54.791	-118.429	M270	7.65	16.62	23.11	10.58	2.69	16.27
2018-09-11	54.791	-118.429	M270	7.10	7.20	7.95	6.32	13.61	3.35
2018-09-15	54.791	-118.429	M270	11.80	2.65	30.72	1.49	13.36	23.92
2018-09-26	54.791	-118.429	M270	7.77	2.21	23.03	1.90	6.64	21.00
2018-10-11	54.791	-118.429	M270	14.50	14.10	18.64	6.30	22.71	10.50
2016-08-20	54.523	-118.161	P4107	61.18	165.53	49.37	15.34	17.75	22.98
2016-08-27	54.523	-118.161	P4107	6.57	3.16	4.40	3.53	1.13	4.07
2016-08-27	54.523	-118.161	P4107	13.89	21.47	19.39	8.81	12.71	4.10
2016-08-31	54.523	-118.161	P4107	7.81	8.52	9.00	6.21	21.50	3.67
2016-09-07	54.523	-118.161	P4107	6.79	3.99	21.95	4.02	22.67	16.88
2016-09-30	54.523	-118.161	P4107	18.72	12.73	32.90	4.99	9.25	20.95
2016-10-04	54.523	-118.161	P4107	9.21	2.80	14.36	2.33	11.94	1.33
2016-10-11	54.523	-118.161	P4107	9.54	5.29	3.70	4.26	11.17	0.97
2018-05-16	54.523	-118.161	P4107	8.52	2.96	21.67	2.12	10.67	14.45
2018-05-20	54.523	-118.161	P4107	11.94	29.38	1.63	12.59	15.41	0.47
2018-05-25	54.523	-118.161	P4107	16.61	31.90	14.78	9.44	10.44	10.67
2018-06-03	54.523	-118.161	P4107	10.11	15.13	7.76	8.42	18.91	6.85
2018-06-10	54.523	-118.161	P4107	10.12	6.57	10.32	4.28	20.98	10.03
2018-06-25	54.523	-118.161	P4107	9.95	15.57	2.55	9.05	11.08	0.52
2018-07-02	54.523	-118.161	P4107	92.73	162.77	51.97	10.46	0.40	51.45
2018-07-19	54.523	-118.161	P4107	71.44	454.23	41.02	31.41	15.72	3.73
2018-07-21	54.523	-118.161	P4107	12.27	22.35	8.40	10.04	16.55	3.42
2018-07-22	54.523	-118.161	P4107	37.01	73.36	29.70	11.10	10.19	5.83
2018-08-12	54.523	-118.161	P4107	8.43	8.01	11.68	6.04	0.39	2.27
2018-08-26	54.523	-118.161	P4107	16.55	38.73	21.96	11.95	1.68	17.98
2018-08-30	54.523	-118.161	P4107	7.82	6.88	10.09	5.56	9.36	2.85
2018-09-11	54.523	-118.161	P4107	9.17	5.29	17.00	3.71	7.81	8.97

Date	Lat	Long	Station	Depth	EI30	Dur	I30	Start Time	Peak Delay
Y-M-D	DD	DD		mm	MJ*mm/ha*hr	hr	mm/hr	hr	hr
2018-09-15	54.523	-118.161	P4107	10.39	2.88	28.45	1.82	13.34	2.93
2018-09-26	54.523	-118.161	P4107	15.59	6.38	33.36	2.65	5.69	9.03
2018-10-11	54.523	-118.161	P4107	7.56	3.22	16.48	2.76	22.86	10.90
2018-05-16	54.388	-118.003	P4128	8.99	3.04	12.90	2.31	22.73	6.57
2018-05-25	54.388	-118.003	P4128	9.96	16.60	16.07	8.53	13.45	7.53
2018-05-31	54.388	-118.003	P4128	2.65	2.42	2.75	4.48	13.17	2.33
2018-06-01	54.388	-118.003	P4128	1.90	1.04	4.96	3.37	13.68	4.82
2018-06-02	54.388	-118.003	P4128	2.51	2.54	3.47	4.29	2.12	2.58
2018-06-10	54.388	-118.003	P4128	12.96	7.85	23.38	4.08	8.34	23.22
2018-06-21	54.388	-118.003	P4128	13.33	75.00	0.83	22.82	23.30	0.45
2018-06-25	54.388	-118.003	P4128	9.26	13.24	2.58	8.43	10.72	0.72
2018-06-29	54.388	-118.003	P4128	3.97	3.86	2.12	4.57	12.49	1.12
2018-07-02	54.388	-118.003	P4128	123.08	262.48	52.04	12.42	0.72	9.02
2018-08-12	54.388	-118.003	P4128	13.67	11.84	11.47	5.65	0.18	10.02
2018-08-26	54.388	-118.003	P4128	25.05	44.89	21.65	9.53	2.15	17.68
2018-08-28	54.388	-118.003	P4128	2.73	2.92	4.89	5.03	12.41	4.75
2018-08-30	54.388	-118.003	P4128	8.23	6.48	16.28	5.03	1.57	12.68
2018-09-11	54.388	-118.003	P4128	12.63	14.36	13.34	6.53	8.46	8.90
2018-09-17	54.388	-118.003	P4128	9.03	3.19	8.26	2.40	11.13	1.98
2018-09-26	54.388	-118.003	P4128	32.01	33.31	36.22	6.70	3.85	14.65
2016-05-19	55.197	-119.396	Beaverlodge	38.39	33.59	30.25	6.79	5.50	25.52
2016-05-27	55.197	-119.396	Beaverlodge	16.79	5.75	12.00	3.04	21.25	2.33
2016-05-29	55.197	-119.396	Beaverlodge	8.90	4.39	6.75	4.24	6.25	3.23
2016-06-08	55.197	-119.396	Beaverlodge	37.40	18.26	33.50	4.22	20.25	17.03
2016-06-11	55.197	-119.396	Beaverlodge	17.90	14.08	13.25	5.86	9.25	3.68
2016-06-14	55.197	-119.396	Beaverlodge	46.96	21.75	50.50	4.01	18.75	6.22
2016-06-24	55.197	-119.396	Beaverlodge	6.36	6.69	12.50	7.38	5.75	6.02
2016-07-09	55.197	-119.396	Beaverlodge	6.68	3.67	8.25	5.03	11.50	7.13
2016-07-10	55.197	-119.396	Beaverlodge	10.35	37.65	1.00	20.11	13.75	0.52
2016-07-12	55.197	-119.396	Beaverlodge	14.99	13.70	4.25	8.20	12.50	4.00
2016-07-13	55.197	-119.396	Beaverlodge	5.35	1.70	5.25	7.51	12.25	0.52
2016-07-20	55.197	-119.396	Beaverlodge	6.41	3.54	14.75	4.80	0.00	14.77
2016-07-31	55.197	-119.396	Beaverlodge	8.31	6.41	11.00	5.88	6.25	7.83
2016-08-01	55.197	-119.396	Beaverlodge	8.09	14.26	6.00	14.59	17.25	0.52
2016-08-05	55.197	-119.396	Beaverlodge	26.07	61.49	11.75	15.19	18.25	7.52
2016-08-06	55.197	-119.396	Beaverlodge	18.73	78.01	7.00	29.91	23.50	0.52
2016-08-21	55.197	-119.396	Beaverlodge	14.21	55.59	1.50	18.87	15.00	1.02
2016-08-21	55.197	-119.396	Beaverlodge	11.99	3.29	18.25	2.60	23.50	7.25
2016-08-27	55.197	-119.396	Beaverlodge	21.06	19.62	13.00	7.76	12.75	1.27
2016-08-31	55.197	-119.396	Beaverlodge	25.51	59.30	17.00	13.64	18.00	4.65
2016-09-30	55.197	-119.396	Beaverlodge	22.58	10.57	26.00	4.20	14.00	17.77
2016-10-04	55.197	-119.396	Beaverlodge	5.00	1.54	4.00	3.02	9.50	0.82

Date	Lat	Long	Station	Depth	EI30	Dur	I30	Start Time	Peak Delay
Y-M-D	DD	DD		mm	MJ*mm/ha*hr	hr	mm/hr	hr	hr
2016-10-13	55.197	-119.396	Beaverlodge	7.79	1.56	7.50	2.00	13.75	4.27
2016-10-14	55.197	-119.396	Beaverlodge	7.49	1.15	24.00	1.60	7.50	17.02
2016-10-24	55.197	-119.396	Beaverlodge	5.78	1.04	20.75	1.80	18.25	18.72
2016-10-31	55.197	-119.396	Beaverlodge	8.58	1.52	23.50	1.82	20.50	4.03
2017-05-11	55.197	-119.396	Beaverlodge	9.36	6.74	6.50	7.14	16.75	0.52
2017-05-12	55.197	-119.396	Beaverlodge	13.07	13.61	10.50	7.76	9.50	3.63
2017-05-13	55.197	-119.396	Beaverlodge	14.28	2.94	20.25	2.04	5.25	6.83
2017-05-23	55.197	-119.396	Beaverlodge	43.90	83.24	10.00	12.23	19.75	4.03
2017-06-09	55.197	-119.396	Beaverlodge	7.60	10.08	2.50	8.47	14.00	1.48
2017-06-10	55.197	-119.396	Beaverlodge	12.47	3.04	19.25	2.47	20.00	5.63
2017-06-14	55.197	-119.396	Beaverlodge	5.67	4.02	1.25	7.61	16.25	0.52
2017-06-27	55.197	-119.396	Beaverlodge	25.68	16.36	16.75	5.00	9.75	14.52
2017-07-07	55.197	-119.396	Beaverlodge	8.89	9.28	4.25	7.14	18.25	3.33
2017-07-16	55.197	-119.396	Beaverlodge	10.90	7.16	7.50	5.20	20.75	1.27
2017-08-23	55.197	-119.396	Beaverlodge	10.12	13.51	6.00	8.47	17.00	4.73
2017-08-24	55.197	-119.396	Beaverlodge	18.78	23.44	4.50	8.31	9.25	2.62
2017-09-02	55.197	-119.396	Beaverlodge	13.89	5.32	8.00	3.40	6.25	5.25
2017-09-19	55.197	-119.396	Beaverlodge	65.39	78.36	27.00	8.67	10.50	6.88
2017-10-24	55.197	-119.396	Beaverlodge	19.47	10.06	17.75	4.57	12.25	17.27
2017-11-13	55.197	-119.396	Beaverlodge	9.18	2.08	8.75	2.21	11.50	4.07
2018-06-03	55.197	-119.396	Beaverlodge	24.67	52.77	9.25	13.69	20.00	5.90
2018-06-25	55.197	-119.396	Beaverlodge	8.10	3.81	3.50	4.20	11.00	0.75
2018-06-29	55.197	-119.396	Beaverlodge	5.30	2.43	4.25	4.00	18.75	4.02
2018-07-01	55.197	-119.396	Beaverlodge	5.11	1.15	10.75	2.21	2.25	9.02
2018-07-01	55.197	-119.396	Beaverlodge	15.98	7.09	11.00	4.02	20.25	6.28
2018-07-03	55.197	-119.396	Beaverlodge	5.19	0.94	15.00	1.83	3.50	9.93
2018-07-07	55.197	-119.396	Beaverlodge	7.60	3.57	10.75	4.41	8.25	0.52
2018-07-19	55.197	-119.396	Beaverlodge	14.50	15.68	5.75	7.24	17.75	0.97
2018-07-20	55.197	-119.396	Beaverlodge	46.82	126.27	18.75	15.46	17.25	8.27
2018-07-21	55.197	-119.396	Beaverlodge	9.60	19.78	7.75	10.56	18.25	2.45
2018-07-22	55.197	-119.396	Beaverlodge	52.18	57.99	17.50	8.00	14.25	5.02
2018-07-30	55.197	-119.396	Beaverlodge	12.94	59.14	0.75	21.65	16.50	0.75
2018-08-01	55.197	-119.396	Beaverlodge	50.64	411.19	2.00	35.72	12.50	1.15
2018-08-11	55.197	-119.396	Beaverlodge	12.67	7.00	11.00	4.60	23.75	1.48
2018-08-26	55.197	-119.396	Beaverlodge	12.30	11.13	9.25	6.54	18.00	1.63
2018-08-30	55.197	-119.396	Beaverlodge	12.98	7.69	7.00	4.87	8.25	2.80
2018-09-08	55.197	-119.396	Beaverlodge	15.26	22.52	5.00	9.54	3.00	3.52
2018-09-11	55.197	-119.396	Beaverlodge	8.99	4.70	23.50	4.61	15.00	23.38
2018-10-11	55.197	-119.396	Beaverlodge	15.12	8.97	13.25	5.05	21.50	11.77
2016-05-18	53.623	-115.894	Carrot Creek	46.41	42.16	43.00	7.36	14.25	43.02
2016-05-22	53.623	-115.894	Carrot Creek	43.09	29.90	26.25	5.62	0.00	8.30
2016-05-26	53.623	-115.894	Carrot Creek	17.49	22.31	30.00	8.88	16.50	1.65

Date	Lat	Long	Station	Depth	EI30	Dur	I30	Start Time	Peak Delay
Y-M-D	DD	DD		mm	MJ*mm/ha*hr	hr	mm/hr	hr	hr
2016-06-08	53.623	-115.894	Carrot Creek	12.36	22.69	14.25	10.17	15.50	6.72
2016-06-11	53.623	-115.894	Carrot Creek	8.97	7.88	3.75	8.78	13.50	0.52
2016-06-13	53.623	-115.894	Carrot Creek	5.93	4.79	4.75	6.65	15.50	0.72
2016-06-14	53.623	-115.894	Carrot Creek	28.85	53.39	17.00	12.37	14.50	0.52
2016-06-25	53.623	-115.894	Carrot Creek	18.07	16.84	16.25	6.67	13.00	10.97
2016-07-10	53.623	-115.894	Carrot Creek	16.18	33.57	2.50	13.92	13.25	0.53
2016-07-29	53.623	-115.894	Carrot Creek	9.67	6.54	15.50	5.93	17.50	0.52
2016-07-31	53.623	-115.894	Carrot Creek	7.58	1.58	15.50	2.18	12.50	1.02
2016-08-03	53.623	-115.894	Carrot Creek	14.05	25.82	8.00	10.19	0.50	1.68
2016-08-06	53.623	-115.894	Carrot Creek	13.16	18.29	13.50	8.85	19.50	4.22
2016-08-08	53.623	-115.894	Carrot Creek	8.50	6.30	12.50	5.60	21.00	0.77
2016-08-21	53.623	-115.894	Carrot Creek	14.70	53.64	3.50	24.46	21.25	0.52
2016-08-22	53.623	-115.894	Carrot Creek	39.23	34.64	15.75	6.63	11.25	6.55
2016-08-31	53.623	-115.894	Carrot Creek	8.95	21.84	6.00	12.37	4.00	0.77
2016-09-02	53.623	-115.894	Carrot Creek	21.40	7.55	15.00	3.20	0.50	3.05
2016-09-08	53.623	-115.894	Carrot Creek	7.89	4.03	27.50	4.41	3.25	18.78
2016-09-30	53.623	-115.894	Carrot Creek	26.89	20.18	29.25	6.21	4.75	3.48
2016-10-07	53.623	-115.894	Carrot Creek	8.70	0.78	48.75	1.00	13.25	42.77
2016-10-14	53.623	-115.894	Carrot Creek	8.60	2.17	6.50	2.40	5.75	4.02
2017-05-12	53.623	-115.894	Carrot Creek	28.83	29.55	35.75	8.00	6.50	10.27
2017-05-24	53.623	-115.894	Carrot Creek	29.86	35.23	11.50	8.18	1.25	1.52
2017-06-08	53.623	-115.894	Carrot Creek	31.95	26.22	30.00	6.61	21.75	8.52
2017-06-20	53.623	-115.894	Carrot Creek	12.27	46.63	2.50	17.18	14.75	1.02
2017-06-26	53.623	-115.894	Carrot Creek	5.32	2.03	7.75	3.23	18.00	0.52
2017-07-11	53.623	-115.894	Carrot Creek	9.10	5.81	4.00	4.92	2.75	3.08
2017-07-12	53.623	-115.894	Carrot Creek	10.93	55.57	6.25	20.83	22.25	0.75
2017-07-21	53.623	-115.894	Carrot Creek	11.82	6.43	5.75	4.40	3.00	2.77
2017-07-23	53.623	-115.894	Carrot Creek	6.87	3.18	7.25	3.79	15.00	2.02
2017-08-03	53.623	-115.894	Carrot Creek	20.86	48.07	11.25	29.35	19.50	0.52
2017-08-07	53.623	-115.894	Carrot Creek	6.17	3.99	6.50	4.96	2.00	6.52
2017-08-13	53.623	-115.894	Carrot Creek	11.35	11.81	7.75	7.20	17.00	1.02
2017-08-18	53.623	-115.894	Carrot Creek	6.49	8.56	2.00	8.45	18.00	1.03
2017-08-24	53.623	-115.894	Carrot Creek	5.02	0.38	2.00	9.84	14.25	0.52
2017-09-08	53.623	-115.894	Carrot Creek	5.58	3.10	17.25	4.81	21.25	1.28
2017-09-09	53.623	-115.894	Carrot Creek	5.29	3.89	5.50	5.48	21.00	0.63
2017-09-13	53.623	-115.894	Carrot Creek	20.47	9.74	31.00	4.15	1.00	13.02
2017-09-18	53.623	-115.894	Carrot Creek	61.12	29.49	75.25	4.60	19.50	16.48
2017-10-10	53.623	-115.894	Carrot Creek	8.61	3.73	17.25	4.00	17.50	17.00
2017-10-31	53.623	-115.894	Carrot Creek	9.00	0.98	63.25	1.20	18.75	15.02
2018-05-10	53.623	-115.894	Carrot Creek	5.40	0.50	18.25	1.04	0.50	16.08
2018-05-16	53.623	-115.894	Carrot Creek	6.70	0.78	17.25	1.26	18.25	5.40
2018-05-30	53.623	-115.894	Carrot Creek	6.10	1.86	10.25	3.01	4.00	7.03

Date	Lat	Long	Station	Depth	EI30	Dur	I30	Start Time	Peak Delay
Y-M-D	DD	DD		mm	MJ*mm/ha*hr	hr	mm/hr	hr	hr
2018-06-10	53.623	-115.894	Carrot Creek	27.41	11.05	26.75	3.60	4.00	10.27
2018-06-15	53.623	-115.894	Carrot Creek	7.10	5.72	5.50	6.00	12.75	5.02
2018-06-16	53.623	-115.894	Carrot Creek	5.86	6.09	0.75	11.57	17.00	0.52
2018-06-21	53.623	-115.894	Carrot Creek	22.29	186.64	1.75	33.59	15.25	0.78
2018-07-02	53.623	-115.894	Carrot Creek	59.97	63.39	53.25	8.02	1.00	33.00
2018-07-07	53.623	-115.894	Carrot Creek	5.50	3.46	9.00	5.11	21.75	1.57
2018-07-12	53.623	-115.894	Carrot Creek	11.43	20.66	8.25	21.87	23.00	0.52
2018-07-13	53.623	-115.894	Carrot Creek	5.90	2.28	11.25	3.60	13.75	0.75
2018-07-17	53.623	-115.894	Carrot Creek	14.42	60.31	10.75	20.17	20.50	5.27
2018-07-20	53.623	-115.894	Carrot Creek	23.12	117.72	10.25	23.11	9.75	2.65
2018-07-22	53.623	-115.894	Carrot Creek	11.69	9.22	20.25	6.20	22.25	20.02
2018-07-30	53.623	-115.894	Carrot Creek	12.28	36.50	2.00	16.41	18.50	0.70
2018-08-01	53.623	-115.894	Carrot Creek	11.07	16.07	0.75	21.83	19.25	0.52
2018-08-11	53.623	-115.894	Carrot Creek	41.40	61.62	24.75	9.99	16.00	12.03
2018-08-23	53.623	-115.894	Carrot Creek	11.41	14.13	8.00	8.44	21.50	4.28
2018-08-30	53.623	-115.894	Carrot Creek	10.18	9.74	3.25	18.26	15.50	0.52
2018-09-11	53.623	-115.894	Carrot Creek	13.70	7.18	42.75	5.08	18.50	0.73
2018-09-14	53.623	-115.894	Carrot Creek	15.00	3.42	39.75	2.40	21.50	36.02
2018-09-20	53.623	-115.894	Carrot Creek	18.40	4.01	52.00	2.31	10.75	48.40
2018-09-26	53.623	-115.894	Carrot Creek	8.50	1.09	17.50	1.41	14.75	9.48
2018-11-01	53.623	-115.894	Carrot Creek	7.30	0.97	19.00	1.45	19.00	13.63
2016-05-08	53.583	-116.467	Edson	6.99	5.68	2.00	6.06	3.25	1.28
2016-05-18	53.583	-116.467	Edson	42.97	44.44	42.75	8.10	14.50	3.93
2016-05-21	53.583	-116.467	Edson	43.28	28.79	27.25	5.40	22.75	10.00
2016-05-26	53.583	-116.467	Edson	12.17	6.52	32.75	4.88	14.75	23.57
2016-06-08	53.583	-116.467	Edson	37.39	542.08	14.00	55.03	15.00	5.75
2016-06-13	53.583	-116.467	Edson	5.50	4.37	9.00	7.41	19.00	0.63
2016-06-14	53.583	-116.467	Edson	15.09	6.51	12.75	3.60	15.50	2.52
2016-06-16	53.583	-116.467	Edson	5.69	1.94	4.50	3.26	22.25	1.07
2016-06-22	53.583	-116.467	Edson	6.82	10.05	2.75	9.21	15.25	0.95
2016-06-23	53.583	-116.467	Edson	6.46	4.21	2.00	6.00	15.50	0.52
2016-06-29	53.583	-116.467	Edson	5.10	2.05	2.25	3.41	19.00	0.73
2016-07-08	53.583	-116.467	Edson	6.28	8.19	1.00	9.45	22.50	0.63
2016-07-12	53.583	-116.467	Edson	8.03	8.82	2.00	7.60	6.00	2.02
2016-08-02	53.583	-116.467	Edson	19.00	55.87	5.25	16.84	23.75	0.77
2016-08-06	53.583	-116.467	Edson	19.57	60.95	8.25	17.62	19.25	3.52
2016-08-08	53.583	-116.467	Edson	5.60	4.84	3.00	6.41	10.50	0.75
2016-08-08	53.583	-116.467	Edson	9.37	6.50	2.50	6.94	20.00	0.52
2016-08-21	53.583	-116.467	Edson	14.37	79.90	1.00	25.11	20.50	0.70
2016-08-22	53.583	-116.467	Edson	5.70	1.20	6.25	2.01	20.75	5.77
2016-08-25	53.583	-116.467	Edson	8.71	18.91	1.50	12.55	18.50	1.43
2016-08-27	53.583	-116.467	Edson	5.95	3.97	1.50	9.18	18.25	0.52

Date	Lat	Long	Station	Depth	EI30	Dur	I30	Start Time	Peak Delay
Y-M-D	DD	DD		mm	MJ*mm/ha*hr	hr	mm/hr	hr	hr
2016-08-31	53.583	-116.467	Edson	9.18	5.24	3.75	5.02	4.75	0.70
2016-09-01	53.583	-116.467	Edson	21.93	10.32	19.00	4.11	22.75	13.15
2016-09-30	53.583	-116.467	Edson	20.19	11.83	38.50	5.12	4.50	3.38
2016-10-07	53.583	-116.467	Edson	5.19	0.87	18.00	1.81	11.50	1.53
2016-10-08	53.583	-116.467	Edson	5.09	0.58	8.50	1.19	13.75	2.77
2016-10-14	53.583	-116.467	Edson	7.80	1.80	5.25	2.25	5.25	3.88
2016-10-28	53.583	-116.467	Edson	8.77	2.73	9.25	2.83	0.25	6.07
2016-10-31	53.583	-116.467	Edson	7.48	1.36	19.50	1.83	18.75	5.80
2017-05-12	53.583	-116.467	Edson	17.99	10.78	20.25	5.00	21.00	8.52
2017-05-24	53.583	-116.467	Edson	22.59	16.53	13.50	5.60	2.75	3.50
2017-06-08	53.583	-116.467	Edson	34.95	17.95	28.25	4.40	22.25	27.27
2017-08-07	53.583	-116.467	Edson	9.38	7.11	7.00	6.41	0.75	0.65
2017-08-18	53.583	-116.467	Edson	7.60	5.79	5.75	6.22	13.75	5.00
2017-09-12	53.583	-116.467	Edson	22.38	10.18	21.75	4.00	21.50	2.02
2017-09-18	53.583	-116.467	Edson	5.50	1.08	9.75	2.00	17.50	3.27
2017-09-19	53.583	-116.467	Edson	48.68	19.17	50.00	3.61	11.25	18.78
2017-10-10	53.583	-116.467	Edson	8.00	1.75	19.00	2.20	15.75	3.77
2017-10-31	53.583	-116.467	Edson	5.36	1.59	5.50	5.33	7.00	0.52
2018-05-17	53.583	-116.467	Edson	6.58	0.91	17.75	1.40	5.00	12.27
2018-05-30	53.583	-116.467	Edson	8.49	6.63	8.00	6.21	11.50	7.53
2018-06-10	53.583	-116.467	Edson	25.09	12.10	28.50	4.21	7.00	12.80
2018-06-16	53.583	-116.467	Edson	5.51	2.16	7.00	3.60	0.50	0.73
2018-06-25	53.583	-116.467	Edson	17.15	103.38	2.25	33.91	2.50	0.52
2018-07-02	53.583	-116.467	Edson	48.60	28.87	32.50	5.00	13.00	28.63
2018-07-13	53.583	-116.467	Edson	11.10	9.09	11.50	6.40	20.00	1.25
2018-07-18	53.583	-116.467	Edson	8.03	2.68	1.00	13.68	2.00	0.52
2018-07-20	53.583	-116.467	Edson	6.80	1.97	9.00	2.83	19.50	7.33
2018-07-21	53.583	-116.467	Edson	5.20	0.70	7.75	1.43	12.25	6.32
2018-08-11	53.583	-116.467	Edson	19.39	21.30	21.75	8.01	22.50	8.77
2018-08-24	53.583	-116.467	Edson	11.49	9.83	4.75	6.42	7.25	1.28
2018-09-10	53.583	-116.467	Edson	5.81	13.26	1.25	10.72	22.25	0.63
2018-09-12	53.583	-116.467	Edson	13.08	2.67	34.00	2.07	0.50	4.08
2018-09-15	53.583	-116.467	Edson	14.57	2.05	40.50	1.43	3.00	37.38
2018-09-20	53.583	-116.467	Edson	19.26	3.81	57.25	2.00	13.00	52.77
2018-09-26	53.583	-116.467	Edson	10.09	1.82	14.50	1.81	23.25	9.03
2018-11-02	53.583	-116.467	Edson	10.79	1.47	24.25	1.40	1.50	13.27
2018-11-16	53.583	-116.467	Edson	8.99	3.52	7.75	3.60	0.75	4.02
2016-05-18	54.751	-116.033	GooseMtnLO	73.59	59.12	50.50	6.44	11.25	17.53
2016-05-22	54.751	-116.033	GooseMtnLO	17.39	21.87	10.75	9.18	11.25	4.02
2016-05-26	54.751	-116.033	GooseMtnLO	44.34	49.35	39.25	8.39	16.50	2.02
2016-06-08	54.751	-116.033	GooseMtnLO	77.22	94.26	25.25	8.46	18.00	13.23
2016-06-10	54.751	-116.033	GooseMtnLO	8.80	3.79	17.25	3.69	22.75	5.72

Date	Lat	Long	Station	Depth	EI30	Dur	I30	Start Time	Peak Delay
Y-M-D	DD	DD		mm	MJ*mm/ha*hr	hr	mm/hr	hr	hr
2016-06-14	54.751	-116.033	GooseMtnLO	67.34	76.59	63.25	9.66	13.75	4.28
2016-06-24	54.751	-116.033	GooseMtnLO	5.18	2.03	7.25	3.59	9.25	1.00
2016-06-30	54.751	-116.033	GooseMtnLO	19.94	85.27	2.25	19.60	12.25	1.07
2016-07-03	54.751	-116.033	GooseMtnLO	9.96	7.08	3.75	6.72	6.00	0.52
2016-07-06	54.751	-116.033	GooseMtnLO	11.77	13.60	8.00	8.88	15.75	1.97
2016-07-08	54.751	-116.033	GooseMtnLO	26.26	242.61	1.50	37.74	2.25	0.75
2016-07-09	54.751	-116.033	GooseMtnLO	21.17	84.70	10.50	20.80	7.75	5.52
2016-07-12	54.751	-116.033	GooseMtnLO	22.02	109.77	2.00	32.09	16.00	0.52
2016-07-14	54.751	-116.033	GooseMtnLO	5.79	2.59	6.00	3.62	15.00	1.77
2016-07-20	54.751	-116.033	GooseMtnLO	11.61	5.18	14.25	4.04	3.25	13.77
2016-07-30	54.751	-116.033	GooseMtnLO	5.39	2.61	9.00	4.88	14.00	5.73
2016-07-31	54.751	-116.033	GooseMtnLO	50.61	95.49	21.00	12.70	5.00	17.67
2016-08-01	54.751	-116.033	GooseMtnLO	5.34	1.56	1.00	9.50	22.00	0.52
2016-08-03	54.751	-116.033	GooseMtnLO	8.18	5.51	2.50	6.80	2.50	0.52
2016-08-03	54.751	-116.033	GooseMtnLO	6.23	17.62	0.75	12.17	12.50	0.52
2016-08-08	54.751	-116.033	GooseMtnLO	6.39	3.83	2.00	7.24	1.50	0.52
2016-08-08	54.751	-116.033	GooseMtnLO	8.74	12.26	1.00	13.23	15.25	0.53
2016-08-09	54.751	-116.033	GooseMtnLO	12.46	19.37	2.75	23.42	11.50	0.52
2016-08-21	54.751	-116.033	GooseMtnLO	76.61	134.24	33.00	12.00	16.25	3.77
2016-08-27	54.751	-116.033	GooseMtnLO	11.83	3.48	25.00	2.83	5.50	11.52
2016-08-31	54.751	-116.033	GooseMtnLO	18.97	38.03	9.00	12.75	2.25	1.77
2016-09-01	54.751	-116.033	GooseMtnLO	12.23	8.98	2.50	18.51	6.75	0.52
2016-09-02	54.751	-116.033	GooseMtnLO	10.77	3.74	16.75	3.24	7.00	11.05
2016-09-03	54.751	-116.033	GooseMtnLO	9.40	3.28	15.75	3.30	8.75	7.45
2016-09-10	54.751	-116.033	GooseMtnLO	8.19	1.58	19.75	2.00	19.75	5.27
2016-09-30	54.751	-116.033	GooseMtnLO	11.59	4.91	11.00	3.80	7.00	0.65
2016-10-06	54.751	-116.033	GooseMtnLO	5.99	0.22	34.50	0.40	21.00	34.52
2016-10-08	54.751	-116.033	GooseMtnLO	8.99	1.34	38.25	1.60	18.00	3.02
2016-10-13	54.751	-116.033	GooseMtnLO	5.40	1.09	18.00	2.00	4.25	4.27
2016-10-14	54.751	-116.033	GooseMtnLO	5.20	1.22	7.25	2.40	6.75	5.52
2016-10-31	54.751	-116.033	GooseMtnLO	6.20	0.92	17.50	1.60	20.00	2.77
2017-05-12	54.751	-116.033	GooseMtnLO	46.62	45.36	26.25	7.21	8.75	19.27
2017-05-23	54.751	-116.033	GooseMtnLO	40.17	45.94	10.50	7.63	22.25	6.47
2017-06-02	54.751	-116.033	GooseMtnLO	11.61	11.18	6.50	7.47	1.25	0.93
2017-06-09	54.751	-116.033	GooseMtnLO	37.08	52.23	14.25	9.18	8.50	3.52
2017-06-14	54.751	-116.033	GooseMtnLO	11.99	4.15	9.50	3.20	11.00	8.52
2017-06-20	54.751	-116.033	GooseMtnLO	6.61	2.72	7.00	3.65	0.50	5.80
2017-06-20	54.751	-116.033	GooseMtnLO	7.99	4.84	2.25	5.37	14.25	0.58
2017-06-21	54.751	-116.033	GooseMtnLO	7.79	1.90	8.50	2.40	18.75	3.77
2017-06-26	54.751	-116.033	GooseMtnLO	16.66	24.20	3.50	23.31	17.50	0.52
2017-06-27	54.751	-116.033	GooseMtnLO	40.54	28.28	27.25	5.60	5.50	24.27
2017-07-02	54.751	-116.033	GooseMtnLO	22.69	103.92	13.25	18.36	16.25	4.52

Date	Lat	Long	Station	Depth	EI30	Dur	I30	Start Time	Peak Delay
Y-M-D	DD	DD		mm	MJ*mm/ha*hr	hr	mm/hr	hr	hr
2017-07-07	54.751	-116.033	GooseMtnLO	6.03	6.48	1.75	7.08	22.00	0.95
2017-07-09	54.751	-116.033	GooseMtnLO	27.96	394.02	6.50	51.93	16.25	6.28
2017-07-13	54.751	-116.033	GooseMtnLO	23.52	186.26	2.00	32.69	14.75	1.02
2017-07-16	54.751	-116.033	GooseMtnLO	17.01	4.26	23.00	2.40	19.25	10.52
2017-07-23	54.751	-116.033	GooseMtnLO	5.00	1.06	14.00	2.12	4.25	12.13
2017-07-29	54.751	-116.033	GooseMtnLO	19.09	91.02	8.25	22.73	21.00	4.77
2017-08-03	54.751	-116.033	GooseMtnLO	10.22	16.50	12.00	10.42	18.50	0.75
2017-08-04	54.751	-116.033	GooseMtnLO	6.56	9.02	6.00	8.33	13.50	2.77
2017-09-08	54.751	-116.033	GooseMtnLO	10.60	5.32	23.25	4.39	13.50	23.00
2017-09-18	54.751	-116.033	GooseMtnLO	82.80	104.71	68.50	10.71	18.00	30.02
2017-10-01	54.751	-116.033	GooseMtnLO	6.60	0.77	14.75	1.26	9.00	13.63
2017-10-07	54.751	-116.033	GooseMtnLO	12.59	2.55	28.25	2.04	3.25	5.63
2017-10-10	54.751	-116.033	GooseMtnLO	21.58	7.15	31.00	3.20	15.75	5.27
2017-10-17	54.751	-116.033	GooseMtnLO	5.79	0.89	13.00	1.60	10.00	11.77
2017-10-24	54.751	-116.033	GooseMtnLO	12.01	5.17	30.25	4.03	12.25	17.27
2017-10-31	54.751	-116.033	GooseMtnLO	17.62	8.29	50.25	4.44	4.00	12.52
2018-05-16	54.751	-116.033	GooseMtnLO	8.78	2.10	18.50	2.40	14.50	12.27
2018-05-25	54.751	-116.033	GooseMtnLO	10.98	12.23	2.25	11.56	22.25	0.52
2018-06-03	54.751	-116.033	GooseMtnLO	8.40	5.46	9.00	4.98	21.25	6.10
2018-06-10	54.751	-116.033	GooseMtnLO	73.20	64.39	56.00	7.68	9.25	13.77
2018-06-21	54.751	-116.033	GooseMtnLO	17.35	96.48	1.00	27.47	16.00	0.63
2018-07-01	54.751	-116.033	GooseMtnLO	100.96	153.97	62.00	11.62	4.50	61.27
2018-07-20	54.751	-116.033	GooseMtnLO	41.57	123.00	20.25	16.40	10.75	3.02
2018-08-01	54.751	-116.033	GooseMtnLO	15.25	42.28	2.50	29.06	18.50	0.52
2018-08-04	54.751	-116.033	GooseMtnLO	15.11	55.96	4.75	17.12	13.00	4.52
2018-08-11	54.751	-116.033	GooseMtnLO	8.58	5.15	3.75	4.80	22.75	2.53
2018-08-25	54.751	-116.033	GooseMtnLO	7.00	6.31	9.25	6.80	17.25	0.77
2018-08-28	54.751	-116.033	GooseMtnLO	5.80	6.34	5.00	7.22	18.50	2.77
2018-08-29	54.751	-116.033	GooseMtnLO	12.99	4.05	23.50	2.87	22.75	0.72
2018-09-08	54.751	-116.033	GooseMtnLO	8.17	5.14	8.25	4.81	2.25	6.27
2018-09-11	54.751	-116.033	GooseMtnLO	16.19	6.40	21.00	3.71	21.00	8.90
2018-10-11	54.751	-116.033	GooseMtnLO	18.59	7.58	19.00	4.02	22.75	8.48
2018-10-28	54.751	-116.033	GooseMtnLO	8.61	2.16	6.25	2.40	16.25	5.27
2016-05-18	54.014	-115.214	Greencourt	21.69	22.76	14.00	7.80	17.50	6.02
2016-05-19	54.014	-115.214	Greencourt	46.47	52.83	19.00	8.41	15.00	4.78
2016-05-22	54.014	-115.214	Greencourt	39.14	27.29	23.75	5.60	1.00	7.77
2016-05-25	54.014	-115.214	Greencourt	10.41	12.53	0.50	20.82	13.25	0.52
2016-05-28	54.014	-115.214	Greencourt	5.06	2.44	0.50	10.12	20.50	0.52
2016-06-08	54.014	-115.214	Greencourt	14.80	22.49	17.25	9.49	16.75	6.88
2016-06-11	54.014	-115.214	Greencourt	13.90	34.88	5.25	14.58	12.75	0.53
2016-06-14	54.014	-115.214	Greencourt	9.69	5.78	12.25	5.01	20.00	3.77
2016-06-24	54.014	-115.214	Greencourt	11.39	20.61	12.00	11.90	13.00	1.43

Date	Lat	Long	Station	Depth	EI30	Dur	I30	Start Time	Peak Delay
Y-M-D	DD	DD		mm	MJ*mm/ha*hr	hr	mm/hr	hr	hr
2016-07-01	54.014	-115.214	Greencourt	5.37	3.02	2.75	7.58	19.00	0.52
2016-07-06	54.014	-115.214	Greencourt	8.98	6.49	3.00	6.27	15.75	0.63
2016-07-10	54.014	-115.214	Greencourt	12.27	10.14	13.75	6.00	7.50	5.00
2016-07-18	54.014	-115.214	Greencourt	5.60	6.78	0.75	7.98	17.25	0.77
2016-08-03	54.014	-115.214	Greencourt	16.35	37.66	16.25	13.47	8.50	13.03
2016-08-04	54.014	-115.214	Greencourt	6.40	18.73	1.00	12.41	14.25	0.52
2016-08-08	54.014	-115.214	Greencourt	5.01	1.79	10.25	3.43	14.50	0.52
2016-08-20	54.014	-115.214	Greencourt	11.46	14.17	11.00	8.42	17.25	7.50
2016-08-21	54.014	-115.214	Greencourt	11.62	12.69	3.25	7.27	21.75	1.97
2016-08-22	54.014	-115.214	Greencourt	58.56	115.88	16.50	12.07	9.75	2.50
2016-08-31	54.014	-115.214	Greencourt	5.81	7.15	5.00	6.99	0.50	4.77
2016-09-02	54.014	-115.214	Greencourt	19.00	7.65	17.00	3.80	1.75	10.98
2016-09-08	54.014	-115.214	Greencourt	5.11	0.99	13.00	2.00	6.00	4.02
2016-09-30	54.014	-115.214	Greencourt	12.98	11.22	10.50	6.72	3.50	6.70
2016-10-01	54.014	-115.214	Greencourt	18.58	10.52	16.50	4.61	6.75	3.68
2016-10-08	54.014	-115.214	Greencourt	6.29	0.95	8.00	1.60	15.25	3.02
2016-10-14	54.014	-115.214	Greencourt	7.69	1.44	7.50	1.83	6.75	3.85
2017-05-12	54.014	-115.214	Greencourt	28.68	16.43	18.25	4.90	17.00	2.38
2017-05-24	54.014	-115.214	Greencourt	16.70	14.69	6.00	6.40	5.00	3.28
2017-06-01	54.014	-115.214	Greencourt	5.40	0.85	9.75	1.61	21.50	5.53
2017-06-09	54.014	-115.214	Greencourt	50.14	139.70	18.75	15.75	5.25	12.77
2017-06-20	54.014	-115.214	Greencourt	6.58	3.81	11.25	4.84	7.00	9.73
2017-06-26	54.014	-115.214	Greencourt	7.11	2.68	19.50	3.40	20.25	1.00
2017-06-28	54.014	-115.214	Greencourt	5.30	1.08	18.25	2.02	2.50	12.27
2017-07-02	54.014	-115.214	Greencourt	7.14	22.37	2.75	13.16	18.75	2.63
2017-07-20	54.014	-115.214	Greencourt	47.61	61.85	17.25	9.00	16.25	12.00
2017-07-23	54.014	-115.214	Greencourt	26.70	78.90	21.00	17.67	4.75	11.27
2017-07-27	54.014	-115.214	Greencourt	5.75	13.39	2.25	10.76	18.25	0.52
2017-08-01	54.014	-115.214	Greencourt	6.69	2.92	9.00	3.84	5.00	3.62
2017-08-03	54.014	-115.214	Greencourt	8.62	19.44	1.75	11.90	19.50	1.25
2017-08-04	54.014	-115.214	Greencourt	6.39	3.78	16.75	4.44	4.00	12.27
2017-08-07	54.014	-115.214	Greencourt	8.60	5.71	9.00	5.22	3.00	6.35
2017-08-24	54.014	-115.214	Greencourt	5.11	3.67	2.25	5.21	15.00	0.75
2017-09-08	54.014	-115.214	Greencourt	6.90	5.62	2.00	5.70	22.00	1.57
2017-09-09	54.014	-115.214	Greencourt	9.49	6.55	4.00	5.20	21.50	2.52
2017-09-19	54.014	-115.214	Greencourt	59.59	27.86	67.50	4.29	0.00	9.88
2017-10-10	54.014	-115.214	Greencourt	12.69	3.49	17.25	2.63	18.25	3.07
2018-05-16	54.014	-115.214	Greencourt	5.81	1.21	12.00	2.05	18.00	4.45
2018-05-24	54.014	-115.214	Greencourt	7.49	11.83	2.25	10.60	17.25	0.75
2018-06-09	54.014	-115.214	Greencourt	17.16	28.08	5.00	23.18	17.25	0.52
2018-06-10	54.014	-115.214	Greencourt	42.50	29.91	21.00	5.62	7.75	16.78
2018-07-02	54.014	-115.214	Greencourt	54.91	75.85	42.50	10.41	2.25	15.75

Date	Lat	Long	Station	Depth	EI30	Dur	I30	Start Time	Peak Delay
Y-M-D	DD	DD		mm	MJ*mm/ha*hr	hr	mm/hr	hr	hr
2018-07-13	54.014	-115.214	Greencourt	34.60	501.03	5.75	55.23	12.00	1.03
2018-07-17	54.014	-115.214	Greencourt	13.56	8.47	9.00	5.20	21.75	3.77
2018-07-18	54.014	-115.214	Greencourt	7.38	8.36	1.00	11.36	20.00	0.52
2018-07-20	54.014	-115.214	Greencourt	14.91	56.74	6.00	18.73	10.50	3.52
2018-07-30	54.014	-115.214	Greencourt	10.49	8.32	2.00	11.58	17.50	0.52
2018-08-11	54.014	-115.214	Greencourt	18.80	20.59	17.50	8.24	22.00	14.53
2018-08-23	54.014	-115.214	Greencourt	10.90	14.90	7.00	8.70	20.75	6.22
2018-09-11	54.014	-115.214	Greencourt	18.81	36.06	43.50	12.98	6.50	13.52
2018-09-15	54.014	-115.214	Greencourt	14.90	4.34	45.75	2.99	0.00	33.52
2018-09-20	54.014	-115.214	Greencourt	6.19	1.86	11.75	2.75	23.50	4.88
2018-10-07	54.014	-115.214	Greencourt	5.30	0.82	6.00	1.60	15.25	1.77
2018-10-12	54.014	-115.214	Greencourt	5.59	1.64	11.50	2.82	4.00	2.23
2016-05-08	53.800	-118.450	Hendrick	8.17	3.05	22.25	3.99	19.25	4.72
2016-05-18	53.800	-118.450	Hendrick	44.43	18.02	49.00	3.56	9.50	0.75
2016-05-22	53.800	-118.450	Hendrick	20.30	24.04	30.75	8.53	2.25	6.52
2016-05-26	53.800	-118.450	Hendrick	8.40	2.78	18.75	3.14	2.25	14.45
2016-05-27	53.800	-118.450	Hendrick	7.11	1.16	35.50	1.73	6.25	13.75
2016-05-29	53.800	-118.450	Hendrick	5.39	0.75	41.25	1.43	4.25	9.52
2016-06-08	53.800	-118.450	Hendrick	15.52	21.60	19.00	9.06	13.25	9.85
2016-06-22	53.800	-118.450	Hendrick	5.61	5.61	6.75	6.79	10.75	5.80
2016-06-23	53.800	-118.450	Hendrick	32.27	23.50	40.50	5.77	15.75	1.38
2016-06-30	53.800	-118.450	Hendrick	9.39	9.90	11.00	8.14	9.25	8.02
2016-07-03	53.800	-118.450	Hendrick	6.59	4.46	10.00	5.57	2.25	3.52
2016-07-04	53.800	-118.450	Hendrick	6.36	9.66	1.25	9.25	17.00	1.23
2016-07-09	53.800	-118.450	Hendrick	5.33	2.47	9.50	4.05	15.50	1.02
2016-07-10	53.800	-118.450	Hendrick	11.42	6.67	11.50	5.08	8.50	11.02
2016-07-12	53.800	-118.450	Hendrick	71.38	1045.91	31.00	68.55	5.25	12.77
2016-07-14	53.800	-118.450	Hendrick	29.95	26.73	30.50	6.62	7.00	10.47
2016-07-16	53.800	-118.450	Hendrick	13.77	24.22	18.00	11.21	6.75	11.25
2016-07-30	53.800	-118.450	Hendrick	16.79	8.02	36.00	4.10	7.00	31.52
2016-08-05	53.800	-118.450	Hendrick	14.08	23.75	26.00	9.92	5.50	21.27
2016-08-07	53.800	-118.450	Hendrick	6.93	9.88	24.75	8.71	9.00	10.43
2016-08-08	53.800	-118.450	Hendrick	9.57	36.18	9.50	17.49	16.00	0.52
2016-08-13	53.800	-118.450	Hendrick	5.74	2.40	1.50	8.03	14.50	0.52
2016-08-21	53.800	-118.450	Hendrick	54.55	58.80	31.00	7.89	11.50	24.93
2016-09-04	53.800	-118.450	Hendrick	5.94	1.55	29.00	2.54	17.50	22.02
2016-09-11	53.800	-118.450	Hendrick	6.18	2.42	17.50	3.61	1.25	2.52
2016-09-17	53.800	-118.450	Hendrick	7.19	1.51	30.00	2.06	4.25	21.43
2016-09-30	53.800	-118.450	Hendrick	7.91	2.21	32.25	2.84	6.50	15.02
2016-10-07	53.800	-118.450	Hendrick	6.83	1.00	19.00	1.51	7.50	11.02
2016-10-08	53.800	-118.450	Hendrick	9.62	0.99	18.00	1.08	12.50	6.63
2016-10-14	53.800	-118.450	Hendrick	5.57	1.14	11.75	2.04	0.00	7.02

Date	Lat	Long	Station	Depth	EI30	Dur	I30	Start Time	Peak Delay
Y-M-D	DD	DD		mm	MJ*mm/ha*hr	hr	mm/hr	hr	hr
2017-05-24	53.800	-118.450	Hendrick	20.61	30.06	16.25	10.40	2.50	8.00
2017-06-08	53.800	-118.450	Hendrick	90.61	98.44	29.25	7.82	22.00	17.03
2017-06-11	53.800	-118.450	Hendrick	11.21	3.95	14.00	3.20	0.00	9.52
2017-06-14	53.800	-118.450	Hendrick	11.76	13.80	8.25	13.30	14.00	0.52
2017-06-28	53.800	-118.450	Hendrick	40.61	40.50	17.50	7.48	1.00	9.42
2017-07-02	53.800	-118.450	Hendrick	15.44	64.13	13.25	20.05	19.50	2.32
2017-07-20	53.800	-118.450	Hendrick	5.40	1.36	18.25	2.42	15.50	11.77
2017-07-23	53.800	-118.450	Hendrick	11.59	3.88	13.00	3.20	1.50	3.77
2017-07-23	53.800	-118.450	Hendrick	7.78	2.40	11.00	3.02	23.75	0.78
2017-07-27	53.800	-118.450	Hendrick	14.19	43.75	5.75	16.40	13.50	3.77
2017-08-03	53.800	-118.450	Hendrick	8.96	5.71	21.00	5.60	20.00	1.27
2017-08-06	53.800	-118.450	Hendrick	16.87	119.27	2.00	29.58	20.75	2.02
2017-09-08	53.800	-118.450	Hendrick	13.32	7.62	26.50	4.61	9.25	22.75
2017-09-12	53.800	-118.450	Hendrick	22.85	10.10	28.00	3.81	16.00	7.73
2017-09-19	53.800	-118.450	Hendrick	73.66	410.43	50.00	32.30	13.75	46.27
2017-10-01	53.800	-118.450	Hendrick	6.29	0.84	20.00	1.40	7.25	1.77
2017-10-07	53.800	-118.450	Hendrick	5.49	1.56	7.50	2.78	21.00	3.52
2017-10-10	53.800	-118.450	Hendrick	29.69	9.51	34.50	3.03	0.25	3.63
2017-10-12	53.800	-118.450	Hendrick	16.10	7.81	15.75	4.62	19.25	0.53
2017-10-17	53.800	-118.450	Hendrick	5.39	3.41	2.25	5.40	9.50	0.77
2017-10-25	53.800	-118.450	Hendrick	5.98	2.00	8.25	3.59	7.50	0.52
2017-10-28	53.800	-118.450	Hendrick	5.70	2.67	2.75	3.86	12.75	1.40
2018-06-10	53.800	-118.450	Hendrick	7.40	2.36	4.75	3.00	10.25	2.00
2018-07-02	53.800	-118.450	Hendrick	68.66	80.45	57.50	8.98	3.75	6.77
2018-07-13	53.800	-118.450	Hendrick	6.81	1.90	14.75	2.61	9.00	12.52
2018-07-17	53.800	-118.450	Hendrick	14.13	61.25	12.75	20.39	20.00	5.27
2018-07-19	53.800	-118.450	Hendrick	57.04	688.58	13.50	73.58	17.00	0.52
2018-07-20	53.800	-118.450	Hendrick	48.88	67.50	31.25	10.24	14.50	1.12
2018-07-22	53.800	-118.450	Hendrick	7.19	5.09	9.75	5.69	16.00	2.55
2018-08-23	53.800	-118.450	Hendrick	15.44	14.85	11.25	7.20	18.25	6.52
2018-08-26	53.800	-118.450	Hendrick	24.27	15.93	25.25	5.70	4.50	13.22
2018-09-03	53.800	-118.450	Hendrick	11.59	4.01	15.50	3.20	7.50	5.52
2018-09-11	53.800	-118.450	Hendrick	19.48	8.40	42.75	4.00	10.00	23.75
2018-09-20	53.800	-118.450	Hendrick	6.19	1.02	19.75	1.60	5.50	19.77
2018-09-21	53.800	-118.450	Hendrick	9.68	4.29	28.25	6.79	13.00	0.52
2018-09-26	53.800	-118.450	Hendrick	13.97	8.43	20.25	5.59	21.00	0.52
2018-10-01	53.800	-118.450	Hendrick	5.19	1.30	17.25	4.79	22.00	0.52
2018-10-12	53.800	-118.450	Hendrick	6.19	2.81	12.25	4.19	7.00	5.52
2018-11-01	53.800	-118.450	Hendrick	9.69	1.94	16.50	2.00	16.50	14.02
2018-11-04	53.800	-118.450	Hendrick	7.77	2.13	28.25	2.58	14.50	9.77
2018-11-15	53.800	-118.450	Hendrick	13.00	5.70	7.75	3.84	16.25	2.55
2018-12-29	53.800	-118.450	Hendrick	7.10	1.93	16.50	2.61	2.25	15.98

Date	Lat	Long	Station	Depth	EI30	Dur	I30	Start Time	Peak Delay
Y-M-D	DD	DD		mm	MJ*mm/ha*hr	hr	mm/hr	hr	hr
2019-01-04	53.800	-118.450	Hendrick	10.46	6.08	11.00	4.76	4.50	2.02
2016-05-19	55.163	-116.415	HighPr	65.19	34.51	32.25	4.32	3.00	3.65
2016-05-26	55.163	-116.415	HighPr	19.08	8.77	31.50	4.02	14.50	5.53
2016-06-09	55.163	-116.415	HighPr	56.35	86.56	16.00	10.28	2.50	1.78
2016-06-10	55.163	-116.415	HighPr	7.09	4.15	13.00	4.63	23.75	13.00
2016-06-14	55.163	-116.415	HighPr	73.94	146.79	62.75	14.65	13.75	5.12
2016-06-19	55.163	-116.415	HighPr	6.08	16.72	3.50	11.38	16.00	3.52
2016-06-25	55.163	-116.415	HighPr	5.75	5.06	0.75	11.36	16.50	0.52
2016-06-30	55.163	-116.415	HighPr	73.02	1926.60	4.50	98.73	12.00	0.75
2016-07-08	55.163	-116.415	HighPr	7.40	12.00	2.75	10.01	12.25	0.53
2016-07-20	55.163	-116.415	HighPr	9.04	5.60	5.50	5.04	10.75	3.77
2016-07-29	55.163	-116.415	HighPr	11.91	53.90	2.00	19.32	19.25	0.75
2016-07-30	55.163	-116.415	HighPr	34.81	30.27	29.75	7.00	18.50	0.52
2017-05-23	55.163	-116.415	HighPr	17.92	12.69	10.25	5.62	21.50	8.27
2017-06-02	55.163	-116.415	HighPr	10.60	7.50	6.25	5.93	1.50	2.57
2017-06-14	55.163	-116.415	HighPr	8.80	2.88	7.75	2.99	13.75	5.52
2017-06-27	55.163	-116.415	HighPr	13.83	6.37	20.50	4.21	19.25	8.27
2017-07-17	55.163	-116.415	HighPr	7.31	2.02	18.00	2.80	15.75	12.27
2017-07-29	55.163	-116.415	HighPr	12.07	6.76	7.25	4.41	20.75	4.53
2017-08-03	55.163	-116.415	HighPr	23.76	20.52	10.25	6.81	18.50	6.52
2017-08-24	55.163	-116.415	HighPr	7.48	1.49	18.25	2.37	13.50	0.52
2017-09-09	55.163	-116.415	HighPr	6.01	4.17	3.25	5.09	9.50	0.53
2017-09-19	55.163	-116.415	HighPr	85.87	68.71	54.25	6.60	5.50	2.53
2017-10-10	55.163	-116.415	HighPr	9.88	3.33	23.25	3.37	17.75	17.95
2017-10-24	55.163	-116.415	HighPr	10.49	2.20	22.25	2.19	15.25	22.27
2017-10-31	55.163	-116.415	HighPr	10.50	2.01	32.25	2.00	4.00	15.25
2018-05-25	55.163	-116.415	HighPr	11.94	14.65	2.50	9.83	21.50	0.53
2018-06-03	55.163	-116.415	HighPr	9.49	13.03	7.00	9.07	21.50	5.48
2018-06-08	55.163	-116.415	HighPr	13.77	23.11	2.75	9.57	23.50	2.02
2018-06-10	55.163	-116.415	HighPr	82.54	86.38	52.50	8.40	13.25	34.52
2018-06-25	55.163	-116.415	HighPr	7.95	19.34	1.50	13.52	12.00	0.52
2018-06-26	55.163	-116.415	HighPr	6.39	1.23	13.00	2.00	18.75	5.02
2018-07-01	55.163	-116.415	HighPr	37.73	35.36	42.50	7.49	20.75	13.57
2018-07-07	55.163	-116.415	HighPr	5.96	7.61	2.75	8.23	10.75	2.02
2018-07-19	55.163	-116.415	HighPr	78.43	361.78	23.75	24.23	22.25	3.78
2018-08-29	55.163	-116.415	HighPr	5.50	8.41	1.50	8.85	22.25	0.75
2018-08-30	55.163	-116.415	HighPr	9.49	5.27	14.50	4.60	6.75	9.00
2018-09-11	55.163	-116.415	HighPr	11.43	5.46	20.75	4.61	20.25	16.02
2018-10-11	55.163	-116.415	HighPr	17.29	5.06	20.50	2.80	17.25	14.52
2018-10-31	55.163	-116.415	HighPr	7.30	2.84	4.75	3.43	17.25	2.05
2018-11-03	55.163	-116.415	HighPr	16.60	3.30	24.75	2.04	22.00	10.82
2018-11-14	55.163	-116.415	HighPr	5.50	0.51	23.00	1.03	23.25	19.13

Date	Lat	Long	Station	Depth	EI30	Dur	I30	Start Time	Peak Delay
Y-M-D	DD	DD		mm	MJ*mm/ha*hr	hr	mm/hr	hr	hr
2018-12-21	55.163	-116.415	HighPr	5.00	0.46	13.00	1.01	4.75	7.28
2018-12-29	55.163	-116.415	HighPr	17.29	6.16	20.75	3.20	9.75	6.75
2016-05-04	52.930	-118.030	Jasper	5.00	1.34	12.50	2.62	20.00	6.32
2016-05-18	52.930	-118.030	Jasper	6.81	3.54	13.25	4.65	16.50	2.72
2016-05-22	52.930	-118.030	Jasper	27.48	9.43	19.00	3.06	4.00	10.90
2016-05-26	52.930	-118.030	Jasper	5.29	1.61	18.75	2.79	22.75	17.77
2016-06-10	52.930	-118.030	Jasper	6.60	2.62	6.75	3.43	16.50	1.55
2016-07-03	52.930	-118.030	Jasper	8.30	4.46	3.50	4.40	6.00	2.27
2016-07-10	52.930	-118.030	Jasper	11.58	2.22	27.00	1.89	15.50	17.15
2016-07-12	52.930	-118.030	Jasper	16.00	7.79	23.25	4.40	22.75	19.27
2016-08-08	52.930	-118.030	Jasper	8.69	6.11	5.50	5.23	17.25	3.15
2016-08-09	52.930	-118.030	Jasper	13.36	39.95	13.00	16.16	6.25	9.53
2016-08-13	52.930	-118.030	Jasper	5.30	1.77	3.50	3.20	19.75	1.77
2016-08-22	52.930	-118.030	Jasper	14.29	3.95	9.75	2.48	8.00	2.87
2016-08-27	52.930	-118.030	Jasper	7.60	2.27	20.00	2.80	3.50	13.02
2016-08-31	52.930	-118.030	Jasper	5.21	5.01	10.00	6.76	22.25	7.72
2016-09-30	52.930	-118.030	Jasper	12.70	9.78	13.75	5.86	7.25	13.72
2016-10-01	52.930	-118.030	Jasper	6.20	1.61	5.75	2.83	5.25	1.97
2016-10-08	52.930	-118.030	Jasper	5.70	0.89	10.00	1.61	10.00	4.03
2017-08-18	52.930	-118.030	Jasper	5.49	1.90	3.50	3.19	16.25	1.27
2017-09-08	52.930	-118.030	Jasper	8.76	10.10	9.50	7.09	11.00	7.27
2017-09-09	52.930	-118.030	Jasper	9.29	4.17	18.50	3.84	5.50	15.18
2017-09-20	52.930	-118.030	Jasper	47.60	38.03	31.25	6.20	2.00	11.03
2018-03-15	52.930	-118.030	Jasper	10.99	6.65	20.00	5.40	14.50	18.52
2018-03-29	52.930	-118.030	Jasper	5.39	0.85	9.75	1.60	23.50	3.00
2018-06-10	52.930	-118.030	Jasper	14.37	4.52	12.50	3.00	2.25	8.02
2018-06-21	52.930	-118.030	Jasper	7.43	23.80	0.75	14.33	15.25	0.75
2018-07-02	52.930	-118.030	Jasper	56.60	44.03	49.25	6.26	5.25	9.58
2018-07-12	52.930	-118.030	Jasper	10.90	4.14	17.25	3.41	23.50	2.20
2018-07-21	52.930	-118.030	Jasper	7.99	1.47	24.25	1.83	7.25	10.97
2018-07-30	52.930	-118.030	Jasper	8.73	11.02	13.75	7.14	7.25	7.02
2018-08-11	52.930	-118.030	Jasper	7.77	11.62	2.50	9.96	20.25	0.72
2018-08-12	52.930	-118.030	Jasper	8.89	7.13	16.00	6.41	6.00	8.77
2018-08-23	52.930	-118.030	Jasper	12.40	7.21	15.75	4.89	21.25	1.82
2018-08-26	52.930	-118.030	Jasper	7.99	1.47	16.75	1.82	7.00	14.77
2018-08-29	52.930	-118.030	Jasper	6.09	1.57	18.75	2.60	4.75	3.77
2018-11-01	52.930	-118.030	Jasper	6.60	0.89	16.00	1.43	18.25	9.07
2018-12-29	52.930	-118.030	Jasper	12.19	3.03	18.75	2.40	1.50	5.77
2019-01-03	52.930	-118.030	Jasper	7.89	1.06	15.00	1.39	3.50	12.77
2016-05-08	55.422	-119.255	LaGlance	9.99	4.11	15.25	3.80	8.25	8.50
2016-05-19	55.422	-119.255	LaGlance	19.48	6.10	29.00	3.02	6.25	0.78
2016-05-27	55.422	-119.255	LaGlance	19.80	6.22	17.00	2.84	17.25	8.18

Date	Lat	Long	Station	Depth	EI30	Dur	I30	Start Time	Peak Delay
Y-M-D	DD	DD		mm	MJ*mm/ha*hr	hr	mm/hr	hr	hr
2016-05-29	55.422	-119.255	LaGlance	7.78	3.14	6.25	3.59	7.50	3.27
2016-06-08	55.422	-119.255	LaGlance	29.11	13.35	38.75	4.00	6.75	28.52
2016-06-11	55.422	-119.255	LaGlance	15.68	15.57	13.75	7.39	9.75	6.00
2016-06-14	55.422	-119.255	LaGlance	70.10	58.87	52.25	6.94	17.50	3.30
2016-06-24	55.422	-119.255	LaGlance	27.51	164.41	7.75	24.62	9.75	3.52
2016-07-07	55.422	-119.255	LaGlance	7.48	11.16	4.00	14.77	17.75	0.52
2016-07-16	55.422	-119.255	LaGlance	14.31	85.30	9.00	25.09	13.00	3.52
2016-07-19	55.422	-119.255	LaGlance	5.21	1.68	23.50	2.80	17.50	4.77
2016-07-21	55.422	-119.255	LaGlance	9.72	27.10	5.75	14.36	13.50	0.77
2016-07-31	55.422	-119.255	LaGlance	6.22	4.07	6.25	5.00	8.00	5.25
2016-08-02	55.422	-119.255	LaGlance	5.84	0.50	12.00	11.08	18.00	0.52
2016-08-05	55.422	-119.255	LaGlance	7.51	8.20	12.25	7.57	17.50	9.42
2016-08-09	55.422	-119.255	LaGlance	5.24	1.97	6.50	10.11	15.00	0.52
2016-08-13	55.422	-119.255	LaGlance	10.94	52.18	1.75	20.11	23.00	1.52
2016-08-21	55.422	-119.255	LaGlance	16.71	10.11	28.25	5.20	13.75	2.52
2016-08-26	55.422	-119.255	LaGlance	5.79	0.76	28.00	1.40	21.00	5.78
2016-08-31	55.422	-119.255	LaGlance	25.14	61.62	19.25	14.38	17.00	13.80
2016-09-30	55.422	-119.255	LaGlance	32.20	19.52	30.00	5.04	12.00	23.25
2016-10-14	55.422	-119.255	LaGlance	7.99	1.07	25.00	1.45	6.50	10.88
2016-10-24	55.422	-119.255	LaGlance	6.49	0.97	23.00	1.60	19.75	18.02
2016-10-31	55.422	-119.255	LaGlance	7.89	0.73	25.50	1.03	18.75	10.13
2017-05-12	55.422	-119.255	LaGlance	7.10	3.90	11.25	4.42	10.00	4.30
2017-05-13	55.422	-119.255	LaGlance	10.09	1.91	21.25	2.00	5.00	2.52
2017-05-23	55.422	-119.255	LaGlance	34.69	55.06	10.25	10.50	19.50	3.13
2017-06-09	55.422	-119.255	LaGlance	16.40	25.86	4.50	9.37	13.25	2.93
2017-06-10	55.422	-119.255	LaGlance	6.01	1.04	20.25	1.81	21.25	0.77
2017-06-14	55.422	-119.255	LaGlance	6.13	4.45	11.00	5.23	16.75	0.75
2017-06-27	55.422	-119.255	LaGlance	18.25	21.97	24.25	9.12	9.00	11.02
2017-07-07	55.422	-119.255	LaGlance	14.40	19.74	5.00	8.63	17.75	4.17
2017-07-16	55.422	-119.255	LaGlance	7.51	5.00	12.75	5.47	16.50	3.40
2017-07-31	55.422	-119.255	LaGlance	7.30	6.64	3.25	6.84	22.00	1.53
2017-08-23	55.422	-119.255	LaGlance	36.49	67.49	32.25	11.72	17.75	15.75
2017-09-02	55.422	-119.255	LaGlance	7.60	2.02	8.00	2.60	6.00	4.00
2017-09-18	55.422	-119.255	LaGlance	44.02	34.40	49.00	6.80	11.75	29.52
2017-10-16	55.422	-119.255	LaGlance	15.29	3.04	25.75	2.00	11.25	22.27
2017-10-24	55.422	-119.255	LaGlance	29.11	12.46	25.50	3.79	10.50	18.27
2018-06-03	55.422	-119.255	LaGlance	20.23	14.21	10.50	5.60	20.25	3.02
2018-06-14	55.422	-119.255	LaGlance	28.57	95.42	12.00	17.57	13.25	0.52
2018-06-25	55.422	-119.255	LaGlance	7.77	4.29	3.00	6.20	12.00	0.52
2018-07-01	55.422	-119.255	LaGlance	11.70	3.41	13.25	2.80	18.00	7.77
2018-07-07	55.422	-119.255	LaGlance	15.41	19.89	10.50	8.73	7.25	0.80
2018-07-19	55.422	-119.255	LaGlance	14.77	11.63	14.50	5.62	16.50	4.53

Date	Lat	Long	Station	Depth	EI30	Dur	I30	Start Time	Peak Delay
Y-M-D	DD	DD		mm	MJ*mm/ha*hr	hr	mm/hr	hr	hr
2018-07-20	55.422	-119.255	LaGlance	48.95	69.26	19.25	9.71	15.50	7.17
2018-07-22	55.422	-119.255	LaGlance	16.40	9.88	14.25	5.03	15.50	2.38
2018-08-01	55.422	-119.255	LaGlance	16.04	25.98	4.25	19.44	12.75	0.52
2018-08-12	55.422	-119.255	LaGlance	15.58	11.52	10.75	6.00	0.00	1.77
2018-08-26	55.422	-119.255	LaGlance	8.10	3.26	6.50	3.60	17.75	2.02
2018-08-30	55.422	-119.255	LaGlance	8.60	4.03	7.00	4.20	8.25	4.27
2018-09-08	55.422	-119.255	LaGlance	18.96	23.80	6.50	8.72	2.50	4.77
2018-09-09	55.422	-119.255	LaGlance	5.70	1.92	8.50	3.04	23.25	3.97
2018-09-11	55.422	-119.255	LaGlance	8.47	2.87	34.75	5.54	12.75	0.52
2018-10-11	55.422	-119.255	LaGlance	16.20	5.39	12.50	3.03	23.00	7.98
2018-10-31	55.422	-119.255	LaGlance	6.88	2.33	14.00	3.20	12.50	4.23
2018-11-03	55.422	-119.255	LaGlance	17.80	3.46	35.25	2.00	19.75	9.27
2018-12-29	55.422	-119.255	LaGlance	10.59	1.88	22.00	1.80	6.50	5.02
2016-05-18	54.017	-115.500	LPaddle	60.98	56.87	43.25	7.53	15.25	12.45
2016-05-21	54.017	-115.500	LPaddle	36.40	33.09	26.50	7.00	23.25	8.52
2016-05-26	54.017	-115.500	LPaddle	8.72	5.66	12.25	5.20	17.75	0.85
2016-05-28	54.017	-115.500	LPaddle	8.51	14.86	1.75	9.48	19.50	0.87
2016-06-07	54.017	-115.500	LPaddle	6.07	2.26	7.75	3.15	19.25	5.52
2016-06-08	54.017	-115.500	LPaddle	10.68	14.37	19.00	8.99	16.25	6.25
2016-06-11	54.017	-115.500	LPaddle	5.61	6.10	3.75	7.44	11.75	3.02
2016-06-14	54.017	-115.500	LPaddle	17.88	27.17	14.75	10.99	16.75	4.38
2016-06-24	54.017	-115.500	LPaddle	13.29	20.69	17.25	9.89	8.25	5.35
2016-06-25	54.017	-115.500	LPaddle	6.35	8.75	7.75	8.12	16.00	7.00
2016-06-28	54.017	-115.500	LPaddle	14.62	20.10	3.75	8.43	14.25	0.65
2016-07-12	54.017	-115.500	LPaddle	13.80	63.96	2.50	21.14	13.00	0.75
2016-07-13	54.017	-115.500	LPaddle	5.85	12.40	1.50	10.71	13.50	1.02
2016-07-29	54.017	-115.500	LPaddle	6.88	10.79	4.75	8.49	18.25	3.77
2016-07-31	54.017	-115.500	LPaddle	12.71	4.93	17.75	3.46	10.25	8.17
2016-08-03	54.017	-115.500	LPaddle	5.00	4.18	1.75	5.65	8.75	0.75
2016-08-06	54.017	-115.500	LPaddle	9.38	6.77	6.75	6.05	22.50	0.53
2016-08-20	54.017	-115.500	LPaddle	11.07	11.75	7.00	7.18	20.75	6.72
2016-08-21	54.017	-115.500	LPaddle	9.49	15.00	1.75	9.60	21.75	1.02
2016-08-22	54.017	-115.500	LPaddle	57.44	109.08	15.75	12.46	10.25	3.02
2016-08-23	54.017	-115.500	LPaddle	17.70	26.97	8.25	8.97	12.00	8.03
2016-08-27	54.017	-115.500	LPaddle	7.05	6.76	1.75	9.20	19.25	0.52
2016-09-02	54.017	-115.500	LPaddle	26.90	10.70	16.25	3.62	1.25	6.28
2016-09-30	54.017	-115.500	LPaddle	12.81	8.34	9.75	4.97	4.25	4.92
2016-09-30	54.017	-115.500	LPaddle	12.58	6.46	15.00	4.20	20.25	13.75
2016-10-07	54.017	-115.500	LPaddle	11.90	2.06	19.25	1.79	12.25	17.27
2016-10-08	54.017	-115.500	LPaddle	8.79	1.40	8.25	1.63	14.75	6.60
2016-10-14	54.017	-115.500	LPaddle	10.50	3.56	5.75	3.00	6.25	3.77
2017-05-12	54.017	-115.500	LPaddle	29.16	23.98	27.75	6.80	7.25	10.02

Date	Lat	Long	Station	Depth	EI30	Dur	I30	Start Time	Peak Delay
Y-M-D	DD	DD		mm	MJ*mm/ha*hr	hr	mm/hr	hr	hr
2017-05-24	54.017	-115.500	LPaddle	22.51	20.23	17.75	6.47	1.50	5.55
2017-06-09	54.017	-115.500	LPaddle	39.27	63.35	20.00	11.21	5.25	1.02
2017-06-20	54.017	-115.500	LPaddle	13.57	30.27	11.50	12.62	6.25	9.77
2017-06-26	54.017	-115.500	LPaddle	15.84	42.56	15.50	14.72	17.75	2.77
2017-06-27	54.017	-115.500	LPaddle	13.32	12.42	25.00	7.02	18.00	25.02
2017-07-20	54.017	-115.500	LPaddle	30.29	24.10	16.75	6.00	16.25	11.02
2017-07-23	54.017	-115.500	LPaddle	11.31	6.76	15.00	5.22	11.00	6.75
2017-07-27	54.017	-115.500	LPaddle	12.71	52.95	2.75	21.98	17.75	0.52
2017-08-01	54.017	-115.500	LPaddle	7.08	2.94	9.50	3.57	4.75	3.12
2017-08-03	54.017	-115.500	LPaddle	9.89	7.36	10.50	6.06	19.50	0.82
2017-08-07	54.017	-115.500	LPaddle	8.89	5.46	12.00	5.03	3.25	5.53
2017-08-18	54.017	-115.500	LPaddle	6.59	7.65	4.75	7.83	15.00	4.50
2017-09-09	54.017	-115.500	LPaddle	9.40	5.50	13.00	4.76	12.50	10.38
2017-09-13	54.017	-115.500	LPaddle	12.80	5.64	17.50	3.97	0.25	17.10
2017-09-14	54.017	-115.500	LPaddle	5.91	5.95	2.25	7.02	16.25	1.00
2017-09-18	54.017	-115.500	LPaddle	73.69	64.30	68.25	7.31	21.00	5.82
2017-10-10	54.017	-115.500	LPaddle	14.49	4.39	10.25	2.80	17.25	7.52
2018-05-16	54.017	-115.500	LPaddle	6.70	1.56	14.75	2.40	16.75	7.77
2018-05-20	54.017	-115.500	LPaddle	7.21	13.16	2.50	10.67	18.00	2.00
2018-06-09	54.017	-115.500	LPaddle	18.28	127.25	4.75	29.07	16.25	0.75
2018-06-10	54.017	-115.500	LPaddle	49.75	37.56	21.25	6.00	8.50	6.77
2018-06-15	54.017	-115.500	LPaddle	8.25	4.01	4.75	4.39	12.75	4.27
2018-07-02	54.017	-115.500	LPaddle	45.51	50.56	42.75	8.39	2.75	36.77
2018-07-17	54.017	-115.500	LPaddle	28.58	76.48	11.00	16.36	19.25	6.03
2018-07-20	54.017	-115.500	LPaddle	30.90	250.76	7.50	35.94	8.75	5.00
2018-07-23	54.017	-115.500	LPaddle	9.40	3.90	16.25	3.81	1.25	15.48
2018-07-30	54.017	-115.500	LPaddle	11.13	30.55	4.50	14.25	17.50	3.73
2018-08-01	54.017	-115.500	LPaddle	20.61	61.98	2.50	22.78	19.75	0.52
2018-08-11	54.017	-115.500	LPaddle	44.20	55.39	26.25	8.42	14.75	22.22
2018-08-23	54.017	-115.500	LPaddle	11.20	14.62	7.75	8.57	20.25	6.35
2018-09-11	54.017	-115.500	LPaddle	11.51	3.89	36.75	3.21	12.50	1.75
2018-09-14	54.017	-115.500	LPaddle	27.59	4.40	46.75	1.66	22.75	6.15
2018-09-20	54.017	-115.500	LPaddle	8.81	1.96	11.25	2.22	21.00	7.73
2018-09-21	54.017	-115.500	LPaddle	11.80	4.42	18.00	3.64	22.50	17.02
2018-10-12	54.017	-115.500	LPaddle	5.10	1.16	12.00	2.22	3.25	4.02
2018-11-01	54.017	-115.500	LPaddle	10.10	1.53	15.25	1.60	20.00	11.77
2018-11-15	54.017	-115.500	LPaddle	6.20	0.69	9.50	1.20	16.25	6.27
2018-12-29	54.017	-115.500	LPaddle	8.29	3.13	7.25	3.47	5.75	6.13
2019-01-04	54.017	-115.500	LPaddle	14.80	5.77	19.25	3.60	6.50	5.52
2016-05-19	54.781	-119.396	PintoLO	28.70	9.63	33.50	3.20	3.25	8.77
2016-05-27	54.781	-119.396	PintoLO	13.30	2.41	37.00	1.82	21.75	27.77
2016-06-08	54.781	-119.396	PintoLO	9.99	32.77	1.00	16.42	12.75	0.72

Date	Lat	Long	Station	Depth	EI30	Dur	I30	Start Time	Peak Delay
Y-M-D	DD	DD		mm	MJ*mm/ha*hr	hr	mm/hr	hr	hr
2016-06-08	54.781	-119.396	PintoLO	45.49	27.57	32.25	5.35	20.00	2.70
2016-06-11	54.781	-119.396	PintoLO	14.19	4.21	15.50	2.83	9.25	1.45
2016-06-14	54.781	-119.396	PintoLO	10.80	7.08	12.00	5.20	0.00	4.77
2016-06-14	54.781	-119.396	PintoLO	66.21	35.53	52.75	4.80	18.75	7.02
2016-06-24	54.781	-119.396	PintoLO	19.47	34.23	6.75	11.23	7.25	2.52
2016-07-07	54.781	-119.396	PintoLO	5.19	1.52	9.00	2.80	21.75	8.52
2016-07-09	54.781	-119.396	PintoLO	22.58	67.12	10.50	15.60	10.25	1.02
2016-07-11	54.781	-119.396	PintoLO	10.04	18.46	1.25	14.05	22.50	0.52
2016-07-20	54.781	-119.396	PintoLO	6.70	3.28	4.25	4.01	8.50	1.02
2016-07-30	54.781	-119.396	PintoLO	11.08	4.46	19.75	3.56	22.75	19.77
2016-08-04	54.781	-119.396	PintoLO	9.79	19.22	5.00	11.13	19.75	2.98
2016-08-05	54.781	-119.396	PintoLO	24.91	27.28	13.25	7.44	17.75	7.87
2016-08-06	54.781	-119.396	PintoLO	8.00	5.36	6.75	5.39	22.50	0.75
2016-08-20	54.781	-119.396	PintoLO	58.12	121.38	43.25	13.41	20.25	19.27
2016-08-27	54.781	-119.396	PintoLO	6.92	8.90	3.50	8.01	0.50	2.98
2016-08-27	54.781	-119.396	PintoLO	21.29	15.93	21.00	6.19	13.50	1.78
2016-08-31	54.781	-119.396	PintoLO	9.18	4.55	19.75	4.21	19.50	10.48
2016-09-30	54.781	-119.396	PintoLO	22.67	12.23	29.25	4.59	10.50	20.77
2016-10-04	54.781	-119.396	PintoLO	10.30	6.13	6.75	5.01	5.50	2.77
2016-10-13	54.781	-119.396	PintoLO	6.39	1.32	9.75	2.00	9.50	6.28
2016-10-14	54.781	-119.396	PintoLO	11.21	3.29	18.00	2.81	5.75	1.03
2017-05-11	54.781	-119.396	PintoLO	12.09	4.96	6.00	19.76	13.00	0.52
2017-05-12	54.781	-119.396	PintoLO	12.31	16.61	5.25	9.01	9.25	2.78
2017-05-12	54.781	-119.396	PintoLO	11.09	2.41	23.00	2.21	21.50	22.47
2017-05-23	54.781	-119.396	PintoLO	21.48	12.73	12.25	4.83	19.75	10.28
2017-06-09	54.781	-119.396	PintoLO	50.52	80.80	22.50	10.84	0.00	12.12
2017-06-10	54.781	-119.396	PintoLO	28.92	24.16	16.00	6.61	21.00	2.23
2017-06-14	54.781	-119.396	PintoLO	16.71	42.66	8.25	13.39	14.25	0.75
2017-06-21	54.781	-119.396	PintoLO	8.10	1.51	7.50	1.81	19.00	2.52
2017-06-27	54.781	-119.396	PintoLO	33.52	25.66	27.25	5.94	9.50	18.38
2017-07-07	54.781	-119.396	PintoLO	24.44	142.36	5.00	26.39	16.25	1.27
2017-07-16	54.781	-119.396	PintoLO	11.28	3.10	15.75	2.60	18.50	6.28
2017-08-06	54.781	-119.396	PintoLO	6.69	3.91	9.00	4.85	19.75	7.28
2017-08-23	54.781	-119.396	PintoLO	11.16	16.55	4.75	9.60	19.75	1.52
2017-08-24	54.781	-119.396	PintoLO	11.68	9.29	4.50	5.86	8.75	0.53
2017-09-02	54.781	-119.396	PintoLO	19.92	11.49	11.75	4.80	2.50	6.77
2017-09-12	54.781	-119.396	PintoLO	11.17	7.13	23.00	5.22	19.75	2.33
2017-09-19	54.781	-119.396	PintoLO	78.19	60.47	37.75	6.19	11.75	15.77
2017-10-10	54.781	-119.396	PintoLO	6.90	0.76	16.25	1.20	16.25	2.27
2017-10-24	54.781	-119.396	PintoLO	15.22	3.40	34.75	2.20	6.50	20.77
2018-05-31	54.781	-119.396	PintoLO	15.14	23.21	1.50	24.60	15.00	0.52
2018-06-10	54.781	-119.396	PintoLO	7.90	0.86	47.25	1.20	18.50	4.02

Date	Lat	Long	Station	Depth	EI30	Dur	I30	Start Time	Peak Delay
Y-M-D	DD	DD		mm	MJ*mm/ha*hr	hr	mm/hr	hr	hr
2018-06-21	54.781	-119.396	PintoLO	21.43	96.36	2.50	20.37	7.25	0.87
2018-06-25	54.781	-119.396	PintoLO	11.70	8.96	9.00	5.75	4.75	5.83
2018-07-01	54.781	-119.396	PintoLO	30.09	20.38	12.75	5.28	22.50	5.08
2018-07-03	54.781	-119.396	PintoLO	17.81	9.03	18.50	4.40	1.25	13.27
2018-07-07	54.781	-119.396	PintoLO	5.19	2.09	11.00	3.90	8.25	0.67
2018-07-19	54.781	-119.396	PintoLO	28.25	67.93	15.50	13.81	15.00	4.02
2018-07-20	54.781	-119.396	PintoLO	64.79	428.41	11.00	32.99	17.75	10.38
2018-07-21	54.781	-119.396	PintoLO	16.79	20.82	18.50	8.34	11.25	10.98
2018-07-22	54.781	-119.396	PintoLO	49.30	73.13	19.50	10.40	14.75	15.25
2018-08-12	54.781	-119.396	PintoLO	22.60	17.92	12.75	6.21	1.50	4.27
2018-08-26	54.781	-119.396	PintoLO	21.56	47.87	14.50	13.84	16.25	4.03
2018-08-30	54.781	-119.396	PintoLO	11.28	7.21	9.00	5.19	7.00	4.77
2018-09-07	54.781	-119.396	PintoLO	10.24	30.34	6.25	14.92	23.75	6.00
2018-09-11	54.781	-119.396	PintoLO	19.28	8.75	29.25	4.45	13.50	3.02
2018-09-26	54.781	-119.396	PintoLO	15.90	6.15	14.00	3.64	13.50	0.97
2018-10-01	54.781	-119.396	PintoLO	7.20	1.48	19.00	2.20	12.75	7.75
2018-10-07	54.781	-119.396	PintoLO	6.40	1.67	16.25	2.56	5.75	5.15
2018-10-12	54.781	-119.396	PintoLO	8.10	2.10	9.00	2.64	6.75	1.30
2018-11-01	54.781	-119.396	PintoLO	12.09	1.37	20.75	1.20	15.25	14.27
2018-11-03	54.781	-119.396	PintoLO	8.69	1.32	26.75	1.60	17.50	10.02
2018-11-15	54.781	-119.396	PintoLO	12.70	3.72	15.50	2.80	11.50	4.77
2018-11-27	54.781	-119.396	PintoLO	5.40	1.64	4.25	2.80	11.00	1.77
2018-12-29	54.781	-119.396	PintoLO	5.80	0.75	9.25	1.40	2.75	5.77
2019-01-04	54.781	-119.396	PintoLO	7.21	2.19	23.50	3.01	3.25	23.32
2019-01-06	54.781	-119.396	PintoLO	7.70	0.85	22.00	1.20	1.75	3.52
2016-05-08	54.950	-117.733	Spring Creek	10.78	4.23	6.50	3.44	11.25	4.22
2016-05-19	54.950	-117.733	Spring Creek	36.92	51.37	31.50	11.05	3.50	31.27
2016-05-26	54.950	-117.733	Spring Creek	8.10	3.32	7.25	3.61	13.00	1.48
2016-05-27	54.950	-117.733	Spring Creek	7.70	1.50	23.25	2.04	11.75	14.82
2016-06-08	54.950	-117.733	Spring Creek	30.37	92.88	17.25	16.48	4.25	3.50
2016-06-09	54.950	-117.733	Spring Creek	27.69	19.70	13.25	5.66	6.75	8.40
2016-06-14	54.950	-117.733	Spring Creek	109.71	239.43	57.00	16.27	18.00	2.62
2016-06-24	54.950	-117.733	Spring Creek	9.04	6.73	9.75	5.33	10.00	3.02
2016-07-06	54.950	-117.733	Spring Creek	7.30	3.93	4.75	4.24	19.25	0.78
2016-07-09	54.950	-117.733	Spring Creek	9.21	7.10	6.75	5.64	15.75	0.88
2016-07-31	54.950	-117.733	Spring Creek	15.39	9.93	15.00	5.27	6.25	8.13
2016-08-06	54.950	-117.733	Spring Creek	15.12	31.10	7.00	11.74	0.50	0.75
2016-08-20	54.950	-117.733	Spring Creek	25.28	22.70	42.00	7.41	22.25	19.52
2016-08-27	54.950	-117.733	Spring Creek	7.03	5.27	3.75	5.86	2.75	2.97
2016-08-27	54.950	-117.733	Spring Creek	17.07	10.17	13.50	6.15	14.25	0.52
2016-08-31	54.950	-117.733	Spring Creek	11.24	14.93	13.25	8.69	23.50	7.02
2016-09-03	54.950	-117.733	Spring Creek	5.29	0.61	7.00	1.23	9.75	4.35

Date	Lat	Long	Station	Depth	EI30	Dur	I30	Start Time	Peak Delay
Y-M-D	DD	DD		mm	MJ*mm/ha*hr	hr	mm/hr	hr	hr
2016-09-08	54.950	-117.733	Spring Creek	6.30	6.94	6.00	7.20	15.25	5.27
2016-09-30	54.950	-117.733	Spring Creek	17.31	4.99	33.75	2.79	9.50	23.77
2016-10-13	54.950	-117.733	Spring Creek	5.60	0.63	7.25	1.20	14.00	4.52
2016-10-14	54.950	-117.733	Spring Creek	7.61	1.56	9.00	2.00	6.75	2.02
2016-10-26	54.950	-117.733	Spring Creek	9.88	0.00	0.25	19.76	11.25	0.13
2016-10-31	54.950	-117.733	Spring Creek	9.60	0.89	25.25	1.03	19.25	10.63
2017-05-13	54.950	-117.733	Spring Creek	24.81	12.20	20.25	4.21	0.25	3.52
2017-05-23	54.950	-117.733	Spring Creek	35.95	35.17	12.00	6.88	19.50	7.32
2017-06-09	54.950	-117.733	Spring Creek	9.21	7.85	11.25	6.42	9.75	9.27
2017-06-14	54.950	-117.733	Spring Creek	5.29	2.53	7.25	4.20	13.75	6.52
2017-06-20	54.950	-117.733	Spring Creek	7.62	5.48	3.00	5.30	12.00	2.60
2017-06-21	54.950	-117.733	Spring Creek	6.30	1.70	7.75	2.60	18.00	5.98
2017-06-26	54.950	-117.733	Spring Creek	6.08	6.27	6.25	7.22	14.25	2.52
2017-06-27	54.950	-117.733	Spring Creek	31.40	46.10	32.75	10.92	11.75	32.52
2017-07-02	54.950	-117.733	Spring Creek	6.64	6.29	5.50	6.45	18.75	0.77
2017-07-07	54.950	-117.733	Spring Creek	17.96	80.43	4.75	20.34	18.25	3.72
2017-07-16	54.950	-117.733	Spring Creek	13.12	4.68	21.75	3.44	21.25	8.03
2017-08-22	54.950	-117.733	Spring Creek	7.63	12.80	5.25	10.05	23.75	0.75
2017-08-23	54.950	-117.733	Spring Creek	11.13	10.13	4.75	11.82	22.75	0.52
2017-09-02	54.950	-117.733	Spring Creek	5.60	1.07	9.50	2.00	8.00	1.77
2017-09-08	54.950	-117.733	Spring Creek	5.52	4.59	2.50	6.31	9.25	0.58
2017-09-09	54.950	-117.733	Spring Creek	17.77	13.68	0.50	35.54	18.25	0.52
2017-09-18	54.950	-117.733	Spring Creek	97.60	122.74	70.00	9.83	15.00	22.75
2017-10-17	54.950	-117.733	Spring Creek	5.71	0.78	10.25	1.40	4.25	2.02
2018-05-25	54.950	-117.733	Spring Creek	8.20	6.33	2.75	5.60	19.50	2.27
2018-06-10	54.950	-117.733	Spring Creek	12.80	6.06	11.75	4.19	16.25	9.27
2018-06-11	54.950	-117.733	Spring Creek	5.00	0.66	10.00	1.40	23.50	8.52
2018-06-29	54.950	-117.733	Spring Creek	6.10	2.37	5.75	3.20	19.00	3.02
2018-07-01	54.950	-117.733	Spring Creek	53.28	63.75	39.75	9.07	4.25	28.78
2018-07-03	54.950	-117.733	Spring Creek	24.57	53.25	19.50	14.42	2.50	17.77
2018-07-07	54.950	-117.733	Spring Creek	7.39	4.89	11.75	5.18	8.50	4.27
2018-07-19	54.950	-117.733	Spring Creek	62.38	112.55	30.00	11.60	19.00	29.75
2018-07-22	54.950	-117.733	Spring Creek	21.73	17.96	28.50	6.52	8.25	6.02
2018-08-02	54.950	-117.733	Spring Creek	12.04	10.40	5.00	9.92	21.50	0.52
2018-08-11	54.950	-117.733	Spring Creek	5.10	1.50	4.50	2.80	23.75	1.02
2018-08-26	54.950	-117.733	Spring Creek	5.50	8.77	9.25	9.08	8.25	8.98
2018-08-29	54.950	-117.733	Spring Creek	7.00	2.81	20.25	3.81	20.25	0.77
2018-08-31	54.950	-117.733	Spring Creek	8.39	8.72	8.50	7.20	19.25	8.02
2018-09-11	54.950	-117.733	Spring Creek	12.11	2.14	24.75	1.85	15.25	8.95
2018-09-16	54.950	-117.733	Spring Creek	5.20	0.48	11.50	1.03	5.50	9.38
2018-09-26	54.950	-117.733	Spring Creek	6.60	5.61	5.25	6.20	22.25	5.02
2018-10-11	54.950	-117.733	Spring Creek	17.00	5.66	28.75	3.20	23.25	8.52

Date	Lat	Long	Station	Depth	EI30	Dur	I30	Start Time	Peak Delay
Y-M-D	DD	DD		mm	MJ*mm/ha*hr	hr	mm/hr	hr	hr
2016-05-08	55.352	-118.408	TeePeeCr	6.41	1.54	11.25	2.40	10.25	1.27
2016-05-19	55.352	-118.408	TeePeeCr	30.68	20.96	31.50	5.79	4.50	27.27
2016-05-27	55.352	-118.408	TeePeeCr	18.52	6.39	15.75	3.22	17.50	9.98
2016-05-29	55.352	-118.408	TeePeeCr	9.10	5.37	4.75	4.63	5.50	1.28
2016-06-08	55.352	-118.408	TeePeeCr	6.09	2.59	9.50	3.27	7.25	9.32
2016-06-09	55.352	-118.408	TeePeeCr	31.01	20.89	14.75	5.25	6.00	12.30
2016-06-11	55.352	-118.408	TeePeeCr	8.64	17.03	13.75	11.45	11.50	2.52
2016-06-14	55.352	-118.408	TeePeeCr	74.32	181.58	62.50	16.82	8.50	6.25
2016-07-06	55.352	-118.408	TeePeeCr	23.31	36.81	6.50	9.76	18.00	0.98
2016-07-08	55.352	-118.408	TeePeeCr	5.36	2.48	10.75	3.79	6.25	2.52
2016-07-19	55.352	-118.408	TeePeeCr	8.19	4.25	16.00	4.70	18.75	5.30
2016-07-21	55.352	-118.408	TeePeeCr	7.23	8.02	7.75	7.51	13.50	1.83
2016-07-31	55.352	-118.408	TeePeeCr	16.69	23.68	19.00	10.40	0.50	1.02
2016-08-01	55.352	-118.408	TeePeeCr	10.58	34.39	3.00	15.66	17.75	3.02
2016-08-03	55.352	-118.408	TeePeeCr	13.96	69.39	8.75	21.30	6.75	7.95
2016-08-06	55.352	-118.408	TeePeeCr	6.85	2.66	9.50	7.71	2.50	0.52
2016-08-21	55.352	-118.408	TeePeeCr	34.07	52.51	20.25	10.68	16.50	1.10
2016-08-31	55.352	-118.408	TeePeeCr	12.08	15.52	20.25	8.80	18.00	13.52
2016-09-30	55.352	-118.408	TeePeeCr	32.07	25.61	33.75	6.73	11.25	22.60
2016-10-14	55.352	-118.408	TeePeeCr	6.59	0.95	32.00	1.58	8.50	27.77
2017-05-11	55.352	-118.408	TeePeeCr	5.90	4.54	6.50	5.87	20.00	0.78
2017-05-12	55.352	-118.408	TeePeeCr	6.01	1.89	4.00	2.81	11.50	3.48
2017-05-12	55.352	-118.408	TeePeeCr	16.09	5.24	24.75	3.01	22.00	12.23
2017-05-23	55.352	-118.408	TeePeeCr	31.03	31.32	11.00	7.07	19.75	4.13
2017-06-09	55.352	-118.408	TeePeeCr	7.93	16.85	1.25	11.11	14.25	0.97
2017-06-10	55.352	-118.408	TeePeeCr	5.00	1.89	3.25	3.30	21.75	0.90
2017-06-27	55.352	-118.408	TeePeeCr	15.62	13.89	21.75	7.05	13.00	7.77
2017-07-07	55.352	-118.408	TeePeeCr	5.86	2.67	1.50	6.53	21.75	0.52
2017-07-23	55.352	-118.408	TeePeeCr	7.98	8.56	3.00	7.62	17.75	2.23
2017-07-31	55.352	-118.408	TeePeeCr	5.81	2.73	3.75	3.87	23.75	3.15
2017-08-23	55.352	-118.408	TeePeeCr	11.69	11.00	6.50	7.04	21.75	2.40
2017-08-24	55.352	-118.408	TeePeeCr	16.35	62.48	2.50	19.51	10.75	1.73
2017-09-02	55.352	-118.408	TeePeeCr	8.98	4.74	6.50	4.35	8.50	6.52
2017-09-18	55.352	-118.408	TeePeeCr	58.41	39.98	56.25	5.73	16.00	23.90
2017-10-16	55.352	-118.408	TeePeeCr	7.00	2.90	22.25	3.80	13.50	2.52
2017-10-24	55.352	-118.408	TeePeeCr	16.89	3.10	17.50	1.82	13.25	8.55
2018-06-03	55.352	-118.408	TeePeeCr	9.79	6.80	9.25	5.43	21.25	3.28
2018-07-01	55.352	-118.408	TeePeeCr	20.69	8.41	34.00	3.81	2.00	29.75
2018-07-06	55.352	-118.408	TeePeeCr	5.74	12.25	2.75	10.51	13.00	2.52
2018-07-07	55.352	-118.408	TeePeeCr	15.72	28.58	6.75	11.61	8.00	3.22
2018-07-19	55.352	-118.408	TeePeeCr	54.75	187.52	29.50	20.75	18.75	29.27
2018-07-21	55.352	-118.408	TeePeeCr	5.40	3.08	8.00	4.32	12.25	1.18

Date	Lat	Long	Station	Depth	EI30	Dur	I30	Start Time	Peak Delay
Y-M-D	DD	DD		mm	MJ*mm/ha*hr	hr	mm/hr	hr	hr
2018-07-22	55.352	-118.408	TeePeeCr	10.49	6.42	8.25	5.00	17.75	2.75
2018-08-11	55.352	-118.408	TeePeeCr	21.91	12.06	13.25	4.55	23.50	5.13
2018-08-25	55.352	-118.408	TeePeeCr	7.09	1.48	22.25	2.00	21.25	16.27
2018-08-28	55.352	-118.408	TeePeeCr	6.25	6.37	4.25	5.73	15.75	1.02
2018-09-07	55.352	-118.408	TeePeeCr	10.70	35.05	22.75	15.40	20.75	11.27
2018-09-11	55.352	-118.408	TeePeeCr	5.20	0.46	29.25	1.01	13.25	22.52
2018-10-11	55.352	-118.408	TeePeeCr	14.92	4.36	12.75	2.63	23.00	5.00
2018-10-31	55.352	-118.408	TeePeeCr	6.39	2.13	8.50	3.18	14.00	2.75
2018-11-03	55.352	-118.408	TeePeeCr	12.09	1.31	39.25	1.20	20.00	6.27
2018-12-29	55.352	-118.408	TeePeeCr	6.20	0.56	21.25	1.01	7.75	7.03
2016-05-08	55.098	-117.199	Valleyview	15.19	19.59	8.75	9.36	11.00	7.10
2016-05-19	55.098	-117.199	Valleyview	32.78	14.73	41.50	4.01	1.25	31.75
2016-05-26	55.098	-117.199	Valleyview	7.60	2.94	9.50	4.81	13.75	0.52
2016-06-08	55.098	-117.199	Valleyview	23.53	43.29	6.00	11.74	5.50	5.77
2016-06-09	55.098	-117.199	Valleyview	28.82	24.07	15.75	6.41	3.00	9.75
2016-06-10	55.098	-117.199	Valleyview	6.39	2.95	13.00	4.21	18.50	10.77
2016-06-14	55.098	-117.199	Valleyview	31.70	13.06	40.25	3.80	16.75	20.53
2016-06-16	55.098	-117.199	Valleyview	21.25	26.61	11.50	8.36	15.00	10.93
2016-06-24	55.098	-117.199	Valleyview	10.75	16.36	4.25	9.25	10.25	2.00
2016-07-06	55.098	-117.199	Valleyview	10.08	5.89	7.25	6.19	16.50	0.52
2016-07-20	55.098	-117.199	Valleyview	5.98	1.38	14.75	2.99	0.25	0.52
2016-07-29	55.098	-117.199	Valleyview	5.57	4.16	1.25	8.57	19.00	0.52
2016-07-31	55.098	-117.199	Valleyview	24.87	24.69	21.50	7.28	2.25	11.42
2016-08-06	55.098	-117.199	Valleyview	6.60	3.22	6.00	4.23	3.00	5.72
2016-08-07	55.098	-117.199	Valleyview	5.40	1.38	4.25	2.50	1.25	0.58
2016-08-21	55.098	-117.199	Valleyview	42.27	141.32	36.75	20.36	5.50	12.77
2016-09-01	55.098	-117.199	Valleyview	5.32	1.81	8.25	2.79	2.00	7.02
2016-09-03	55.098	-117.199	Valleyview	6.01	0.68	12.50	1.21	7.25	10.77
2016-09-30	55.098	-117.199	Valleyview	23.32	14.61	36.25	5.35	9.00	0.88
2016-10-08	55.098	-117.199	Valleyview	6.09	0.78	39.25	1.42	17.75	16.47
2016-10-13	55.098	-117.199	Valleyview	8.20	1.82	10.50	2.20	14.25	4.27
2016-10-14	55.098	-117.199	Valleyview	6.89	0.75	26.50	1.20	8.00	26.52
2017-05-11	55.098	-117.199	Valleyview	7.16	7.86	3.25	7.76	21.25	1.52
2017-05-12	55.098	-117.199	Valleyview	28.99	12.55	29.00	3.80	9.75	19.02
2017-05-23	55.098	-117.199	Valleyview	19.40	11.16	10.50	4.80	20.50	3.27
2017-06-20	55.098	-117.199	Valleyview	5.00	2.24	3.00	3.89	12.50	0.70
2017-06-27	55.098	-117.199	Valleyview	9.00	13.35	2.00	8.99	4.25	1.58
2017-06-27	55.098	-117.199	Valleyview	17.00	7.92	23.50	4.10	17.25	18.38
2017-07-02	55.098	-117.199	Valleyview	7.80	11.96	5.25	8.38	19.25	2.02
2017-07-07	55.098	-117.199	Valleyview	25.03	233.30	5.75	37.64	22.00	0.77
2017-07-13	55.098	-117.199	Valleyview	8.28	27.52	1.25	14.98	14.50	0.77
2017-07-20	55.098	-117.199	Valleyview	17.60	36.94	2.00	31.57	18.50	0.52

Date	Lat	Long	Station	Depth	EI30	Dur	I30	Start Time	Peak Delay
Y-M-D	DD	DD		mm	MJ*mm/ha*hr	hr	mm/hr	hr	hr
2017-08-03	55.098	-117.199	Valleyview	16.71	47.01	11.00	16.48	17.00	0.78
2017-08-23	55.098	-117.199	Valleyview	18.39	75.75	6.75	17.84	20.75	5.97
2017-09-18	55.098	-117.199	Valleyview	89.60	78.89	64.00	7.20	15.50	22.27
2017-10-07	55.098	-117.199	Valleyview	6.20	1.25	4.50	2.00	2.50	3.53
2017-10-16	55.098	-117.199	Valleyview	6.11	1.71	20.00	2.80	13.00	19.25
2017-10-24	55.098	-117.199	Valleyview	9.09	1.99	23.50	2.22	14.75	2.97
2018-05-25	55.098	-117.199	Valleyview	7.42	7.76	5.25	7.25	20.75	1.55
2018-06-10	55.098	-117.199	Valleyview	19.60	18.13	15.00	7.38	14.50	1.52
2018-06-11	55.098	-117.199	Valleyview	15.20	6.23	29.50	3.61	13.50	9.25
2018-06-15	55.098	-117.199	Valleyview	5.25	6.86	2.25	7.74	11.75	2.02
2018-07-01	55.098	-117.199	Valleyview	32.44	32.67	45.50	8.34	22.75	44.52
2018-07-07	55.098	-117.199	Valleyview	6.93	8.14	11.75	8.05	9.75	2.50
2018-07-19	55.098	-117.199	Valleyview	81.02	114.99	33.50	8.96	19.50	24.98
2018-08-04	55.098	-117.199	Valleyview	17.33	127.35	2.00	29.88	15.00	0.77
2018-08-25	55.098	-117.199	Valleyview	9.89	6.01	27.50	4.79	16.00	23.27
2018-09-11	55.098	-117.199	Valleyview	6.90	0.91	15.25	1.40	19.75	3.77
2018-09-16	55.098	-117.199	Valleyview	6.40	0.57	18.75	1.00	5.25	10.52
2018-10-12	55.098	-117.199	Valleyview	10.30	3.40	12.50	3.07	2.00	5.83
2018-10-31	55.098	-117.199	Valleyview	6.91	1.45	10.75	2.23	16.00	0.55
2018-11-01	55.098	-117.199	Valleyview	7.60	0.97	17.50	1.40	19.25	17.52
2018-11-04	55.098	-117.199	Valleyview	5.49	0.49	27.25	1.02	0.00	4.05
2018-12-29	55.098	-117.199	Valleyview	11.00	2.78	21.50	2.48	9.00	3.40
2016-05-19	56.012	-122.185	Williston	14.97	3.87	21.75	2.00	4.50	0.52
2016-05-20	56.012	-122.185	Williston	10.98	2.76	7.75	2.00	9.75	0.52
2016-05-28	56.012	-122.185	Williston	6.98	1.66	7.75	2.00	5.75	0.52
2016-05-29	56.012	-122.185	Williston	7.99	3.88	11.00	4.00	22.75	1.27
2016-06-08	56.012	-122.185	Williston	44.95	24.36	42.50	4.00	15.75	24.02
2016-06-14	56.012	-122.185	Williston	13.00	20.45	3.75	14.00	11.50	0.52
2016-06-14	56.012	-122.185	Williston	36.96	42.41	20.00	8.03	23.25	2.52
2016-07-13	56.012	-122.185	Williston	5.98	3.80	8.75	5.97	13.50	8.77
2016-07-19	56.012	-122.185	Williston	28.04	116.47	18.25	22.18	16.50	1.48
2016-08-06	56.012	-122.185	Williston	18.02	27.00	10.50	9.98	3.25	6.02
2016-08-21	56.012	-122.185	Williston	6.98	1.66	10.50	2.00	7.50	0.52
2016-08-26	56.012	-122.185	Williston	110.93	1366.73	18.00	54.58	22.75	6.97
2016-08-29	56.012	-122.185	Williston	12.98	6.64	9.75	4.00	1.75	8.02
2016-08-29	56.012	-122.185	Williston	13.99	7.20	8.25	4.00	21.00	5.77
2016-08-31	56.012	-122.185	Williston	12.95	14.61	9.25	8.00	1.50	9.02
2016-08-31	56.012	-122.185	Williston	5.99	2.77	8.25	4.00	17.25	3.77
2016-09-01	56.012	-122.185	Williston	8.98	2.21	15.50	2.00	20.75	0.52
2016-09-30	56.012	-122.185	Williston	14.97	3.87	25.50	2.00	14.75	0.52
2016-10-04	56.012	-122.185	Williston	13.97	3.59	30.50	2.00	7.25	0.52
2016-10-07	56.012	-122.185	Williston	8.98	2.21	14.25	2.00	14.50	0.52

Date	Lat	Long	Station	Depth	EI30	Dur	I30	Start Time	Peak Delay
Y-M-D	DD	DD		mm	MJ*mm/ha*hr	hr	mm/hr	hr	hr
2016-10-16	56.012	-122.185	Williston	6.98	1.66	14.50	2.00	2.25	0.52
2016-10-24	56.012	-122.185	Williston	18.97	9.96	19.00	4.00	20.25	17.77
2017-05-05	56.012	-122.185	Williston	7.97	6.28	8.25	5.97	13.50	4.27
2017-05-11	56.012	-122.185	Williston	50.93	41.78	31.00	5.97	10.50	17.52
2017-05-13	56.012	-122.185	Williston	7.98	1.93	15.00	2.00	13.00	0.52
2017-05-15	56.012	-122.185	Williston	29.94	33.43	22.50	8.00	18.75	1.27
2017-05-23	56.012	-122.185	Williston	14.97	13.07	8.50	6.21	23.75	1.88
2017-06-09	56.012	-122.185	Williston	20.00	17.37	9.50	6.03	4.50	6.77
2017-06-10	56.012	-122.185	Williston	16.98	8.86	10.25	4.00	21.00	7.52
2017-06-21	56.012	-122.185	Williston	5.99	1.38	6.25	2.00	18.50	0.52
2017-06-27	56.012	-122.185	Williston	7.98	4.20	12.75	3.99	15.25	3.27
2017-07-07	56.012	-122.185	Williston	19.00	32.03	4.75	10.00	19.25	1.27
2017-07-13	56.012	-122.185	Williston	24.95	35.27	6.00	8.64	6.75	0.62
2017-08-29	56.012	-122.185	Williston	12.99	34.75	2.25	20.00	20.00	0.52
2017-09-19	56.012	-122.185	Williston	12.98	6.64	10.50	4.00	23.25	9.02
2017-10-24	56.012	-122.185	Williston	14.99	7.75	5.25	4.00	15.00	5.27
2017-10-25	56.012	-122.185	Williston	34.73	141.68	9.25	29.55	2.25	0.52
2018-05-30	56.012	-122.185	Williston	12.98	6.64	11.75	4.00	13.00	9.52
2018-06-03	56.012	-122.185	Williston	32.02	37.64	17.25	8.00	14.50	4.27
2018-06-24	56.012	-122.185	Williston	11.97	3.04	18.00	2.00	21.25	0.52
2018-06-25	56.012	-122.185	Williston	10.99	5.54	5.75	4.00	22.50	3.27
2018-07-01	56.012	-122.185	Williston	24.93	22.60	16.00	6.33	9.00	13.42
2018-07-05	56.012	-122.185	Williston	5.94	2.74	2.00	9.89	18.50	0.52
2018-07-07	56.012	-122.185	Williston	11.99	6.09	6.25	4.00	7.00	4.27
2018-07-19	56.012	-122.185	Williston	62.99	75.28	28.25	8.00	17.25	16.77
2018-07-22	56.012	-122.185	Williston	24.98	13.62	11.25	4.00	5.25	7.77
2018-08-26	56.012	-122.185	Williston	5.00	2.21	6.25	4.00	5.25	5.02
2018-08-30	56.012	-122.185	Williston	9.98	2.49	8.75	2.00	3.25	0.52
2018-09-08	56.012	-122.185	Williston	45.01	85.53	13.50	12.00	1.25	1.27
2018-09-09	56.012	-122.185	Williston	7.99	3.88	10.00	4.00	19.00	4.02
2018-10-12	56.012	-122.185	Williston	15.98	8.30	14.25	4.00	0.75	4.27

Appendix C. Infiltration rates in this study compared with others

Study	Road Type	Estimated Infiltration Rate (mm/hr)
This Study	Glaciolacustrine High Traffic	1.87 ± 0.81
	Glaciolacustrine Low Traffic	3.72 ± 0.90
	Glaciofluvial High Traffic	1.63 ± 0.64
	Glaciofluvial Low Traffic	1.89 ± 1.05
	Morainal High Traffic	1.33 ± 1.18
	Morainal Low Traffic	1.22 ± 0.54
Luce and Cundy, 1994	All (3)	2.13 – 4.75
Reid and Dunne, 1984	In-use gravel	0.3 ± 1
	Abandoned Gravel	0.7
Croke et al., 2006	Main Cut and Fill (2)	0.42 – 10.49
	Feeder Access Cut and Fill (2)	5.2 – 15.88
	Main Ridgetop (1)	17.74 – 22.32
	Feeder Ridgetop (1)	7.88 – 24.87
Sosa-Perez and MacDonald, 2017	Closed	4 ± 1
	Closed – simulated traffic	5 ± 3
Soon et al. 2000	Road near pipeline right-of-way in gray luvisolic soils	~10 – 25
Startsev and McNabb, 2000	Compacted Skid Trail – Grey Luvisol	3
	Non-compactable Skid Trail – Grey Luvisol	13.3

Appendix D. Erosion rates compared across studies in North America

Study	Category	Soils	Production (kg/m ² -yr)	
			Average	Range
<u>This Study</u> (Western Alberta)				
Settling Tanks	High Traffic	Glacial	2.78	0.56 – 6.99
	Low Traffic	Glacial	0.94	0.09 – 1.58
Silt Fences	High Traffic	Glacial	3.18†	0 – 9.15†
Plumes	Road surface	Glacial	7.60*	1.8 – 45*
Gullies	Ditches	Glacial	18.00*	0.2 – 45.6*
Reid and Dunne, 1984 (Western Washington)	Heavy use	Muddy Gravels	125	
	Temporary Nonuse	Muddy Gravels	16.5	
	Moderate use	Muddy Gravels	10.5	
	Light use	Muddy Gravels	0.95	
Bilby et al. 1989 (Western Washington)	Main line	Andesite/Glacial	2.6	2.6 – 2.7
	Secondary	Basalt	1.83	0.68 – 2.75
Luce and Black, 2001 (Oregon)	Graded – Traffic	Basalt	0.23	
	Graded – No Traffic	Basalt	0.2	
	N.G. – Traffic	Basalt	0.05	
	N.G. – No Traffic	Basalt	0.003	
Coe, 2006 (California)	Native surface		0.32	0.0002 – 4.0
	Rocked		0.13	<0.01 – 3.3††
Sugden and Woods, 2007 (Montana)		Belt	0.55	0 – 4.28
		Till	0.53	0 – 9.69
Welsh, 2008 (Colorado)	Low use (≥10%)	Granitic	4.53	0.5 – 7.05
	Low use (6-10%)	Granitic	3.08	1.49 – 5.36
	Low use (<6%)	Granitic	1.92	0.79 – 3.01
Brown et al. 2013 (Virginia)	Bare surface		9.76	3.4 – 28.7
	Rocked		1.28	1.0 – 1.6

†Mean includes two non-producing segments.

††Single large outlier, average without outlier was 0.01 – 0.02 kg/m²-yr

*Time of emplacement of plumes and excavation of ditches not precisely known, but is estimated to be considerably less than one year in most cases due to familiarity with the operating area

Appendix E. Detailed laser particle size plots

